iScience

CellPress

Article

Silver-Catalyzed Regio- and Stereoselective Formal Carbene Insertion into Unstrained C–C σ-Bonds of 1,3-Dicarbonyls

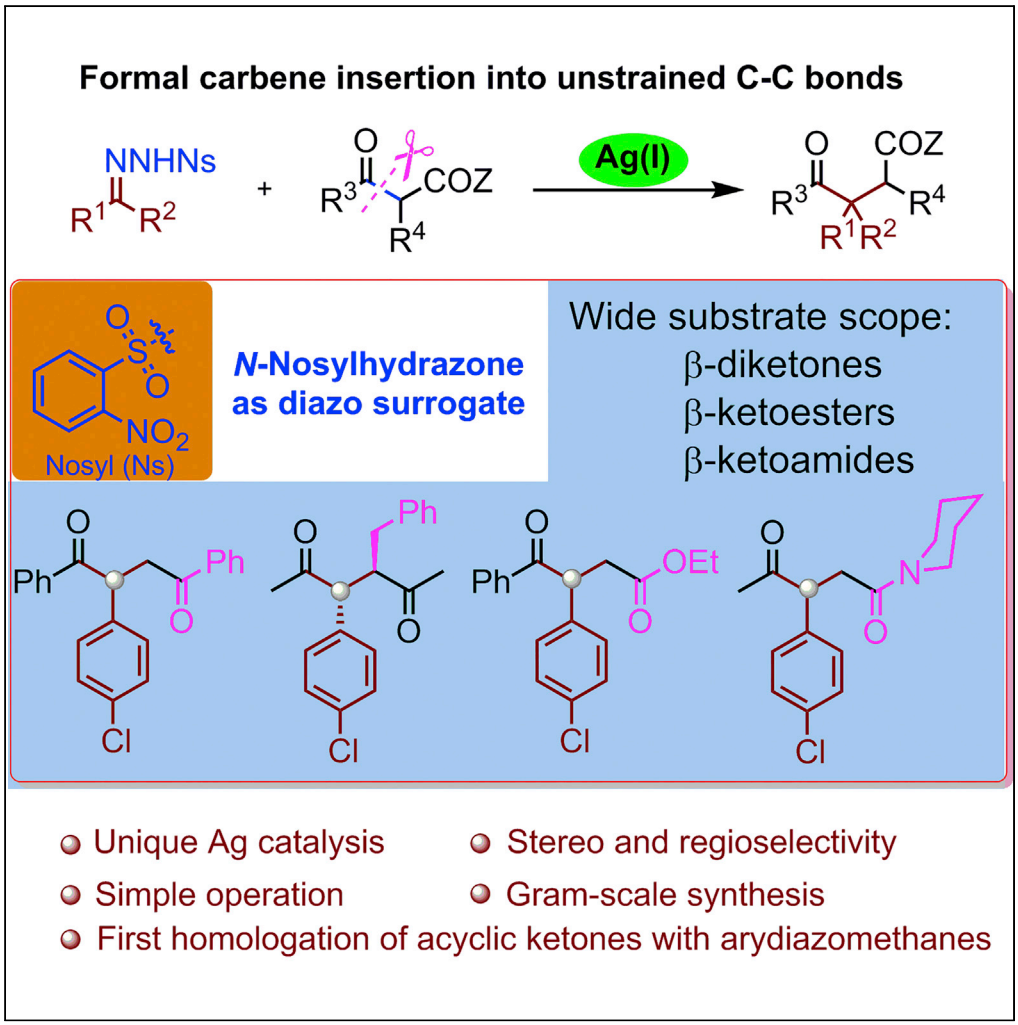

Zhaohong Liu, Xinyu Zhang, Matteo Virelli, Giuseppe Zanoni, Edward A. Anderson, Xihe Bi

bixh507@nenu.edu.cn

HIGHLIGHTS

Regio- and stereoselective carbene insertion into unstrained C–C bonds

Homologation of acyclic ketones with arydiazomethanes

N-nosylhydrazones as room temperature decomposable diazo surrogates

Liu et al., iScience *8*, 54–60
October 26, 2018
https://doi.org/10.1016/j.isci.2018.09.006

iScience

CellPress

Article

Silver-Catalyzed Regio- and Stereoselective Formal Carbene Insertion into Unstrained C–C σ-Bonds of 1,3-Dicarbonyls

Zhaohong Liu,[1] Xinyu Zhang,[1] Matteo Virelli,[3] Giuseppe Zanoni,[3] Edward A. Anderson,[4] and Xihe Bi[1,2,5,*]

SUMMARY

A regio- and stereoselective silver-catalyzed formal carbene insertion into 1,3-dicarbonyls has been developed, using *N*-nosylhydrazones as diazo surrogates. Two new C–C bonds are constructed at the carbenic carbon center through the selective cleavage of the C–C(=O) σ-bond of acyclic 1,3-dicarbonyls, enabling the preparation of various synthetically useful polysubstituted γ-diketones, γ-ketoesters, and γ-ketoamides in high yields. The *in situ* formation of a donor-acceptor cyclopropane, via reaction of the enolate of the 1,3-dicarbonyl with an electrophilic silver carbenoid, is proposed as a key process in the catalytic cycle.

INTRODUCTION

Selective one-carbon insertion into C–C σ-bonds is a highly desirable strategy to homologate organic molecules (Candeias et al., 2016). However, this process is, in general, highly challenging, due to the difficulty of cleaving the relatively inert C–C σ-bonds (Murakami et al., 2016; Fumagalli et al., 2017; Souillart and Cramer, 2015; Chen et al., 2014). Aside from reactions in strained systems, very few efficient strategies are available (Chen et al., 2014); among these, the homologation of ketones with diazo compounds represents one of the most explored strategies, whereby the diazo compound acts as ambiphilic species in sequential nucleophilic addition/1,2-rearrangement cascades (Candeias et al., 2016; Moebius and Kingsbury, 2009; Hashimoto et al., 2009, 2011; Li et al., 2013) (Figure 1A). Diazo compounds have been widely explored as a source of carbenoids under transition metal catalysis (Xia et al., 2017; Ford et al., 2015; Davies and Manning, 2008; Doyle et al., 1998); in the context of C–C insertions, Wang and co-workers have described the formal insertion of diazo-derived rhodium carbenoids into the cyclic C–C bonds of strained benzocyclobutenols (Xia et al., 2014), whereas Murakami's group reported a related enantioselective insertion using *N*-tosylhydrazones as carbene precursors (Yada et al., 2014) (Figure 1B). In both reports, strain release provides a crucial thermodynamic driving force (Fumagalli et al., 2017). In sharp contrast, the selective one-carbon insertion of diazo-derived carbenoids into unstrained acyclic C–C σ-bonds is a formidable challenge (Brogan and Zercher, 1996). Very recently, we have also realized a silver-catalyzed formal carbene insertion into acyclic C-C bonds, affording 1,4-dicarbonyl products bearing an all-carbon quaternary center (Liu et al., 2018). However, the process still has certain deficiencies like the need to synthesize and handle potentially toxic and explosive diazo compounds and the fact that the C-C bond cleavage is limited to 1,3-diketones. As part of our continued interest in the silver-catalyzed activation of diazo compounds (Liu et al., 2017a, 2017b, 2018), we here report the silver-catalyzed formal carbene insertion into the unstrained C–C(=O) bonds of 1,3-dicarbonyls (Xi et al., 2014), using *N*-nosylhydrazones (Xia and Wang, 2017; Xiao et al., 2013; Shao and Zhang, 2012; Barluenga and Valdés, 2011) as diazo surrogates (Figure 1C). This represents the first example of the homologation of acyclic ketones with aryldiazomethanes (Candeias et al., 2016; Xia et al., 2013) and offers a straightforward route to construct synthetically useful polysubstituted 1,4-dicarbonyls, which can be difficult to synthesize by other approaches (DeMartino et al., 2008; Yoo et al., 2010; Liu et al., 2011).

RESULTS AND DISCUSSION

As shown in Scheme 1, initial efforts to achieve the optimal conditions for this insertion process used the reaction of 4-chlorobenzaldehyde *N*-nosylhydrazone **1** and 1,3-diphenylpropane-1,3-dione **2** as the model, AgOTf (10 mol %) and NaH (1.5 equiv) in CH_2Cl_2 at 40°C (please see Table S1 for details), under which the one-carbon insertion product **3** was obtained in 92% yield. The product structure was unambiguously established by single-crystal X-ray analysis (please see Table S2 for details).

[1]Department of Chemistry, Northeast Normal University, Changchun 130024, China

[2]State Key Laboratory of Elemento-Organic Chemistry, Nankai University, Tianjin 300071, China

[3]Department of Chemistry, University of Pavia, Viale Taramelli 12, Pavia 27100, Italy

[4]Chemistry Research Laboratory, University of Oxford, 12 Mansfield Road, Oxford OX1 3TA, UK

[5]Lead Contact

*Correspondence: bixh507@nenu.edu.cn

https://doi.org/10.1016/j.isci.2018.09.006

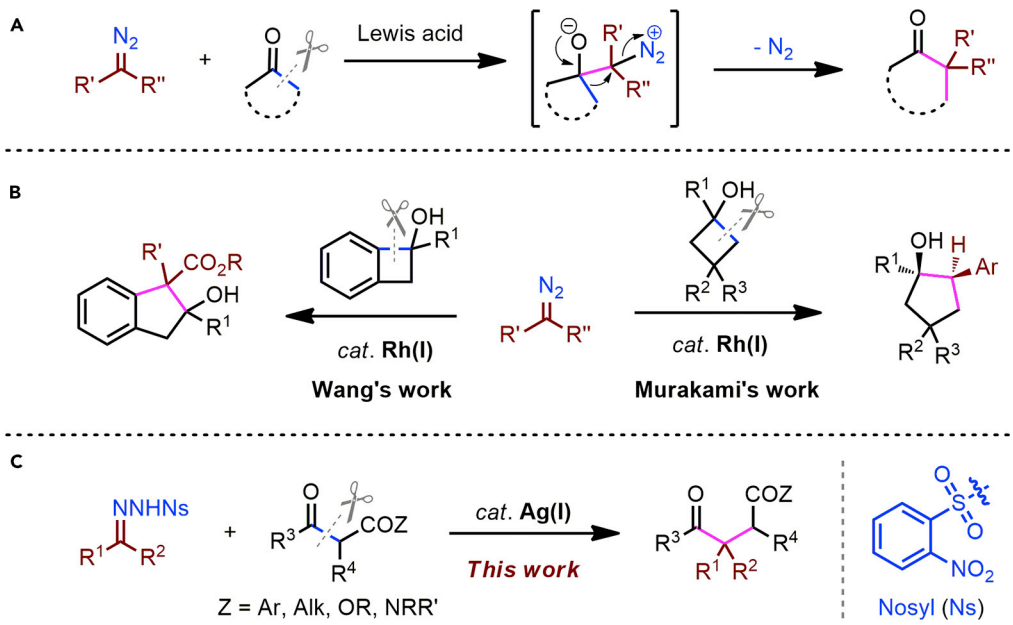

Figure 1. One-Carbon Insertion of Diazo Compounds into C–C σ-Bonds

(A) Lewis acid-promoted nucleophilic addition/1,2-rearrangement.

(B) Rh(I)-catalyzed formal carbene insertion into strained C-C bonds.

(C) This work: Ag(I)-catalyzed formal carbene insertion into unstrained C-C bonds.

With these conditions in hand, the reaction scope was investigated, first focusing on the *N*-nosylhydrazone substrate (Figure 2A). Pleasingly, a wide variety of aldehyde- and ketone-derived *N*-nosylhydrazones proved to be suitable substrates. Benzaldehydes substituted with halogens, and a range of other electron-withdrawing (CO_2Me and CF_3), electron-neutral, and electron-donating groups (Me, OMe, and OBn) at the *para*, *meta*, or *ortho* positions of the phenyl ring were all well-tolerated, affording the desired 1,4-dicarbonyls **4**–**14** in 58%–86% yield. Notably, a potentially reactive benzylic C–H bond in substrate remained intact (Soldi et al., 2014), giving the desired C–C insertion product **14** in 81% yield. More complex aldehyde-derived *N*-nosylhydrazones were also compatible, such as disubstituted arenes, naphthyl, 3-thienyl, 3-furyl, and even cinnamyl groups, leading to the corresponding products **15**–**19** in good yields. To our delight, ketone-derived *N*-nosylhydrazones also underwent successful C–C insertion to give 1,4-dicarbonyls containing an all-carbon α-quaternary stereocenter (Quasdorf and Overman, 2014; Zeng et al., 2016; Feng et al., 2017), requiring only a slight increase of the reaction temperature to 50°C. The scope of these substrates was again broad, with both electron-rich and electron-poor aryl, naphthyl, and heteroaryl methyl ketone-based hydrazones all undergoing smooth reaction with **2** to give 1,4-diketones (**20**–**27**) in 52%–86% yield. *N*-nosylhydrazones bearing a trifluoromethyl group and a 2-methoxyethyl group were also compatible with the reaction conditions, giving α-functionalized 1,4-dicarbonyls **25** and **26** in 86% and 65% yield, respectively. Even the sterically hindered diphenyl *N*-nosylhydrazone delivered the desired product **27** in excellent yield (85%). Collectively, these results demonstrate the breadth of *N*-nosylhydrazones that can be employed in this insertion chemistry.

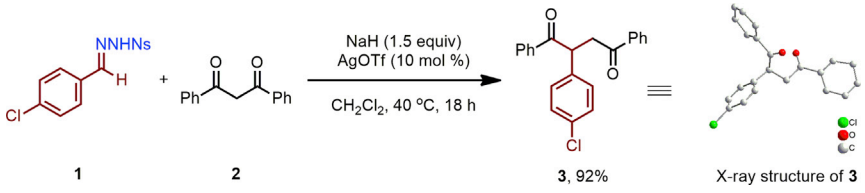

Scheme 1. Optimization of *N*-Nosylhydrazone 1 Insertion into 1,3-Diketone 2

See also Figures S1 and S2.

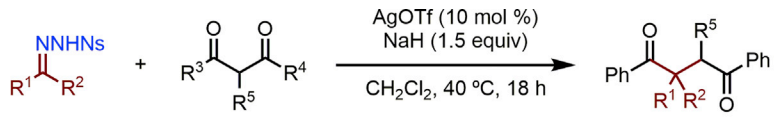

A

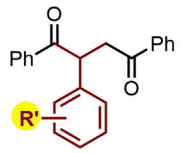

R'	yield	R'	yield	R'	yield
2-Cl, **4**	86%	4-CO_2Me, **8**	72%	3-OMe, **12**	78%
2-Br, **5**	70%	4-CF_3, **9**	80%	2-OMe, **13**	80%
2-I, **6**	74%	4-Me, **10**	58%	2-OBn, **14**	81%
H, **7**	86%	4-Ph, **11**	71%	2-Br-4-F, **15**	55%

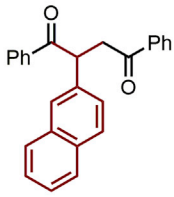

16, 56%

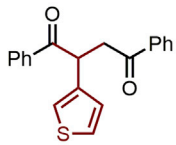

17, 70%

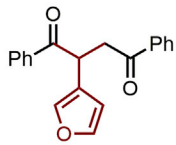

18, 74%

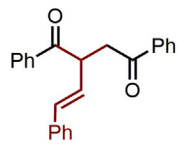

19, 76%

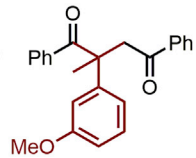

20, 52%

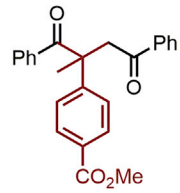

21, 61%

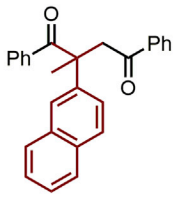

22, 82%

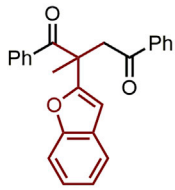

23, 80%

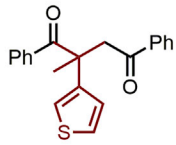

24, 70%

25, 86%

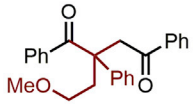

26, 65%

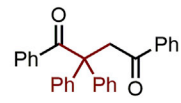

27, 85%

B

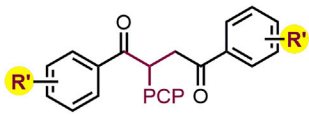

R'	yield
4-OMe, **28**	82%
4-Me, **29**	90%
4-CF_3, **30**	77%
3-Cl, **31**	84%

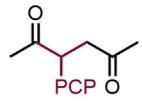

32, 86%

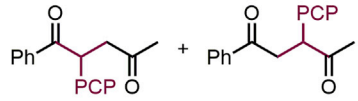

33 + **33'**, 90%, r.r. = 2:1

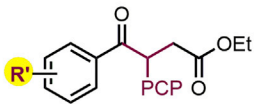

R'	yield	R'	yield
H, **34**	84%	3-OMe, **38**	68%
4-F, **35**	86%	3-Me, **39**	72%
4-NO_2, **36**	92%	3-F, **40**	87%
3-NO_2, **37**	85%		

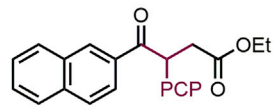

41, 64%

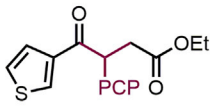

42, 72%

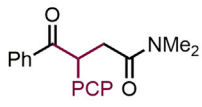

43, 66%

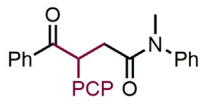

44, 82%

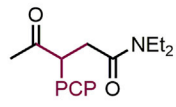

45, 58%

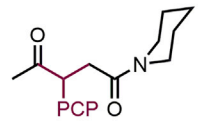

46, 60%

C

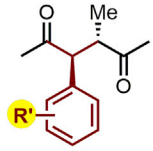

R'	yield
4-Cl, **47**	76% (13:1)
2-F, **48**	46% (8:1)
3-OMe, **49**	78% (4:1)
4-Me, **50**	68% (10:1)

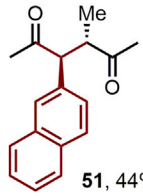

51, 44% (4:1)

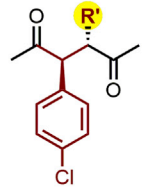

R'	yield
n-Bu, **52**	64% (10:1)
Bn, **53**	63% (8:1)

Figure 2. Substrate Scope Investigation

(A) C-C insertion reaction of *N*-nosylhydrazones.

(B) C-C insertion reaction of 1,3-dicarbonyls.

(C) Diastereoselective insertion into α-substituted 1,3-dicarbonyls.

Reaction conditions: *N*-nosylhydrazones (0.3 mmol), NaH (0.45 mmol), and CH_2Cl_2 (6.0 mL) were stirred at room temperature for 1 hr, then 1,3-dicarbonyls (0.45 mmol) and AgOTf (0.03 mmol) were added, after which the mixture was stirred at 40°C for 18 hr; yields are isolated yields. The reaction was performed at 50°C for compounds **20**–**27**. PCP, *p*-chlorophenyl for compounds **28**–**46**. See also Figures S3–S111.

Next, a variety of 1,3-dicarbonyl compounds, including β-diketones, β-ketoesters, and β-ketoamides, were examined in reactions with 4-chlorophenyl *N*-nosylhydrazone **1** (Figure 2B). Various symmetrical β-diketones with different substituted aryl/alkyl groups were all excellent substrates, affording the corresponding insertion products **28**–**32** in excellent yields (77%–90%). In the case of unsymmetrical phenyl methyl 1,3-diketone, a 2:1 mixture of products **33** and **33′** was obtained in 90% combined yield. This regioselectivity was dramatically enhanced on turning our attention to β-ketoesters: both electron-rich and electron-poor aryl, 2-naphthyl, and 3-thienyl β-ketoesters all smoothly reacted with *N*-nosylhydrazone **1** to deliver the corresponding γ-ketoesters (**34**–**42**) in 62%–92% yield as single regioisomers. The catalytic protocol could also be extended to β-ketoamides, affording γ-ketoamides (**43**–**46**) in moderate to good yields (58–82%), with these one-carbon insertions once again proceeding in a regioselective manner, i.e., into the C(=O)−C bond.

Inspired by the above results, we sought to challenge the scope of the chemistry by using various α-substituted 1,3-diketones (Figure 2C), which have the potential to install two adjacent stereocentres in the product 1,4-dicarbonyls. In the event, 1,3-diketones featuring α-methyl, *n*-butyl, and benzyl groups all participated efficiently in the C−C insertion reaction with a variety of *N*-nosylhydrazones, giving 2,3-disubstituted 1,4-diketones **47**–**53** in moderate to high yields (44%–78%) and, to our delight, with good to excellent diastereoselectivity (4:1–13:1 *dr*) (Dittrich et al., 2016). Such 2,3-disubstituted 1,4-diketones are widespread in biologically active natural products (DeMartino et al., 2008; Yoo et al., 2010) but are not easily accessed in a stereoselective manner by other methods (Liu et al., 2011).

Finally, the robustness of the insertion was tested by performing a multigram-scale synthesis (Scheme 2). We were pleased to find that the reaction could readily be carried out on 15 mmol scale (5.10 g of **1**), affording **3** in high yield (86%, 5.23 g). The synthetic utility of the product 1,4-diketone **3** was briefly explored through its conversion to a 2,3,5-trisubstituted pyrrole **54** on treatment with magnesium nitride (94%) (Veitch et al., 2008); to a 1,2,3,5-tetrasubstituted pyrrole (**55**) on refluxing with aniline in acetic acid (88%); and to a 2,3,5-trisubstituted furan (**56**) on treatment with TsOH in toluene at 110°C (86%) (Liu et al., 2011).

Insight into the possible mechanism of this formal C–C insertion process was obtained through a series of control experiments (Scheme 3, see also Scheme S1). First, attempted reaction of

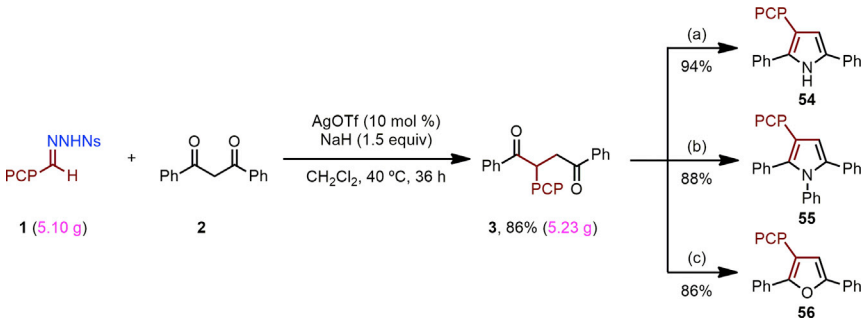

Scheme 2. Multigram-Scale Synthesis of 3 and Further Transformations

Reaction conditions: (a) Mg_3N_2, MeOH, 90°C, 24 hr; (b) aniline (1.5 equiv), AcOH, reflux, 18 hr; (c) TsOH (50 mol %), toluene, 110°C, 8 hr.

See also Figures S112–S117.

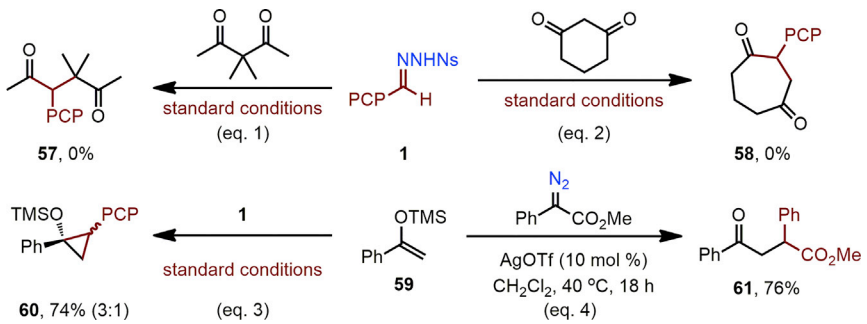

Scheme 3. Mechanistic Studies
See also Figures S118–S123.

3,3-dimethylpentane-2,4-dione (Scheme 3, Equation 1) met with failure, suggesting the ability of the dicarbonyl to form an enol or enolate to be important. Cyclohexane-1,3-dione also proved unsuccessful (Scheme 3, Equation 2); this substrate can clearly undergo enolization but cannot form an enolate capable of chelating to a metal ion through both oxygen atoms (Curini et al., 2006). Under the standard silver catalysis, the reaction of *N*-nosylhydrazone **1** and silylenol ether **59**, which has no an electron-withdrawing group, resulted in cyclopropane **60**, without ring-opening (Scheme 3, Equation 3). In contrast, reaction of methyl phenyldiazoacetate with **59** afforded C-C coupling product **61**, which can be explained by *in situ* formation and ring-opening of a donor-acceptor cyclopropane intermediate (Scheme 3, Equation 4). The intermediacy of a silver enolate was then probed through the reactions of silver acetylacetonate and sodium acetylacetonate with **1** under the standard conditions. Only the former was successful, with product **32** isolated in 40% yield (Scheme S1). This may imply that the silver ion plays a dual role not only in the formation of a silver carbenoid from a diazo compound generated *in situ* from the *N*-nosylhydrazone but also in the delivery of this carbenoid to the dicarbonyl through formation of a bidentate-complexed silver enolate.

On the basis of these observations and related precedents (Brogan and Zercher, 1996; Liu et al., 2018), a plausible mechanism for this formal C−C insertion process is proposed in Scheme 4. Initially, NaH promotes decomposition of the *N*-nosylhydrazone **1** to generate an unstable donor-type diazo species **I**, which then reacts with the silver enolate **II** formed from reaction of AgOTf with 1,3-dicarbonyls to give a key intermediate silver carbenoid **III** (Thompson and Davies, 2007; Caballero et al., 2011; Luo et al., 2015). Intramolecular cyclopropanation of the enolate alkene by a carbene transfer-insertion affords cyclopropane **IV**, which undergoes a ring-opening retro-aldol process to generate intermediate **V** (Cavitt et al., 2014). Protonation of **V** produces the 1,4-dicarbonyl product **P** and regenerates the silver(I) catalyst.

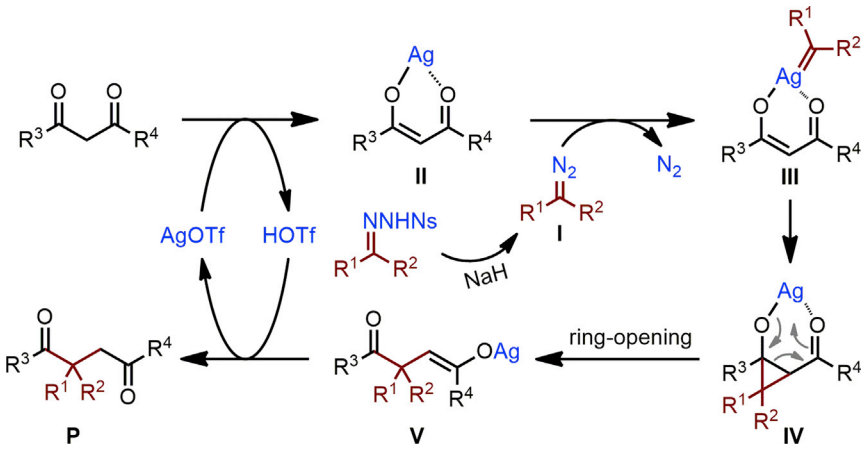

Scheme 4. Proposed Mechanism

Conclusion

In summary, a silver-catalyzed formal carbene insertion into the unstrained C−C σ-bonds of 1,3-dicarbonyls has been developed using *N*-nosylhydrazones as diazo surrogates. In this process, two new C−C bonds are formed to the carbenic carbon atom, along with the regioselective cleavage of a C−C σ-bond. This protocol enables the assembly of synthetically important 1,4-dicarbonyls possessing tertiary/quaternary stereocenters in high yields and with excellent regio- and stereoselectivities. The dual role of the silver catalyst—as a Lewis acid in the formation of a silver enolate and as a transition metal in forming a silver carbenoid—is crucial. Given the mild reaction conditions, broad substrate scope, excellent functional group tolerance, and ready availability of the hydrazone substrates, this one-carbon insertion chemistry has much potential for the construction of useful polysubstituted 1,4-dicarbonyls.

METHODS

All methods can be found in the accompanying Transparent Methods supplemental file.

DATA AND SOFTWARE AVAILABILITY

The data for the X-ray crystallographic structure of **3** has been deposited in the Cambridge Crystallographic Data Center under accession number CCDC: 1563346 (also see Table S1 in Supplemental Information).

SUPPLEMENTAL INFORMATION

Supplemental Information includes Transparent Methods, 123 figures, 1 scheme, 2 tables, and 1 data file and can be found with this article online at https://doi.org/10.1016/j.isci.2018.09.006.

ACKNOWLEDGMENTS

X.B. thanks NSFC (21522202, 21502017), and E.A.A. thanks the EPSRC for support (EP/M019195/1).

AUTHOR CONTRIBUTIONS

Z.L., and X.Z. performed the synthetic experiments and analyzed the experimental data; Z.L., M.V., and G.Z. wrote the original draft; E.A.A. and X.B. performed investigations and prepared the manuscript; X.B. supervised.

DECLARATION OF INTERESTS

The authors declare no competing interests.

Received: July 23, 2018
Revised: August 13, 2018
Accepted: September 6, 2018
Published: October 26, 2018

REFERENCES

Barluenga, J., and Valdés, C. (2011). Tosylhydrazones: new uses for classic reagents in palladium-catalyzed cross-coupling and metal-free reactions. Angew. Chem. Int. Ed. *50*, 7486–7500.

Brogan, J.B., and Zercher, C.K. (1996). Zinc-mediated conversion of β-keto esters to γ-keto esters. J. Org. Chem. *62*, 6444–6446.

Caballero, A., Despagnet-Ayoub, E., Díaz-Requejo, M.M., Díaz-Rodríguez, A., González-Núñez, M.E., Mello, R., Muñoz, B.K., Ojo, W.S., Asensio, G., Etienne, M., and Pérez, P.J. (2011). Silver-catalyzed C-C bond formation between methane and ethyl diazoacetate in supercritical CO_2. Science *332*, 835–838.

Candeias, N.R., Paterna, R., and Gois, P.M.P. (2016). Homologation reaction of ketones with diazo compounds. Chem. Rev. *116*, 2937–2981.

Cavitt, M.A., Phun, L.H., and France, S. (2014). Intramolecular donor-acceptor cyclopropane ring-opening cyclizations. Chem. Soc. Rev. *43*, 804–818.

Chen, F., Wang, T., and Jiao, N. (2014). Recent advances in transition-metal-catalyzed functionalization of unstrained carbon- carbon bonds. Chem. Rev. *114*, 8613–8661.

Curini, M., Epifano, F., and Genovese, S. (2006). Ytterbium triflate catalyzed synthesis of β-keto enol ethers. Tetrahedron Lett. *47*, 4697.

Davies, H.M.L., and Manning, J.R. (2008). Catalytic C-H functionalization by metal carbenoid and nitrenoid insertion. Nature *451*, 417–424.

DeMartino, M.P., Chen, K., and Baran, P.S. (2008). Intermolecular enolate heterocoupling: scope, mechanism, and application. J. Am. Chem. Soc. *130*, 11546–11560.

Dittrich, N., Jung, E.K., Davidson, S.J., and Barker, D. (2016). An Acyl-Claisen/Paal-Knorr approach to fully substituted pyrroles. Tetrahedron *72*, 4676–4689.

Doyle, M.P., McKervey, M.A., and Ye, T. (1998). Modern Catalytic Methods for Organic Synthesis with Diazo Compounds (Wiley-Interscience).

Feng, J., Holmes, M., and Krische, M.J. (2017). Acyclic quaternary carbon stereocenters via enantioselective transition metal catalysis. Chem. Rev. *117*, 12564–12580.

Ford, A., Miel, H., Ring, A., Slattery, C.N., Maguire, A.R., and McKervey, M.A. (2015). Modern organic synthesis with α-diazocarbonyl compounds. Chem. Rev. *115*, 9981–10080.

Fumagalli, G., Stanton, S., and Bower, J.F. (2017). Recent methodologies that exploit C-C single-bond cleavage of strained ring systems by transition metal complexes. Chem. Rev. *117*, 9404–9432.

Hashimoto, T., Naganawa, Y., and Maruoka, K. (2009). Stereoselective construction of seven-membered rings with an all-carbon quaternary center by direct Tiffeneau–Demjanov-type ring expansion. J. Am. Chem. Soc. *131*, 6614–6617.

Hashimoto, T., Naganawa, Y., and Maruoka, K. (2011). Desymmetrizing asymmetric ring expansion of cyclohexanones with α-diazoacetates catalyzed by chiral aluminum Lewis acid. J. Am. Chem. Soc. *133*, 8834–8837.

Li, W., Liu, X., Tan, F., Hao, X., Zheng, J., Lin, L., and Feng, X. (2013). Catalytic asymmetric homologation of α-ketoesters with α-diazoesters: synthesis of succinate derivatives with chiral quaternary centers. Angew. Chem. Int. Ed. *52*, 10883–10886.

Liu, C., Deng, Y., Wang, J., Yang, Y., Tang, S., and Lei, A. (2011). Palladium-catalyzed C-C bond formation to construct 1,4-diketones under mild conditions. Angew. Chem. Int. Ed. *50*, 7337–7341.

Liu, Z., Li, Q., Liao, P., and Bi, X. (2017a). Silver-catalyzed [2+1] cyclopropenation of alkynes with unstable diazoalkanes: *N*-nosylhydrazones as room-temperature decomposable diazo surrogates. Chem. Eur. J. *23*, 4756–4760.

Liu, Z., Li, Q., Yang, Y., and Bi, X. (2017b). Silver(I)-promoted insertion into X–H (X = Si, Sn, and Ge) bonds with *N*-nosylhydrazones. Chem. Commun. *53*, 2503–2506.

Liu, Z., Sivaguru, P., Zanoni, G., Anderson, E.A., and Bi, X. (2018). Catalyst-dependent chemoselective formal insertion of diazo compounds into C-C or C-H bonds of 1,3-dicarbonyl compounds. Angew. Chem. Int. Ed. *57*, 8927–8931.

Luo, H., Wu, G., Zhang, Y., and Wang, J. (2015). Silver(I)-catalyzed *N*-trifluoroethylation of anilines and *O*-trifluoroethylation of amides with 2,2,2-trifluorodiazoethane. Angew. Chem. Int. Ed. *54*, 14503–14507.

Moebius, D.C., and Kingsbury, J.S. (2009). Catalytic homologation of cycloalkanones with substituted diazomethanes. mild and efficient single-step access to α-tertiary and α-quaternary carbonyl compounds. J. Am. Chem. Soc. *131*, 878–879.

Murakami, M., Amii, H., Ito, Y., and Chatani, N. (2016). Cleavage of Carbon-Carbon Single Bonds by Transition Metals (Wiley-VCH).

Quasdorf, K.W., and Overman, L.E. (2014). Catalytic enantioselective synthesis of quaternary carbon stereocentres. Nature *516*, 181–191.

Shao, Z., and Zhang, H. (2012). *N*-Tosylhydrazones: versatile reagents for metal-catalyzed and metal-free cross-coupling reactions. Chem. Soc. Rev. *41*, 560–572.

Soldi, C., Lamb, K.N., Squitieri, R.A., González-López, M., Di Maso, M.J., and Shaw, J.T. (2014). Enantioselective intramolecular C-H insertion reactions of donor-donor metal carbenoids. J. Am. Chem. Soc. *136*, 15142–15145.

Souillart, L., and Cramer, N. (2015). Catalytic C–C bond activations *via* oxidative addition to transition metals. Chem. Rev. *115*, 9410–9464.

Thompson, J.L., and Davies, H.M.L. (2007). Enhancement of cyclopropanation chemistry in the silver-catalyzed reactions of aryldiazoacetates. J. Am. Chem. Soc. *129*, 6090–6091.

Veitch, G.E., Bridgwood, K.L., Rands-Trevor, K., and Ley, S.V. (2008). Magnesium nitride as a convenient source of ammonia: preparation of pyrroles. Synlett *10*, 2597–2600.

Xi, Y., Su, Y., Yu, Z., Dong, B., McClain, E.J., Lan, Y., and Shi, X. (2014). Chemoselective carbophilic addition of α-diazoesters through ligand-controlled gold catalysis. Angew. Chem. Int. Ed. *53*, 9817–9821.

Xia, Y., and Wang, J. (2017). *N*-Tosylhydrazones: versatile synthons in the construction of cyclic compounds. Chem. Soc. Rev. *46*, 2306–2362.

Xia, Y., Liu, Z., Liu, Z., Ge, R., Ye, F., Hossain, M., Zhang, Y., and Wang, J. (2014). Formal carbene insertion into C-C bond: Rh(I)-catalyzed reaction of benzocyclobutenols with diazoesters. J. Am. Chem. Soc. *136*, 3013–3015.

Xia, Y., Qiu, D., and Wang, J. (2017). Transition-metal-catalyzed cross-couplings through carbene migratory insertion. Chem. Rev. *117*, 13810–13889.

Xia, Y., Qu, P., Liu, Z., Ge, R., Xiao, Q., Zhang, Y., and Wang, J. (2013). Catalyst-free intramolecular formal carbon insertion into σ-C-C bonds: a new approach toward phenanthrols and naphthols. Angew. Chem. Int. Ed. *52*, 2543–2546.

Xiao, Q., Zhang, Y., and Wang, J. (2013). Diazo compounds and *N*-tosylhydrazones: novel cross-coupling partners in transition-metal-catalyzed reactions. Acc. Chem. Res. *46*, 236–247.

Yada, A., Fujita, S., and Murakami, M. (2014). Enantioselective insertion of a carbenoid carbon into a C-C bond to expand cyclobutanols to cyclopentanols. J. Am. Chem. Soc. *136*, 7217–7220.

Yoo, E.J., Wasa, M., and Yu, J.-Q. (2010). Pd(II)-catalyzed carbonylation of C(sp^3)-H bonds: a new entry to 1,4-dicarbonyl compounds. J. Am. Chem. Soc. *132*, 17378–17380.

Zeng, X., Cao, Z., Wang, Y., Zhou, F., and Zhou, J. (2016). Catalytic enantioselective desymmetrization reactions to all-carbon quaternary stereocenters. Chem. Rev. *116*, 7330–7396.

ISCI, Volume *8*

Supplemental Information

Silver-Catalyzed Regio- and Stereoselective Formal Carbene Insertion into Unstrained C−C σ-Bonds of 1,3-Dicarbonyls

Zhaohong Liu, Xinyu Zhang, Matteo Virelli, Giuseppe Zanoni, Edward A. Anderson, and Xihe Bi

Supplemental Figures for ^{1}H NMR, ^{13}C NMR, and ^{19}F NMR Spectra

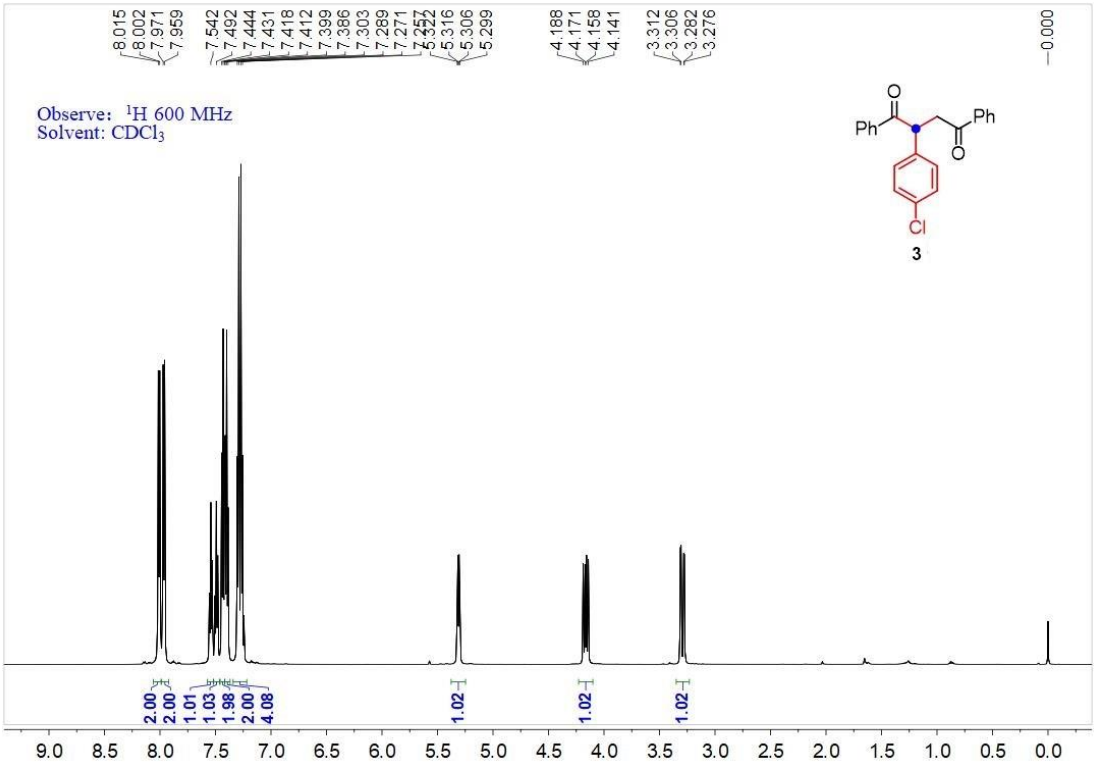

Figure S1. ^{1}H NMR spectrum of compound **3**, related to **Scheme 1.**

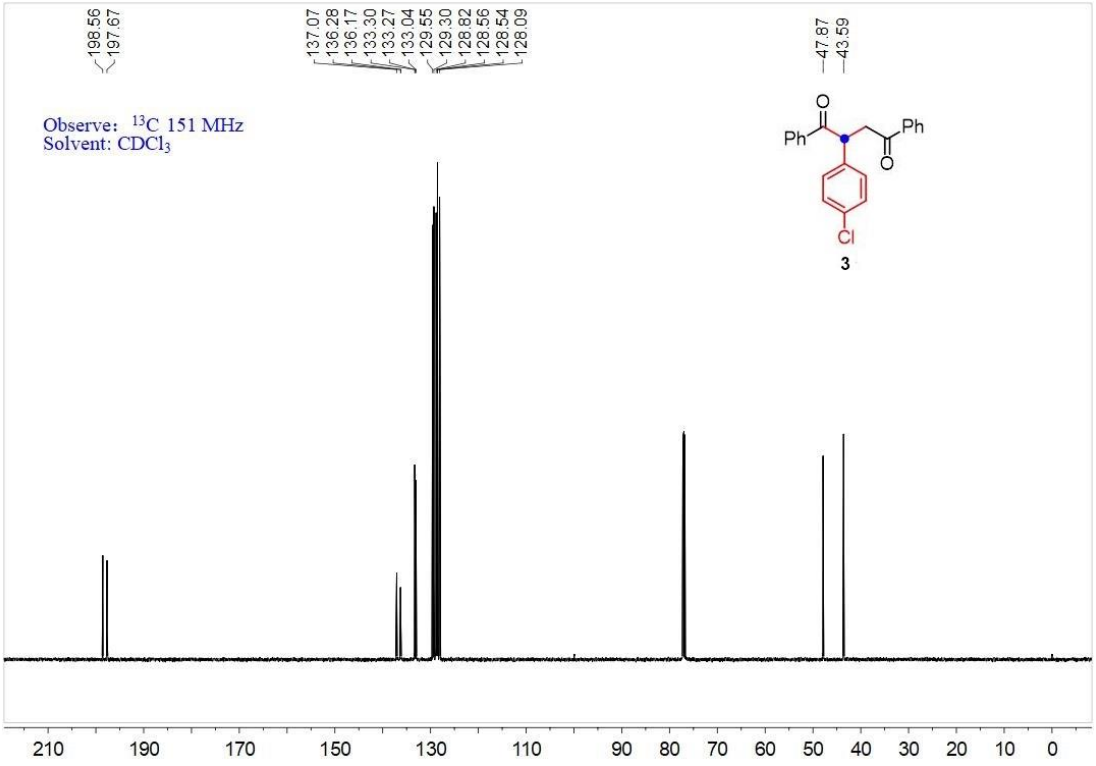

Figure S2. ^{13}C NMR spectrum of compound **3**, related to **Scheme 1.**

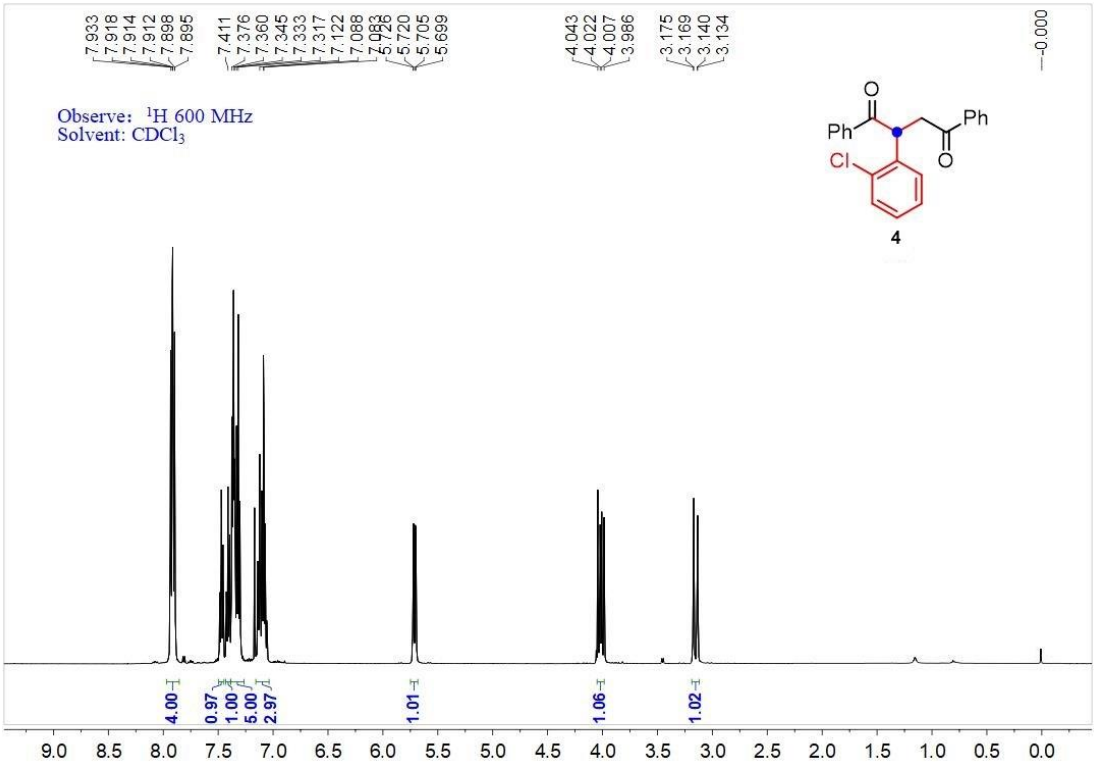

Figure S3. ^{1}H NMR spectrum of compound **4**, related to **Figure 2A.**

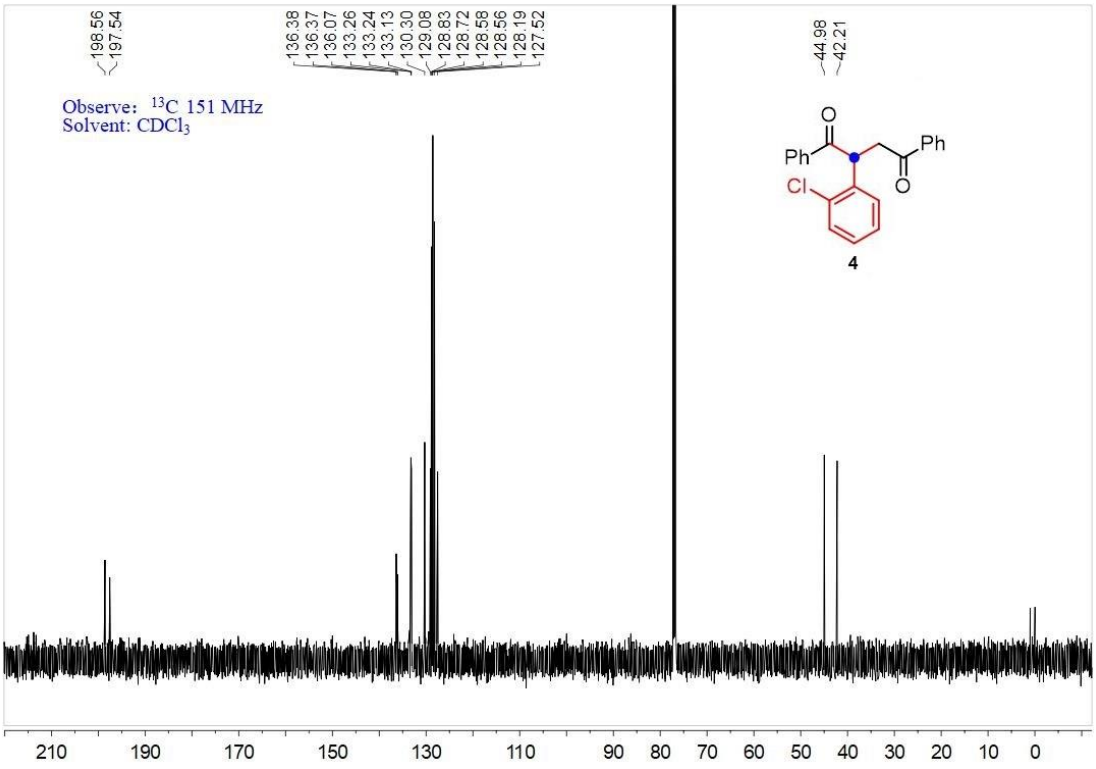

Figure S4. ^{13}C NMR spectrum of compound **4**, related to **Figure 2A.**

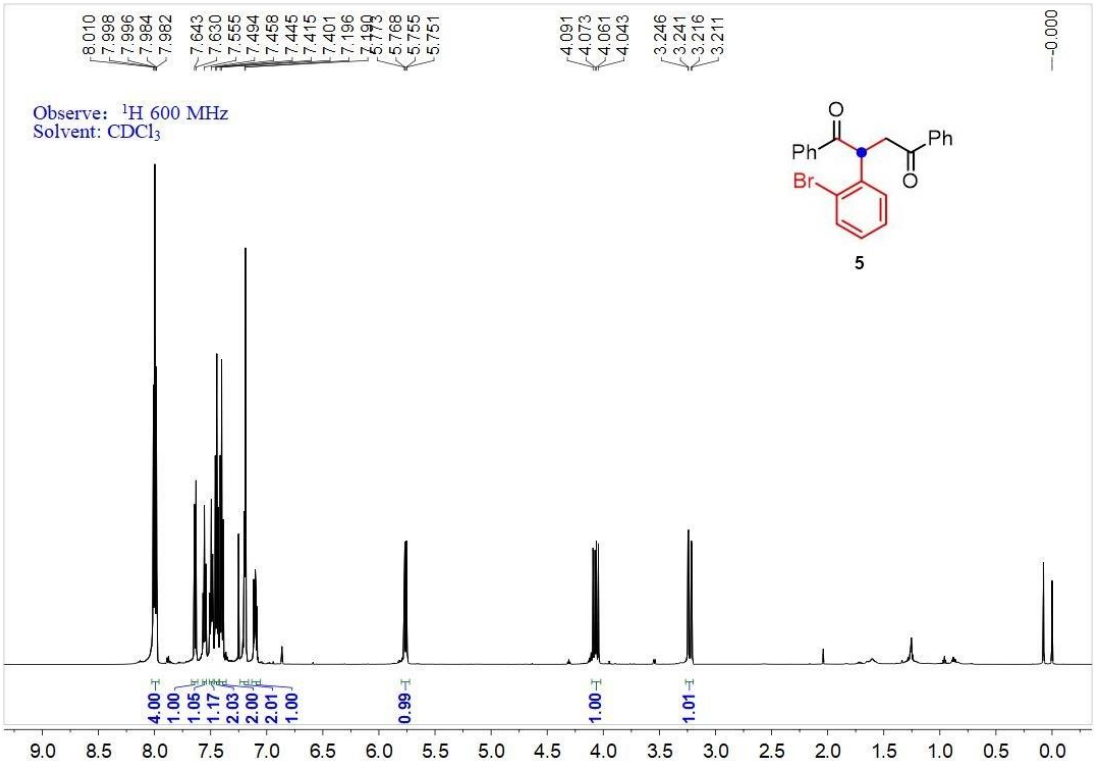

Figure S5. ^{1}H NMR spectrum of compound **5**, related to **Figure 2A.**

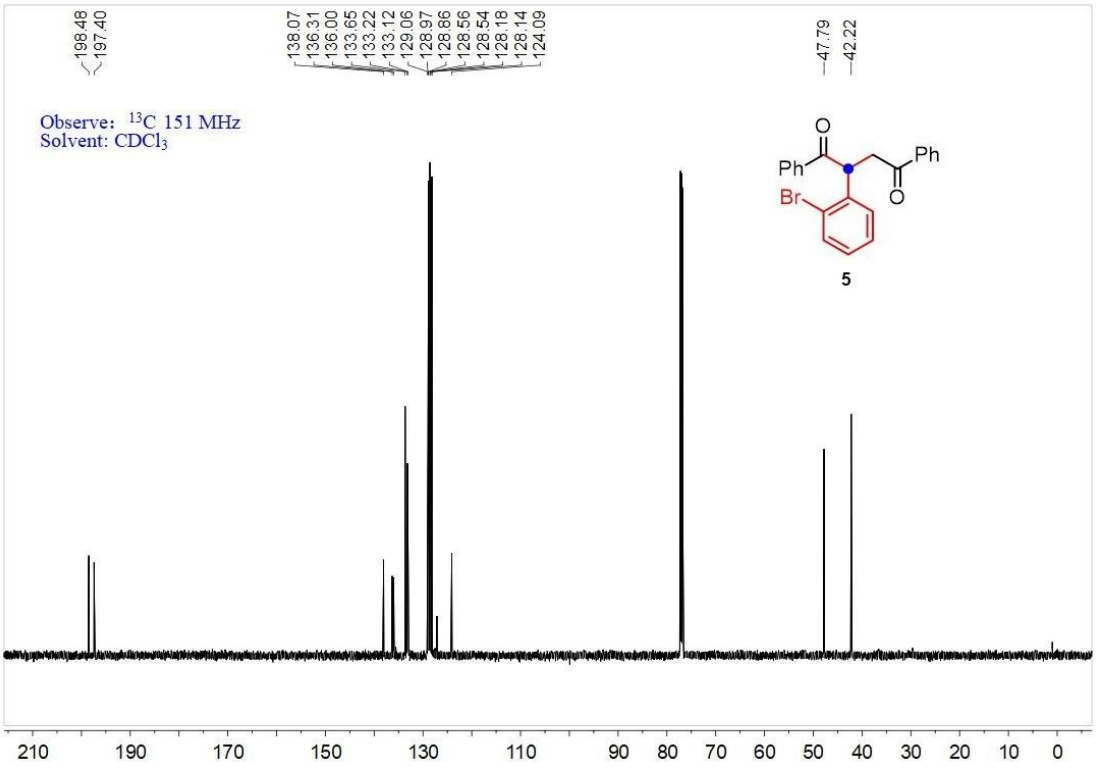

Figure S6. ^{13}C NMR spectrum of compound **5**, related to **Figure 2A.**

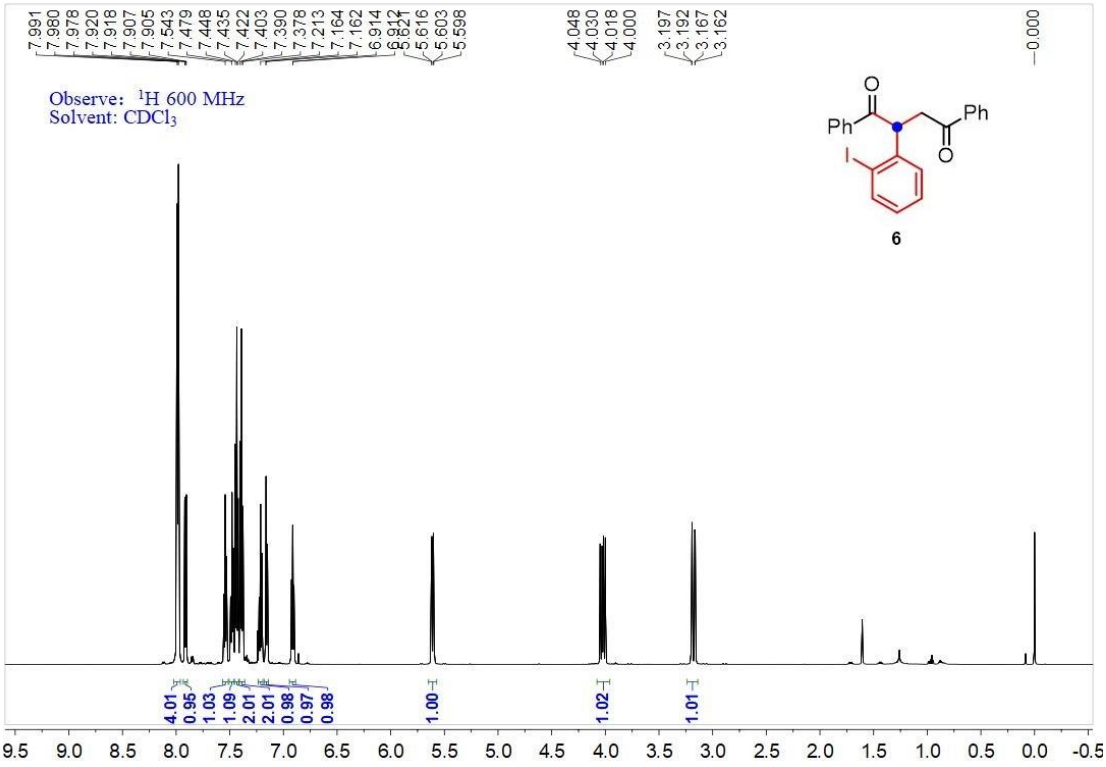

Figure S7. ^{1}H NMR spectrum of compound **6**, related to **Figure 2A.**

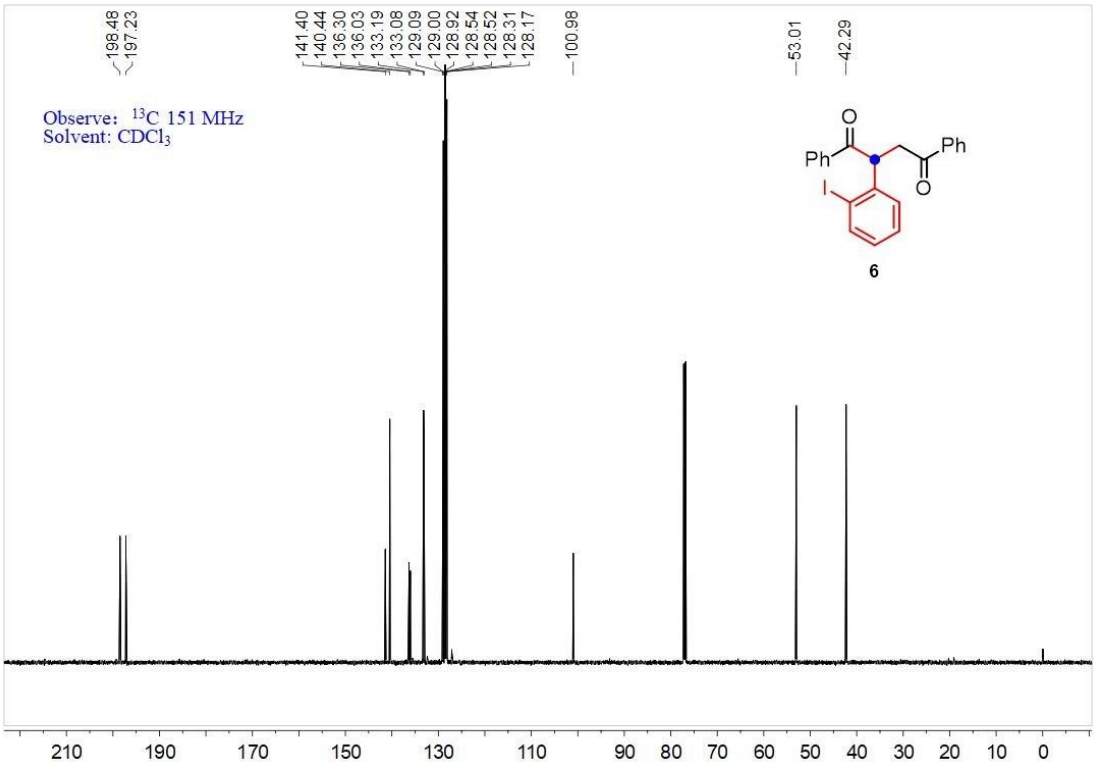

Figure S8. ^{13}C NMR spectrum of compound **6**, related to **Figure 2A.**

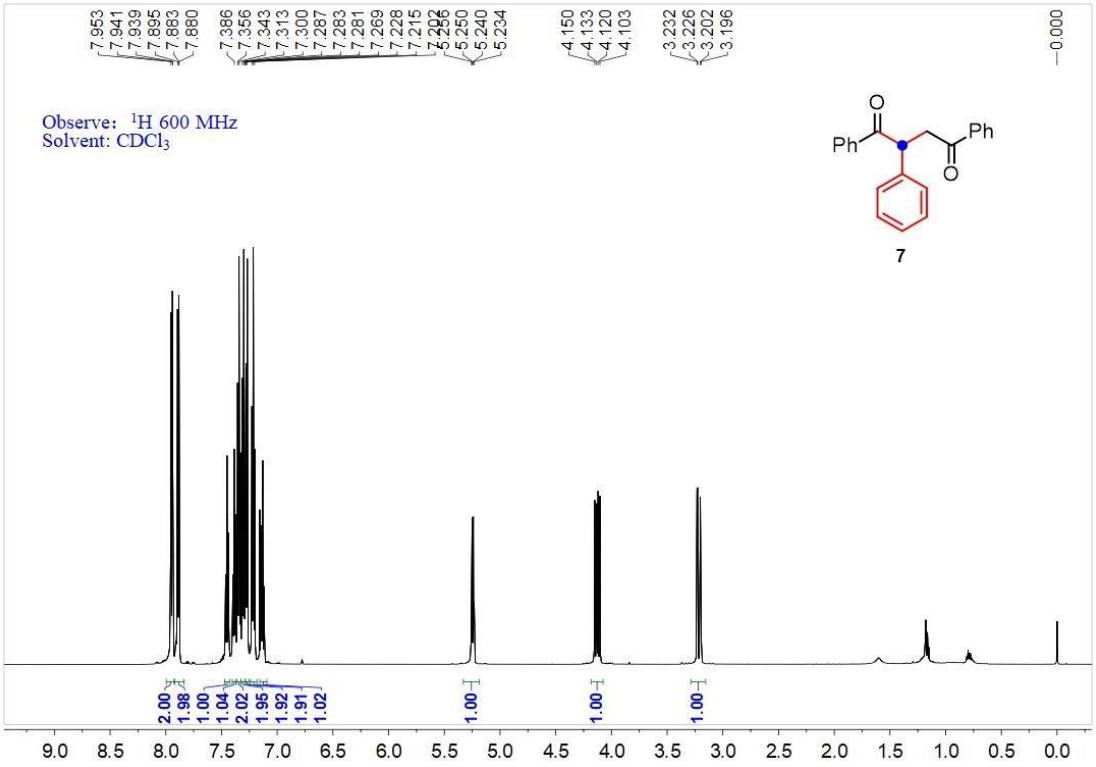

Figure S9. ^{1}H NMR spectrum of compound **7**, related to **Figure 2A.**

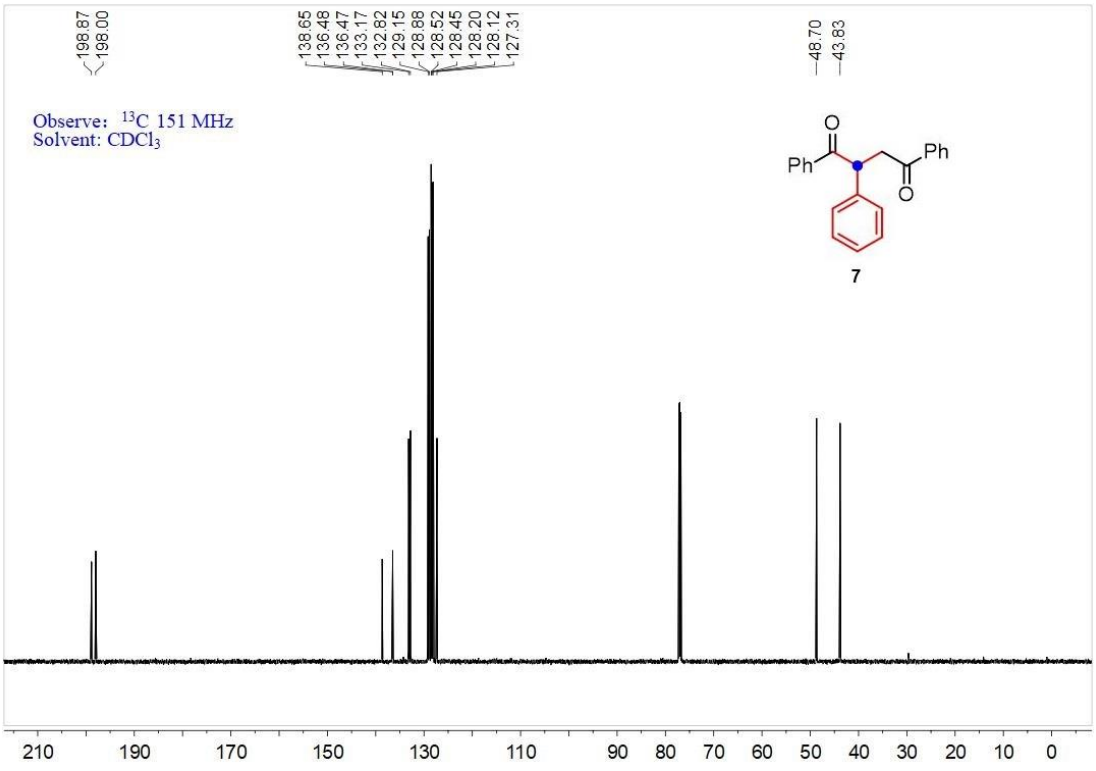

Figure S10. ^{13}C NMR spectrum of compound **7**, related to **Figure 2A.**

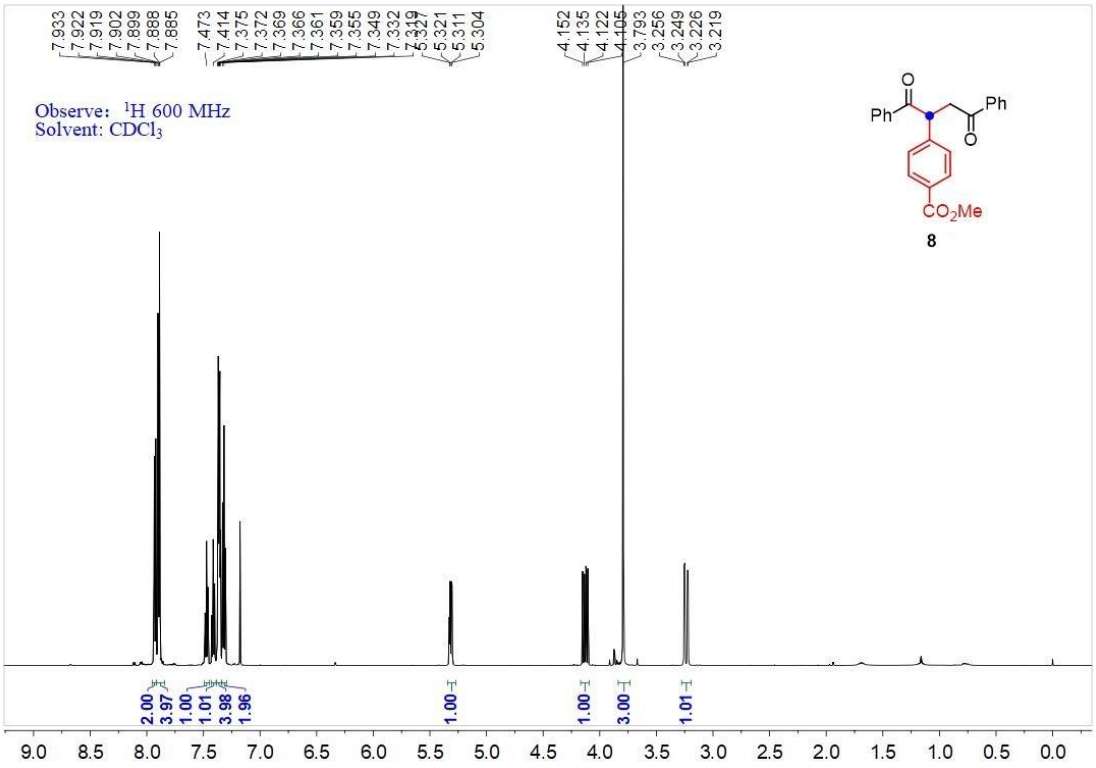

Figure S11. ^{1}H NMR spectrum of compound **8**, related to **Figure 2A.**

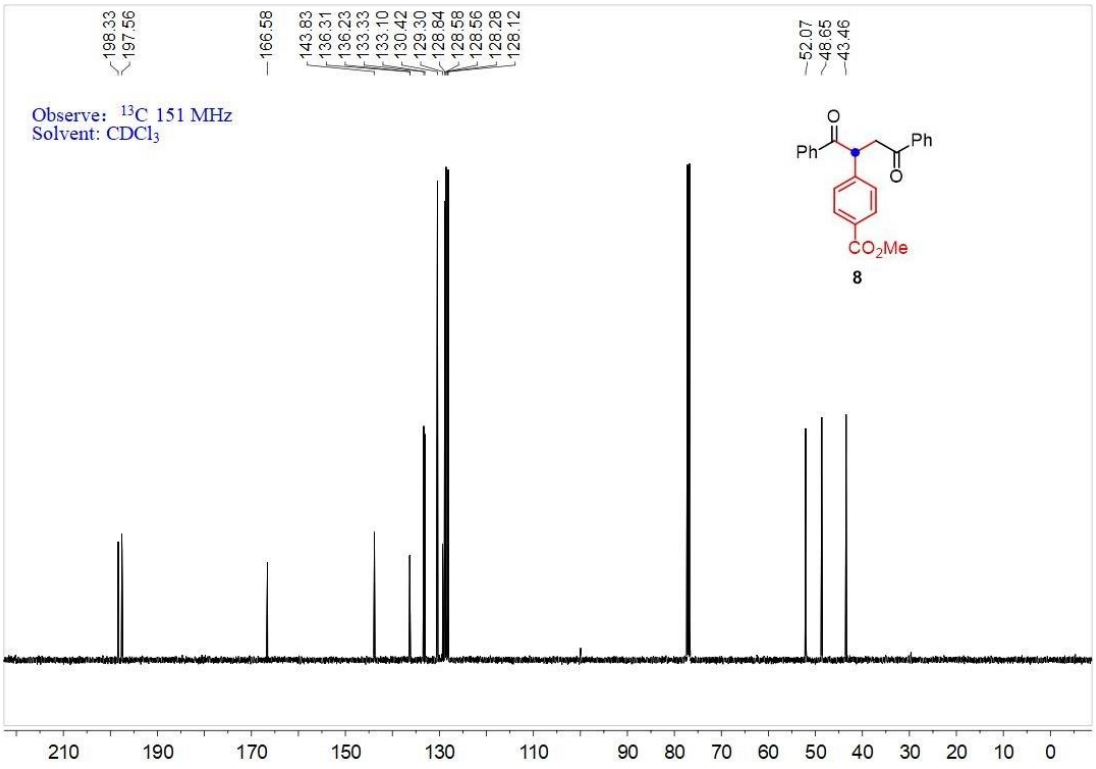

Figure S12. ^{13}C NMR spectrum of compound **8**, related to **Figure 2A.**

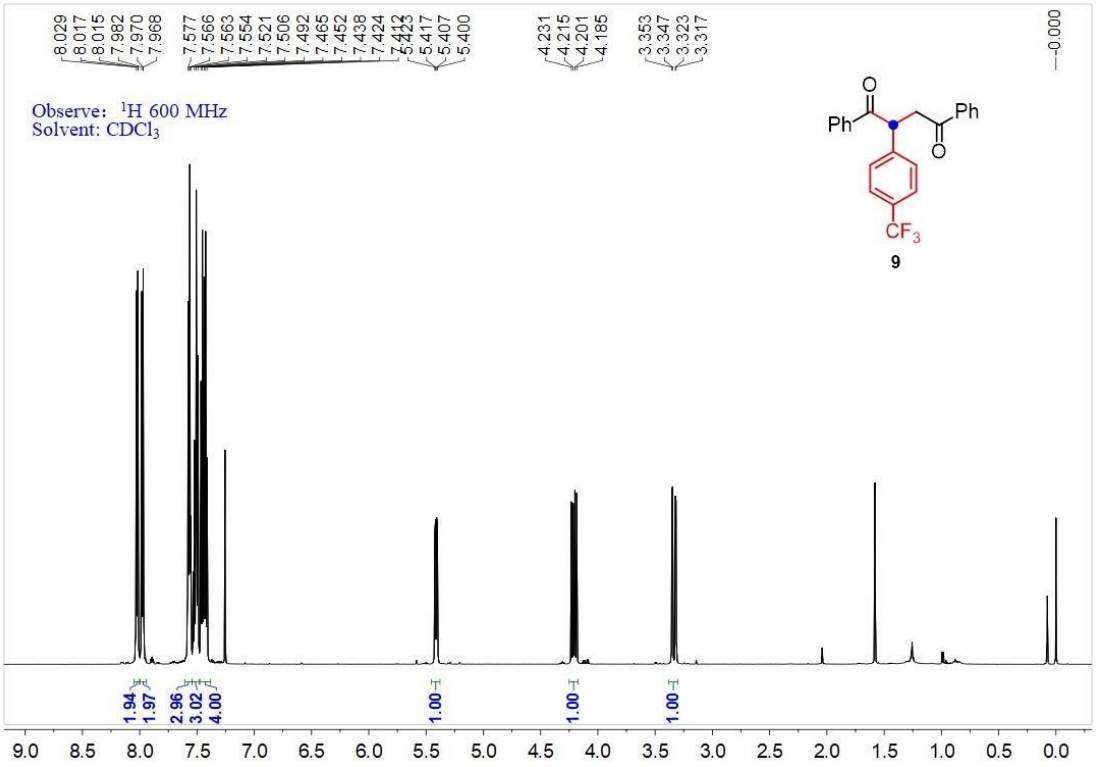

Figure S13. ^{1}H NMR spectrum of compound **9**, related to **Figure 2A.**

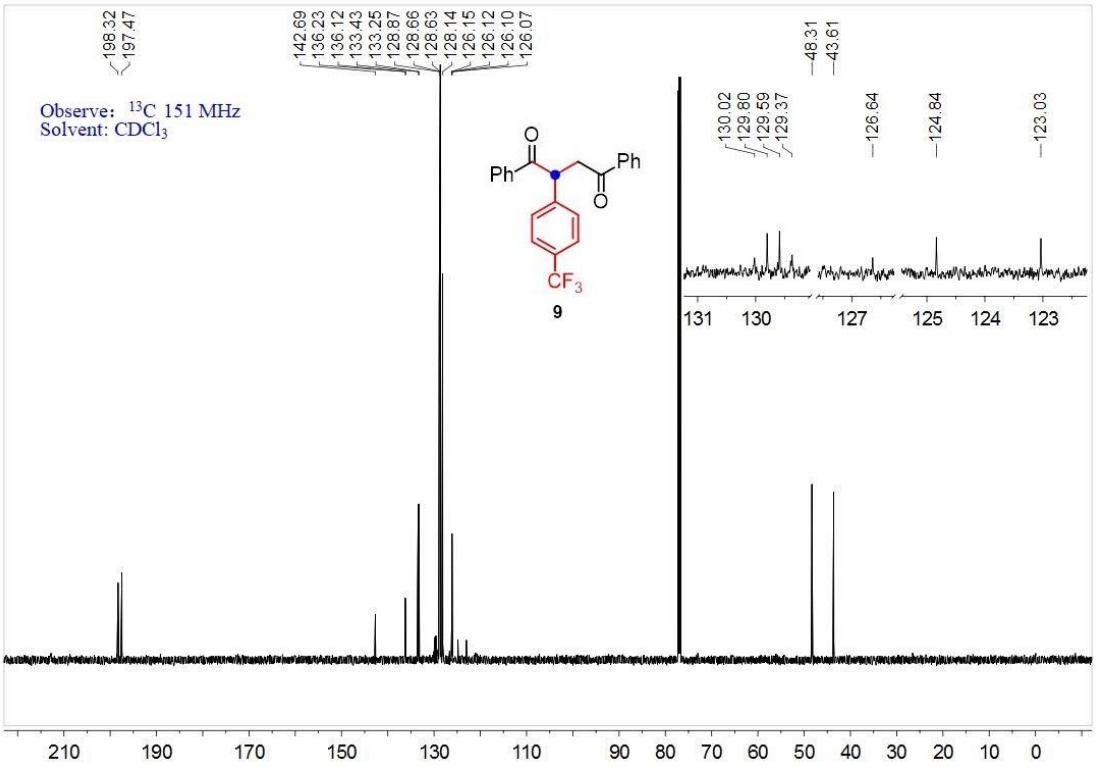

Figure S14. ^{13}C NMR spectrum of compound **9**, related to **Figure 2A.**

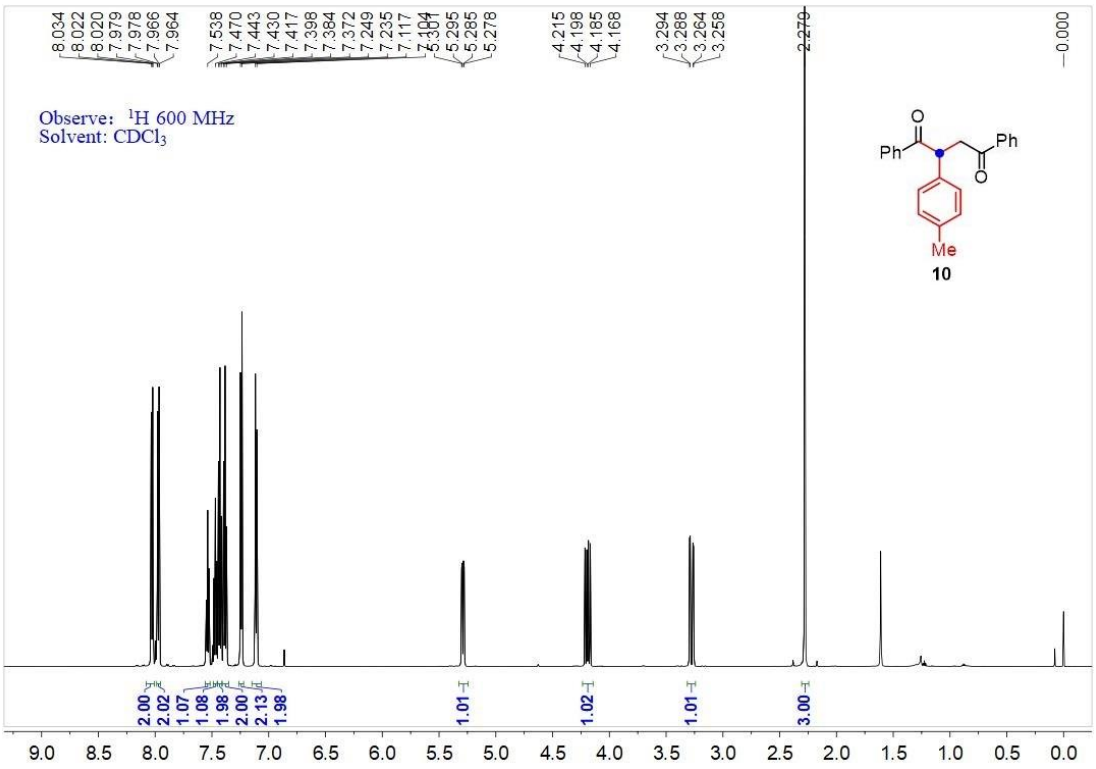

Figure S15. ^{1}H NMR spectrum of compound **10**, related to **Figure 2A.**

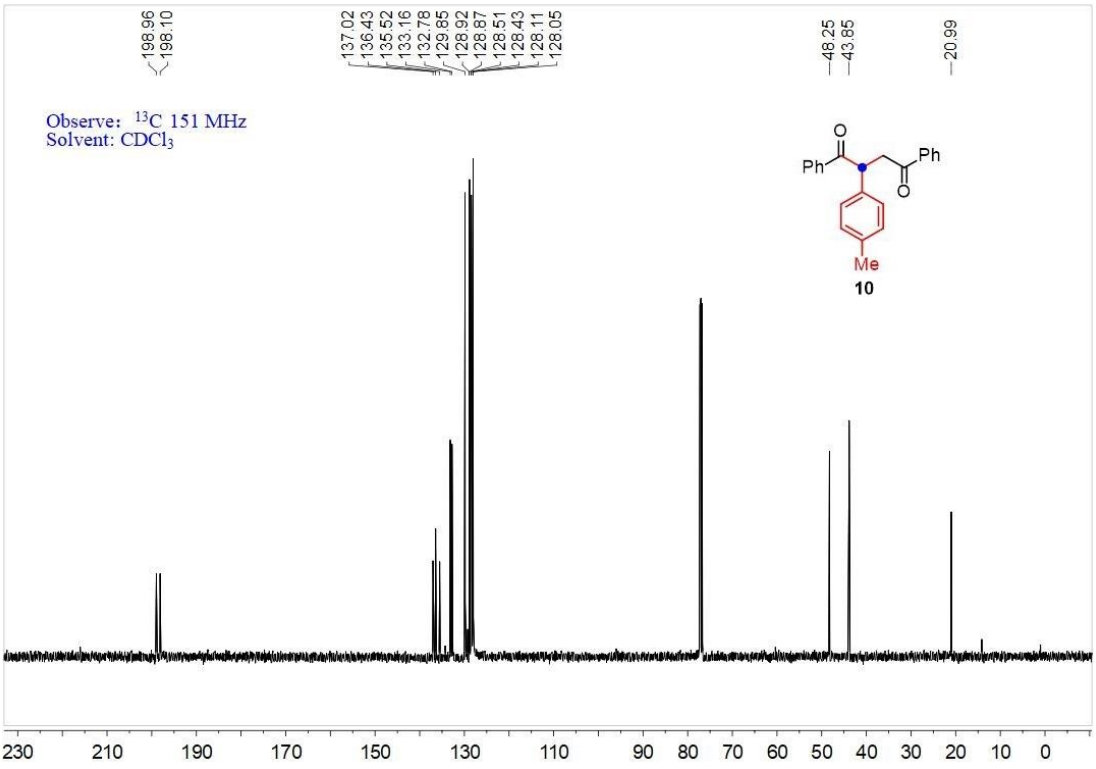

Figure S16. ^{13}C NMR spectrum of compound **10**, related to **Figure 2A.**

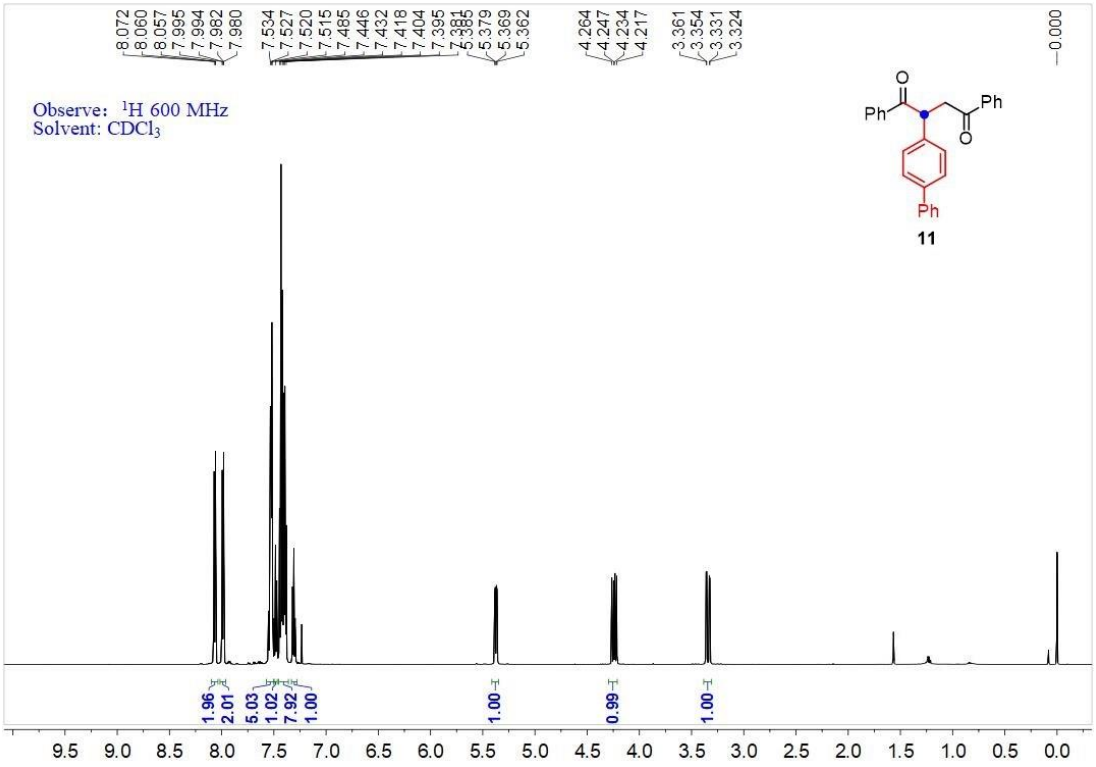

Figure S17. ^{1}H NMR spectrum of compound **11**, related to **Figure 2A.**

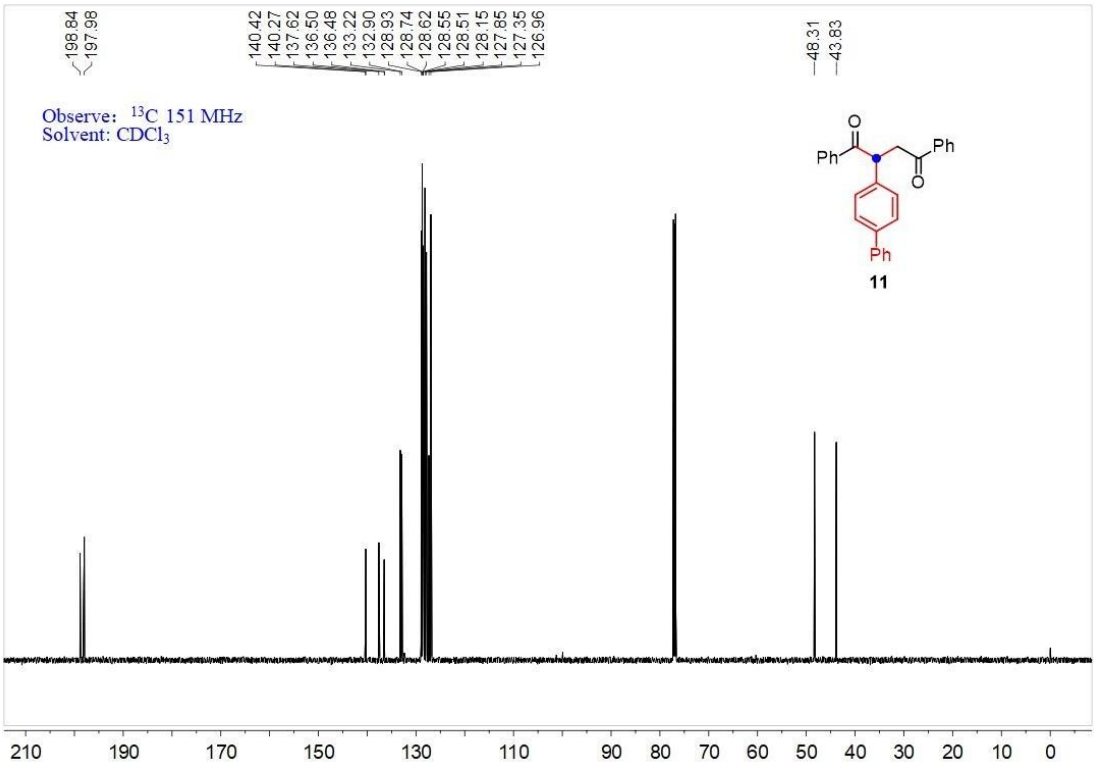

Figure S18. ^{13}C NMR spectrum of compound **11**, related to **Figure 2A.**

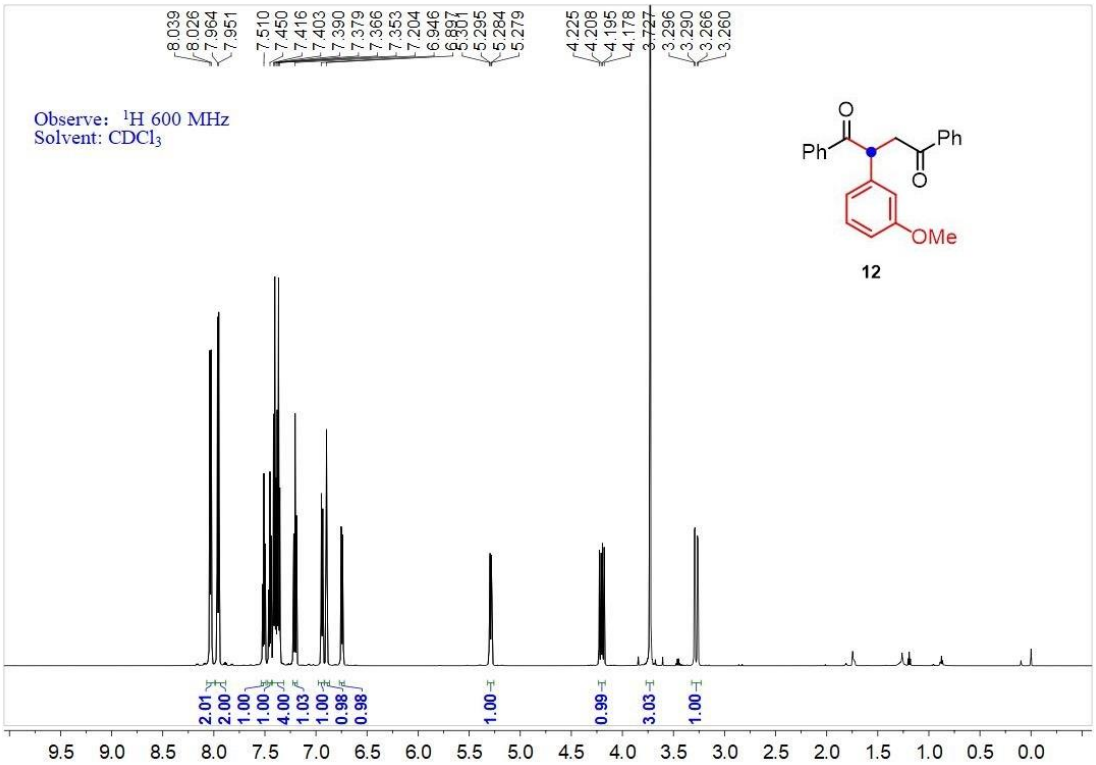

Figure S19. ^{1}H NMR spectrum of compound **12**, related to **Figure 2A.**

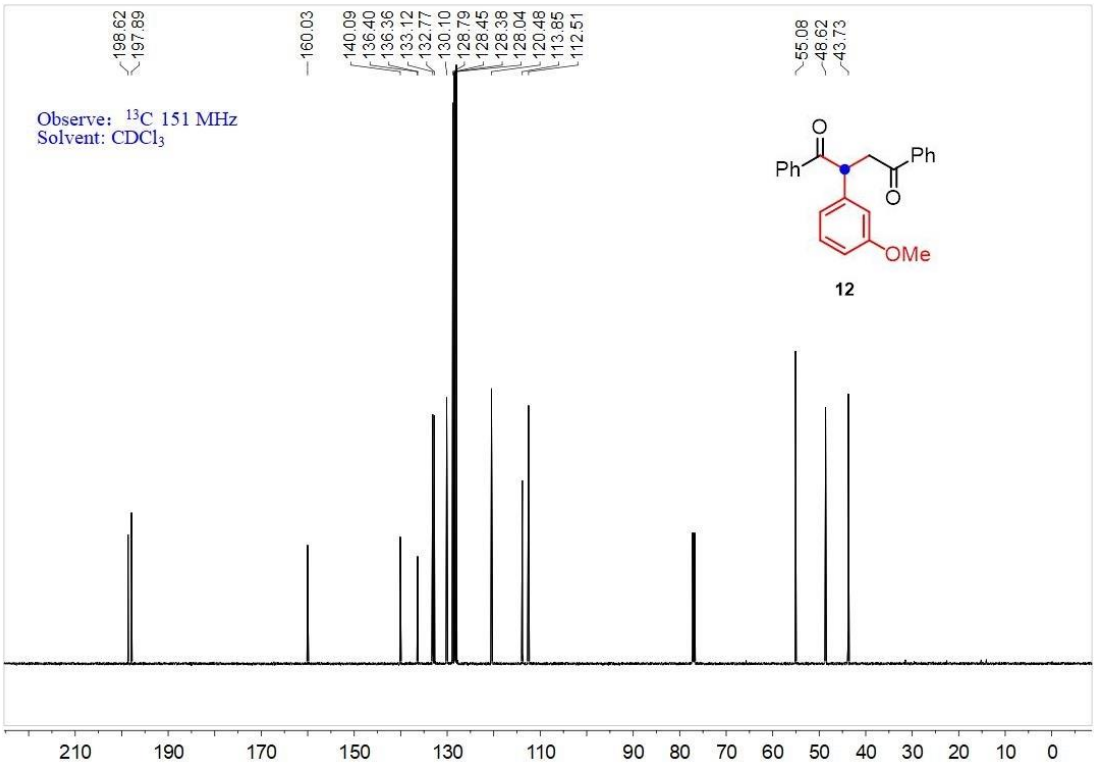

Figure S20. ^{13}C NMR spectrum of compound **12**, related to **Figure 2A.**

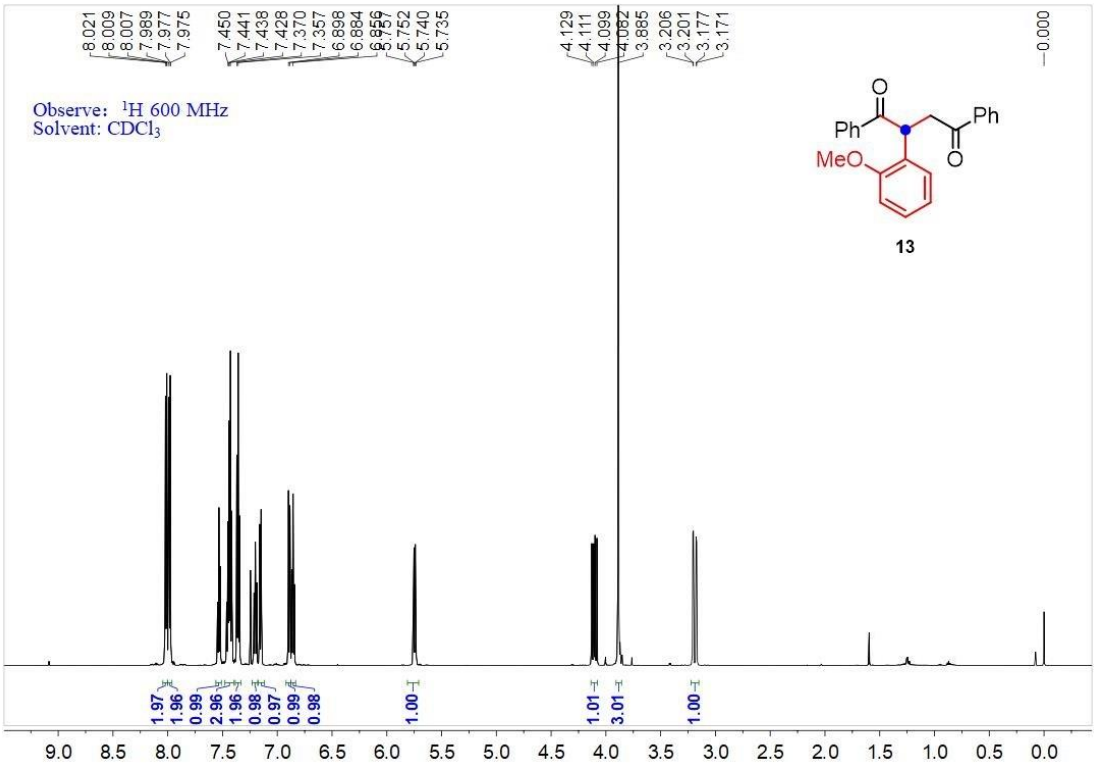

Figure S21. ^{1}H NMR spectrum of compound **13**, related to **Figure 2A.**

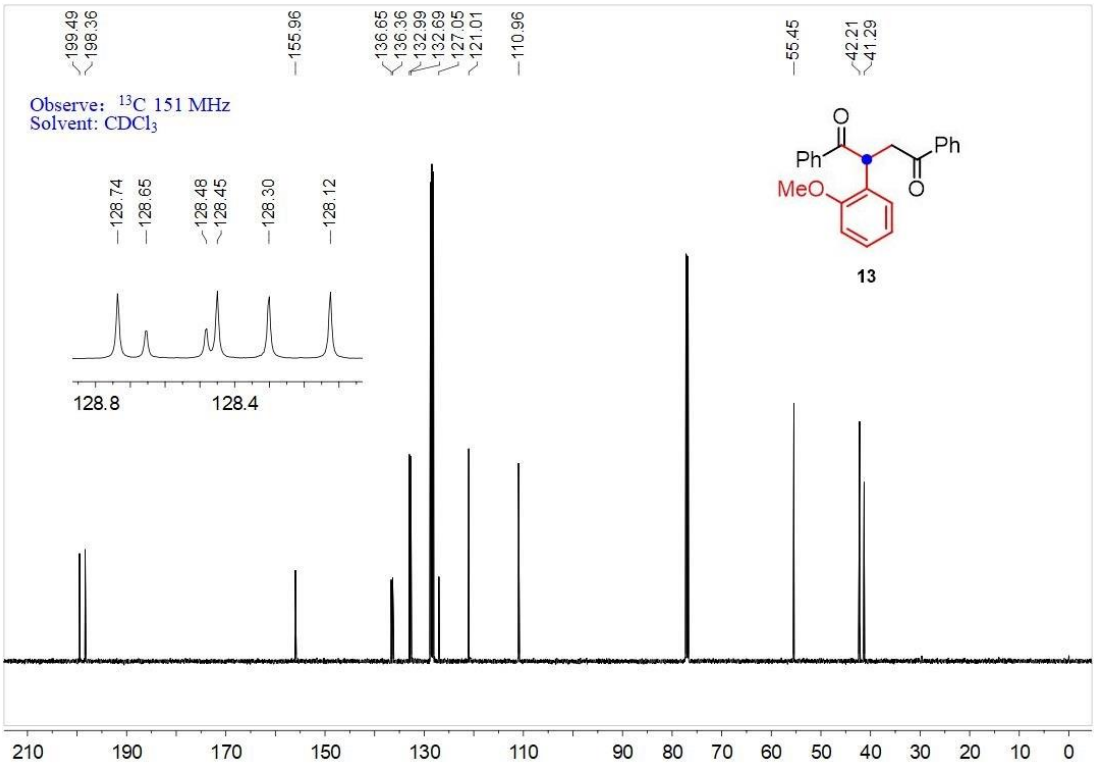

Figure S22. ^{13}C NMR spectrum of compound **13**, related to **Figure 2A.**

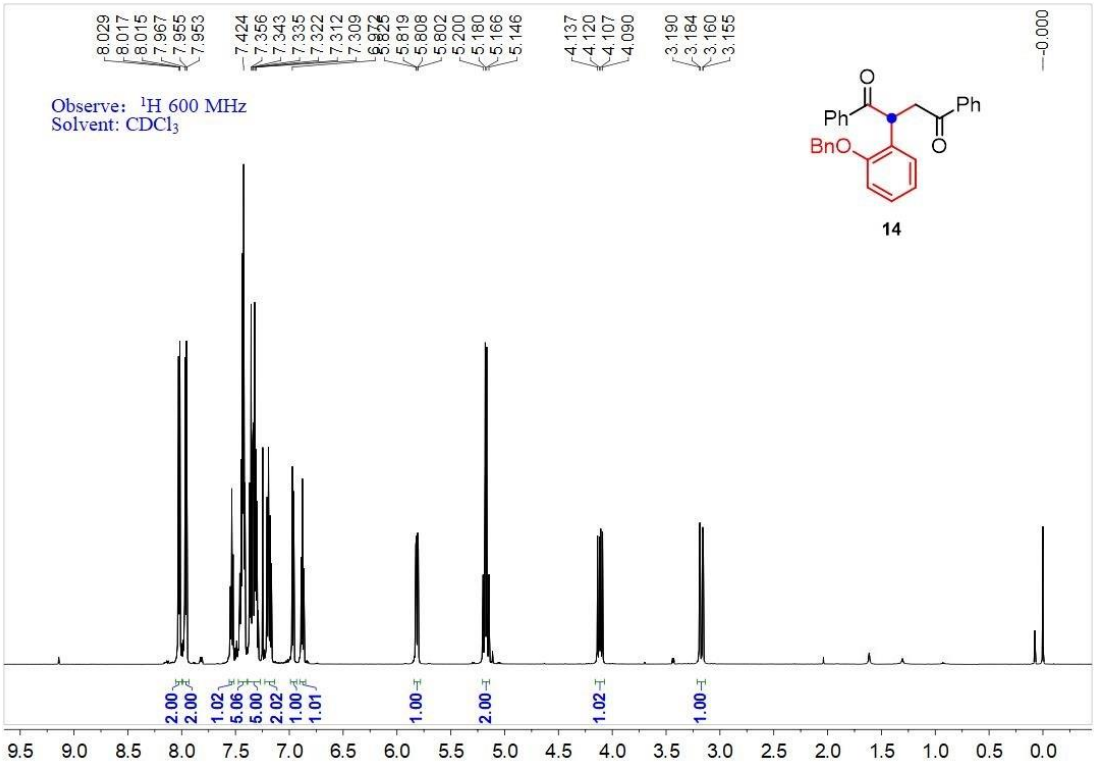

Figure S23. ^{1}H NMR spectrum of compound **14**, related to **Figure 2A.**

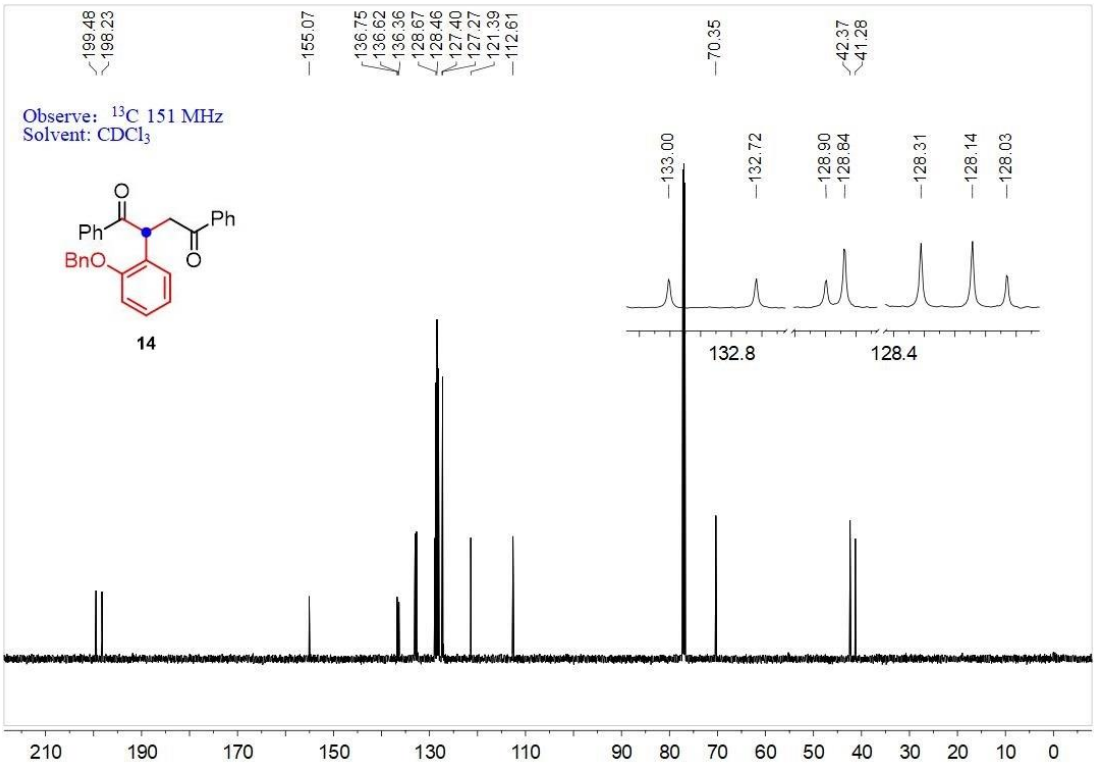

Figure S24. ^{13}C NMR spectrum of compound **14**, related to **Figure 2A.**

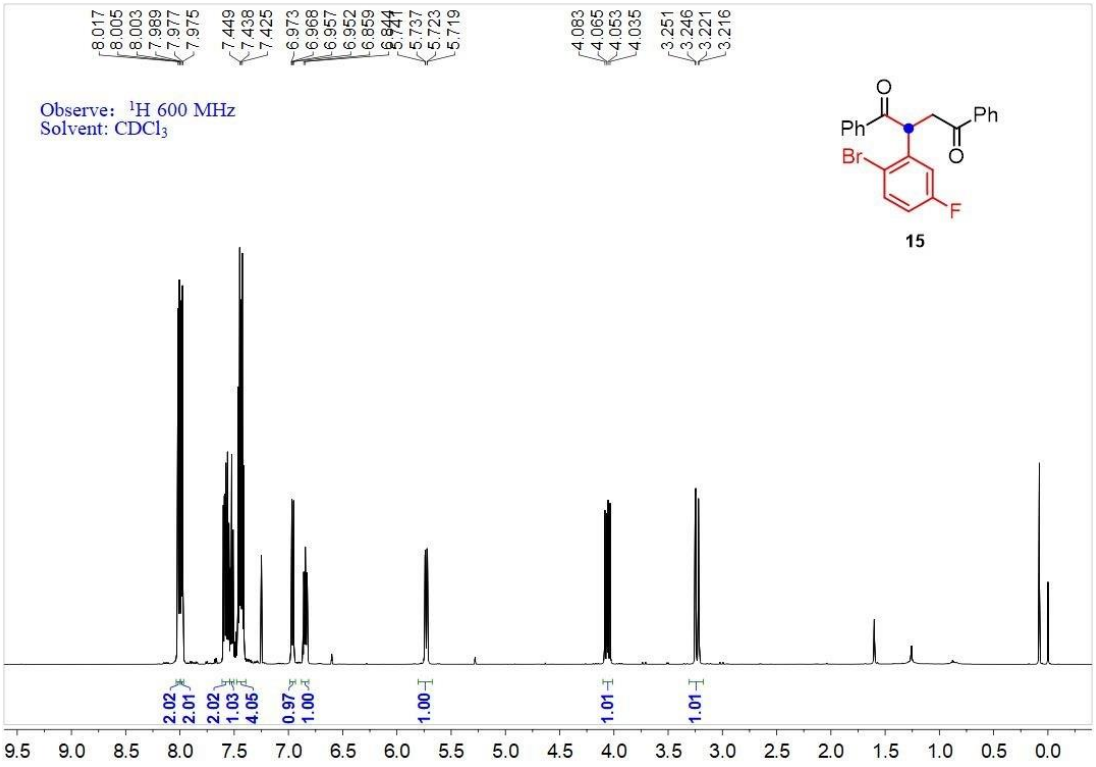

Figure S25. ^{1}H NMR spectrum of compound **15**, related to **Figure 2A.**

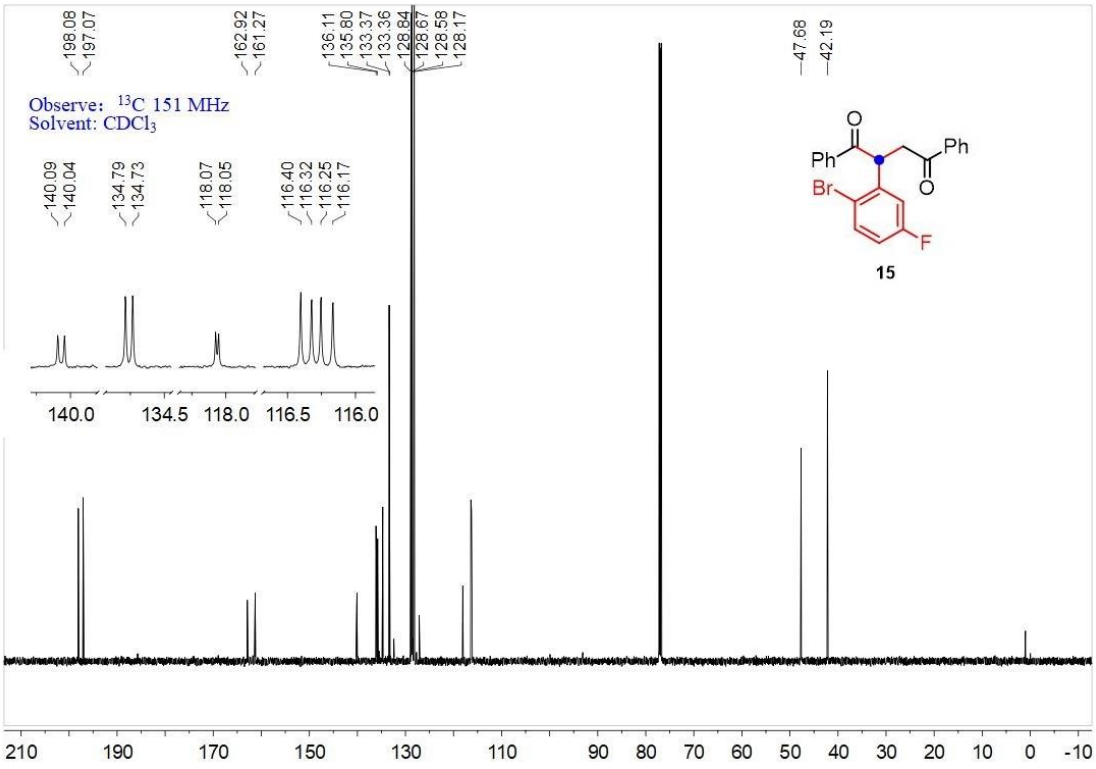

Figure S26. ^{13}C NMR spectrum of compound **15**, related to **Figure 2A.**

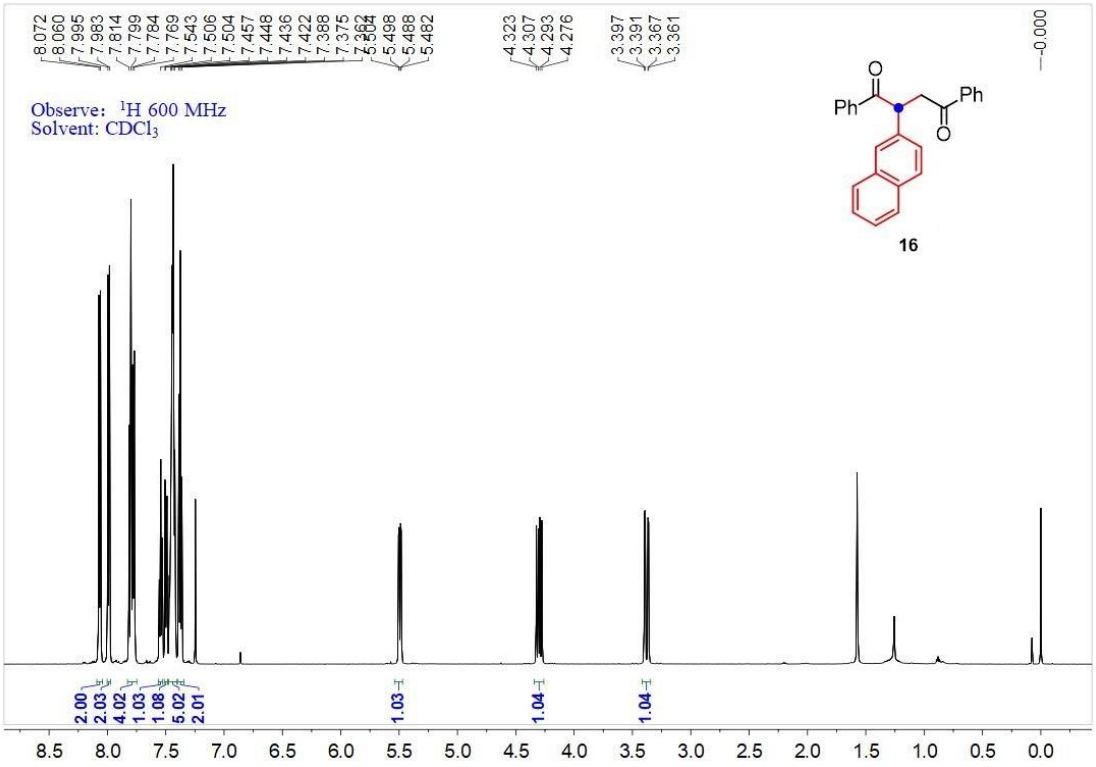

Figure S27. ^{1}H NMR spectrum of compound **16**, related to **Figure 2A.**

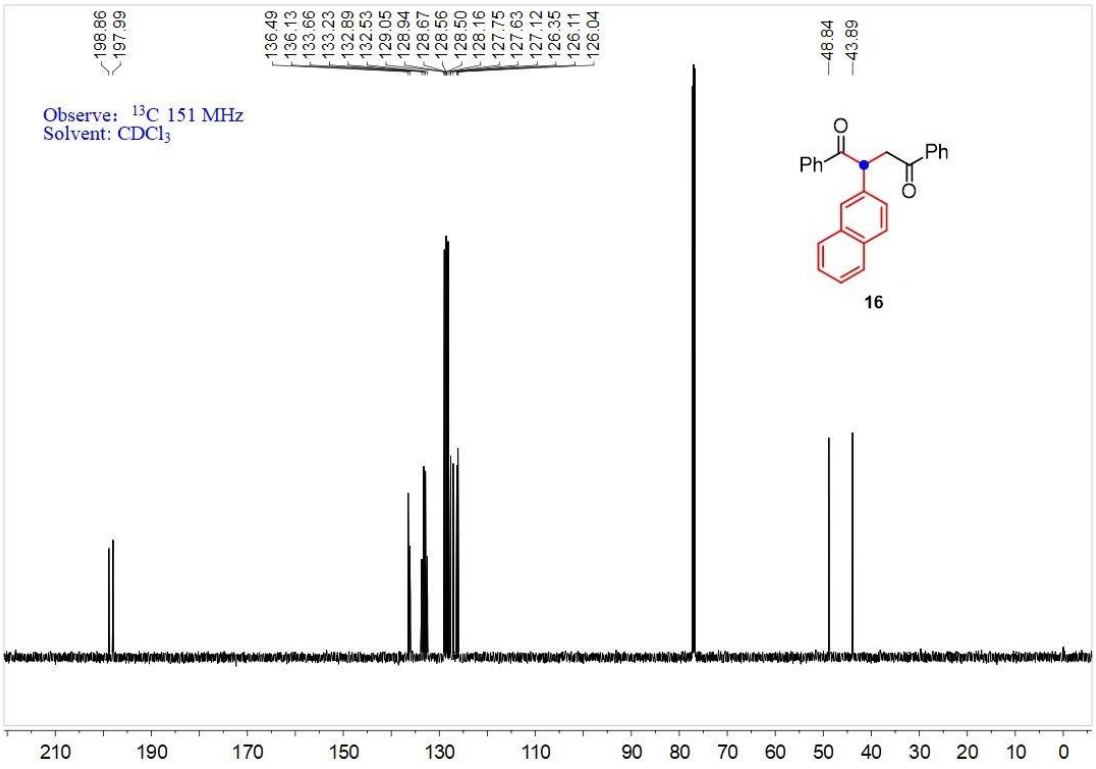

Figure S28. ^{13}C NMR spectrum of compound **16**, related to **Figure 2A.**

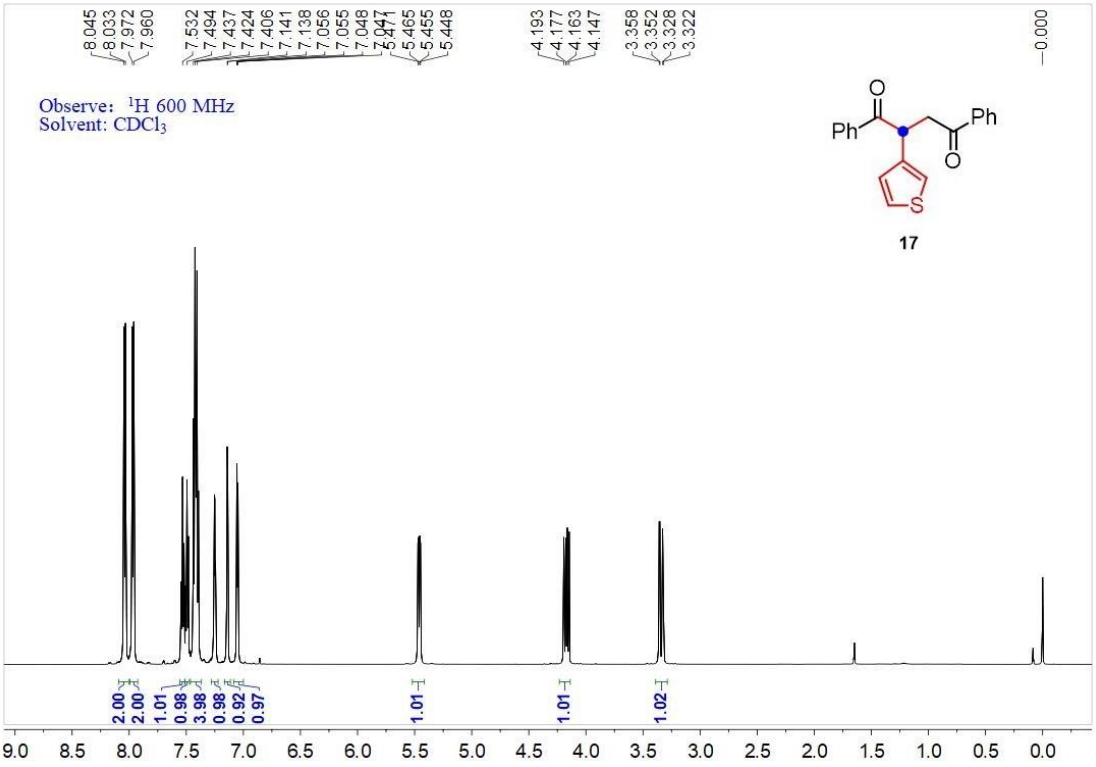

Figure S29. ^{1}H NMR spectrum of compound **17**, related to **Figure 2A.**

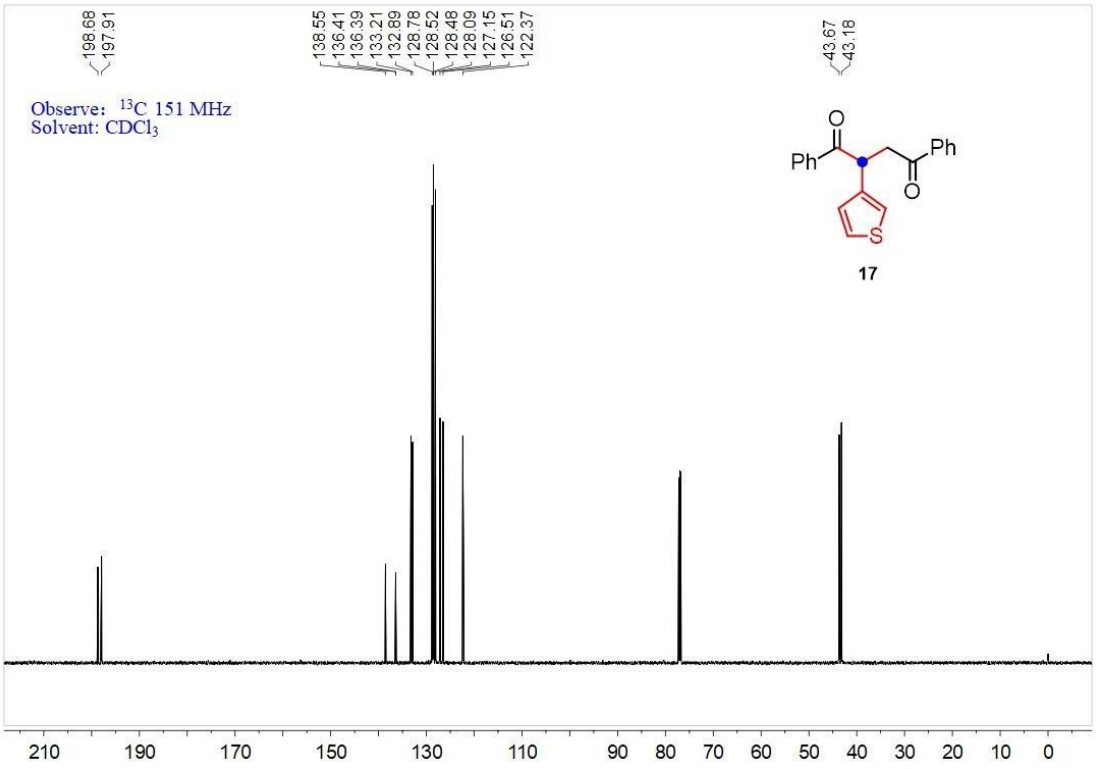

Figure S30. ^{13}C NMR spectrum of compound **17**, related to **Figure 2A.**

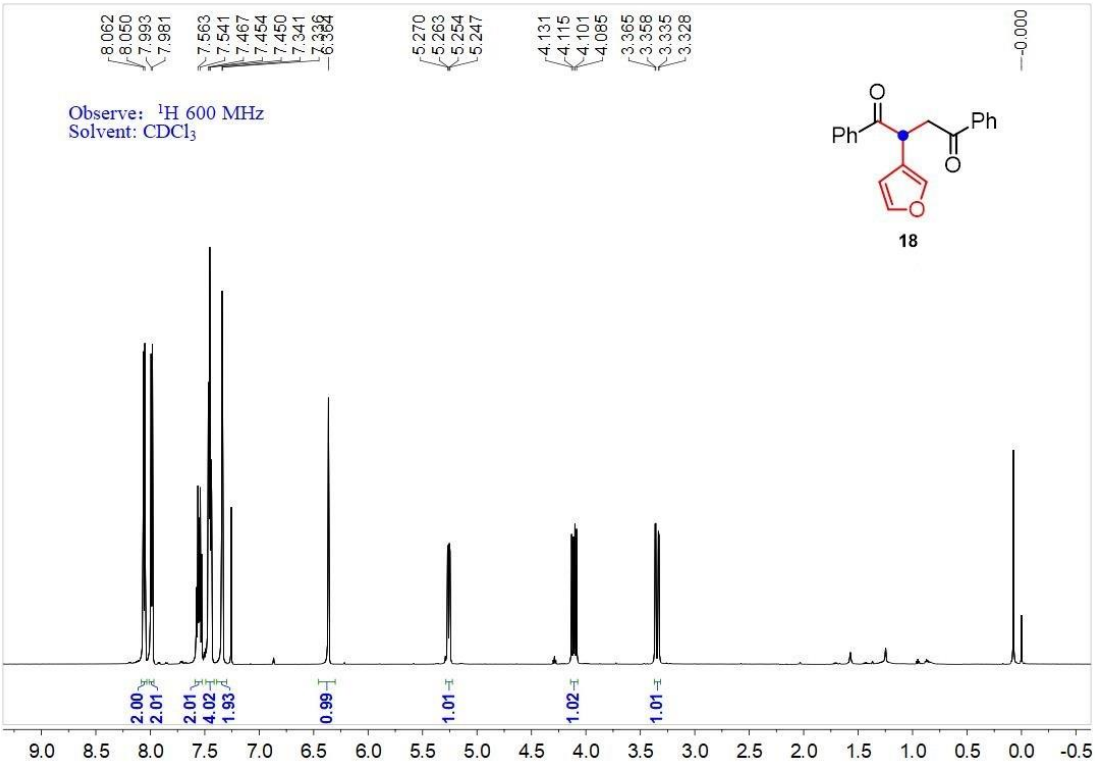

Figure S31. ^{1}H NMR spectrum of compound **18**, related to **Figure 2A.**

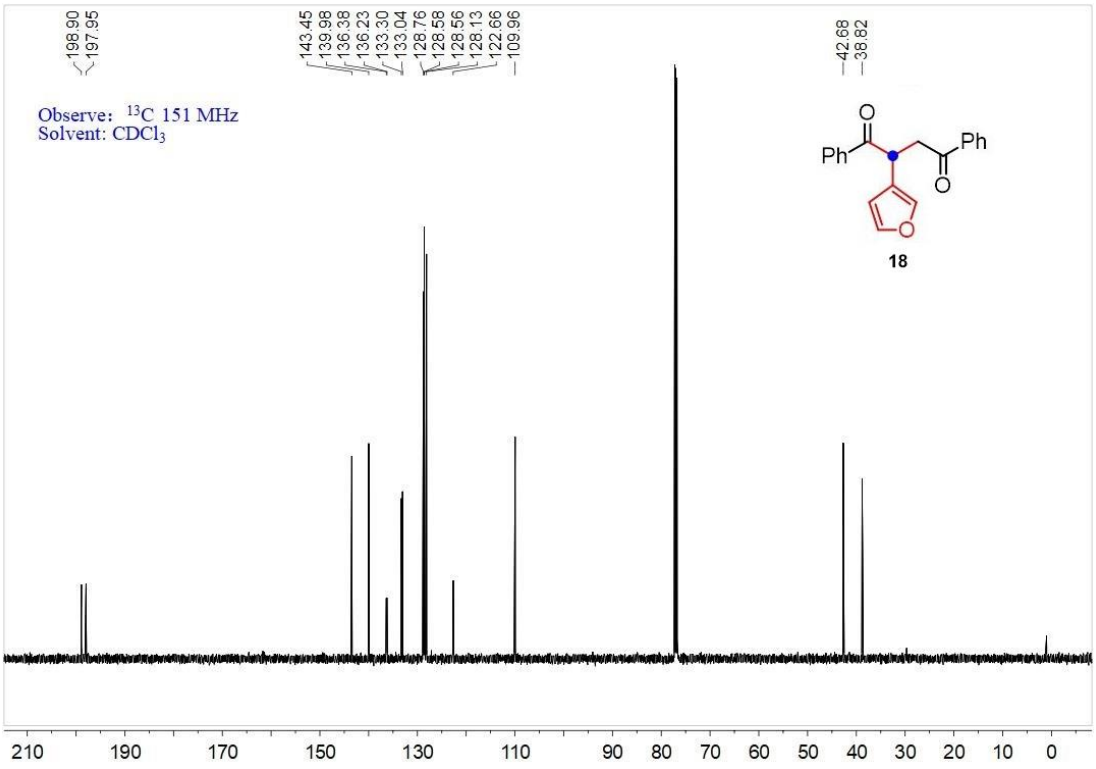

Figure S32. ^{13}C NMR spectrum of compound **18**, related to **Figure 2A.**

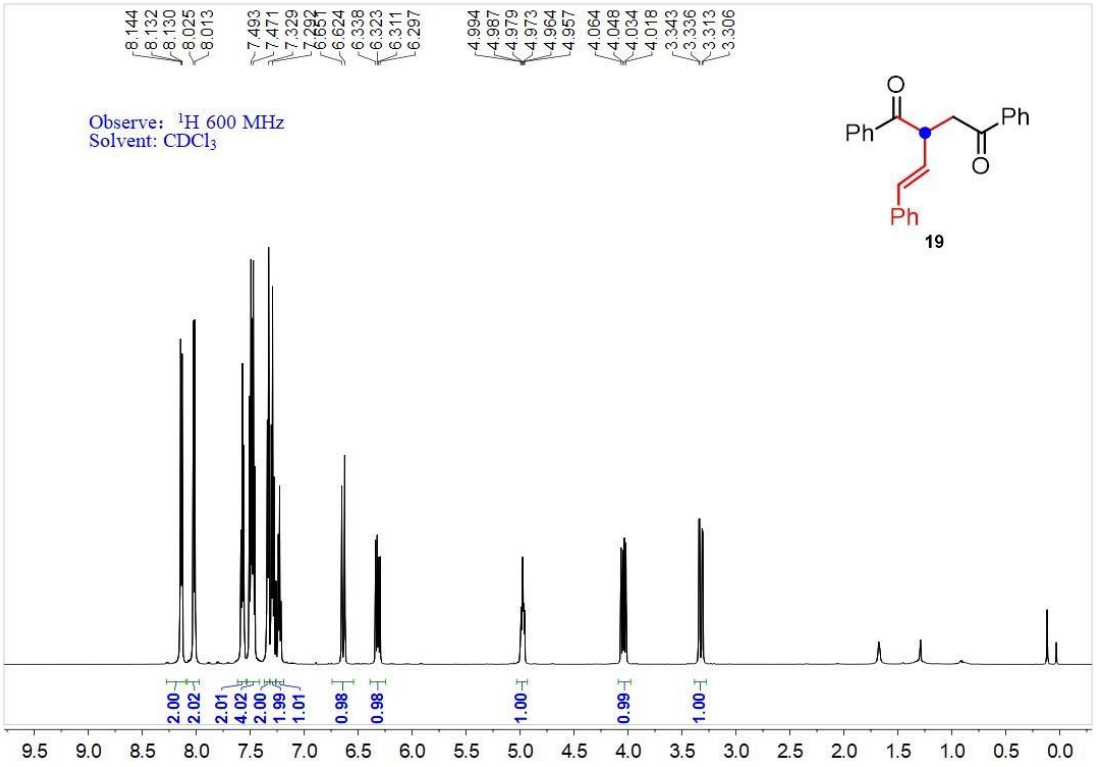

Figure S33. ^{1}H NMR spectrum of compound **19**, related to **Figure 2A.**

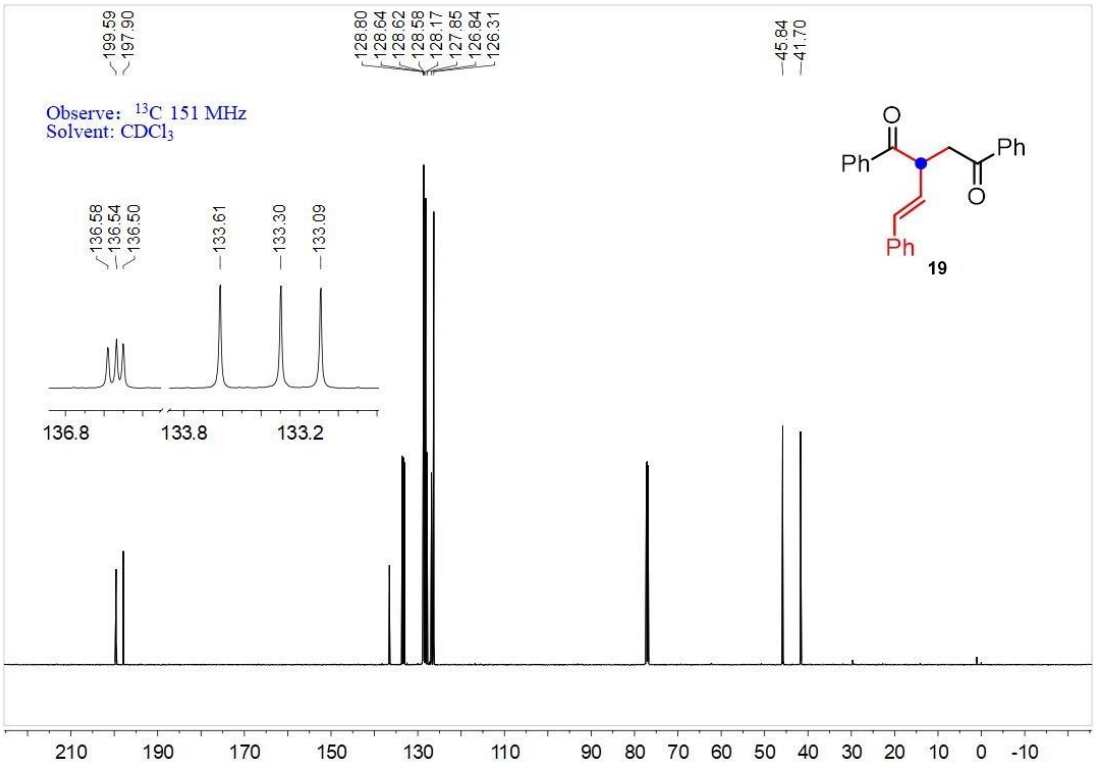

Figure S34. ^{13}C NMR spectrum of compound **19**, related to **Figure 2A.**

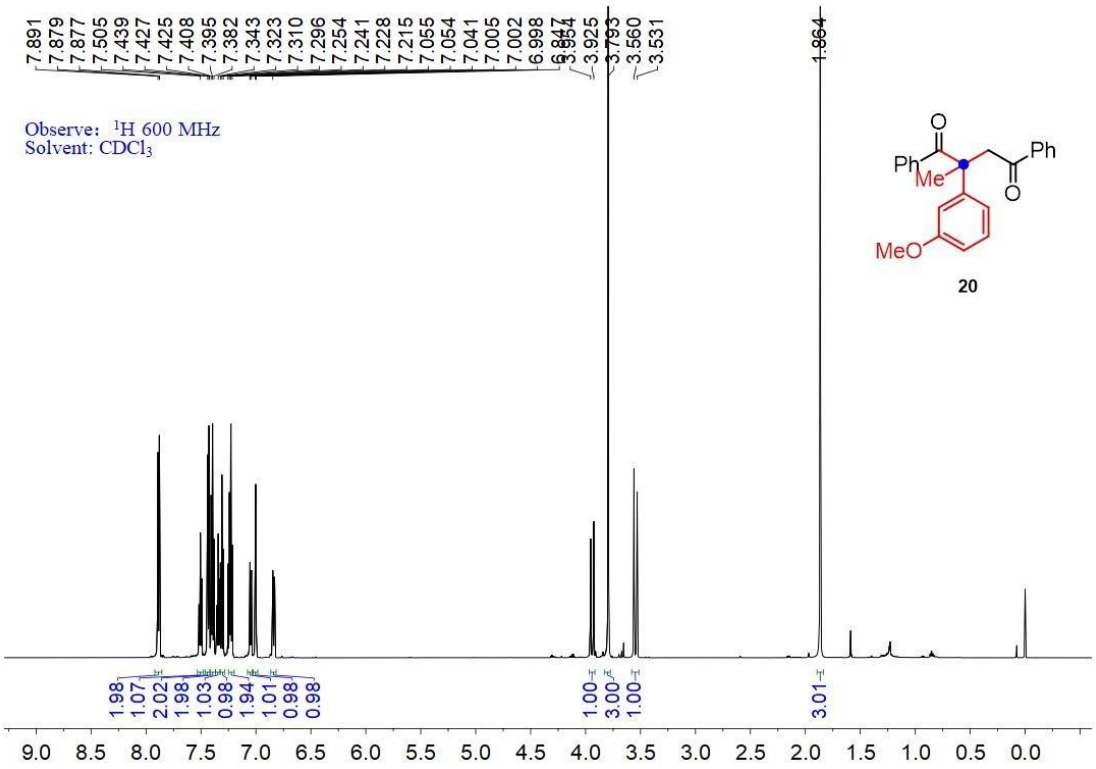

Figure S35. ^{1}H NMR spectrum of compound **20**, related to **Figure 2A.**

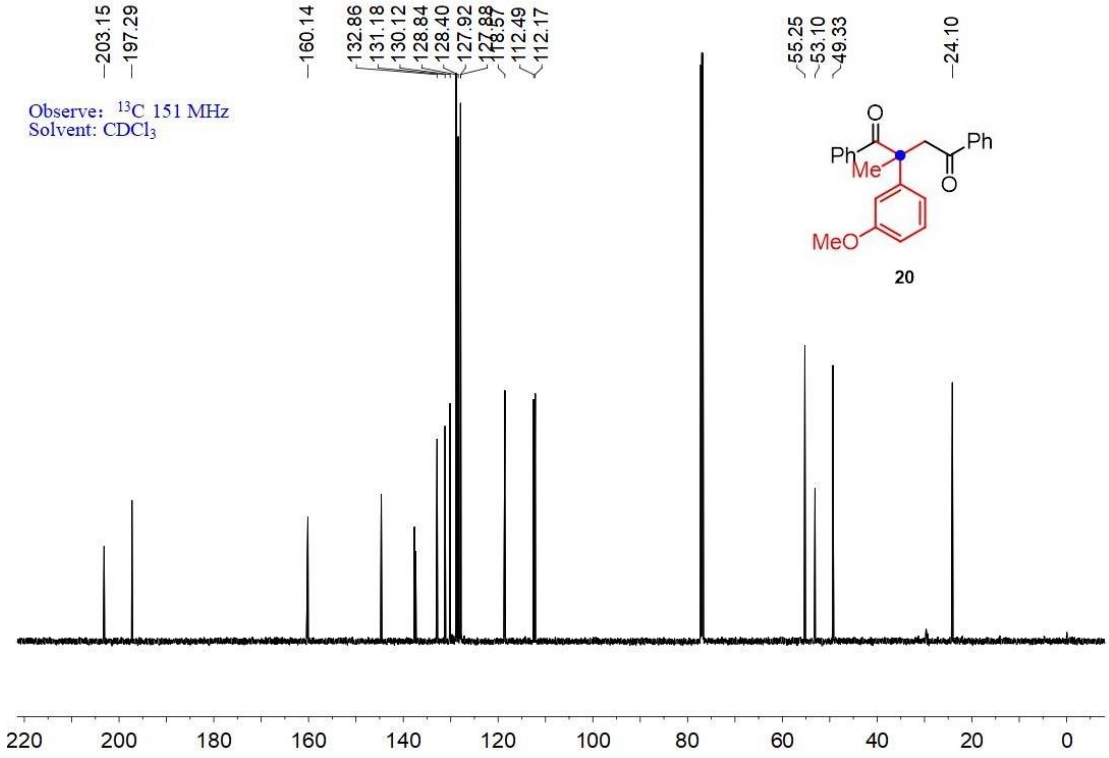

Figure S36. ^{13}C NMR spectrum of compound **20**, related to **Figure 2A.**

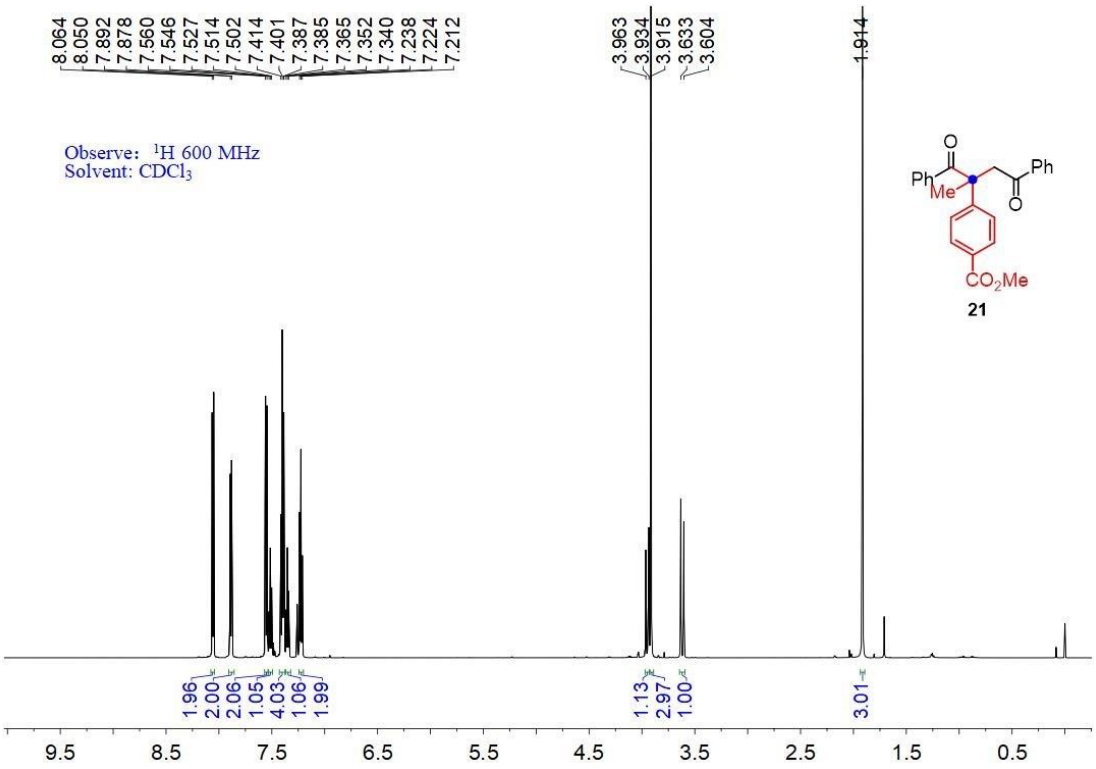

Figure S37. ^{1}H NMR spectrum of compound **21**, related to **Figure 2A.**

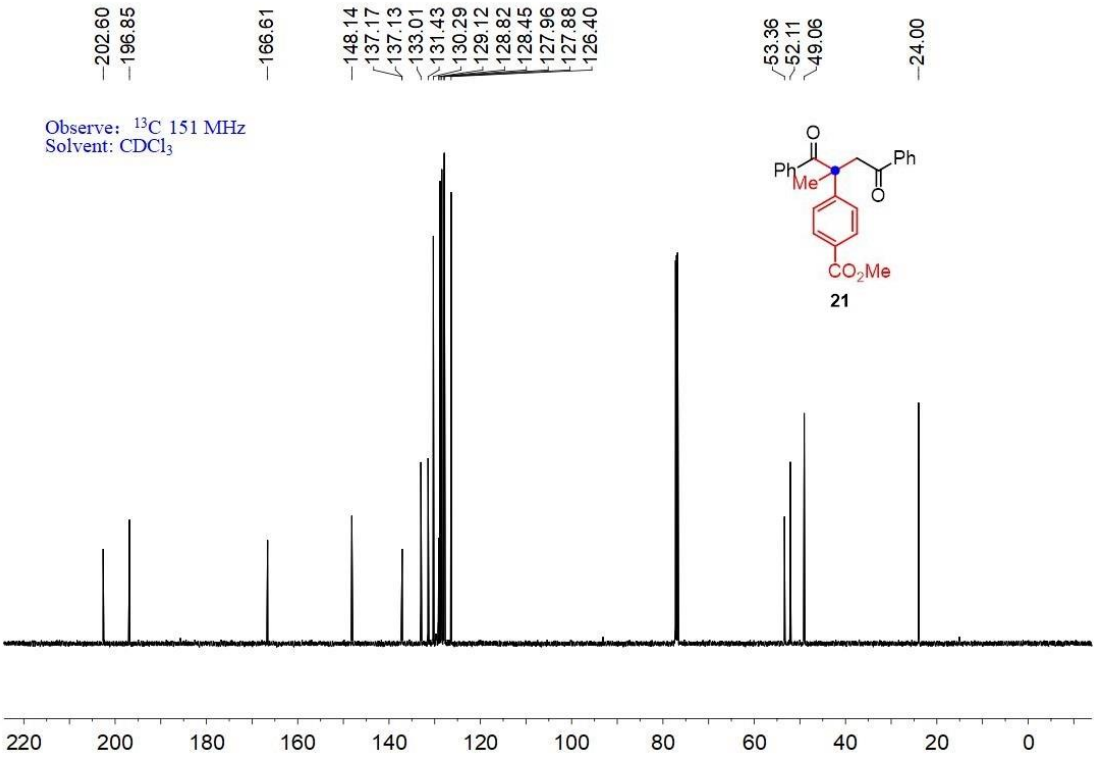

Figure S38. ^{13}C NMR spectrum of compound **21**, related to **Figure 2A.**

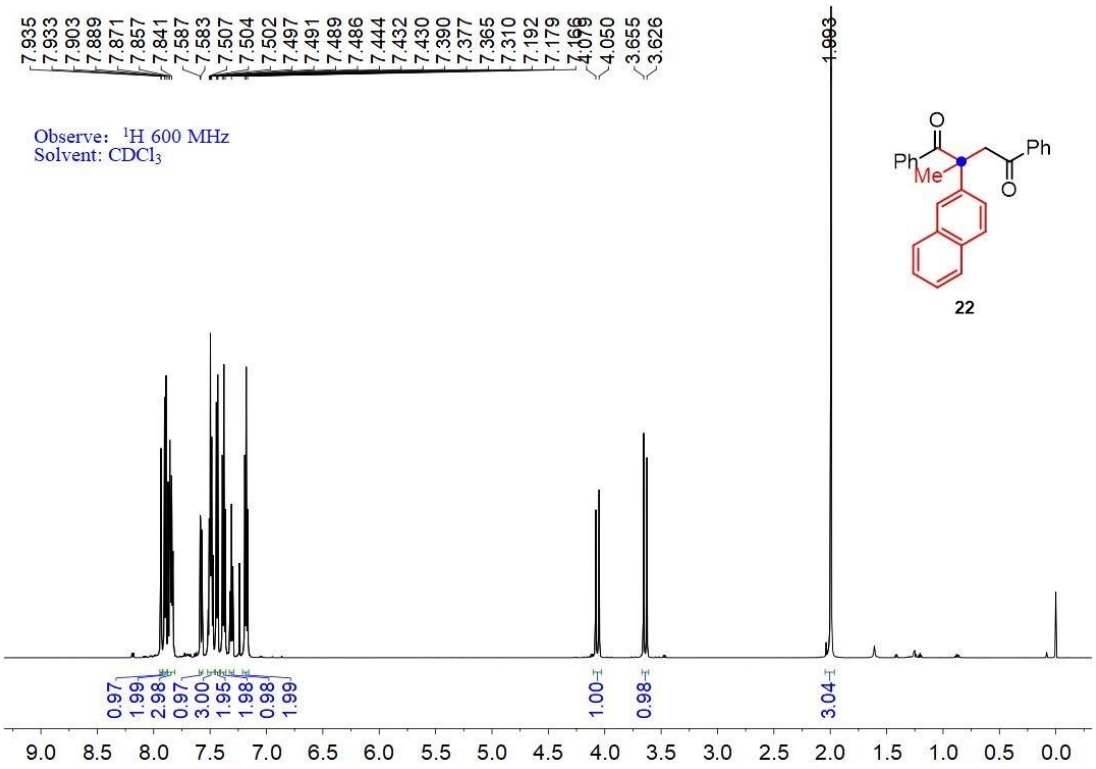

Figure S39. ^{1}H NMR spectrum of compound **22**, related to **Figure 2A.**

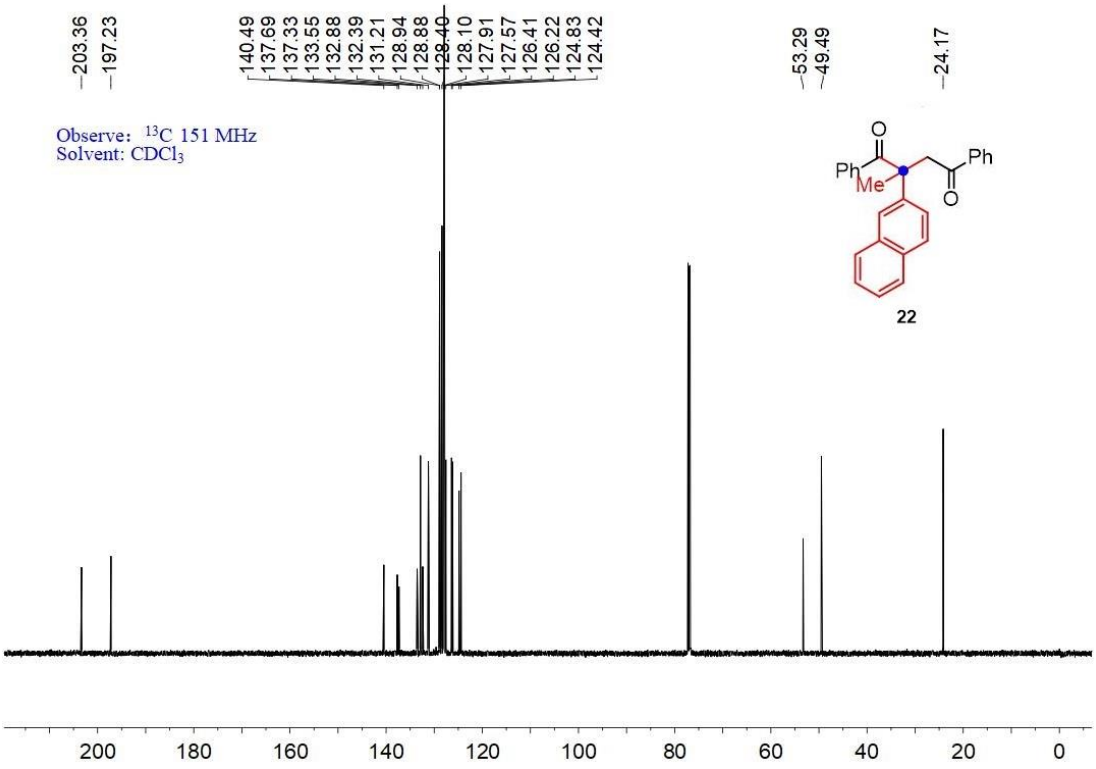

Figure S40. ^{13}C NMR spectrum of compound **22**, related to **Figure 2A.**

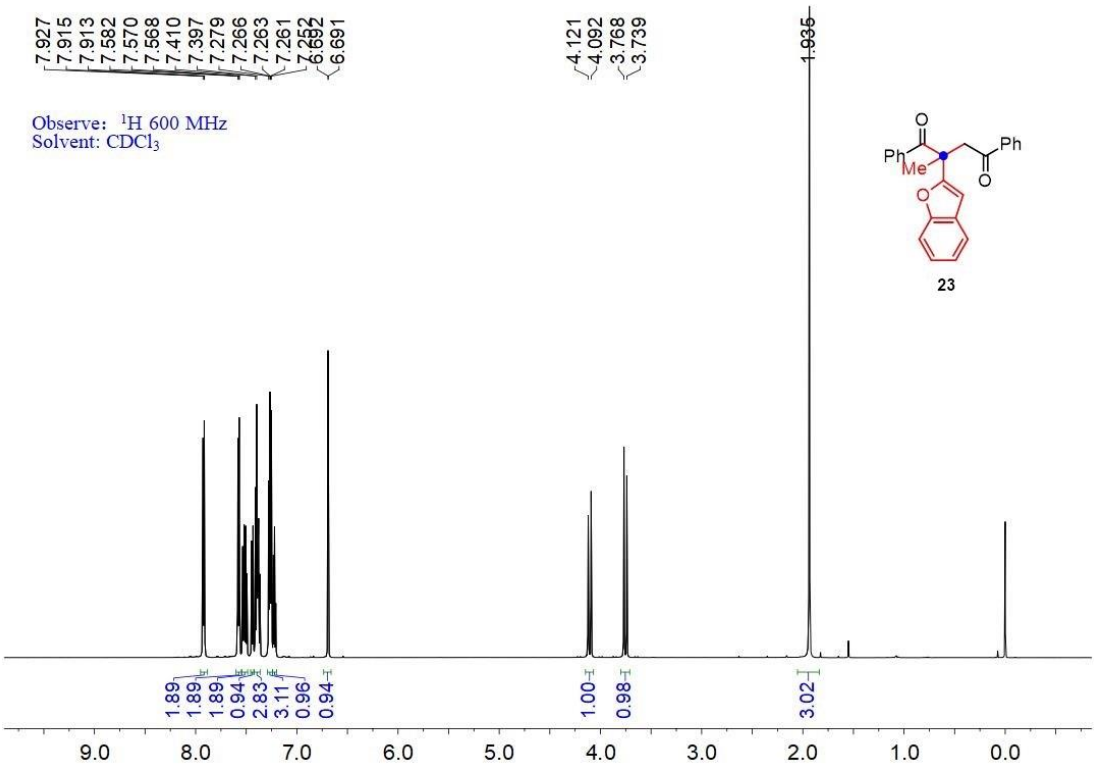

Figure S41. ^{1}H NMR spectrum of compound **23**, related to **Figure 2A.**

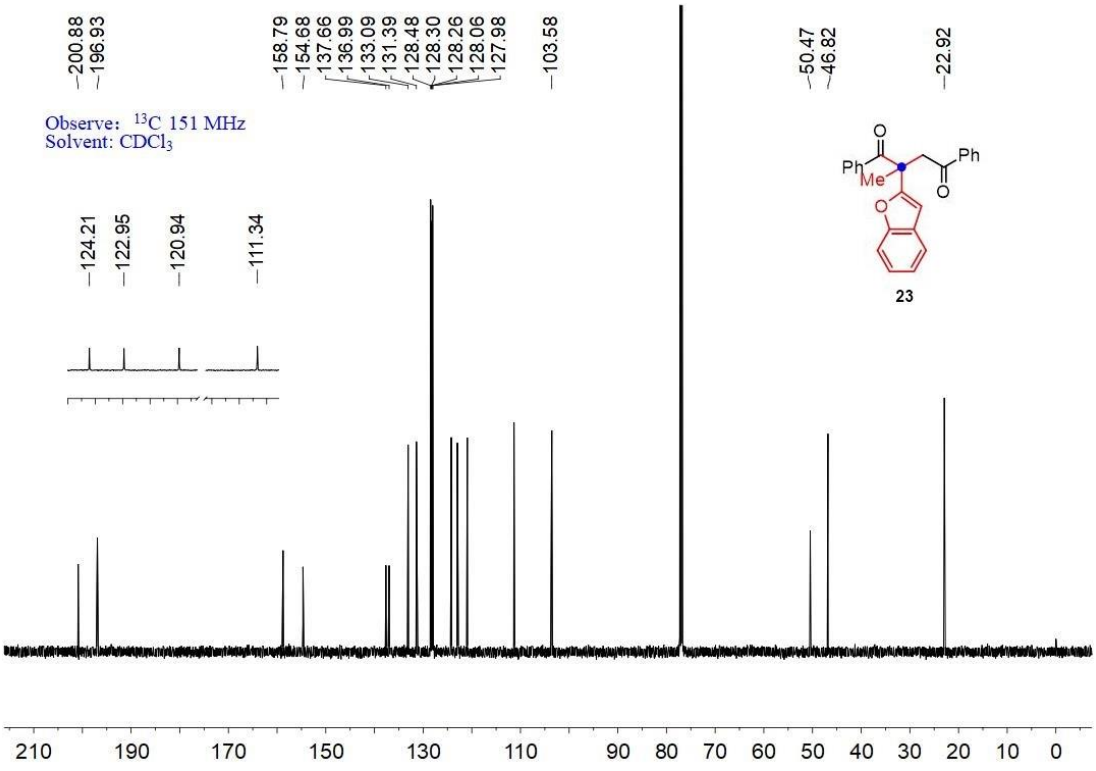

Figure S42. ^{13}C NMR spectrum of compound **23**, related to **Figure 2A.**

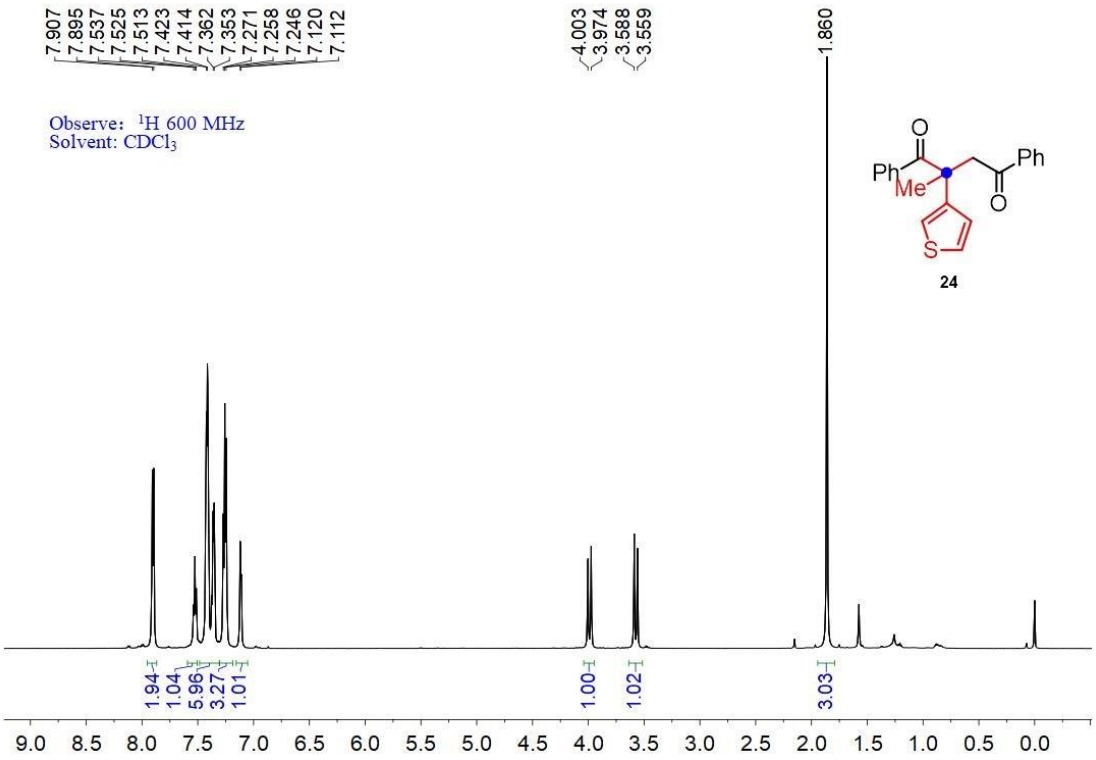

Figure S43. ^{1}H NMR spectrum of compound **24**, related to **Figure 2A.**

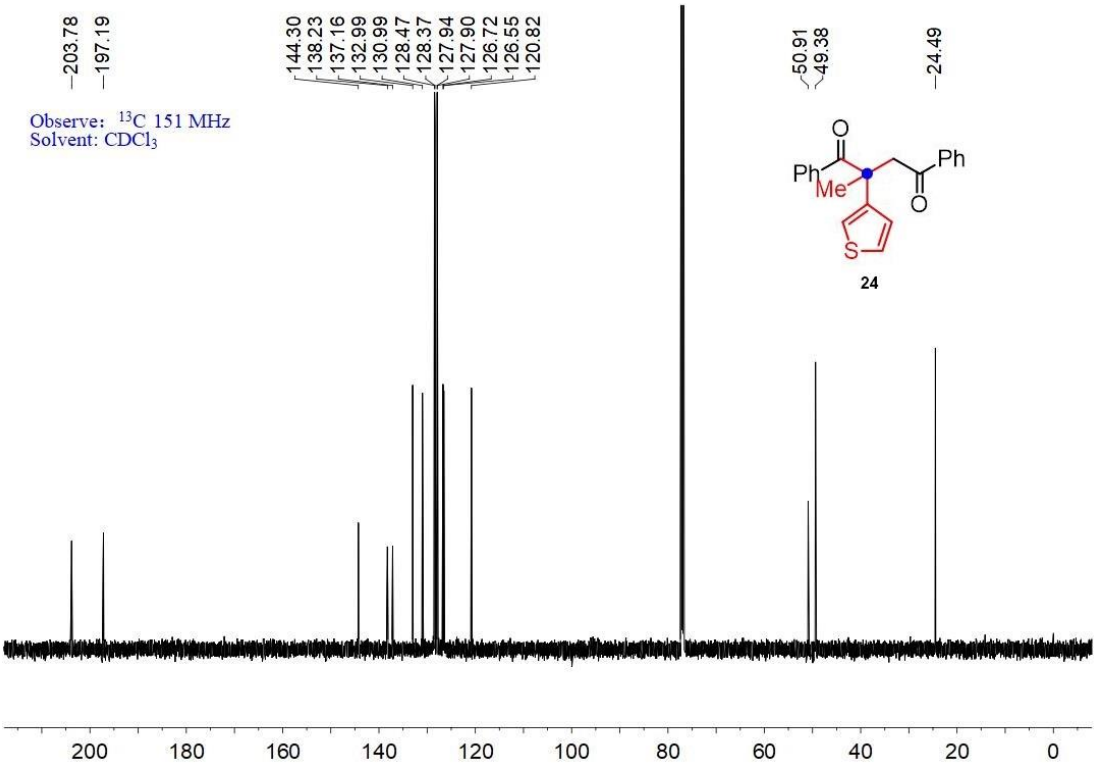

Figure S44. ^{13}C NMR spectrum of compound **24**, related to **Figure 2A.**

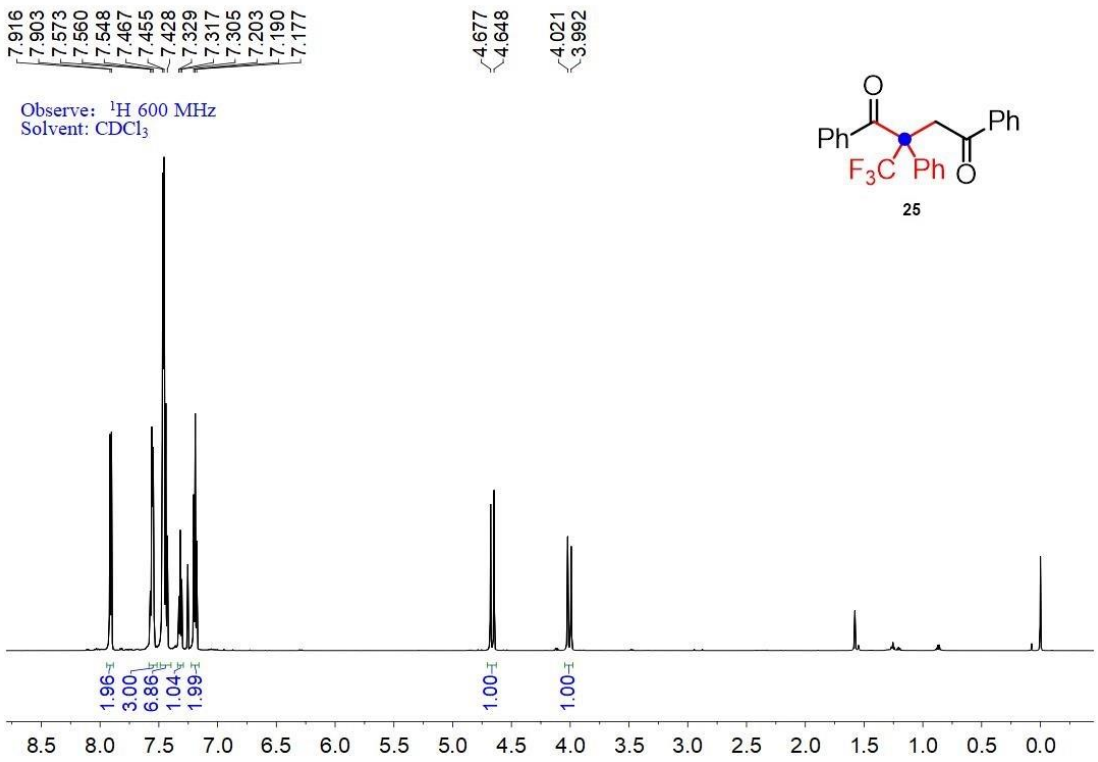

Figure S45. ^{1}H NMR spectrum of compound **25**, related to **Figure 2A.**

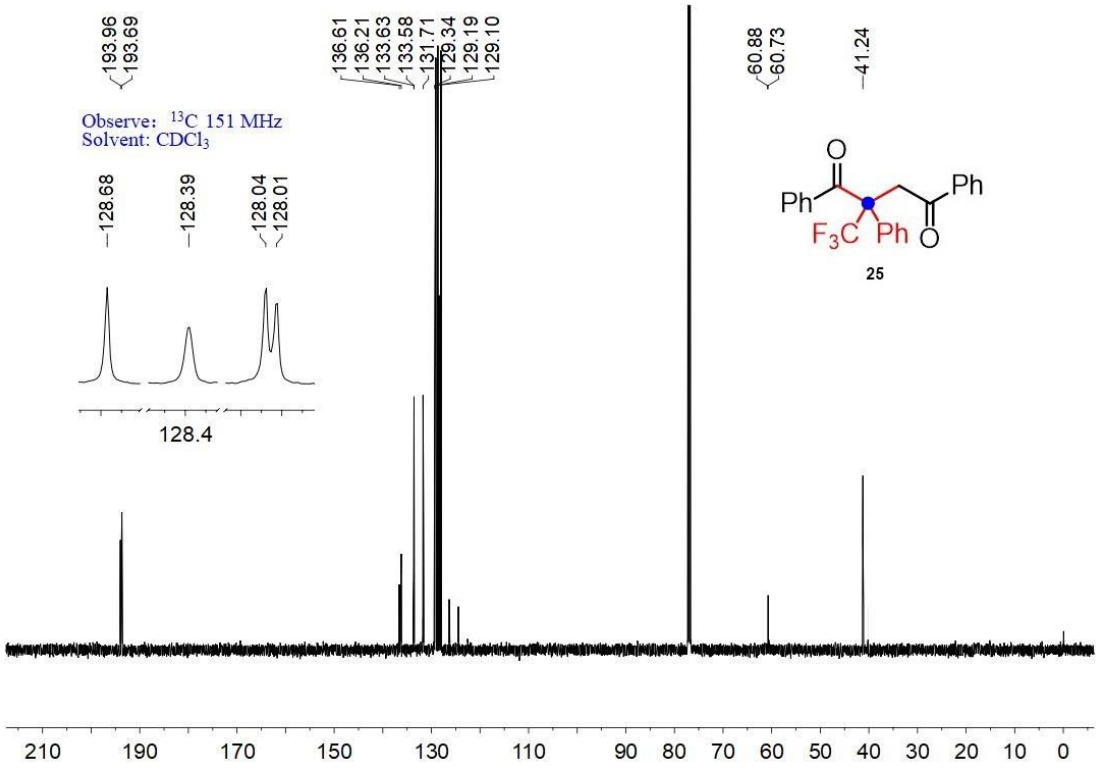

Figure S46. ^{13}C NMR spectrum of compound **25**, related to **Figure 2A.**

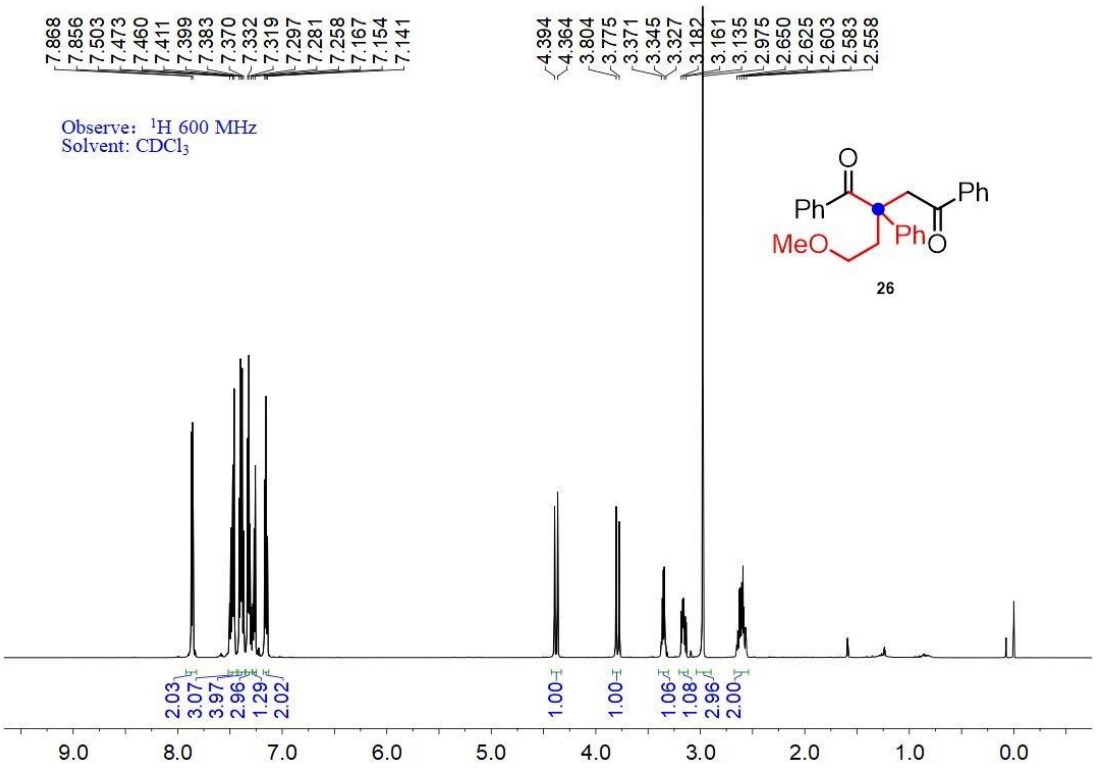

Figure S47. ^{1}H NMR spectrum of compound **26**, related to **Figure 2A.**

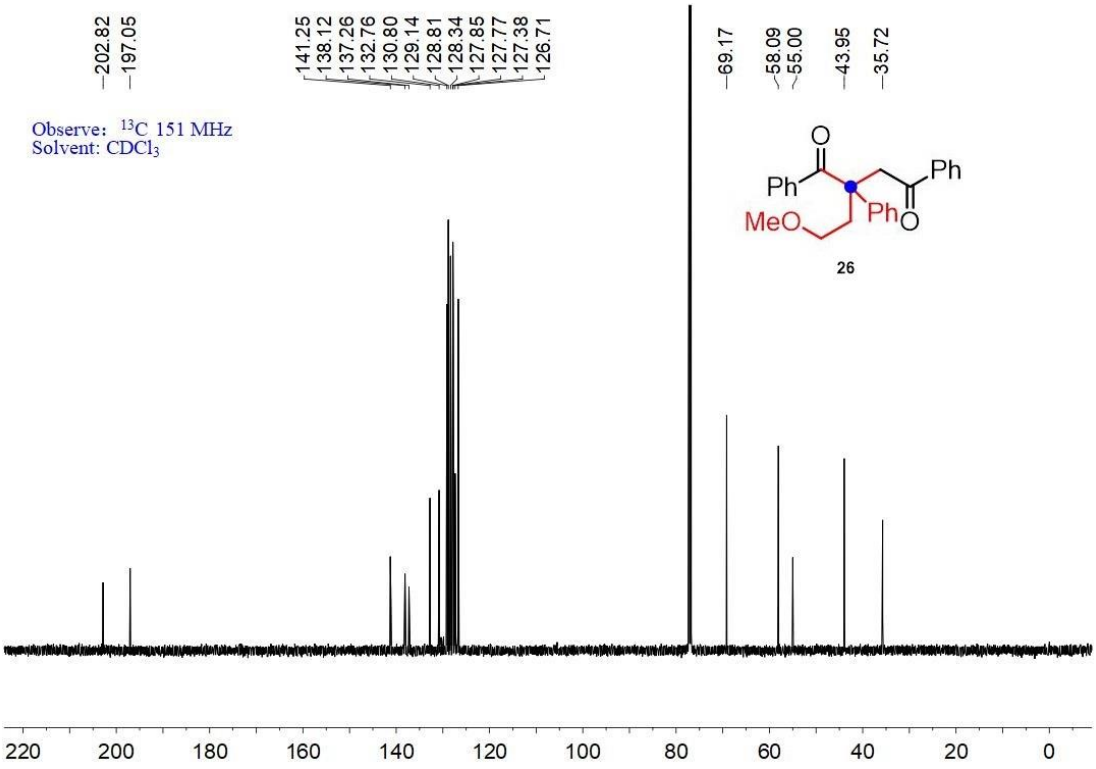

Figure S48. ^{1}H NMR spectrum of compound **26**, related to **Figure 2A.**

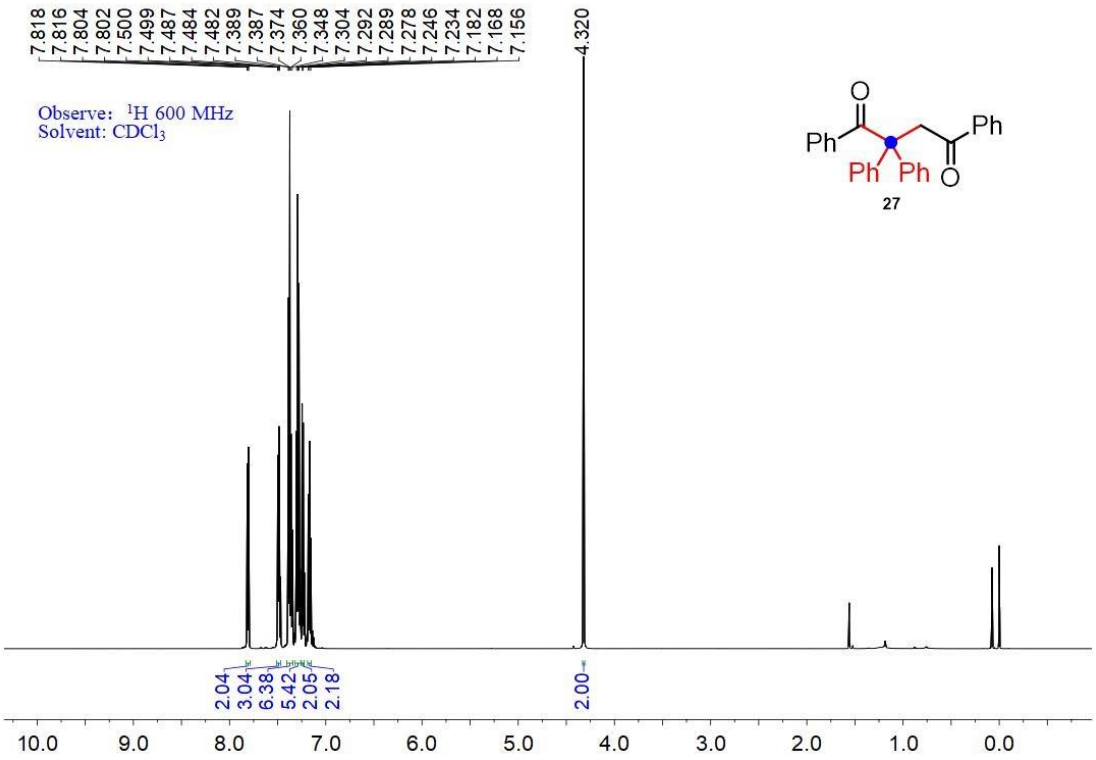

Figure S49. ^{1}H NMR spectrum of compound **27**, related to **Figure 2A.**

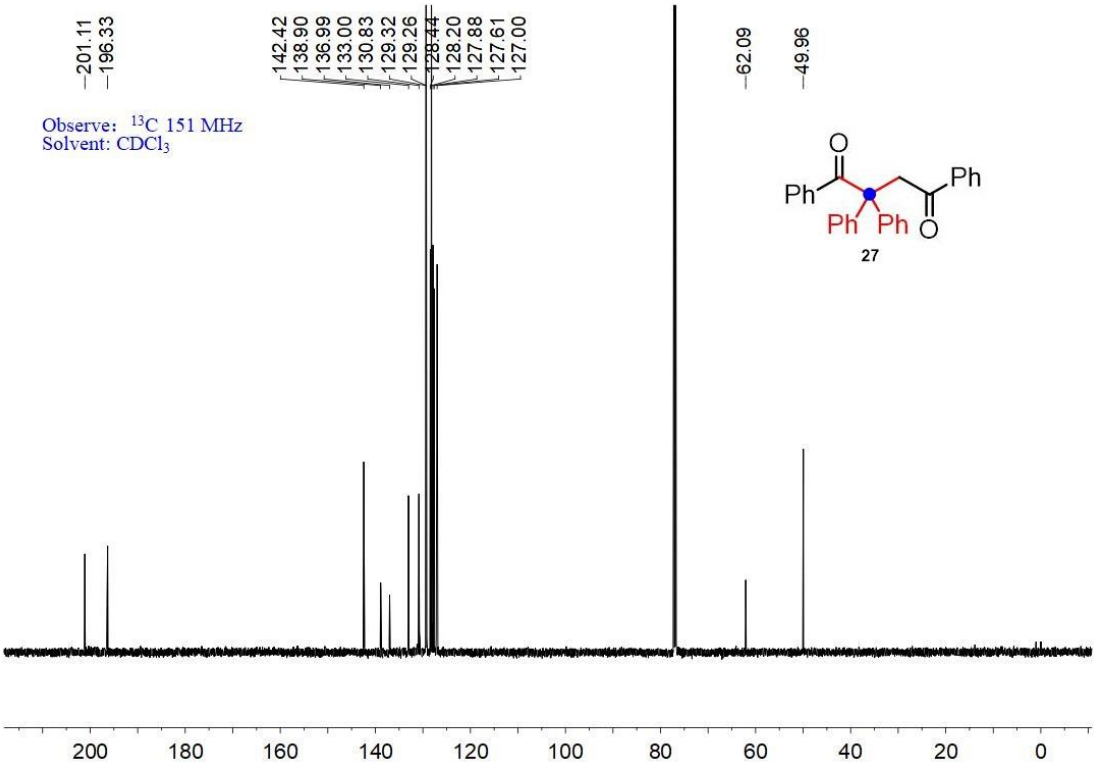

Figure S50. ^{13}C NMR spectrum of compound **27**, related to **Figure 2A.**

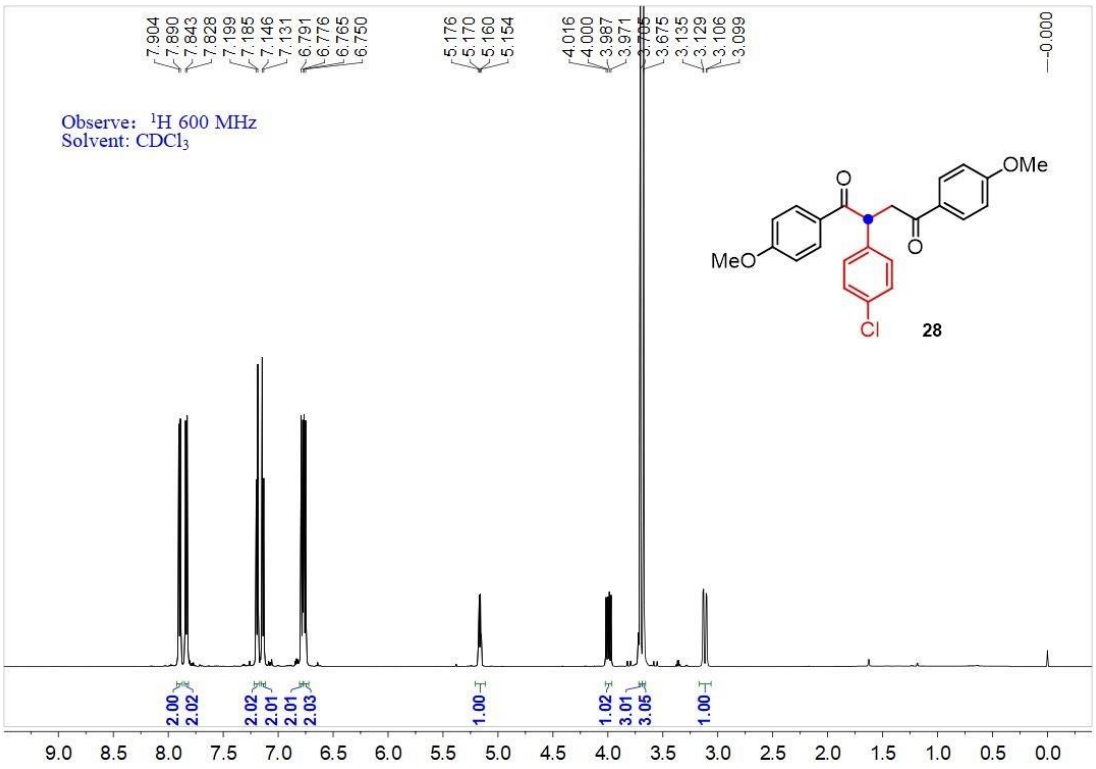

Figure S51. ^{1}H NMR spectrum of compound **28**, related to **Figure 2B.**

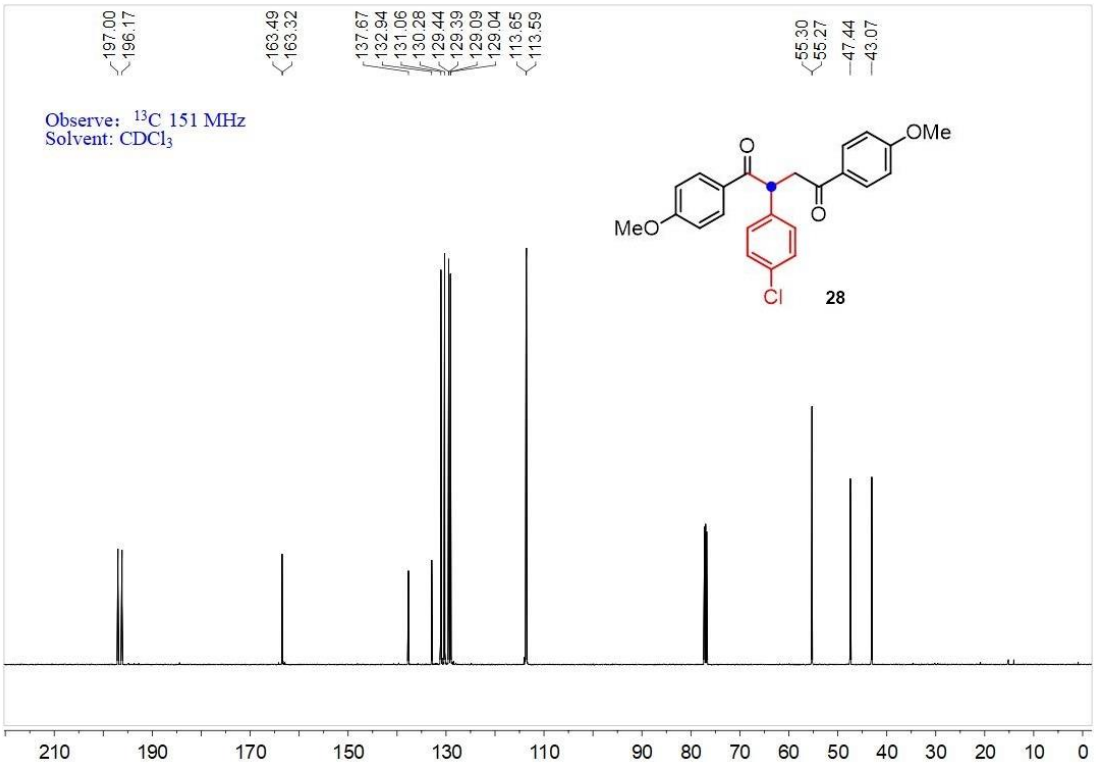

Figure S52. ^{13}C NMR spectrum of compound **28**, related to **Figure 2A.**

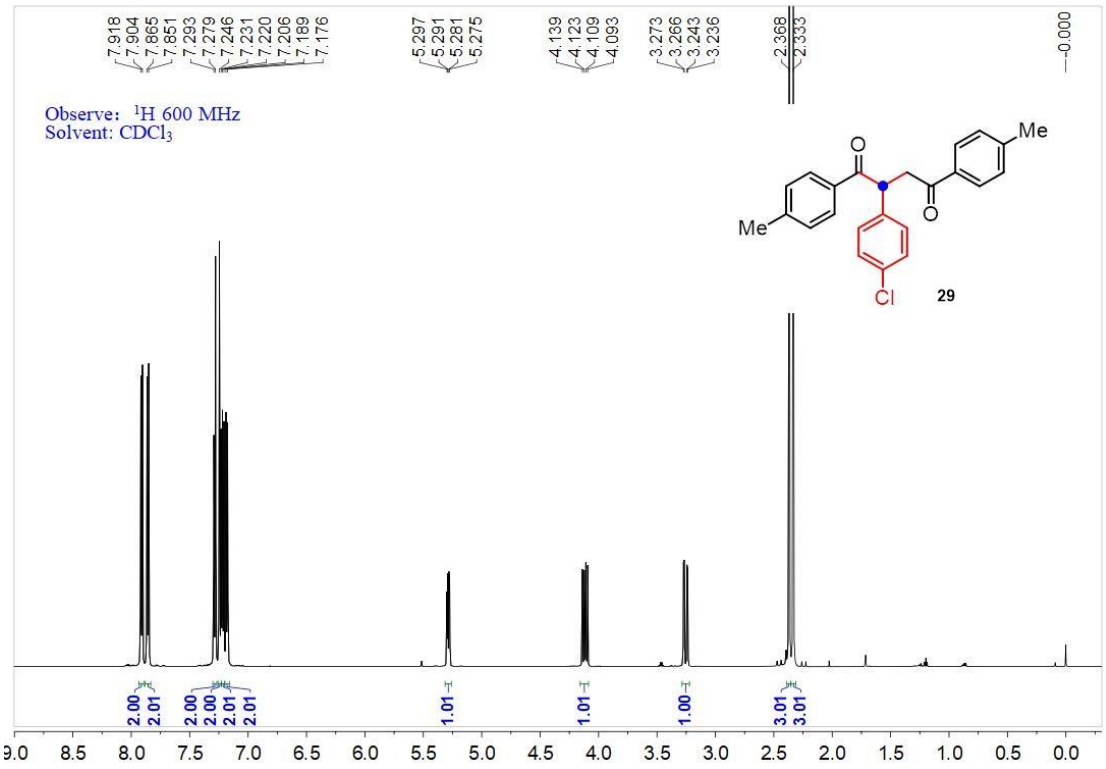

Figure S53. ^{1}H NMR spectrum of compound **29**, related to **Figure 2B.**

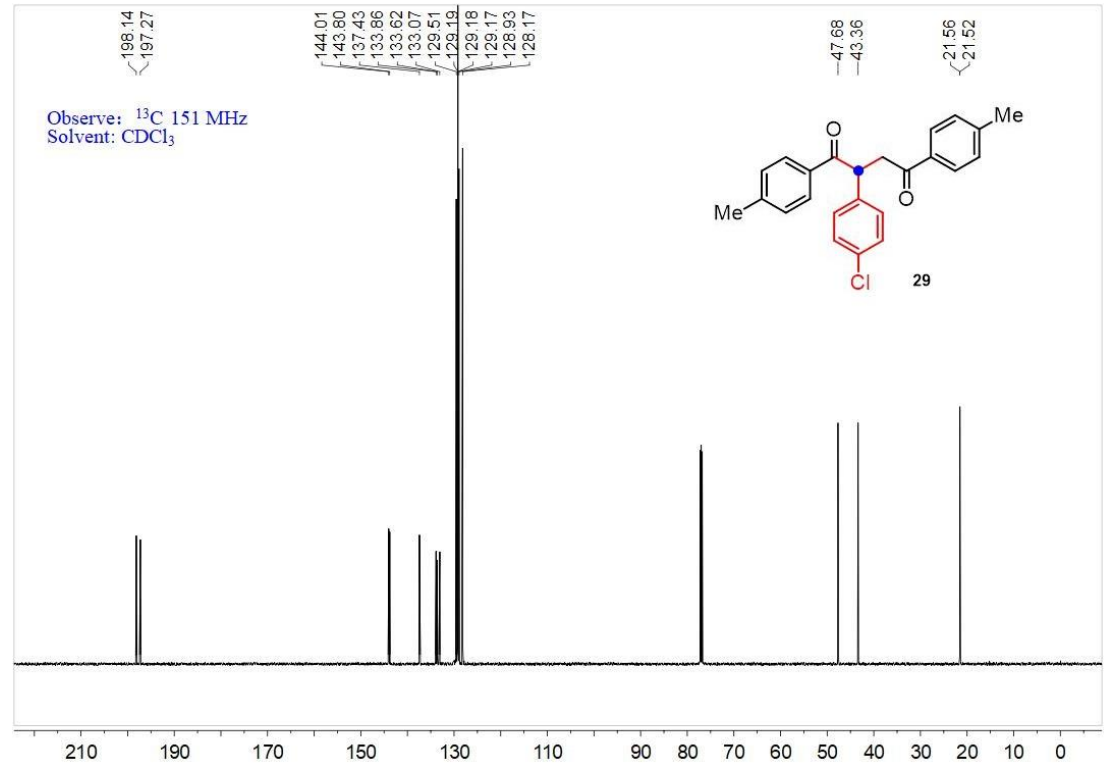

Figure S54. ^{13}C NMR spectrum of compound **29**, related to **Figure 2A.**

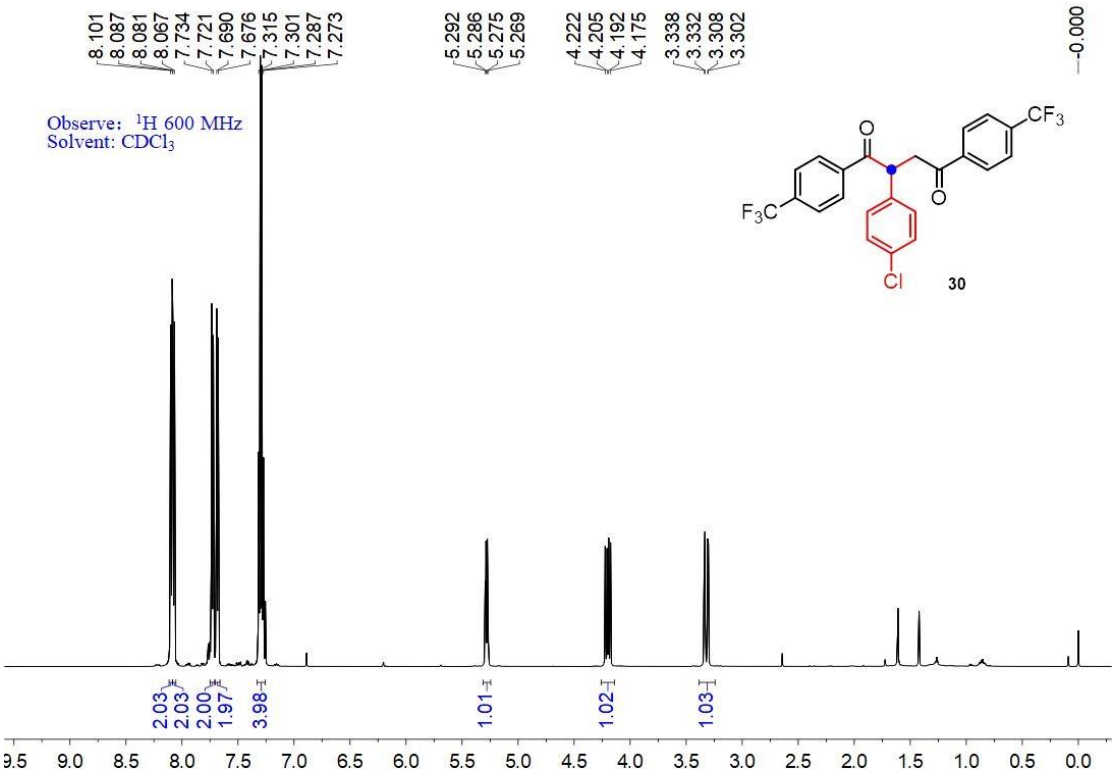

Figure S55. ^{1}H NMR spectrum of compound **30**, related to **Figure 2B.**

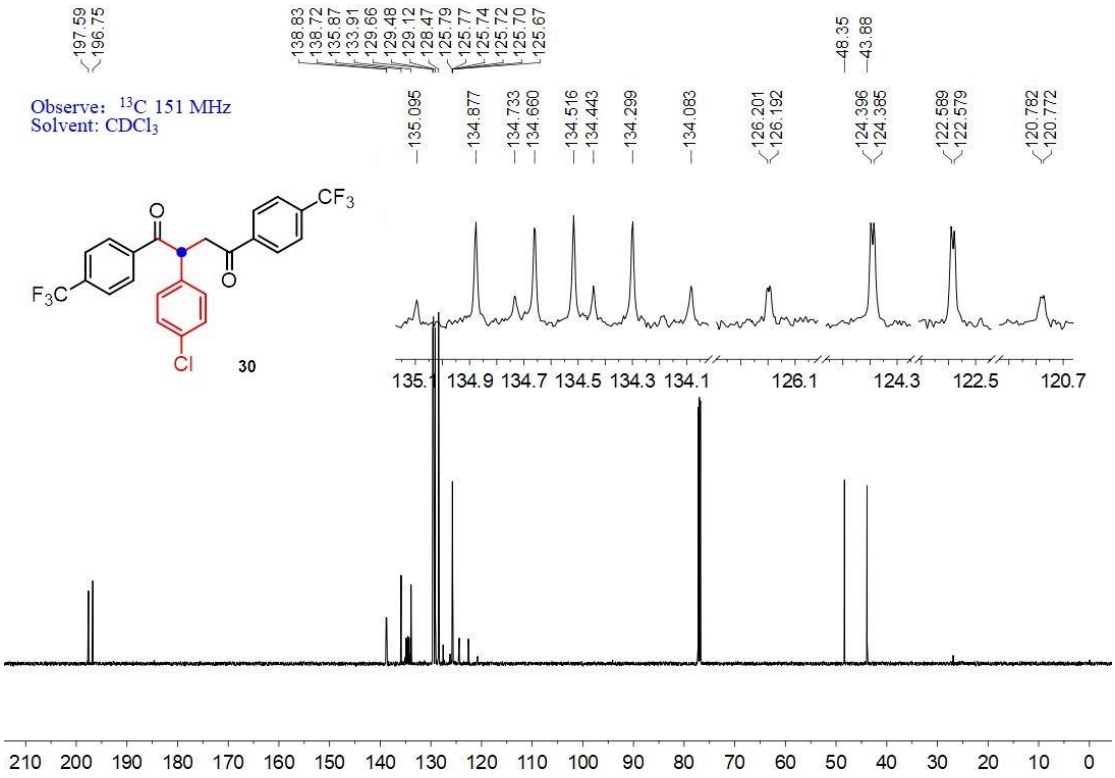

Figure S56. ^{13}C NMR spectrum of compound **30**, related to **Figure 2A.**

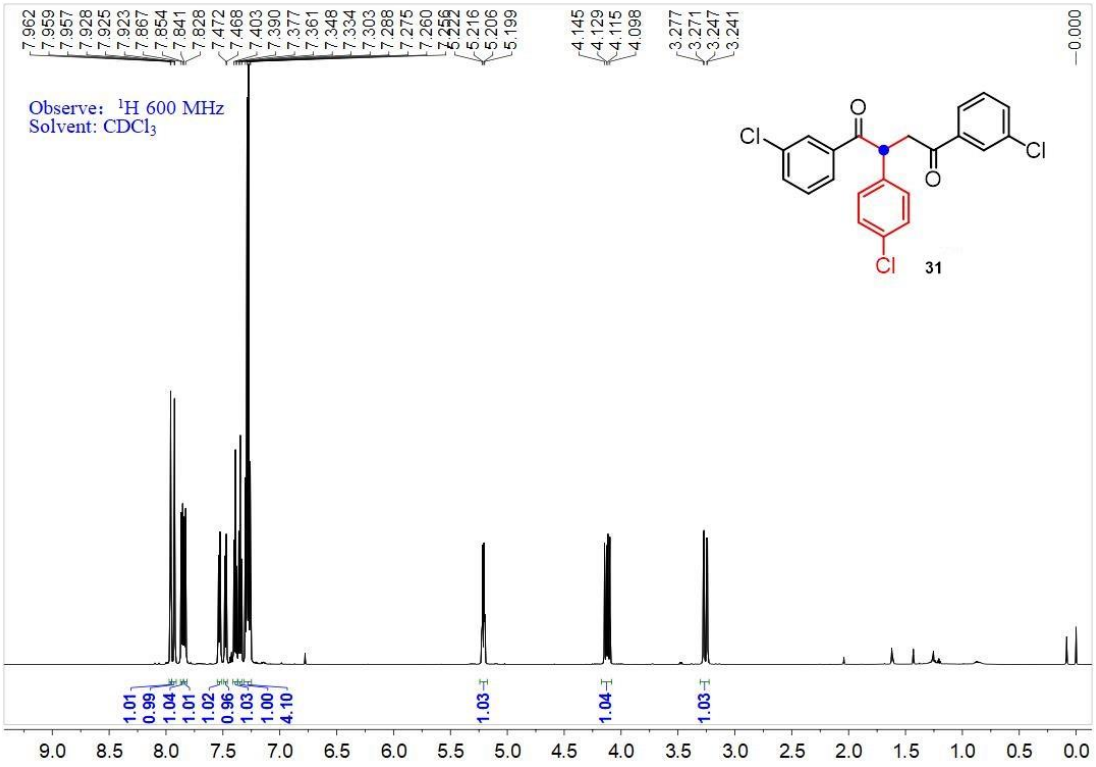

Figure S57. ^{1}H NMR spectrum of compound **31**, related to **Figure 2B.**

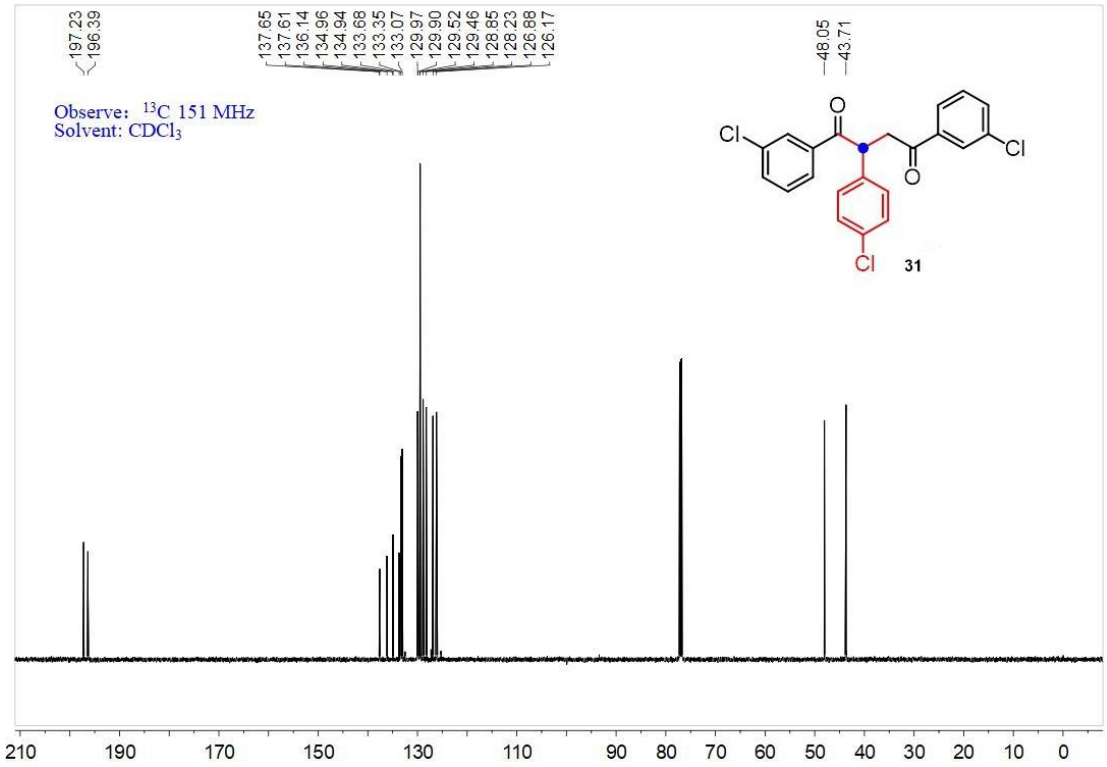

Figure S58. ^{13}C NMR spectrum of compound **31**, related to **Figure 2A.**

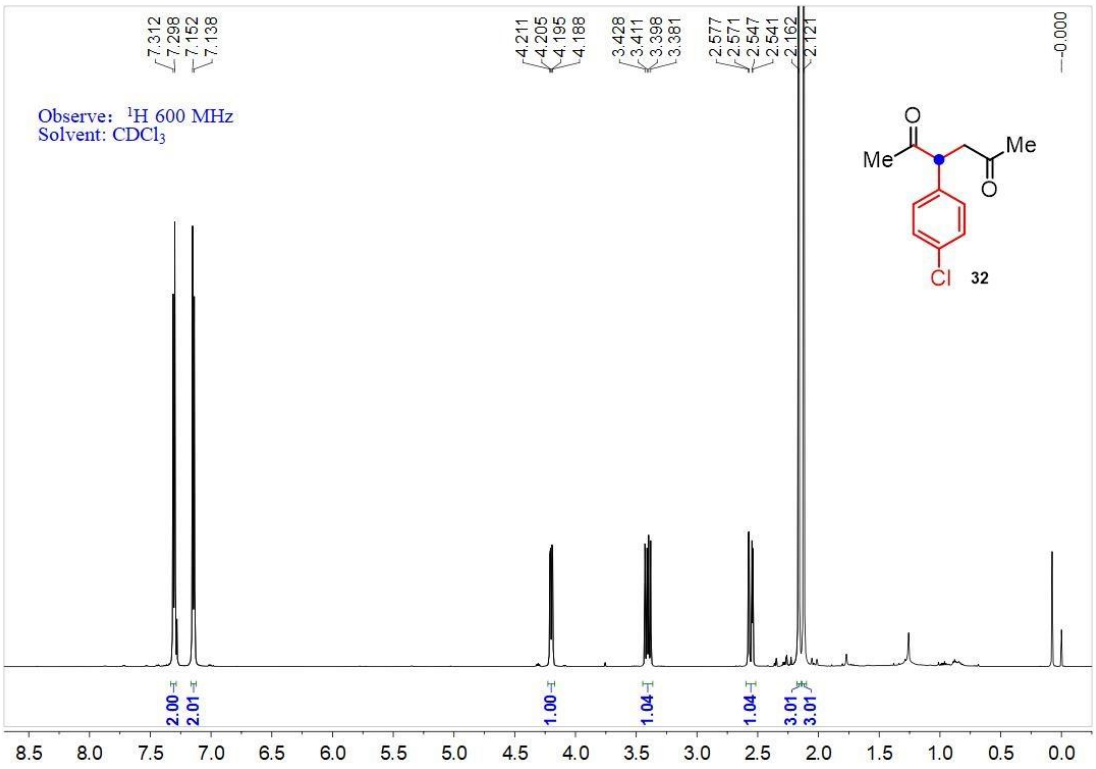

Figure S59. ^{1}H NMR spectrum of compound **32**, related to **Figure 2B.**

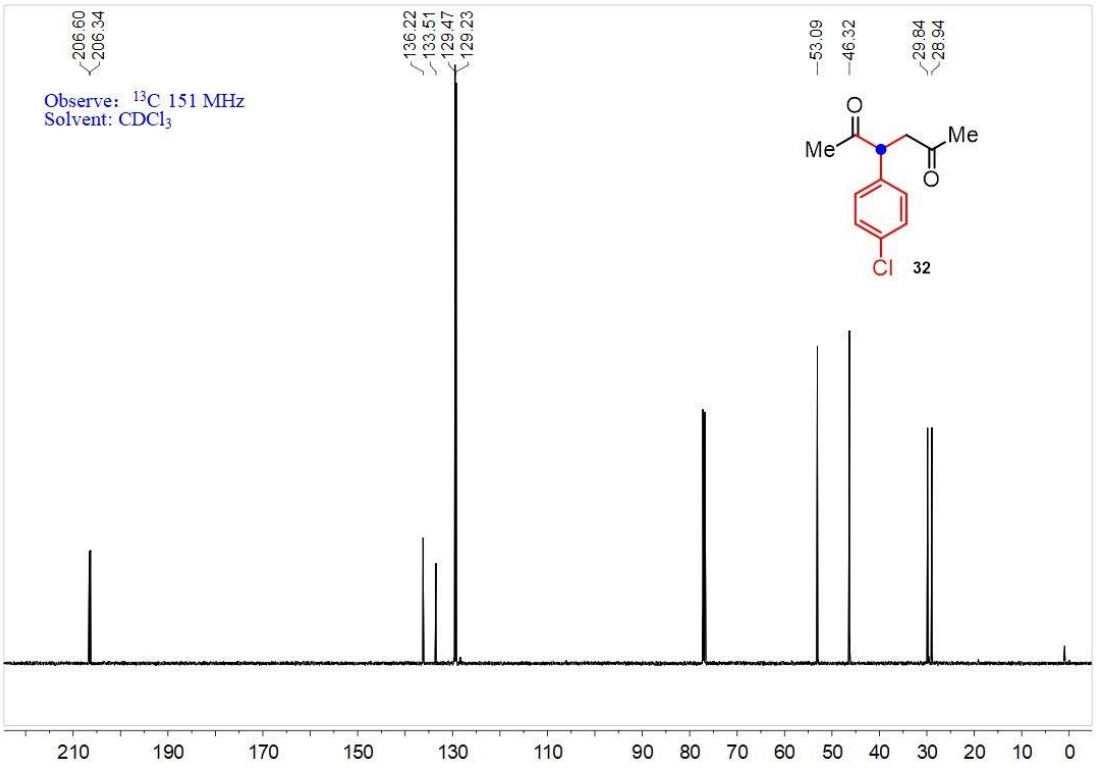

Figure S60. ^{13}C NMR spectrum of compound **32**, related to **Figure 2A.**

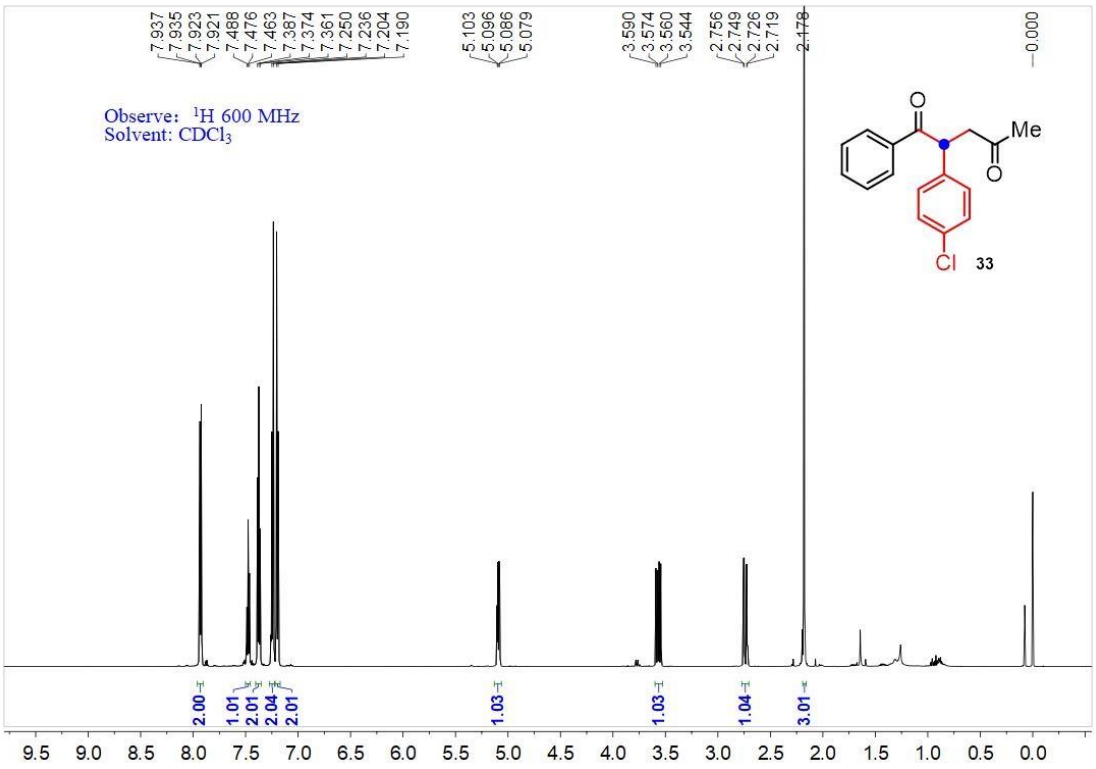

Figure S61. ^{1}H NMR spectrum of compound **33**, related to **Figure 2B.**

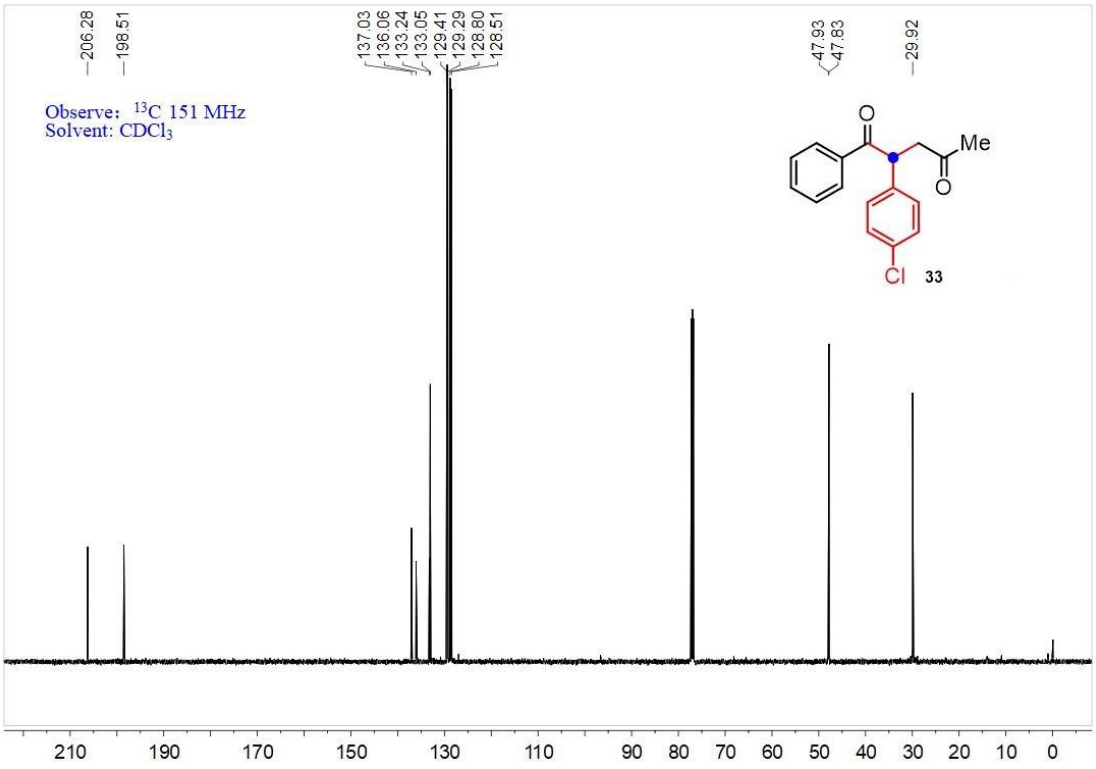

Figure S62. ^{13}C NMR spectrum of compound **33**, related to **Figure 2A.**

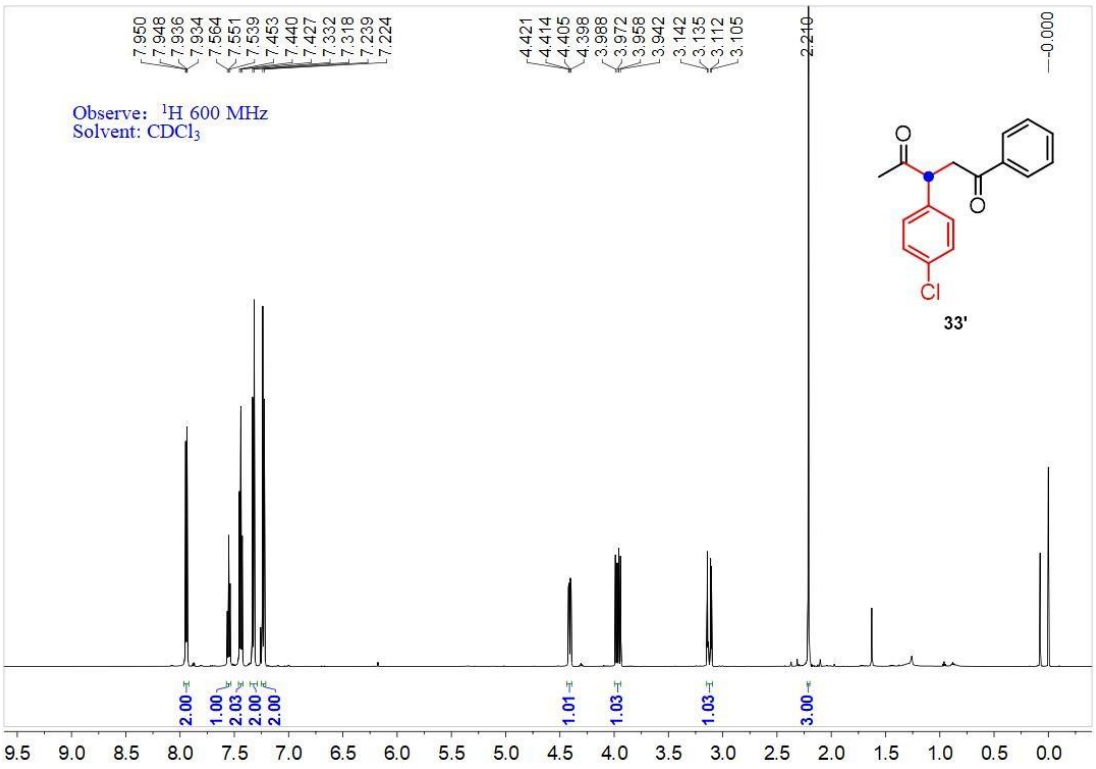

Figure S63. ^{1}H NMR spectrum of compound **33'**, related to **Figure 2B.**

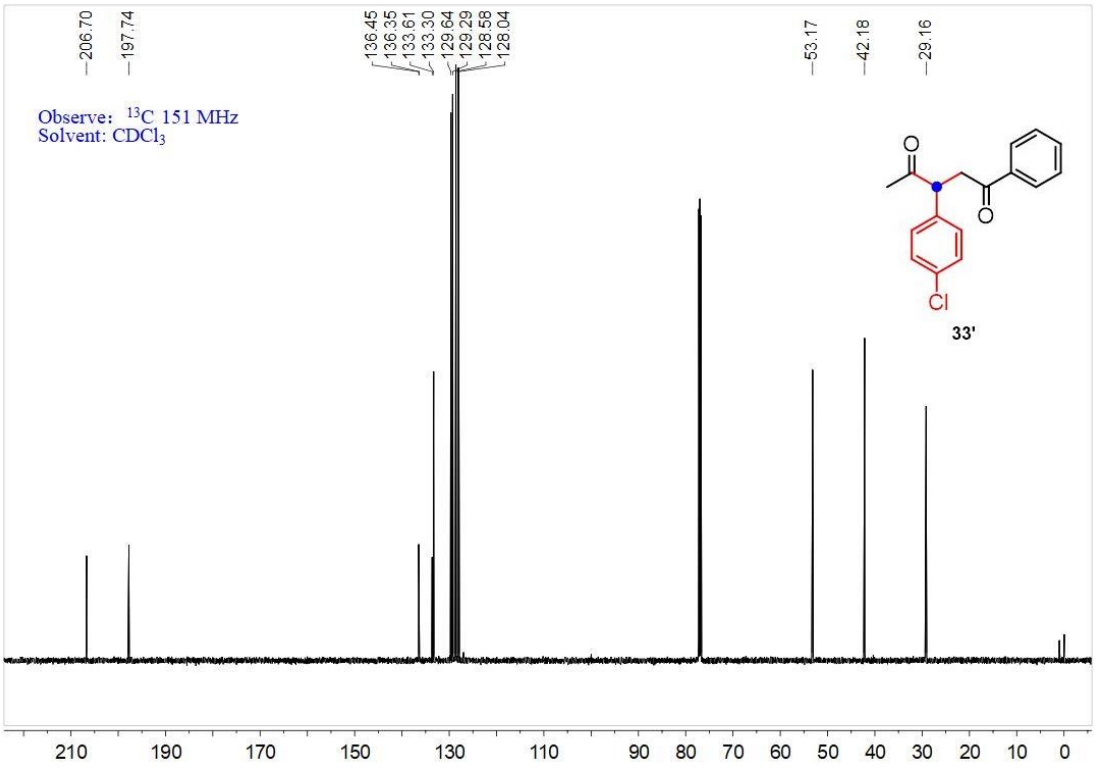

Figure S64. ^{13}C NMR spectrum of compound **33'**, related to **Figure 2A.**

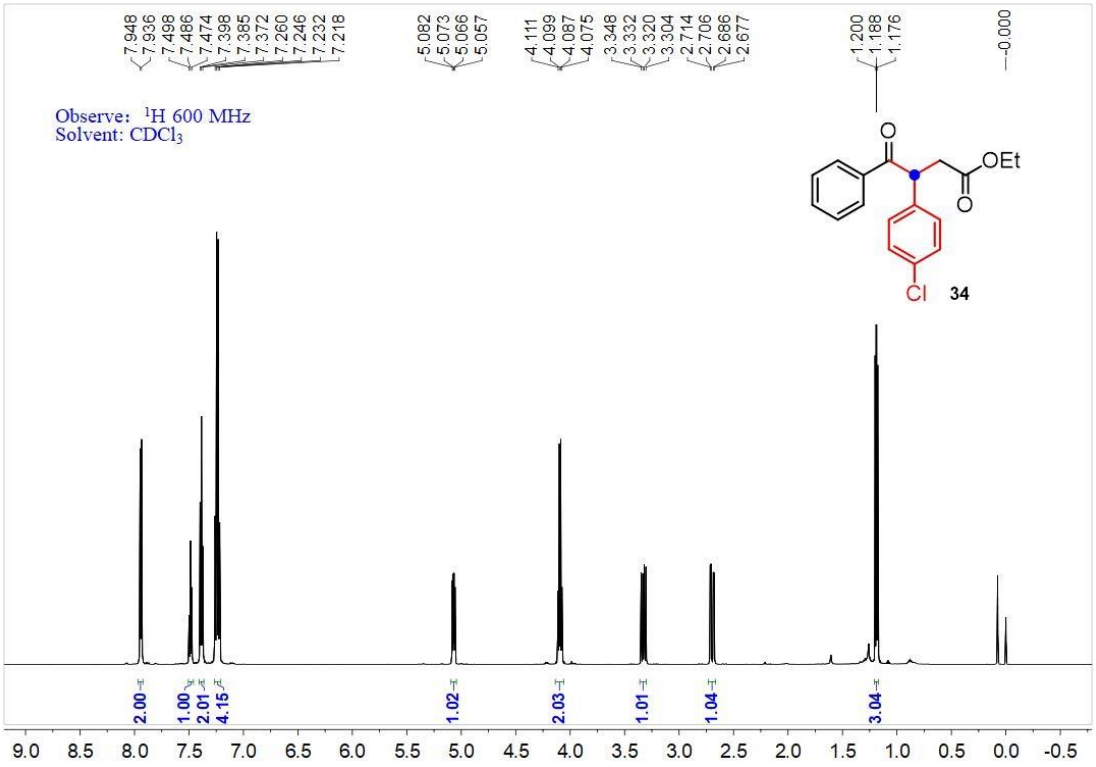

Figure S65. ^{1}H NMR spectrum of compound **34**, related to **Figure 2B.**

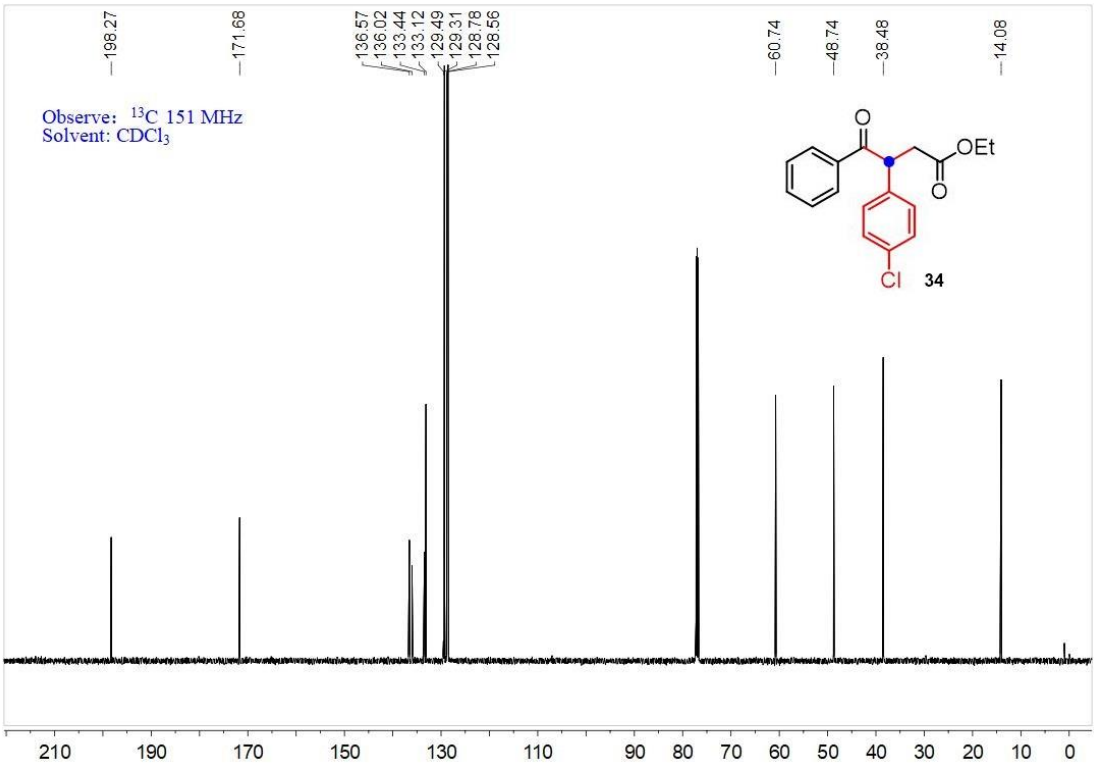

Figure S66. ^{13}C NMR spectrum of compound **34**, related to **Figure 2B.**

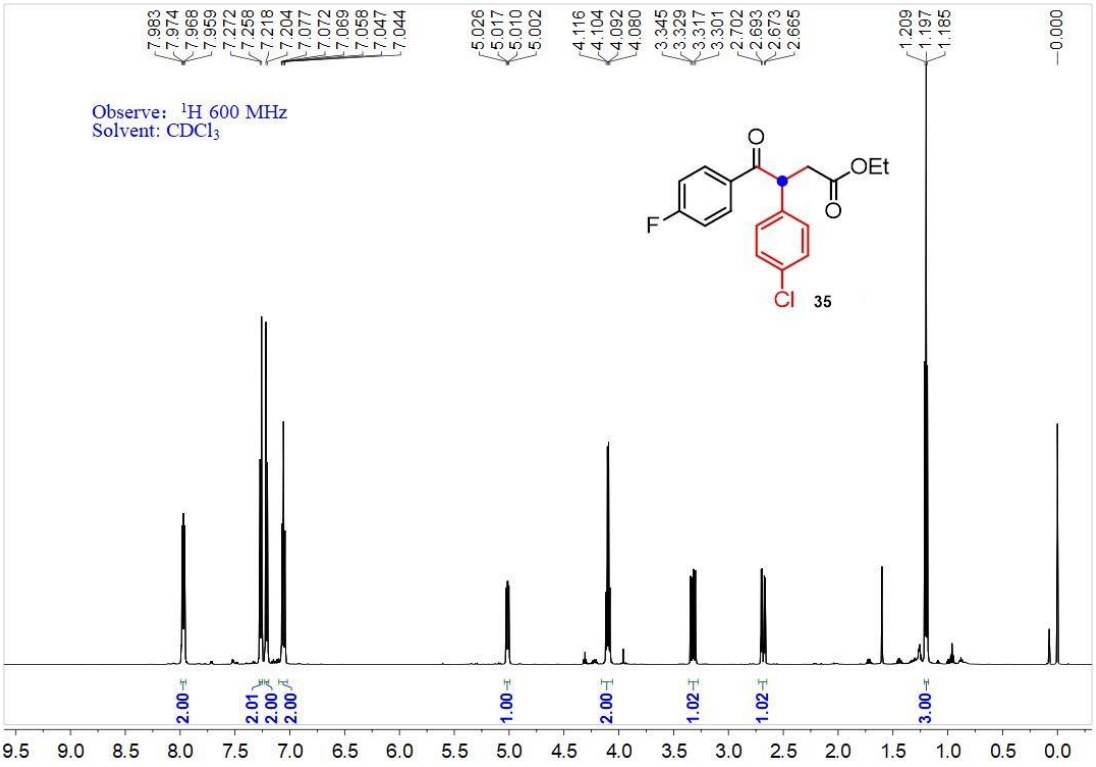

Figure S67. ^{1}H NMR spectrum of compound **35**, related to **Figure 2B.**

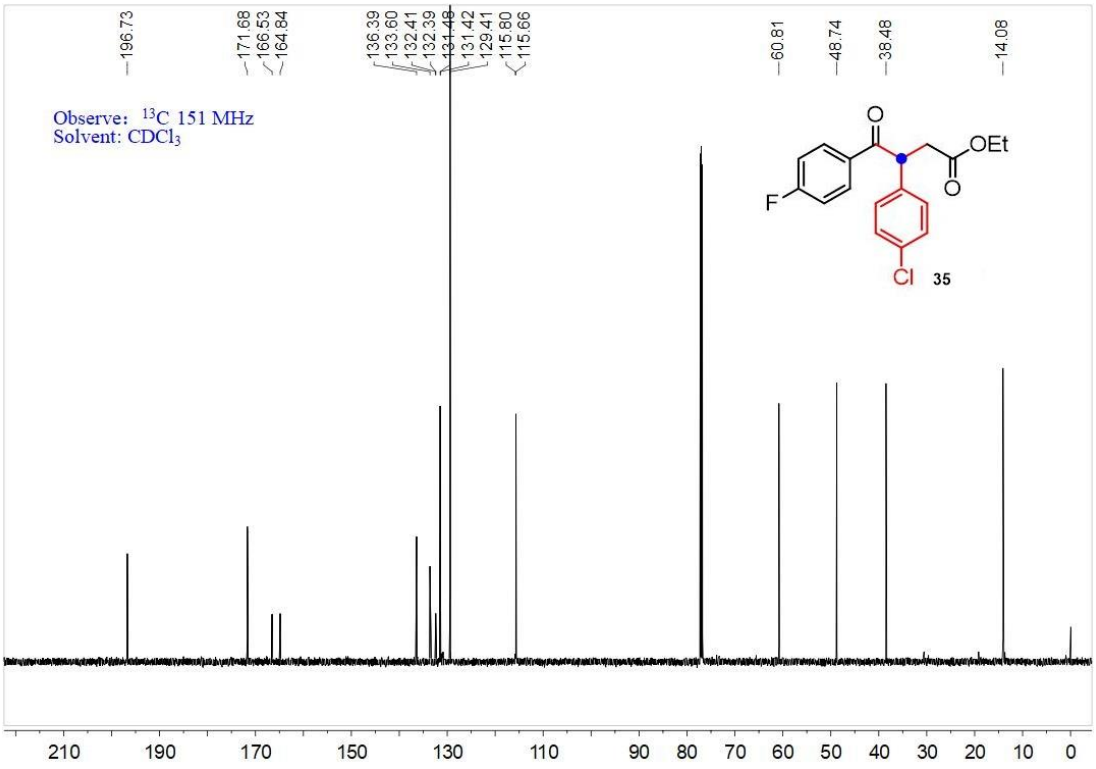

Figure S68. ^{13}C NMR spectrum of compound **35**, related to **Figure 2B.**

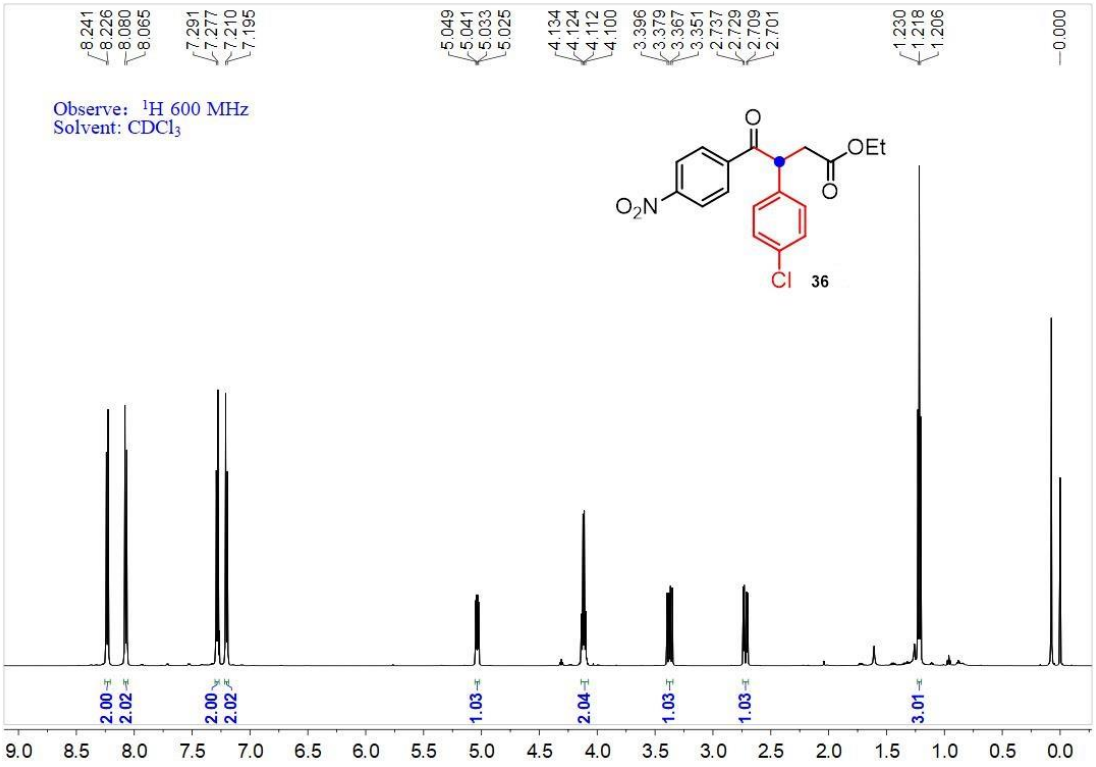

Figure S69. ^{1}H NMR spectrum of compound **36**, related to **Figure 2B.**

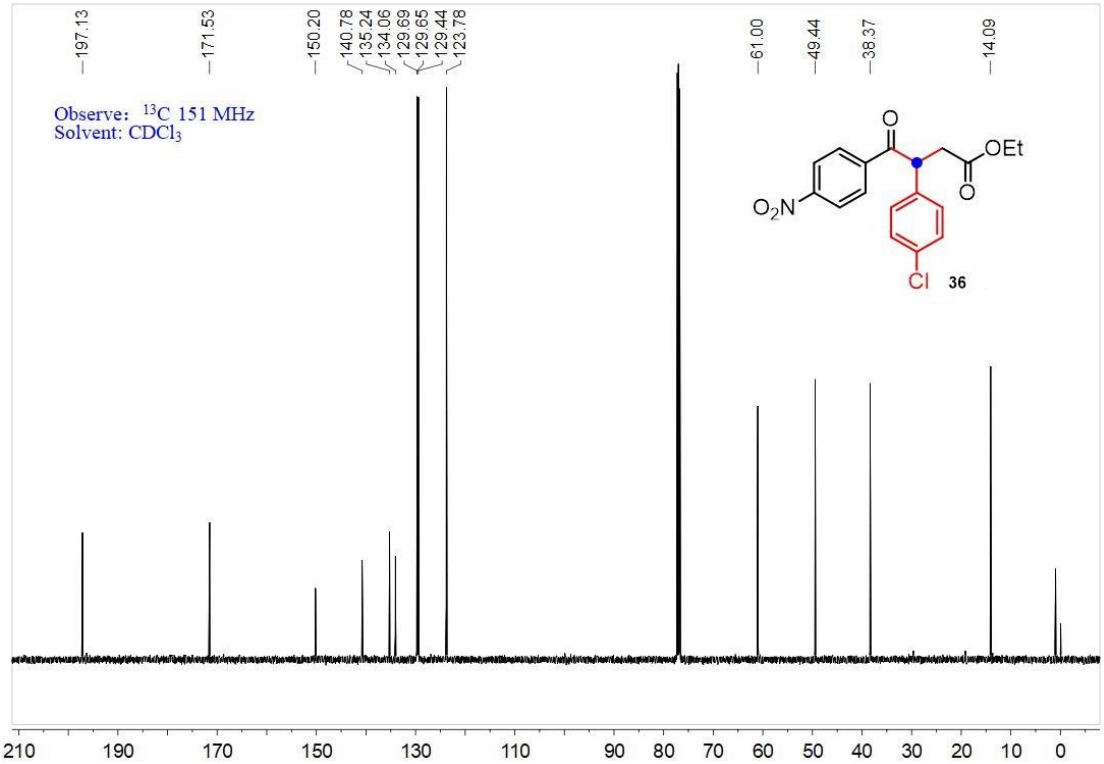

Figure S70. ^{13}C NMR spectrum of compound **36**, related to **Figure 2B.**

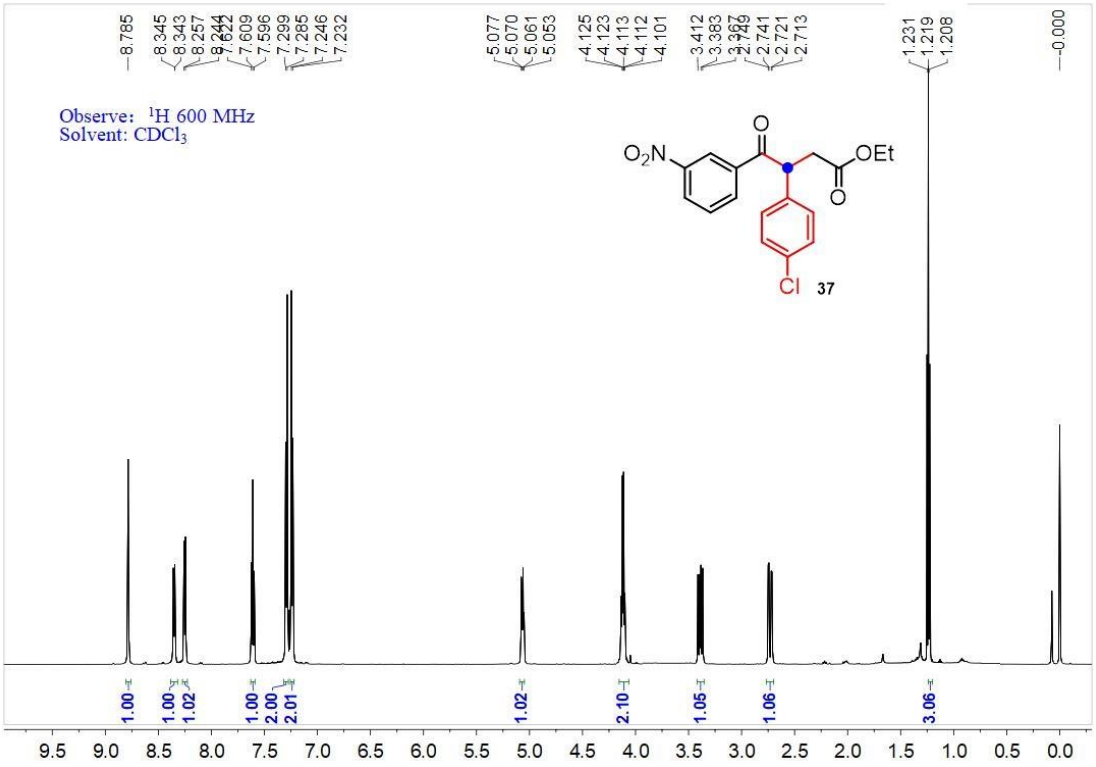

Figure S71. ^{1}H NMR spectrum of compound **37**, related to **Figure 2B.**

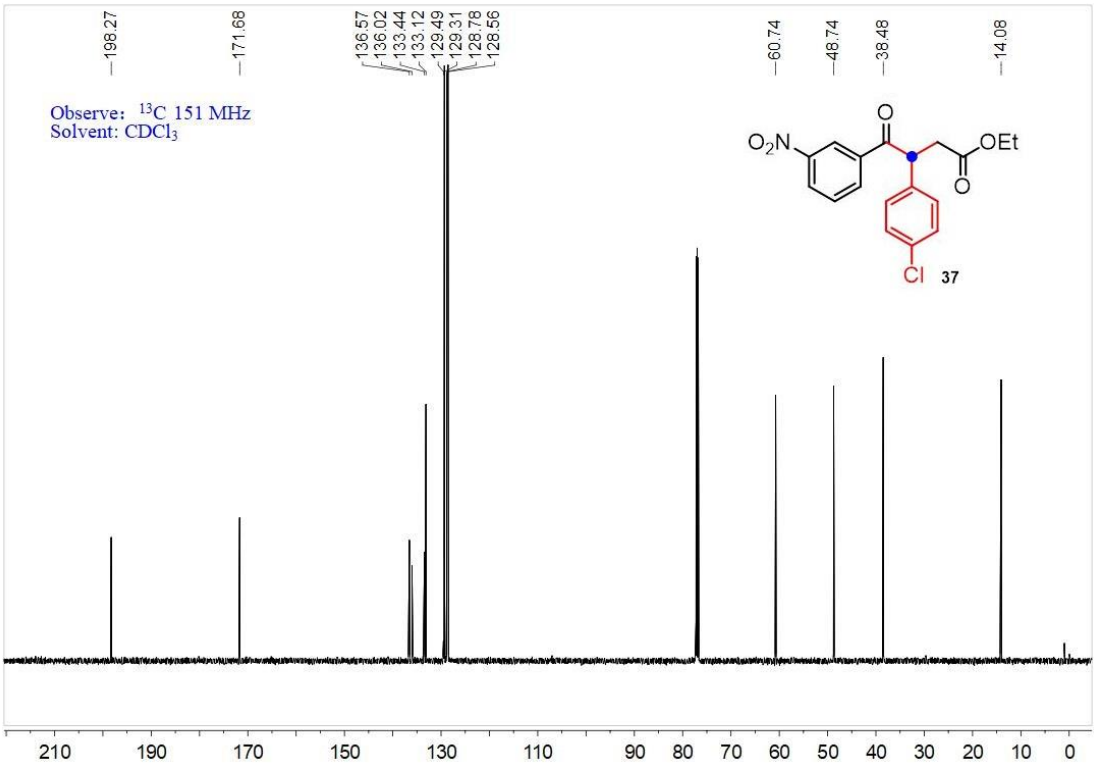

Figure S72. ^{13}C NMR spectrum of compound **37**, related to **Figure 2B.**

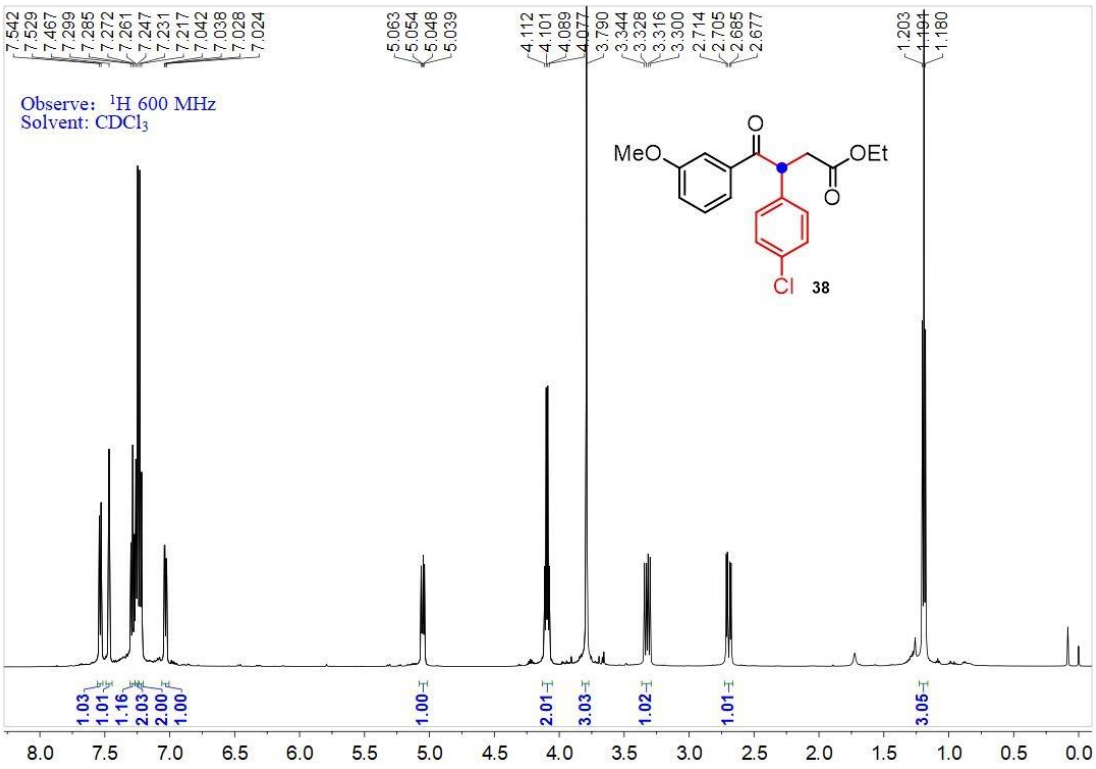

Figure S73. ^{1}H NMR spectrum of compound **38**, related to **Figure 2B.**

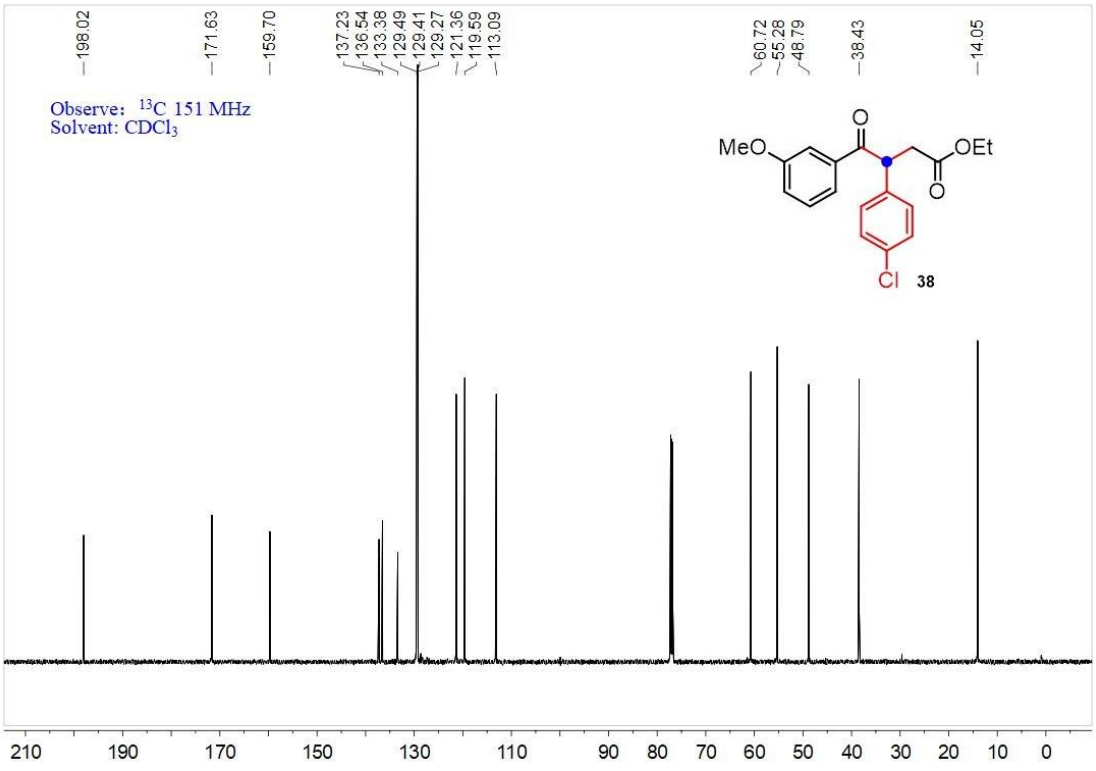

Figure S74. ^{13}C NMR spectrum of compound **38**, related to **Figure 2B.**

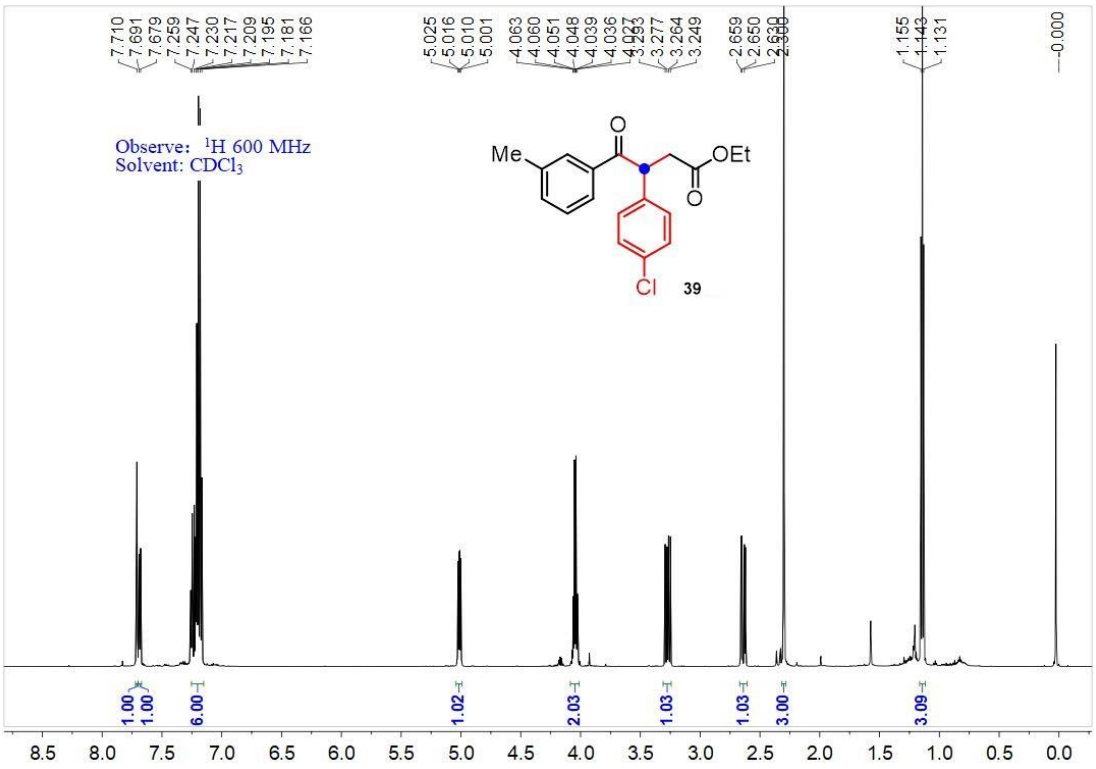

Figure S75. ^{1}H NMR spectrum of compound **39**, related to **Figure 2B.**

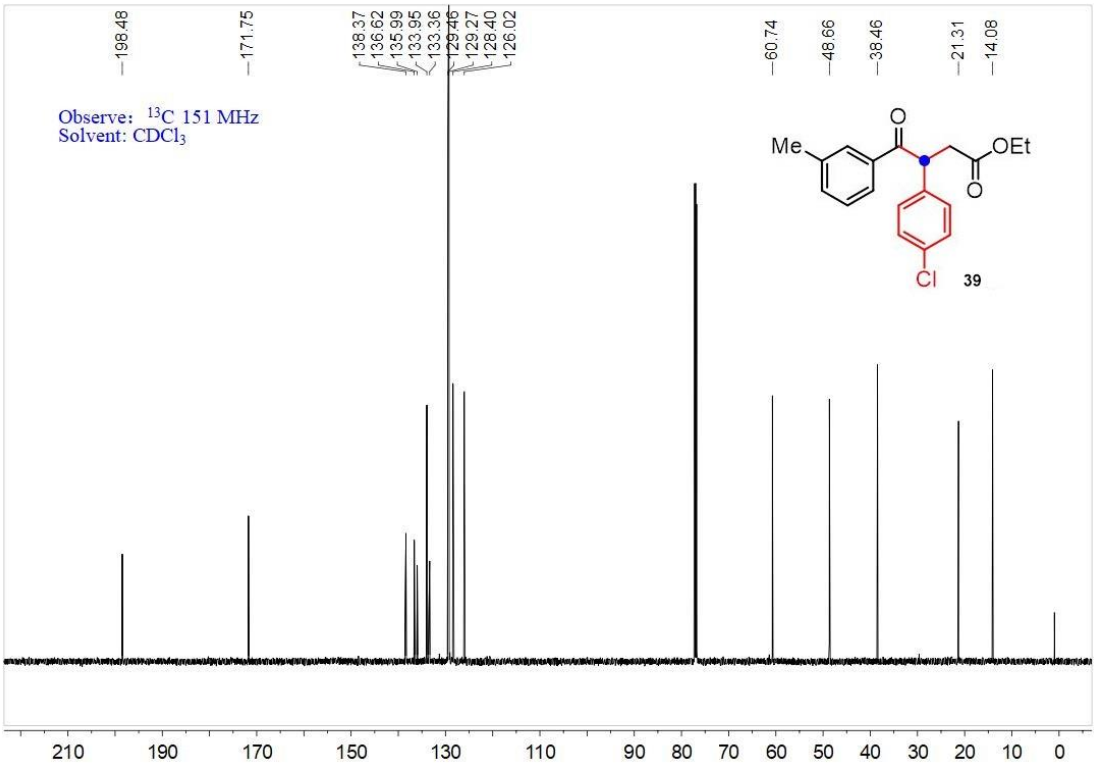

Figure S76. ^{13}C NMR spectrum of compound **39**, related to **Figure 2B.**

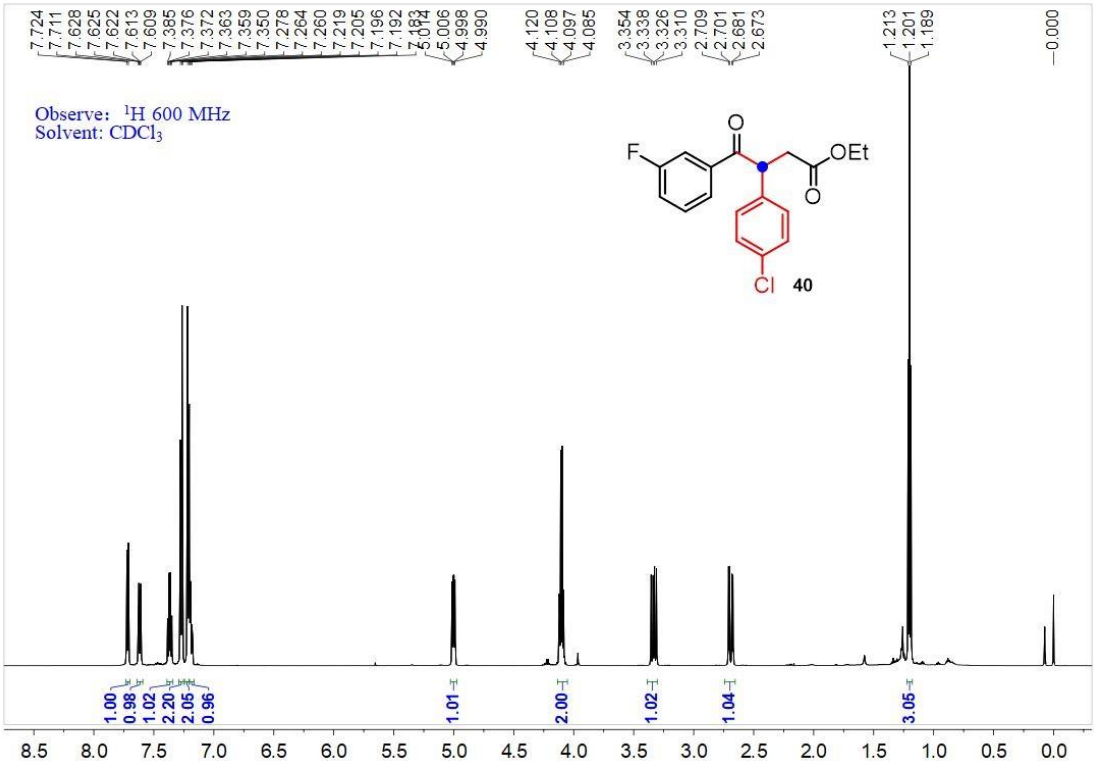

Figure S77. ^{1}H NMR spectrum of compound **40**, related to **Figure 2B.**

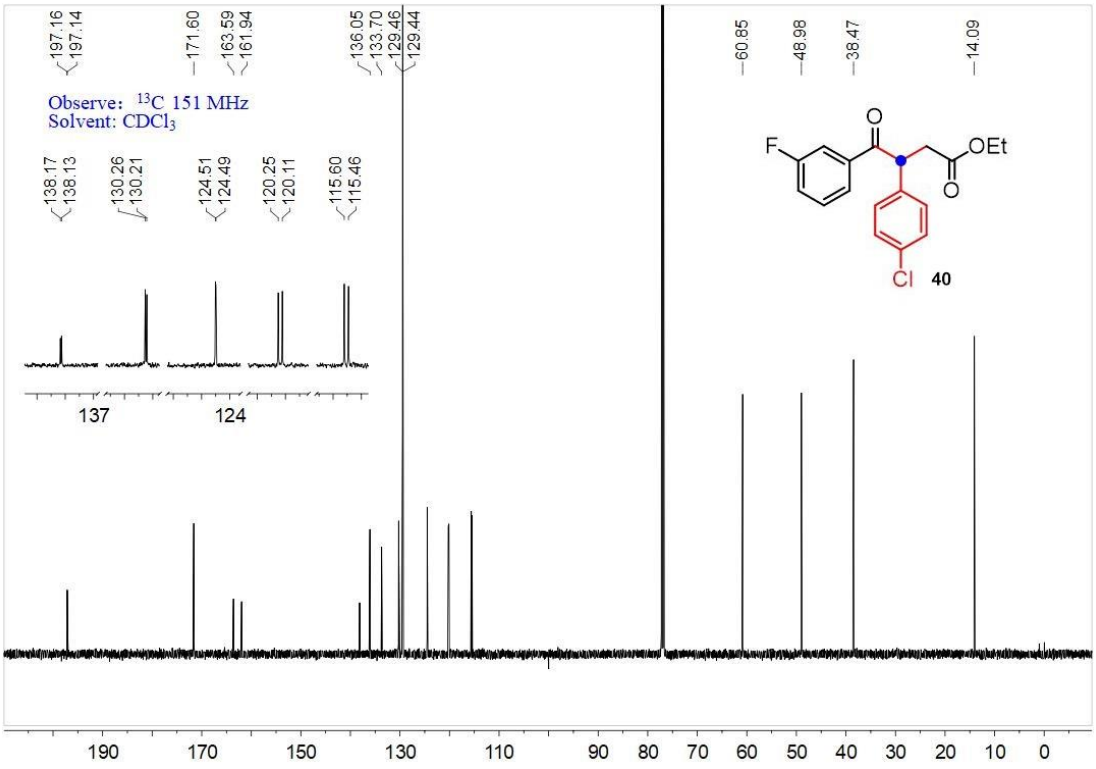

Figure S78. ^{13}C NMR spectrum of compound **40**, related to **Figure 2B.**

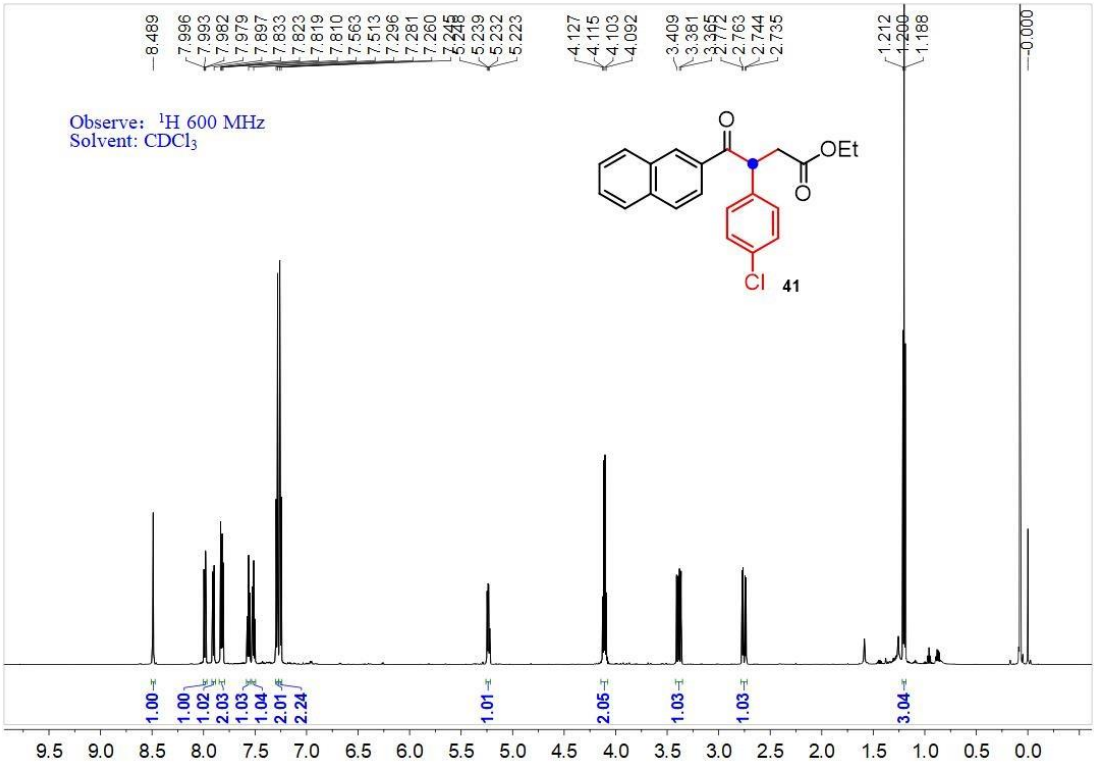

Figure S79. ^{1}H NMR spectrum of compound **41**, related to **Figure 2B.**

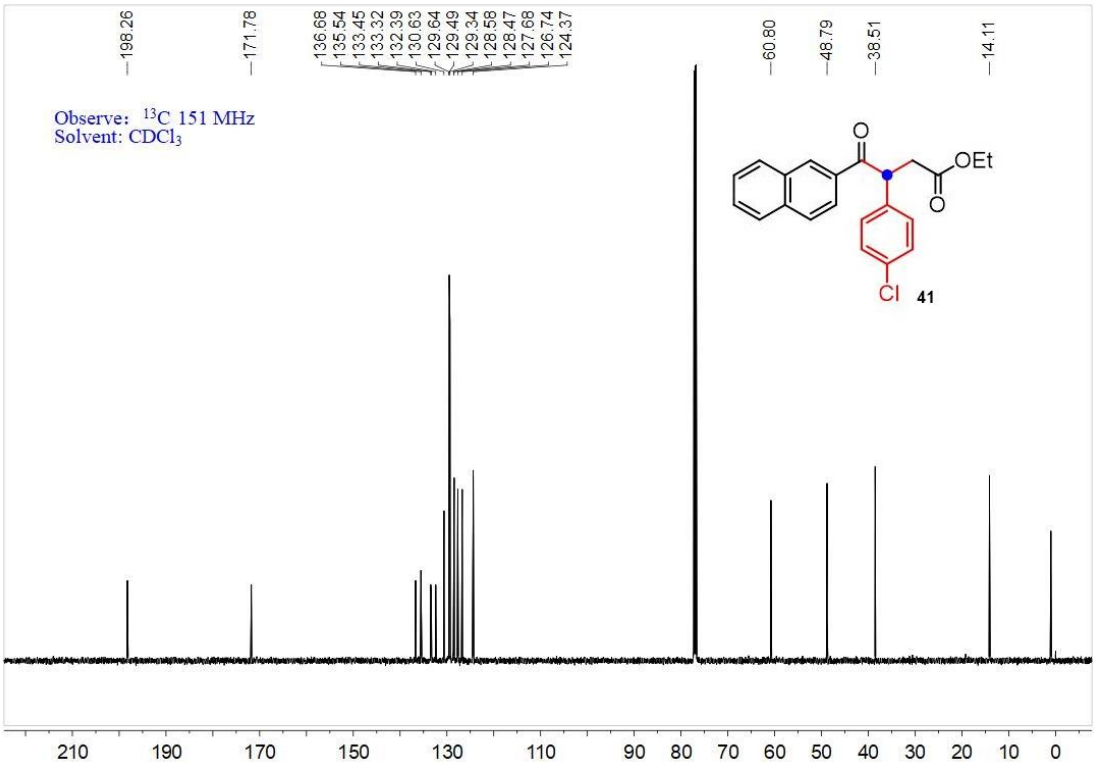

Figure S80. ^{13}C NMR spectrum of compound **41**, related to **Figure 2B.**

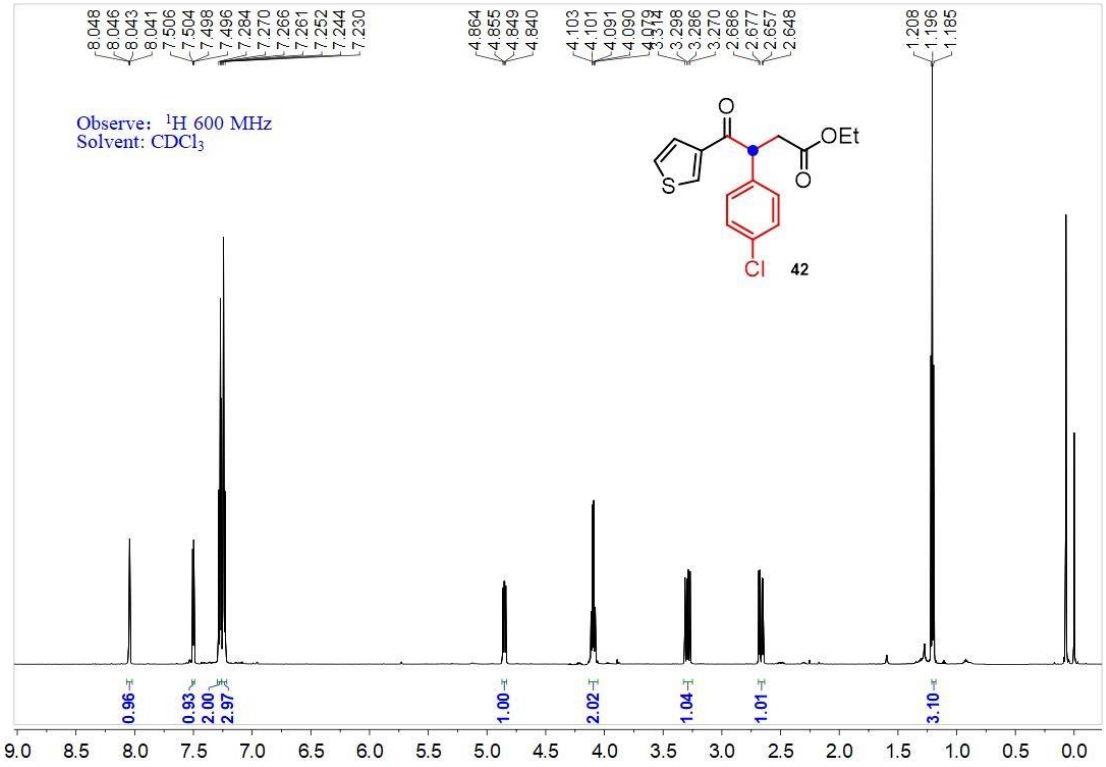

Figure S81. ^{1}H NMR spectrum of compound **42**, related to **Figure 2B.**

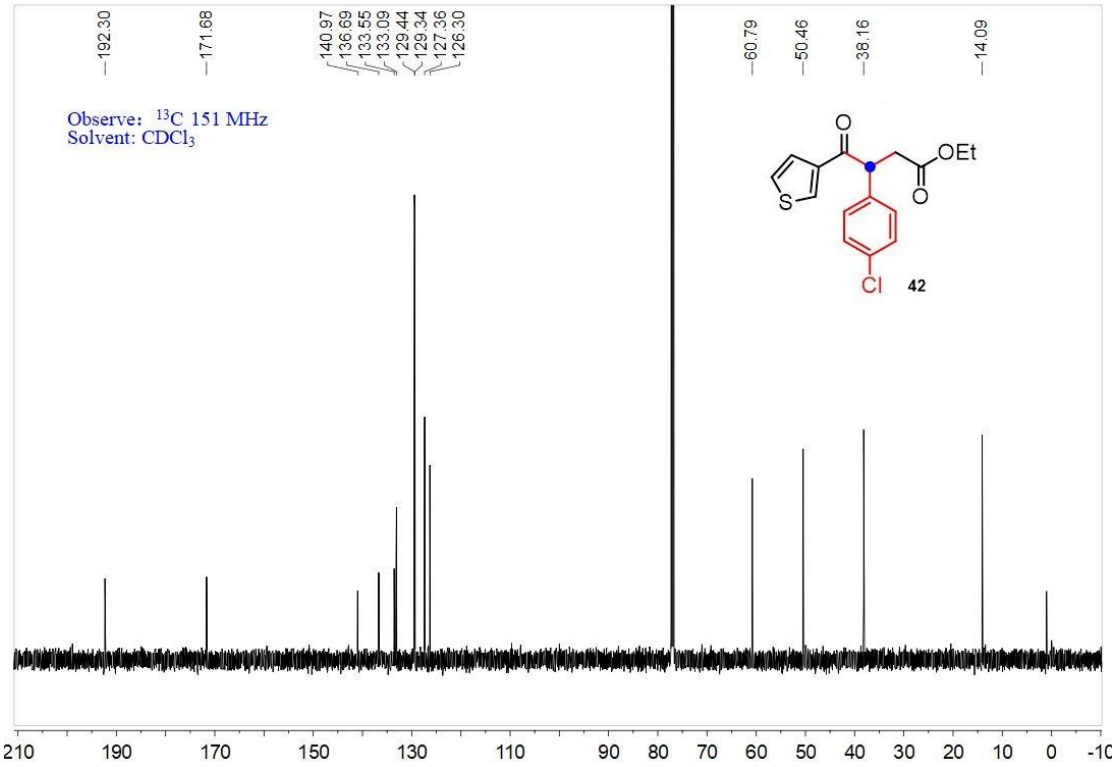

Figure S82. ^{13}C NMR spectrum of compound **42**, related to **Figure 2B.**

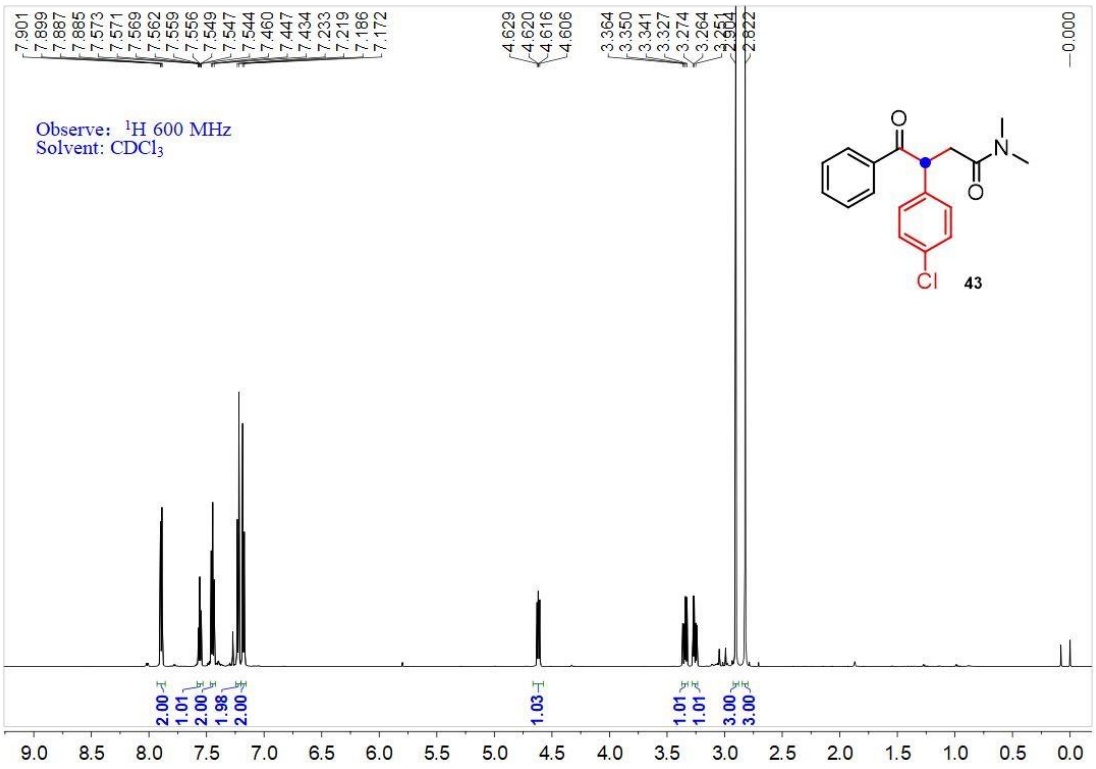

Figure S83. ^{1}H NMR spectrum of compound **43**, related to **Figure 2B.**

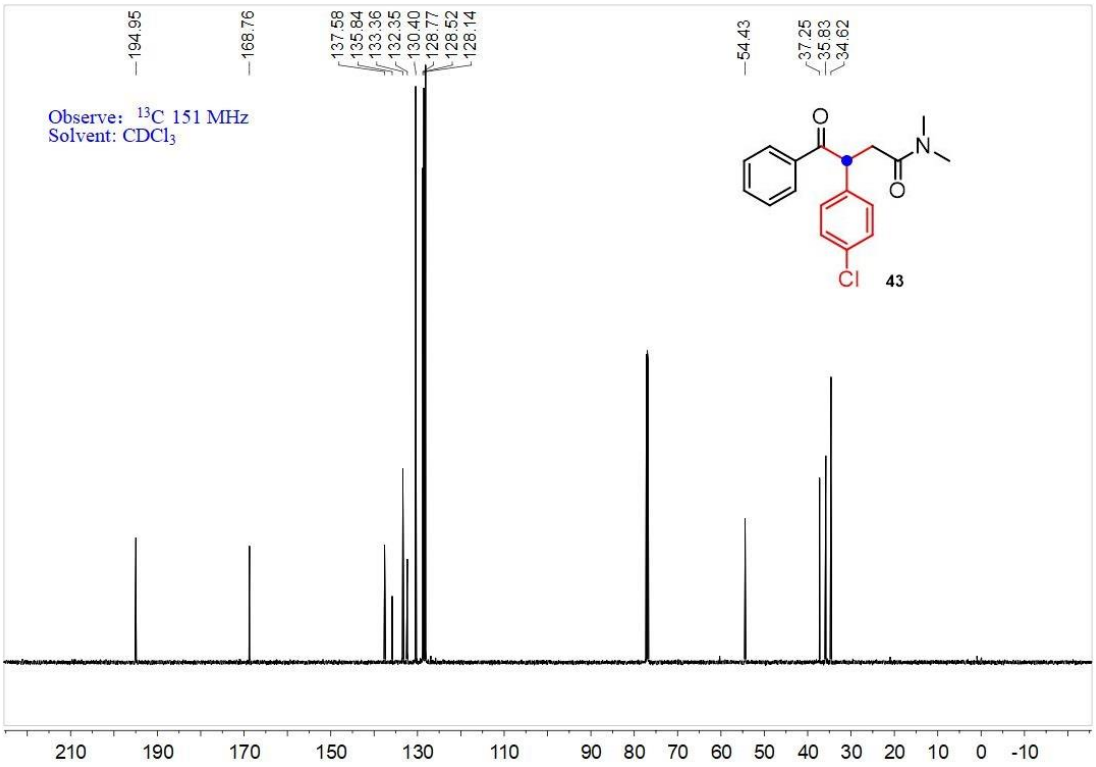

Figure S84. ^{13}C NMR spectrum of compound **43**, related to **Figure 2B.**

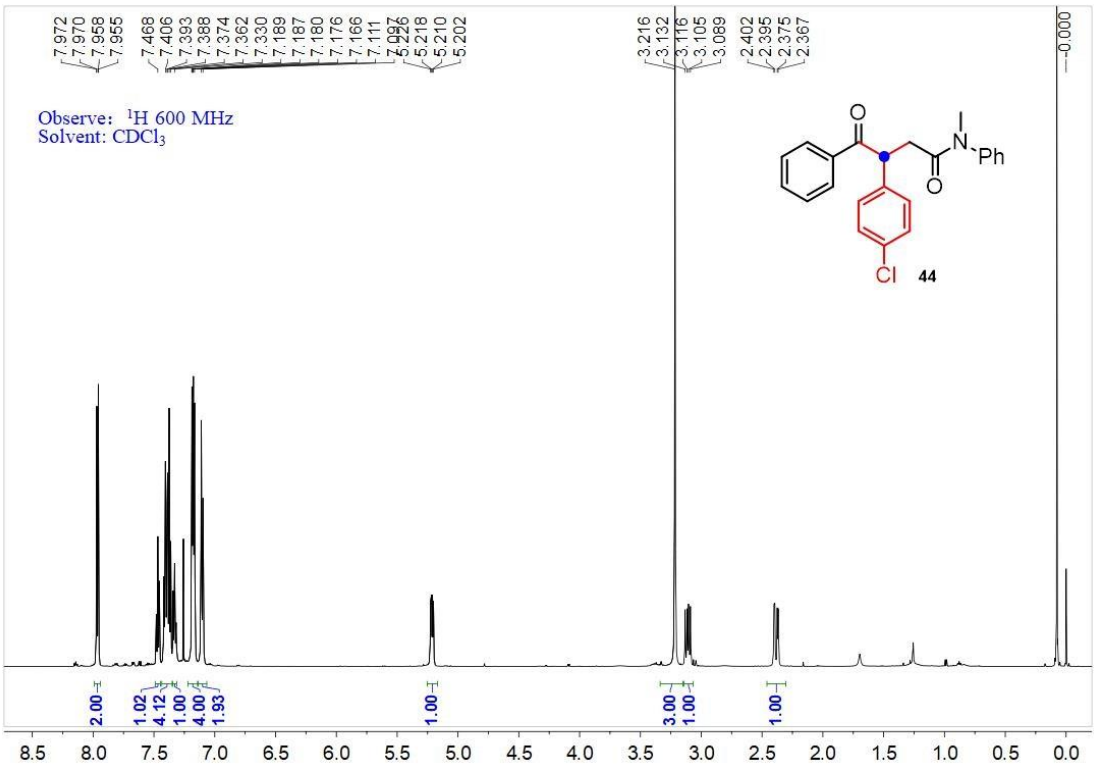

Figure S85. ^{1}H NMR spectrum of compound **44**, related to **Figure 2B.**

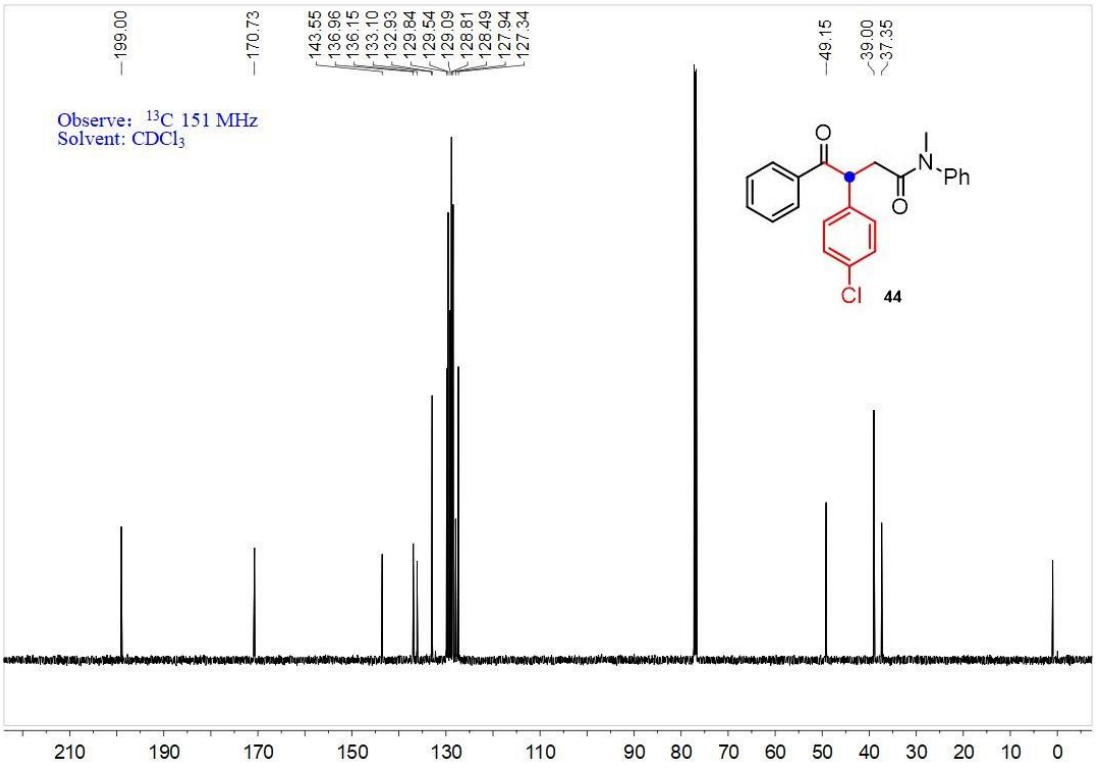

Figure S86. ^{13}C NMR spectrum of compound **44**, related to **Figure 2B.**

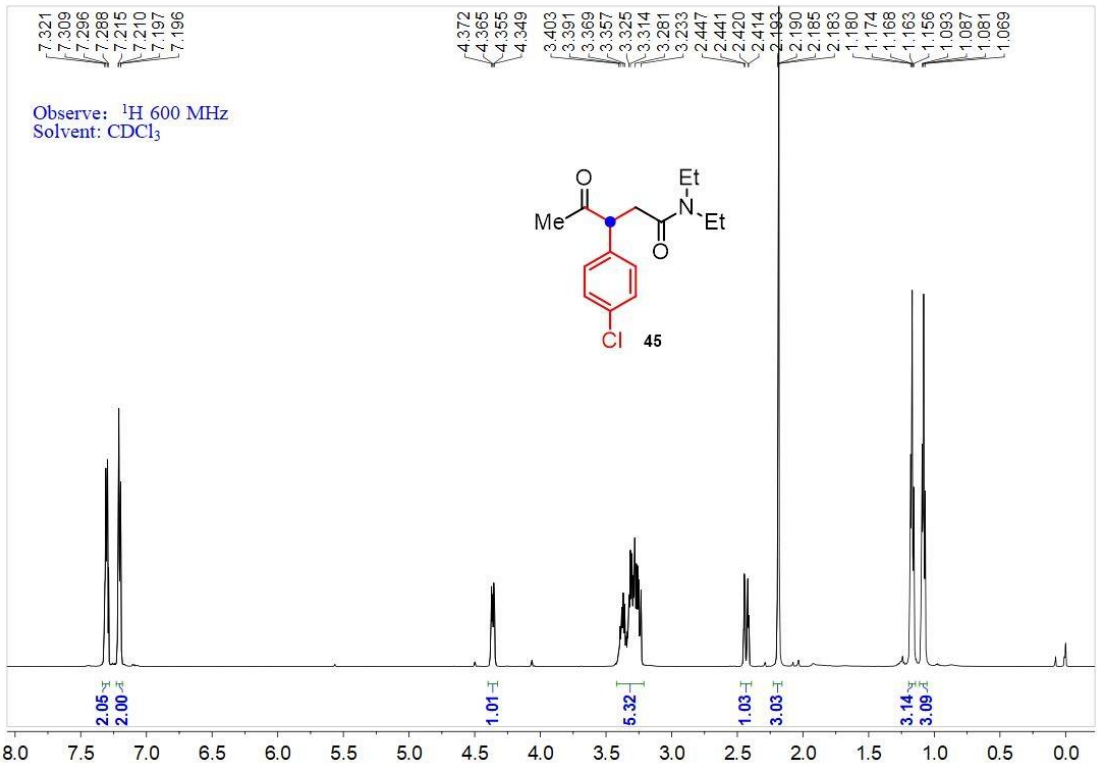

Figure S87. ^{1}H NMR spectrum of compound **45**, related to **Figure 2B.**

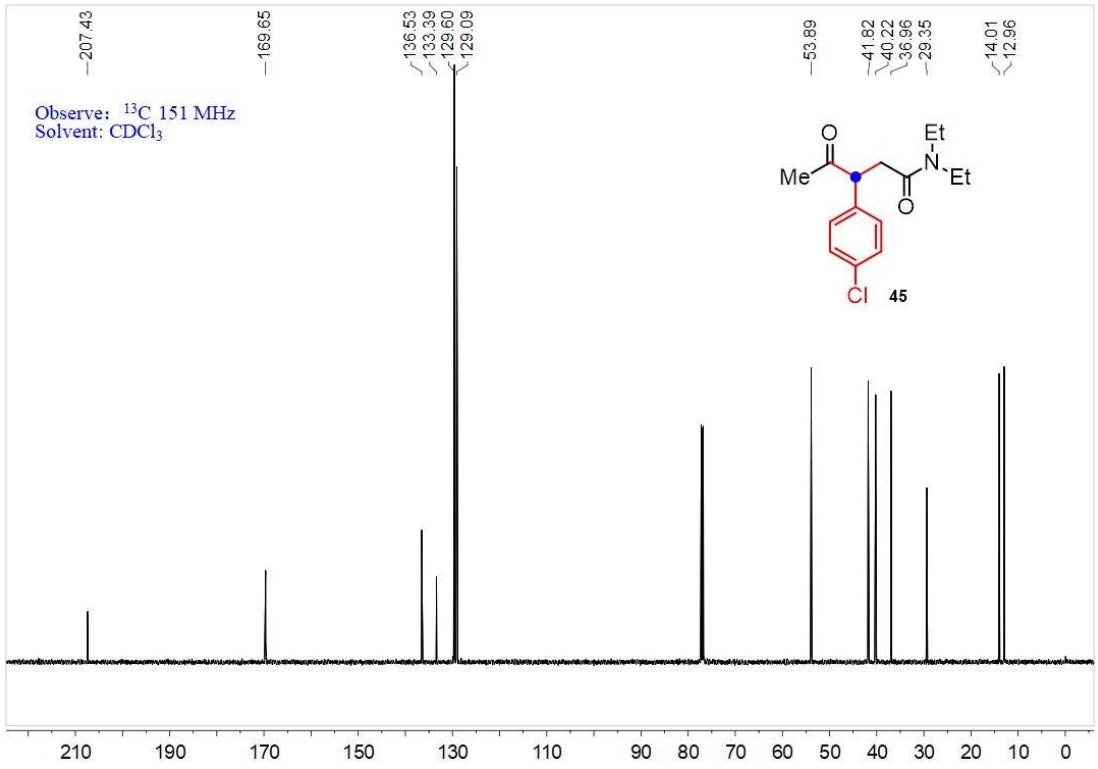

Figure S88. ^{13}C NMR spectrum of compound **45**, related to **Figure 2B.**

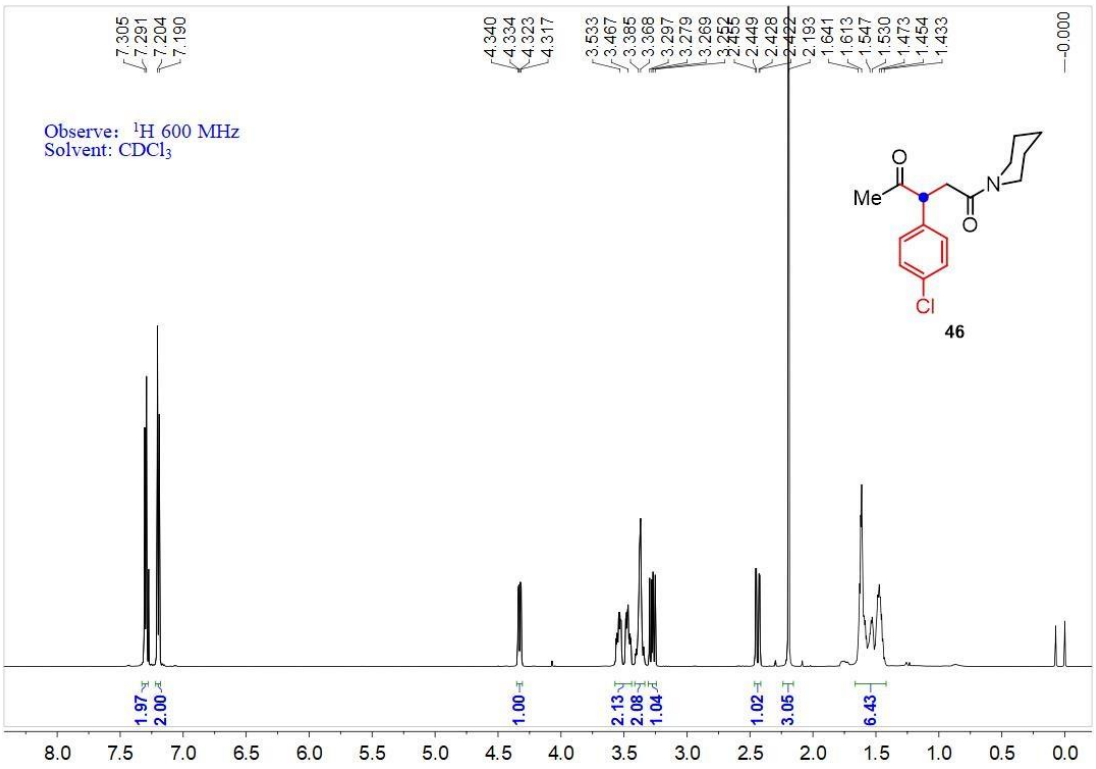

Figure S89. ^{1}H NMR spectrum of compound **46**, related to **Figure 2B.**

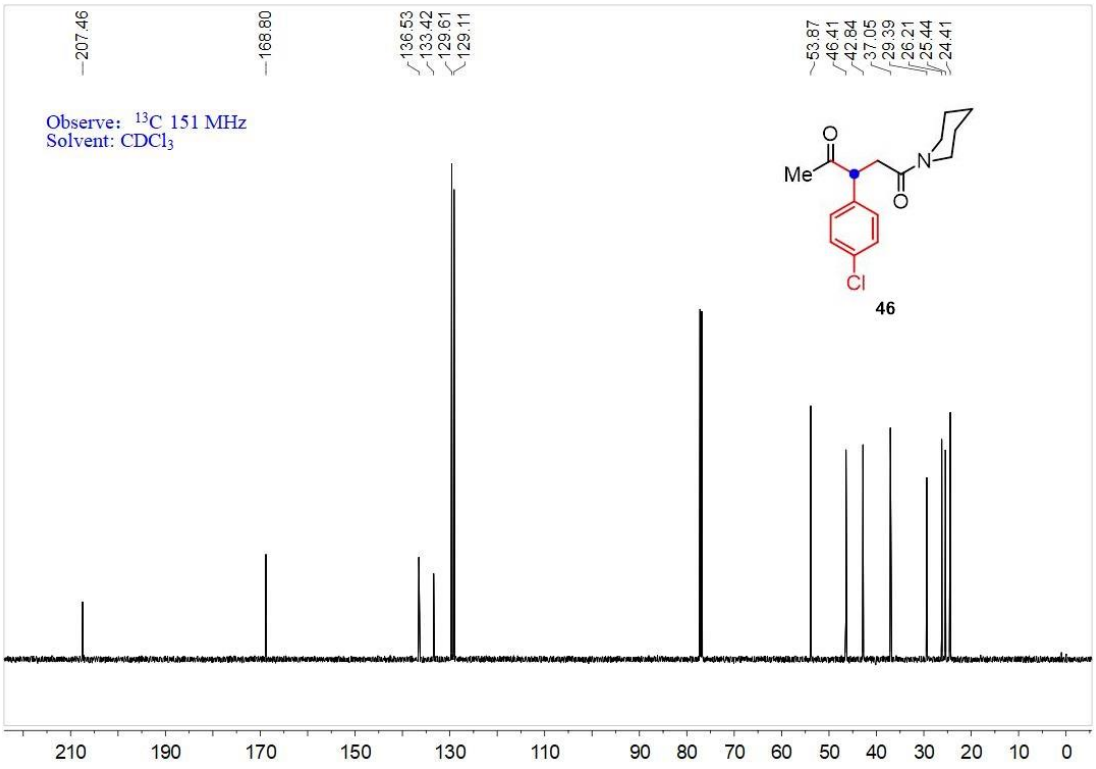

Figure S90. ^{13}C NMR spectrum of compound **46**, related to **Figure 2B.**

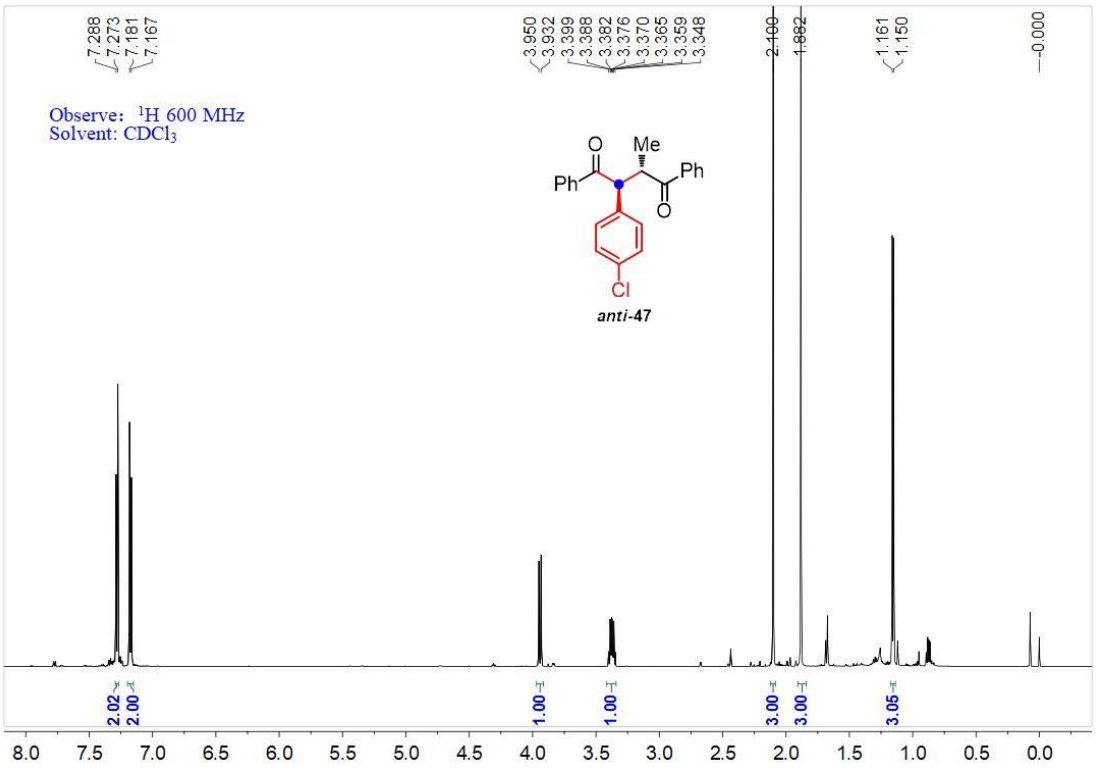

Figure S91. ^{1}H NMR spectrum of compound ***anti-47***, related to **Figure 2C.**

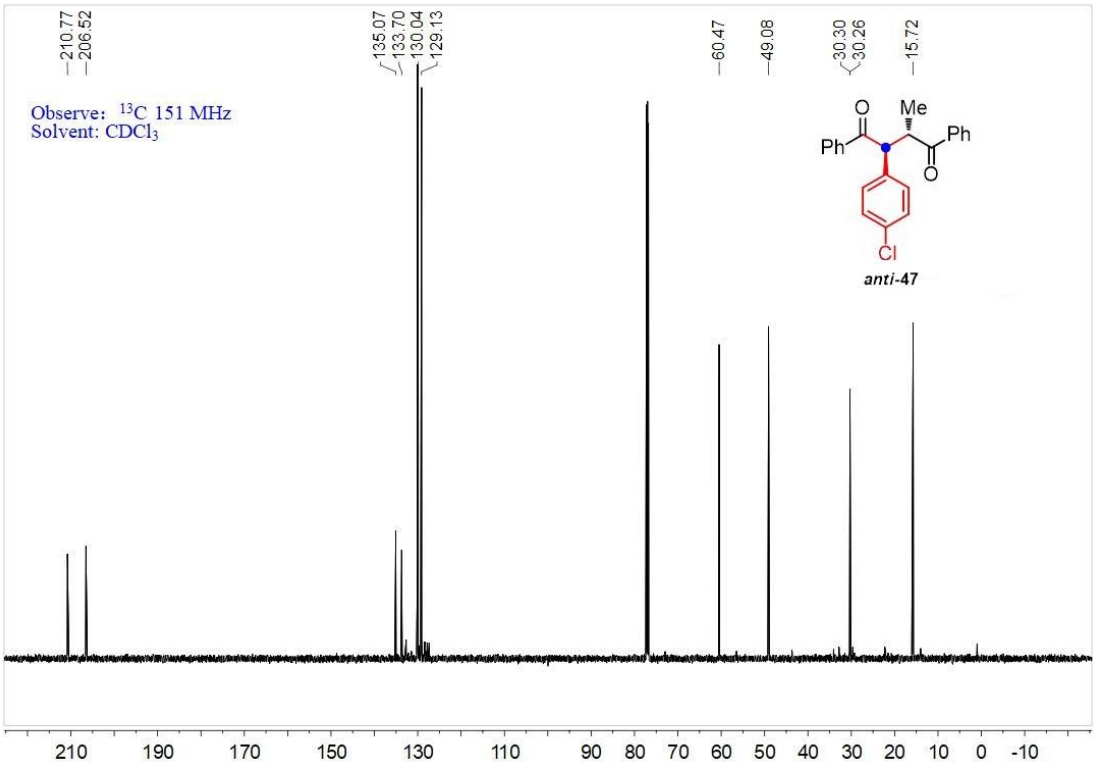

Figure S92. ^{13}C NMR spectrum of compound ***anti*-47**, related to **Figure 2C.**

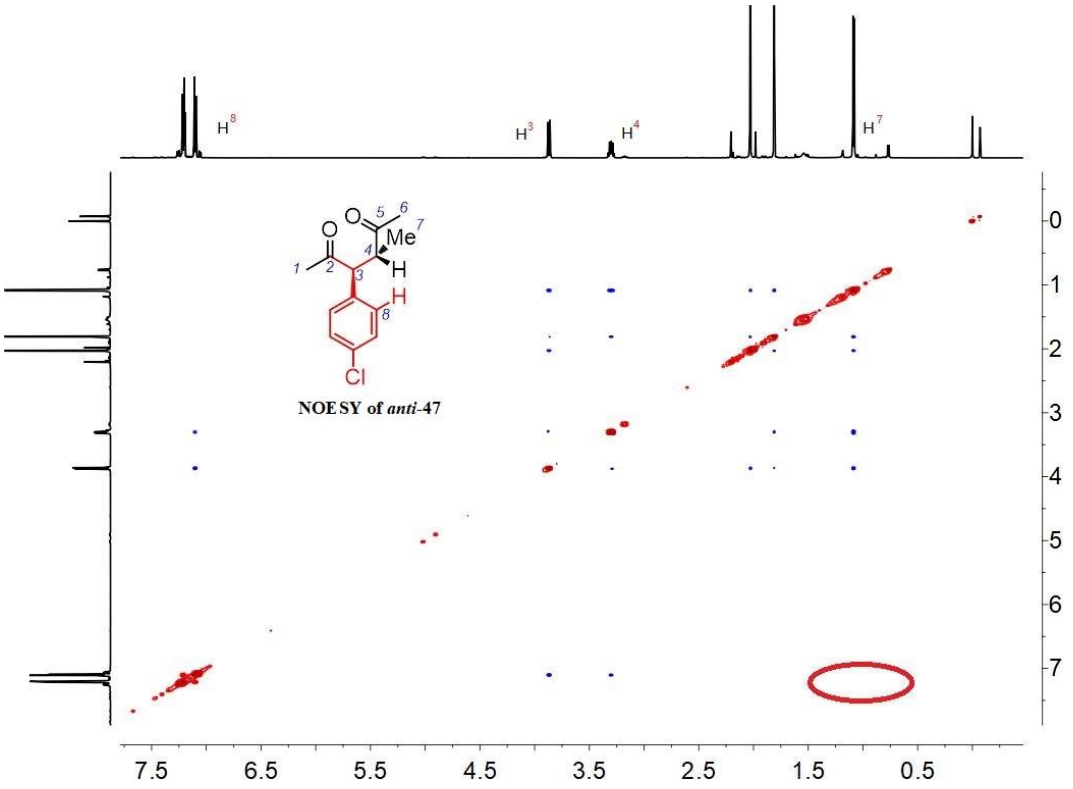

Figure S93. NOE spectrum of compound ***anti-47***, related to **Figure 2C.**

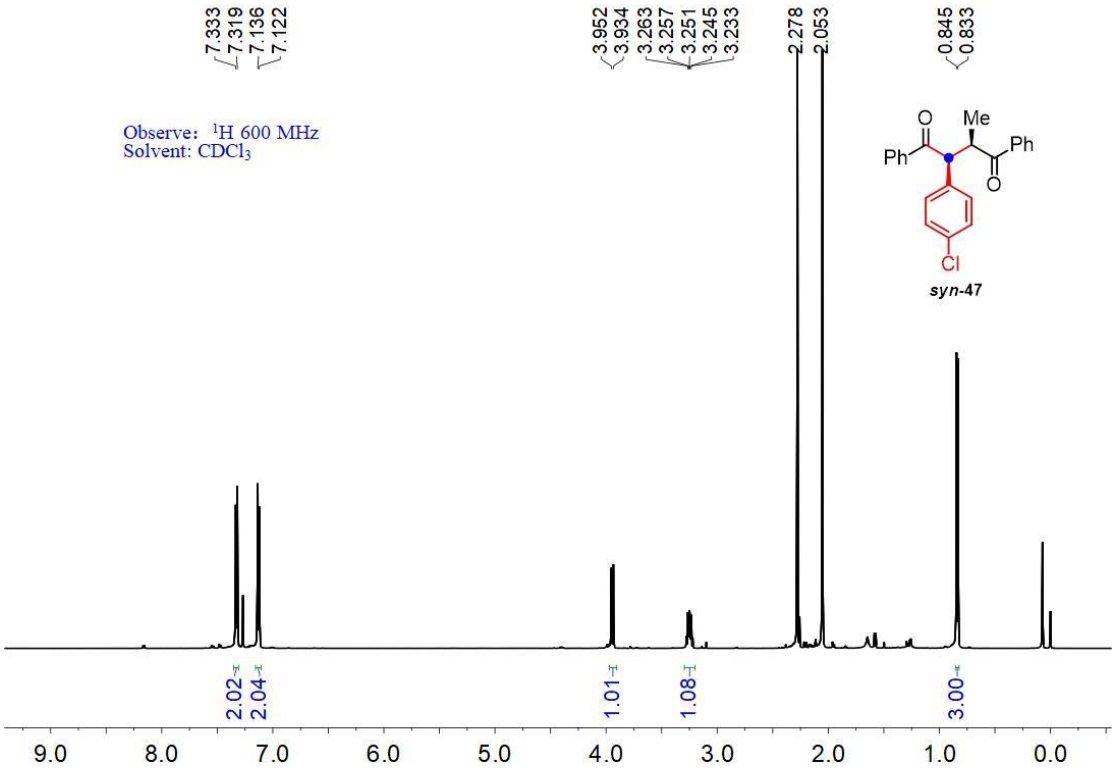

Figure S94. ^{1}H NMR spectrum of compound ***syn*-47**, related to **Figure 2C.**

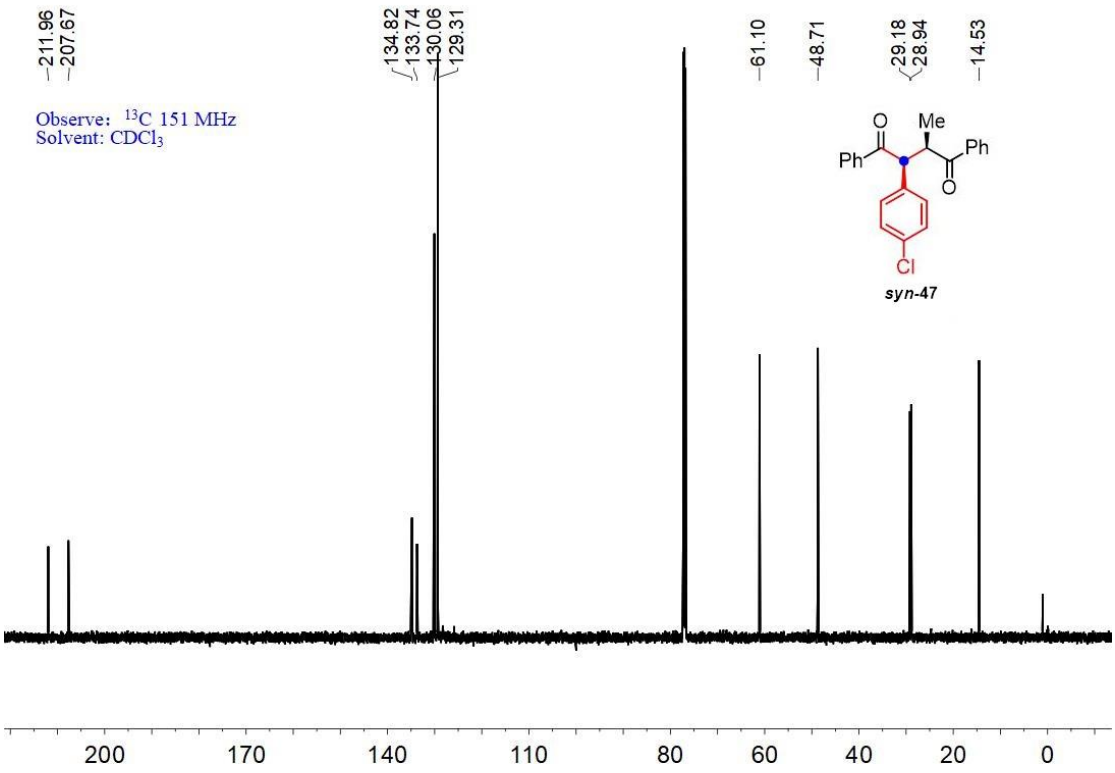

Figure S95. ^{13}C NMR spectrum of compound ***syn-47***, related to **Figure 2C.**

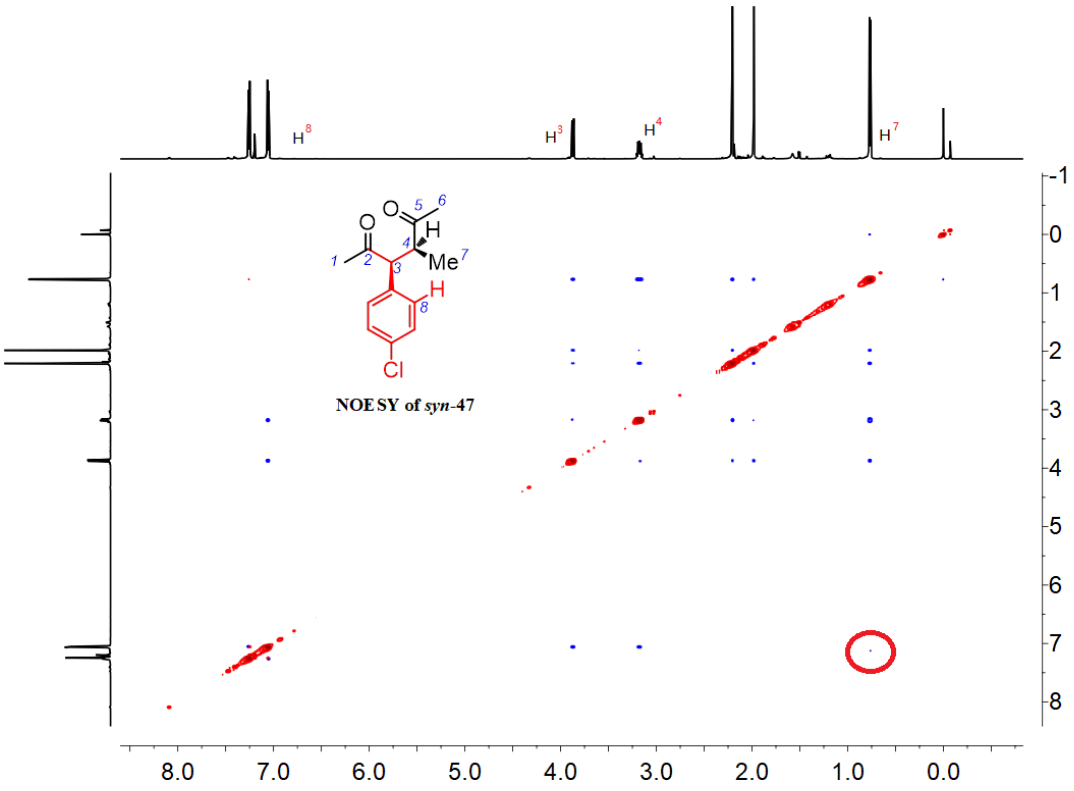

Figure S96. NOE spectrum of compound ***anti-47***, related to **Figure 2C.**

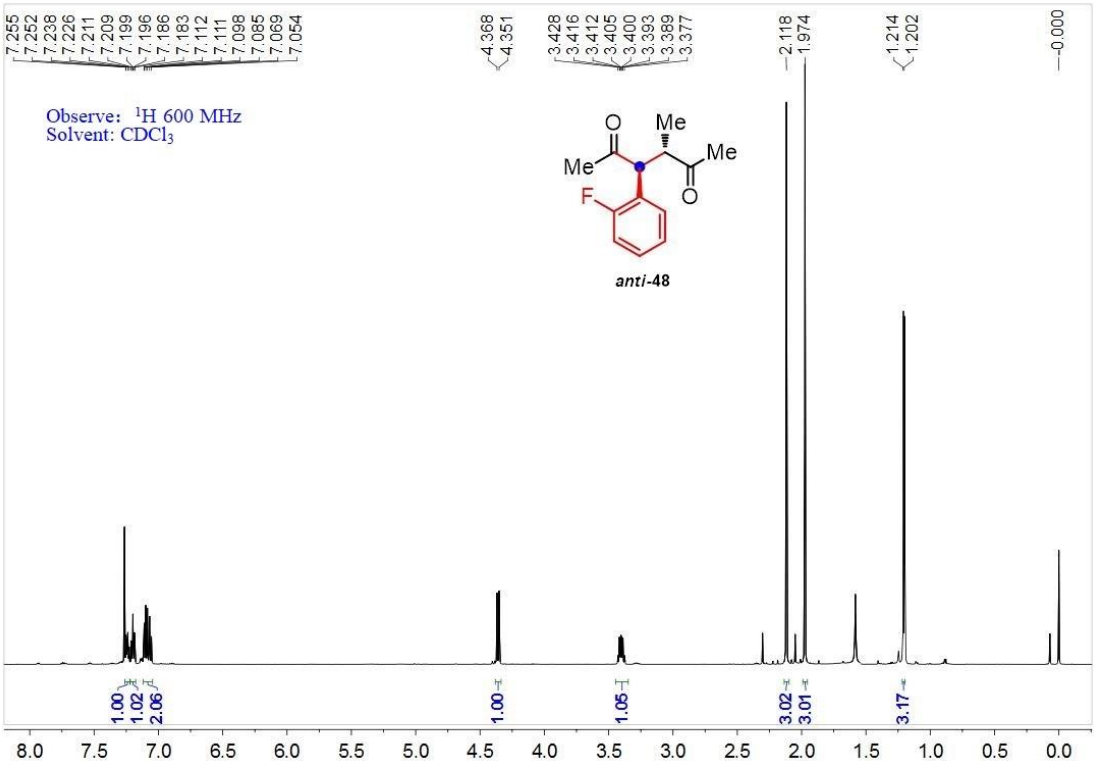

Figure S97. ^{1}H NMR spectrum of compound ***anti-48***, related to **Figure 2C.**

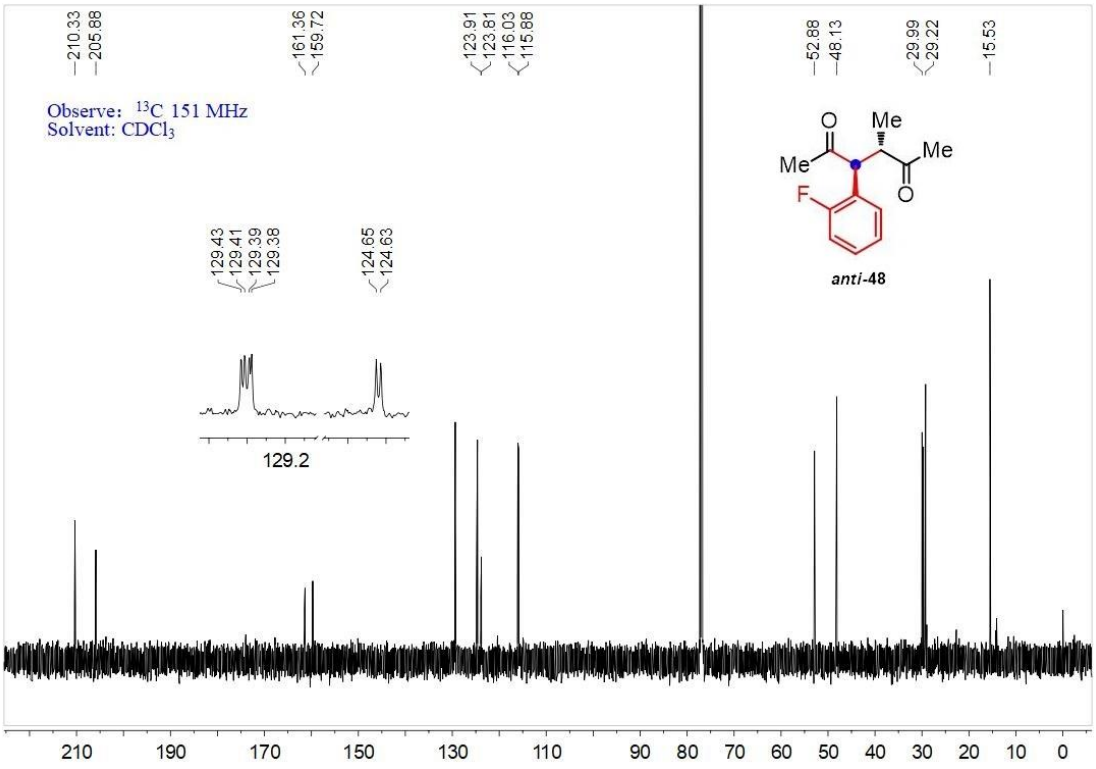

Figure S98. ^{13}C NMR spectrum of compound ***anti-48***, related to **Figure 2C.**

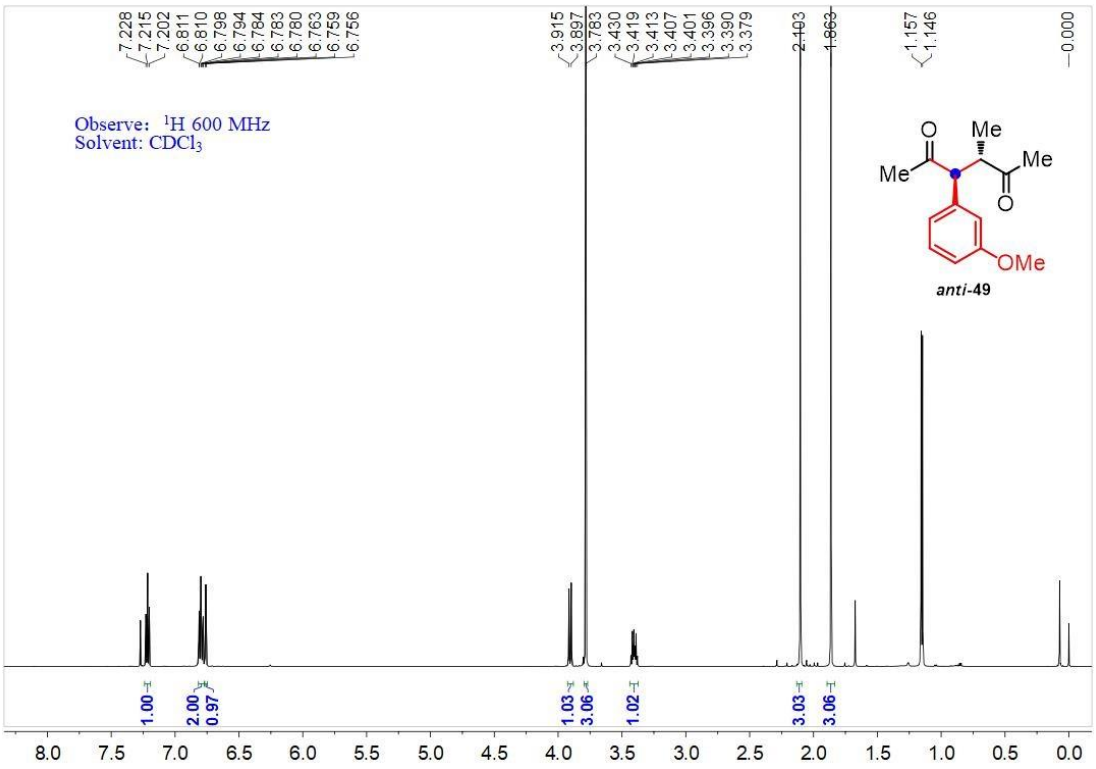

Figure S99. ^{1}H NMR spectrum of compound ***anti-49***, related to **Figure 2C.**

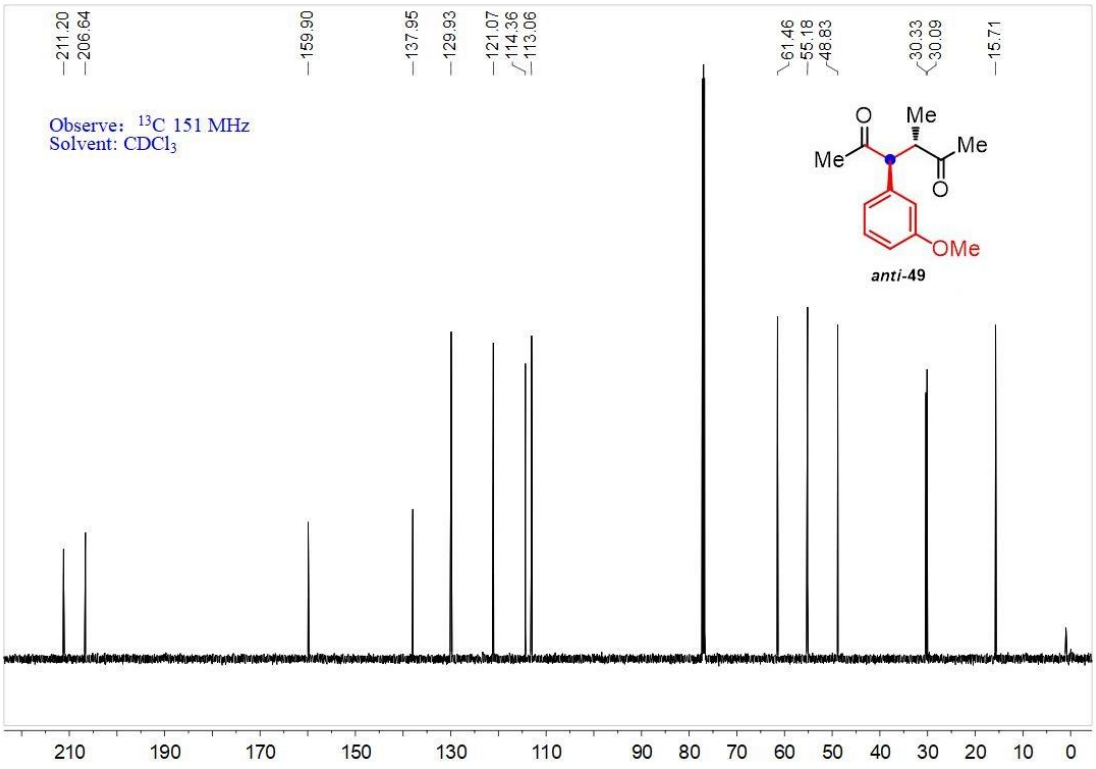

Figure S100. ^{13}C NMR spectrum of compound ***anti-49***, related to **Figure 2C.**

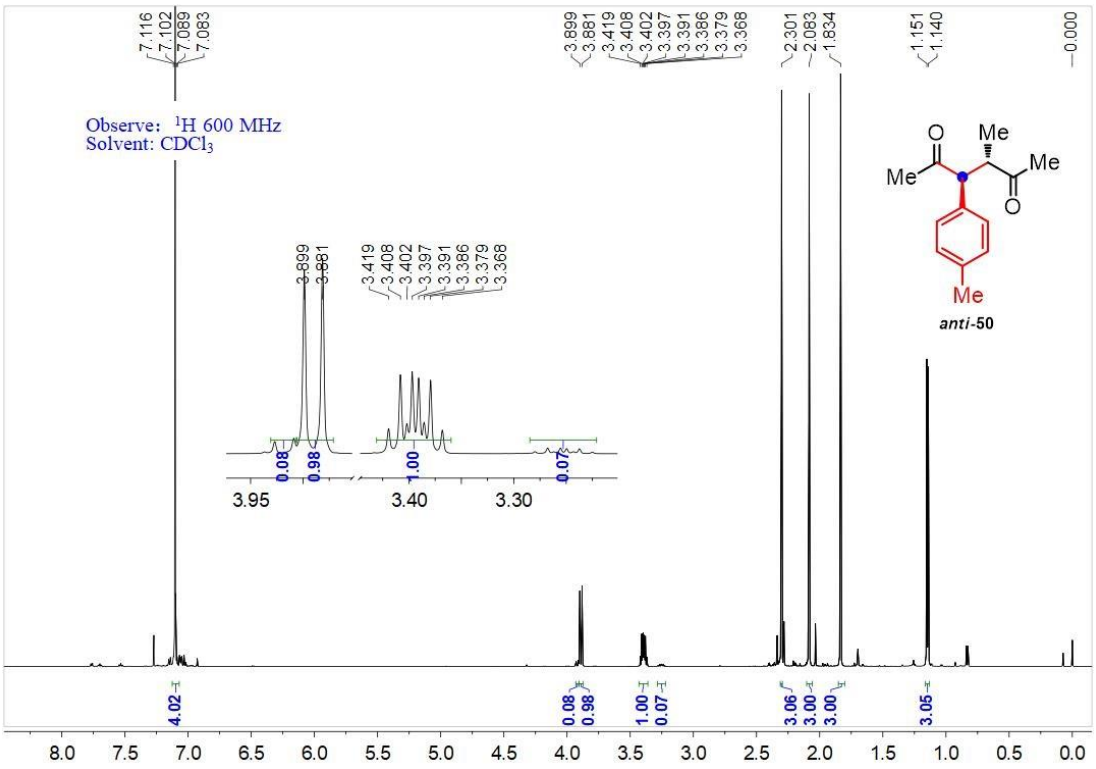

Figure S101. ^{1}H NMR spectrum of compound ***anti-50***, related to **Figure 2C.**

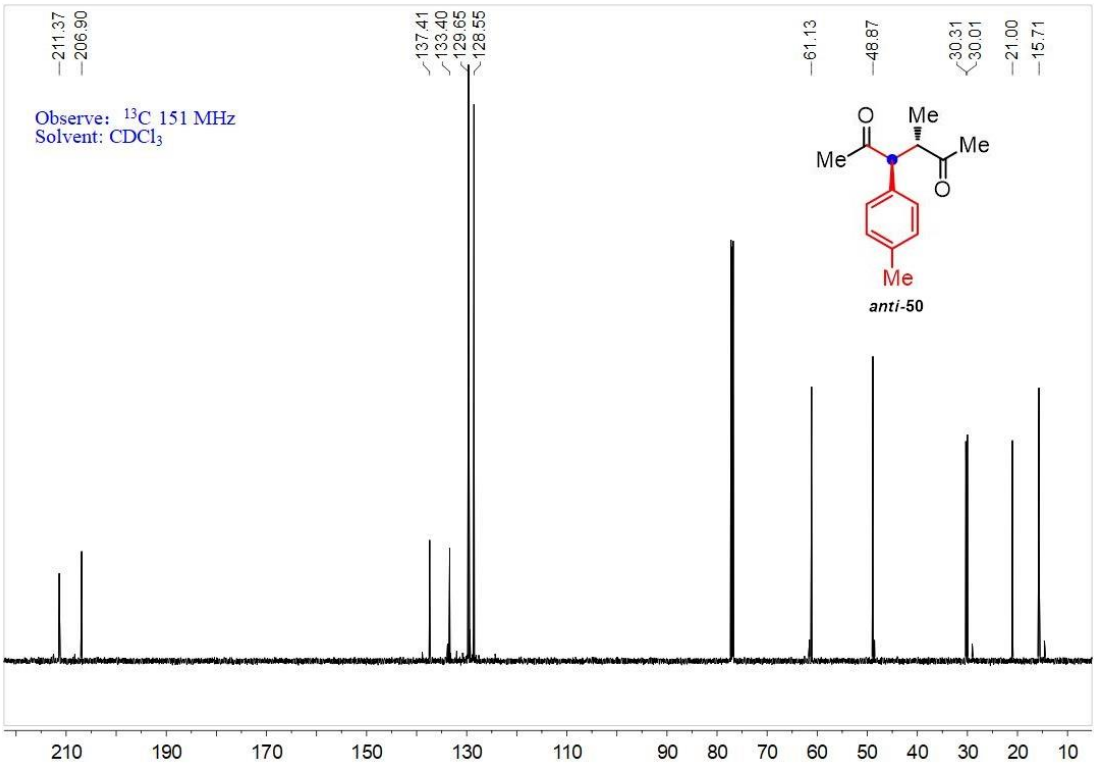

Figure S102. ^{13}C NMR spectrum of compound ***anti-50***, related to **Figure 2C.**

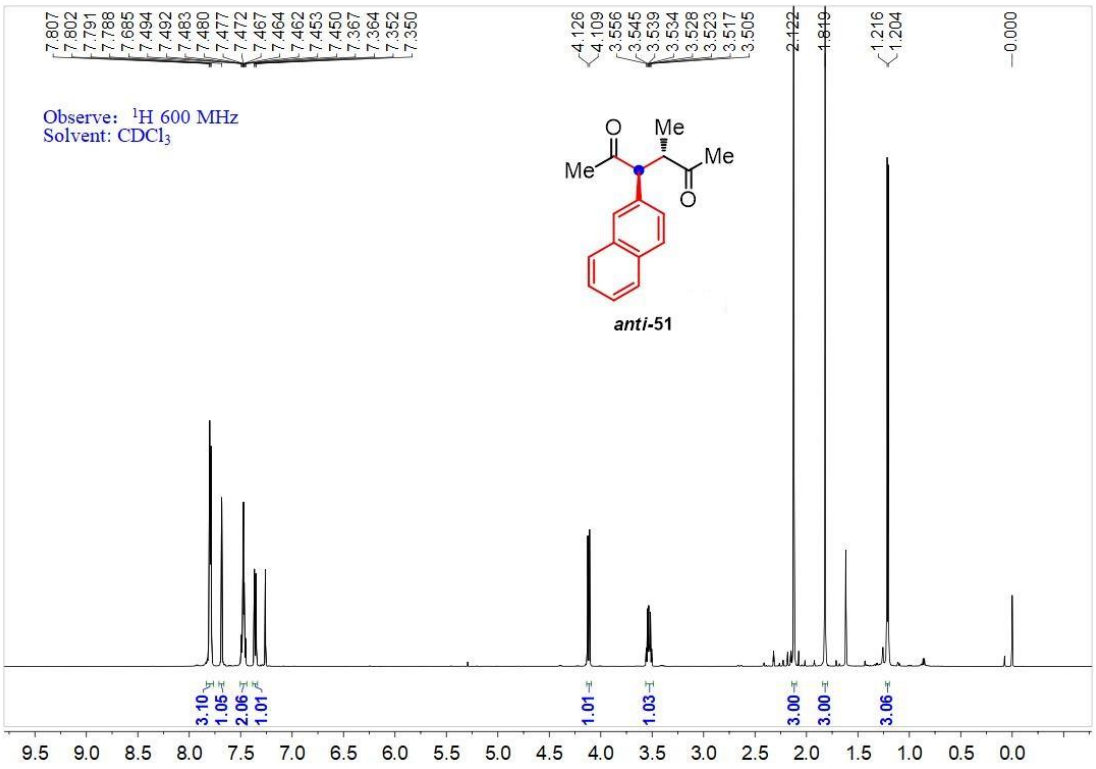

Figure S103. ^{1}H NMR spectrum of compound ***anti-51***, related to **Figure 2C.**

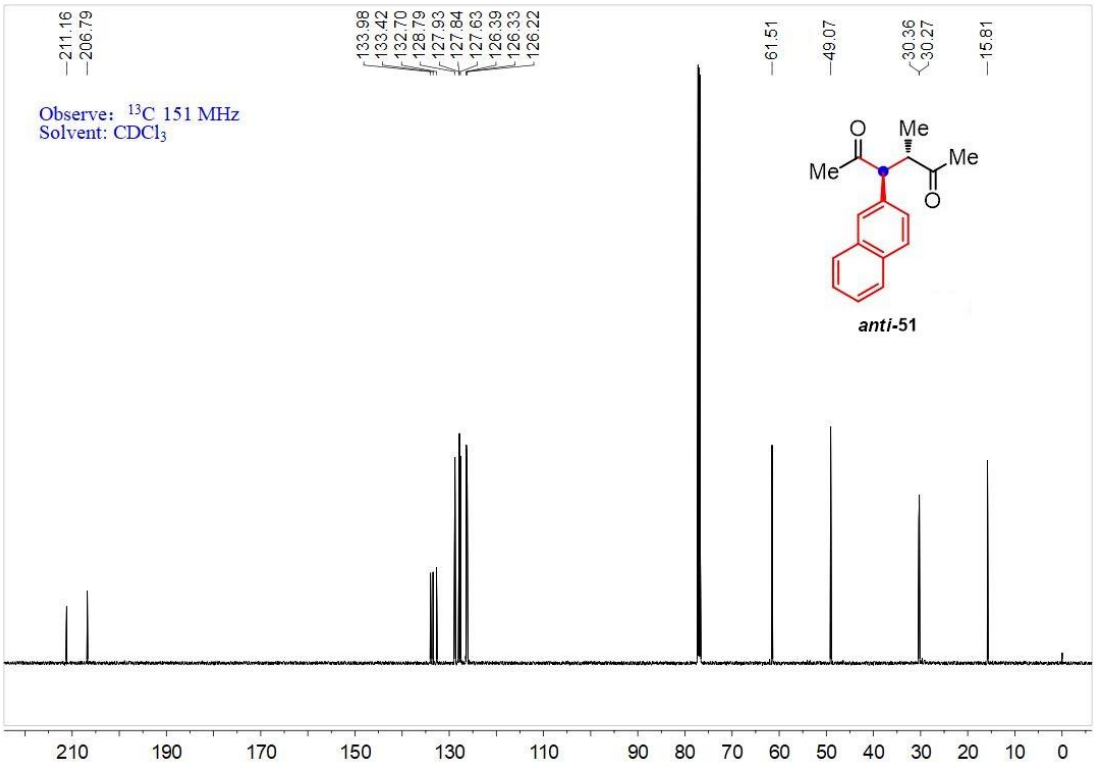

Figure S104. ^{13}C NMR spectrum of compound ***anti-51***, related to **Figure 2C.**

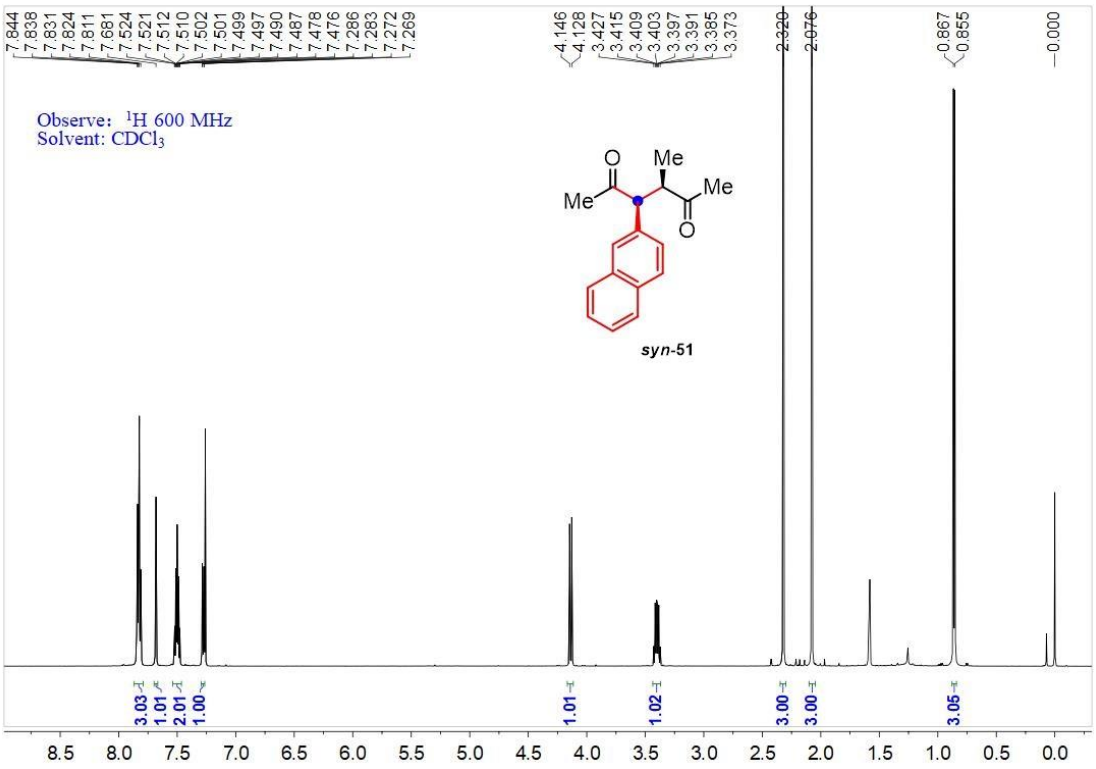

Figure S105. [1]H NMR spectrum of compound ***syn-51***, related to **Figure 2C.**

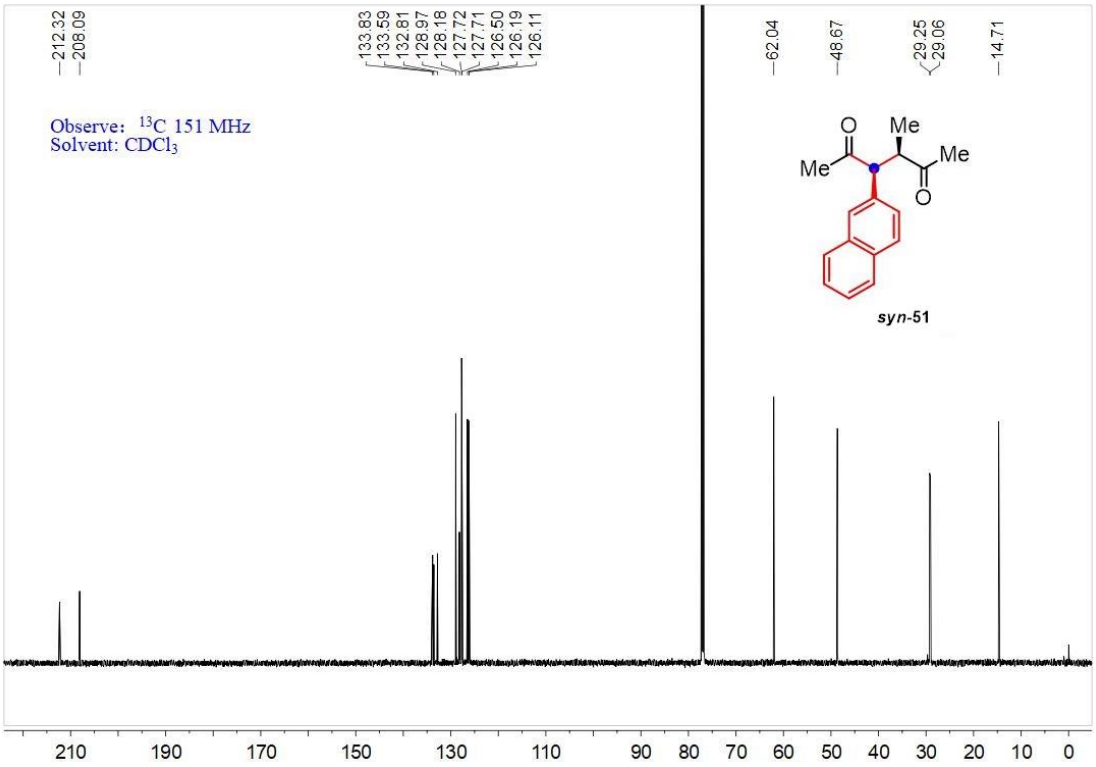

Figure S106. [13]C NMR spectrum of compound ***syn-51***, related to **Figure 2C.**

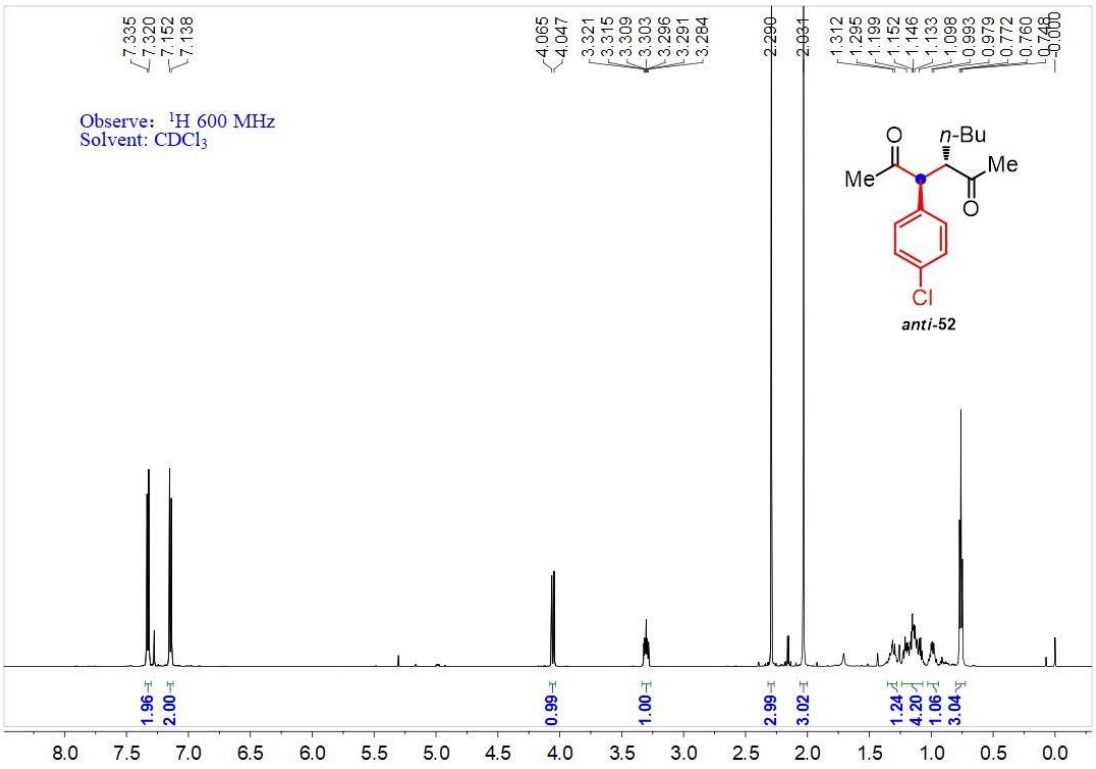

Figure S107. ^{1}H NMR spectrum of compound ***anti-52***, related to **Figure 2C.**

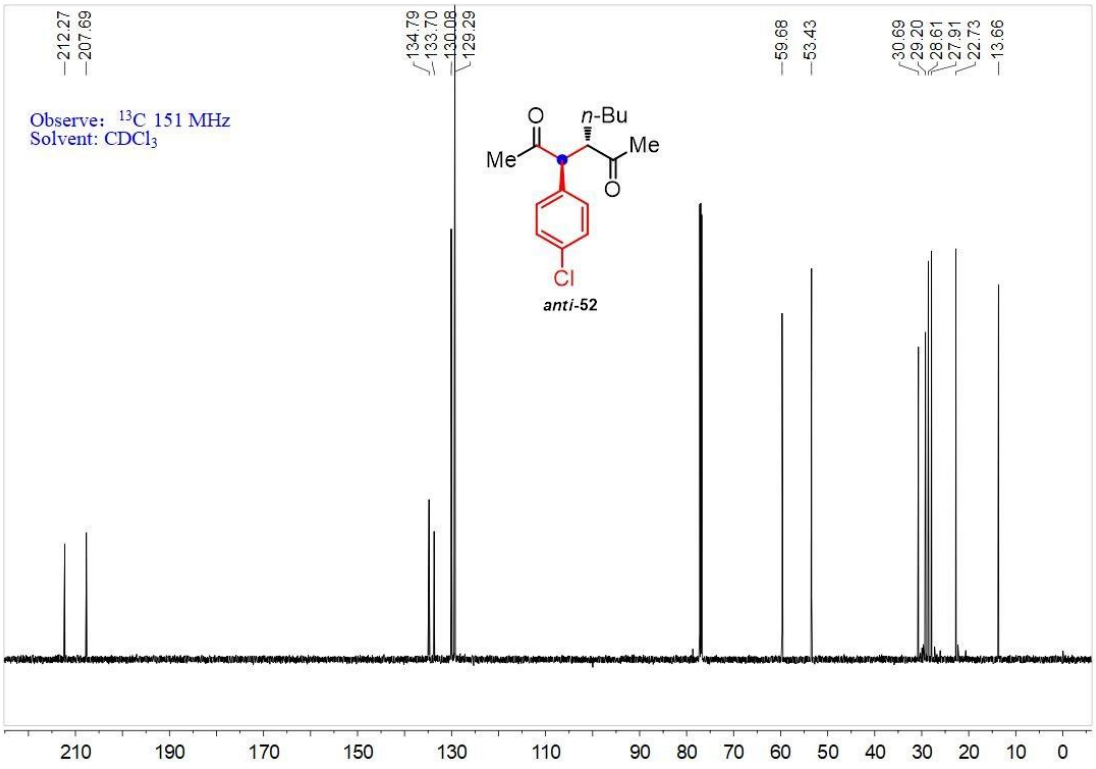

Figure S108. ^{13}C NMR spectrum of compound ***anti*-52**, related to **Figure 2C.**

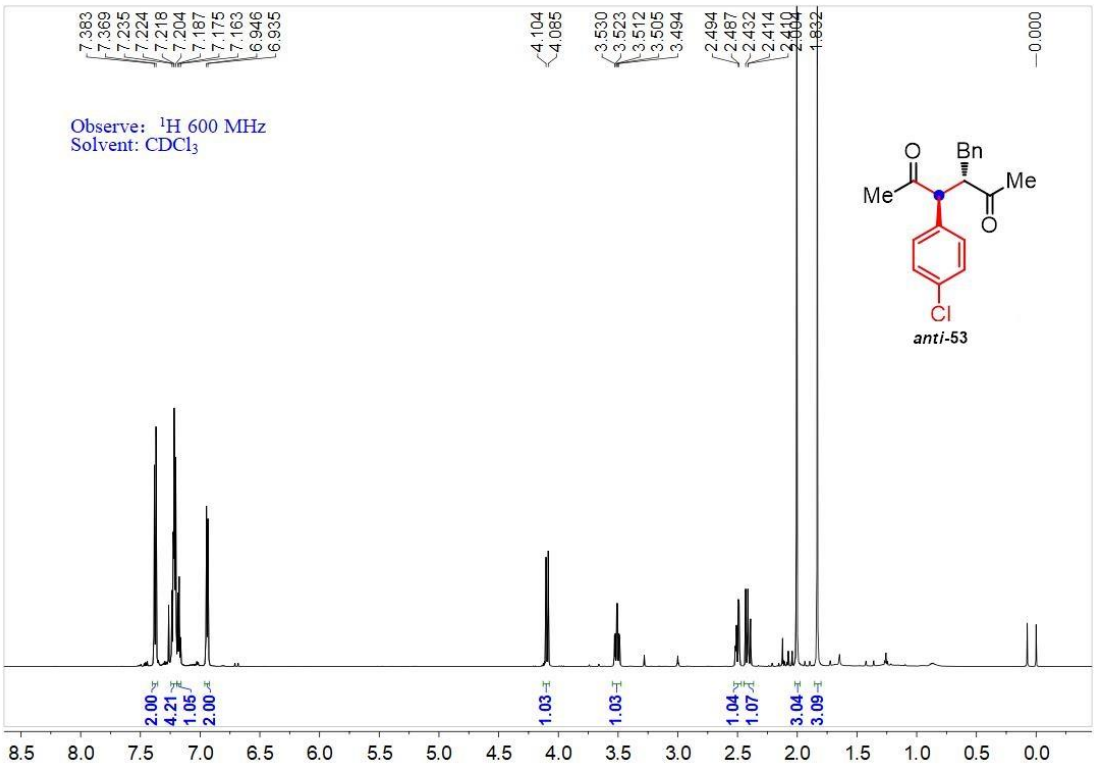

Figure S109. [1]H NMR spectrum of compound *anti*-**53**, related to **Figure 2C.**

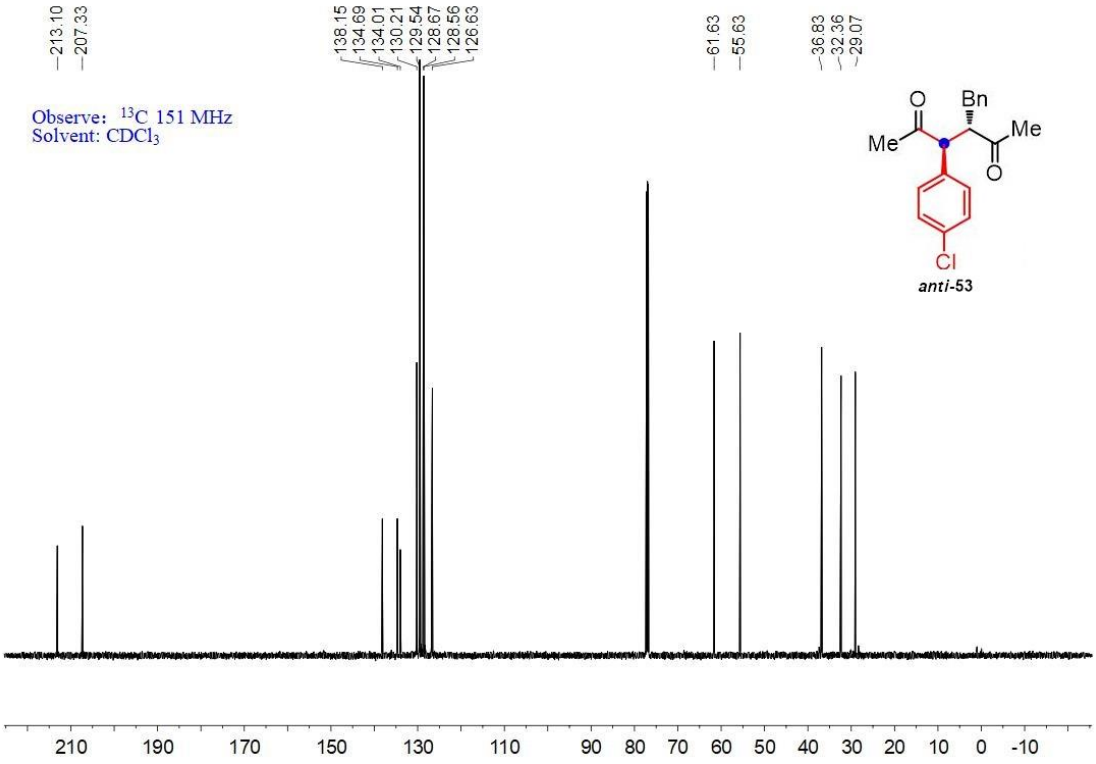

Figure S110. [13]C NMR spectrum of compound *anti*-**53**, related to **Figure 2C.**

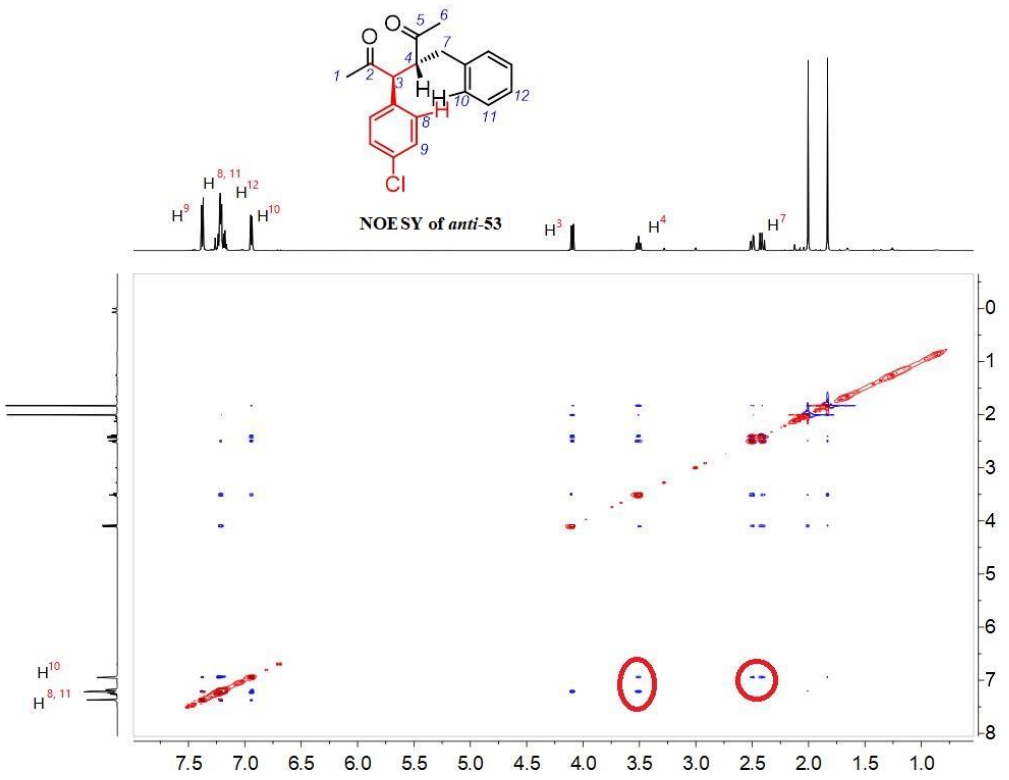

Figure S111. NOE spectrum of compound ***anti*-53**, related to **Figure 2C.**

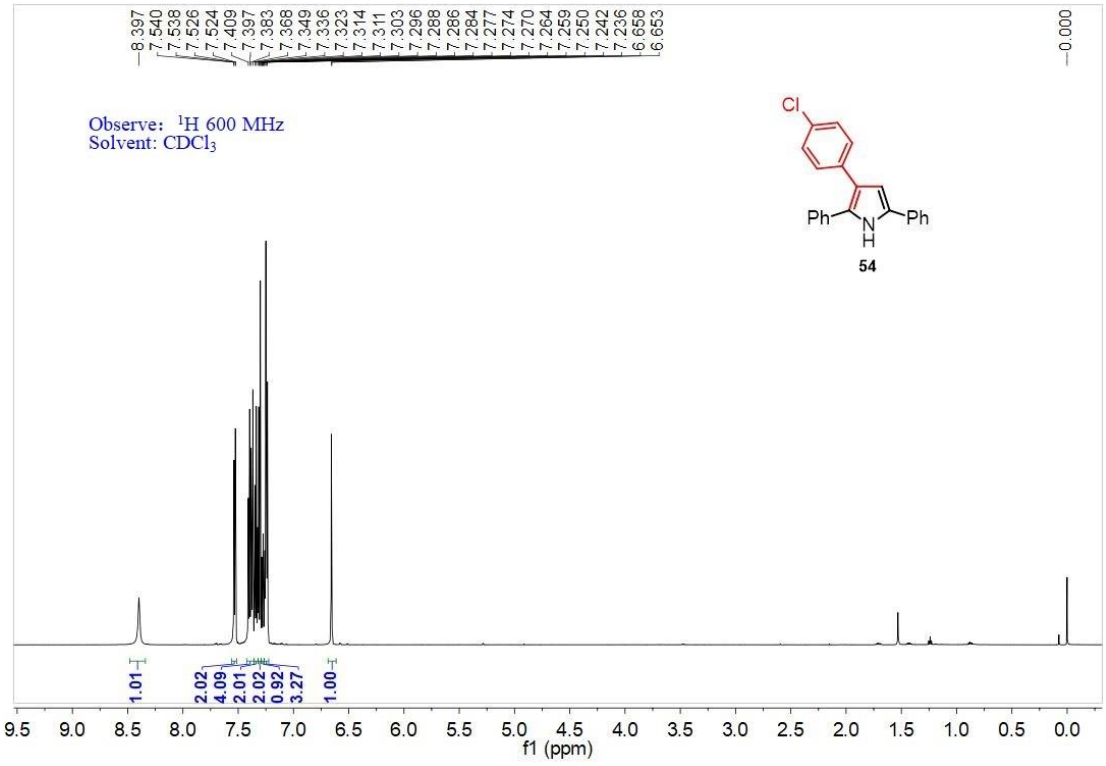

Figure S112. ^{1}H NMR spectrum of compound **54**, related to **Scheme 2.**

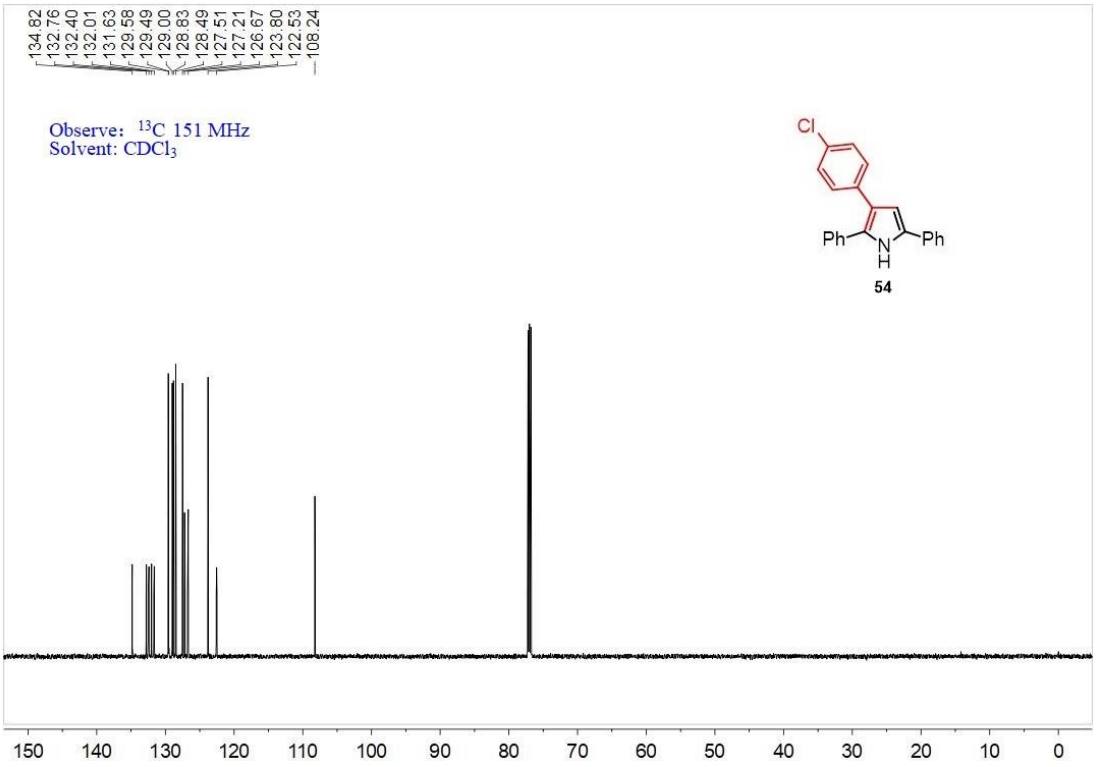

Figure S113. ^{13}C NMR spectrum of compound **54**, related to **Scheme 2.**

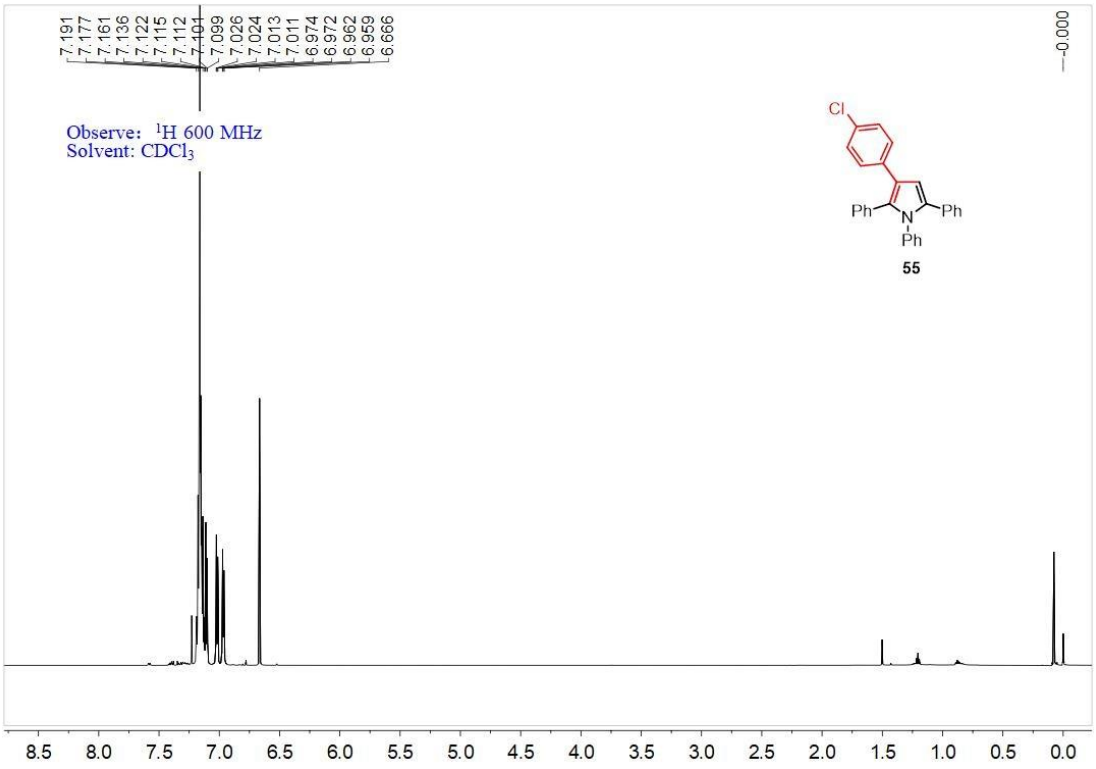

Figure S114. ^{1}H NMR spectrum of compound **55**, related to **Scheme 2.**

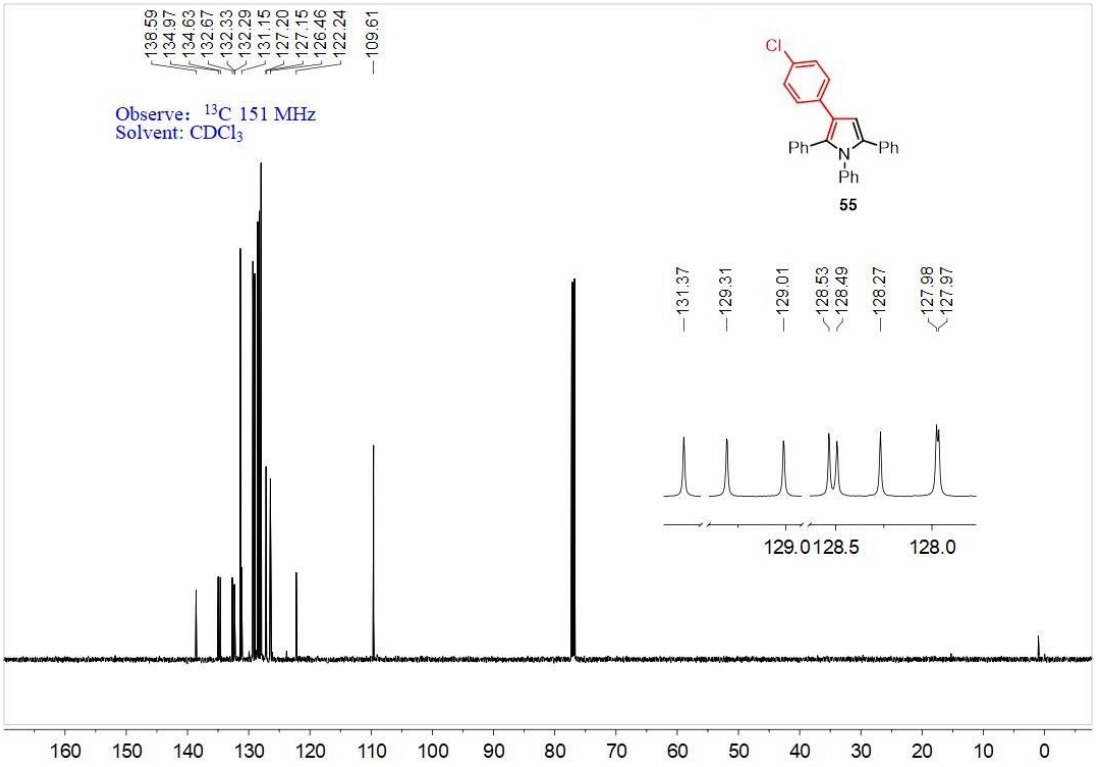

Figure S115. ^{13}C NMR spectrum of compound **55**, related to **Scheme 2.**

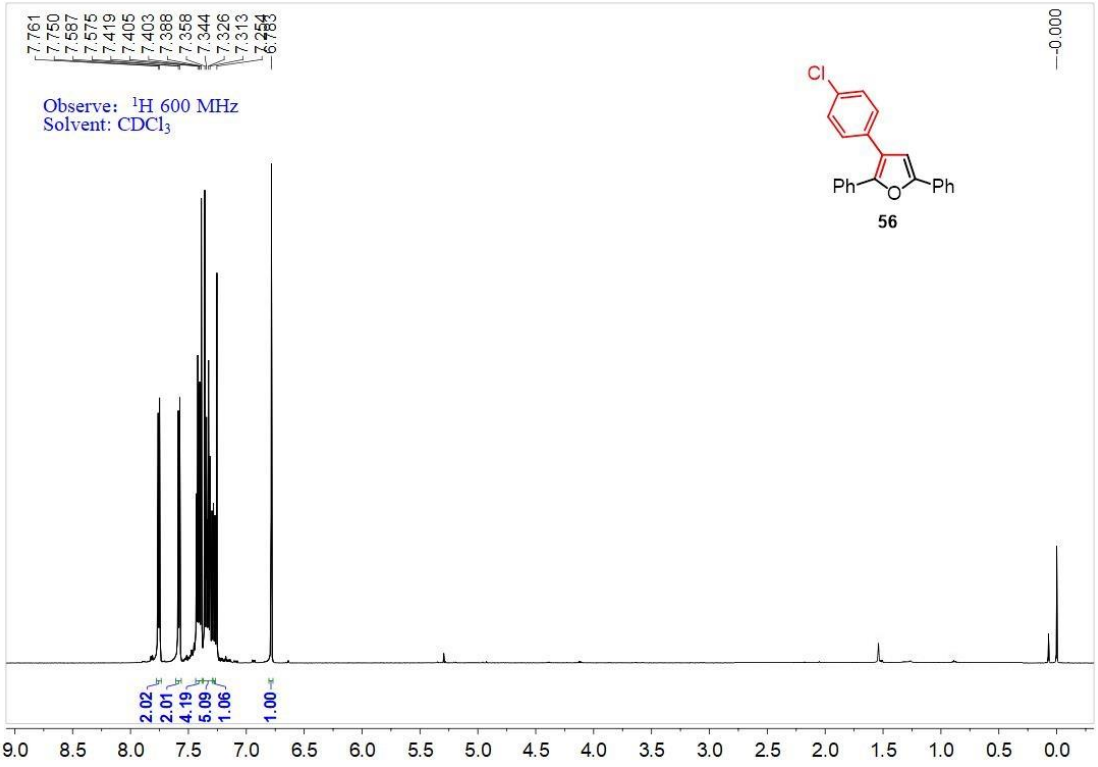

Figure S116. ^{1}H NMR spectrum of compound 5**6**, related to **Scheme 2.**

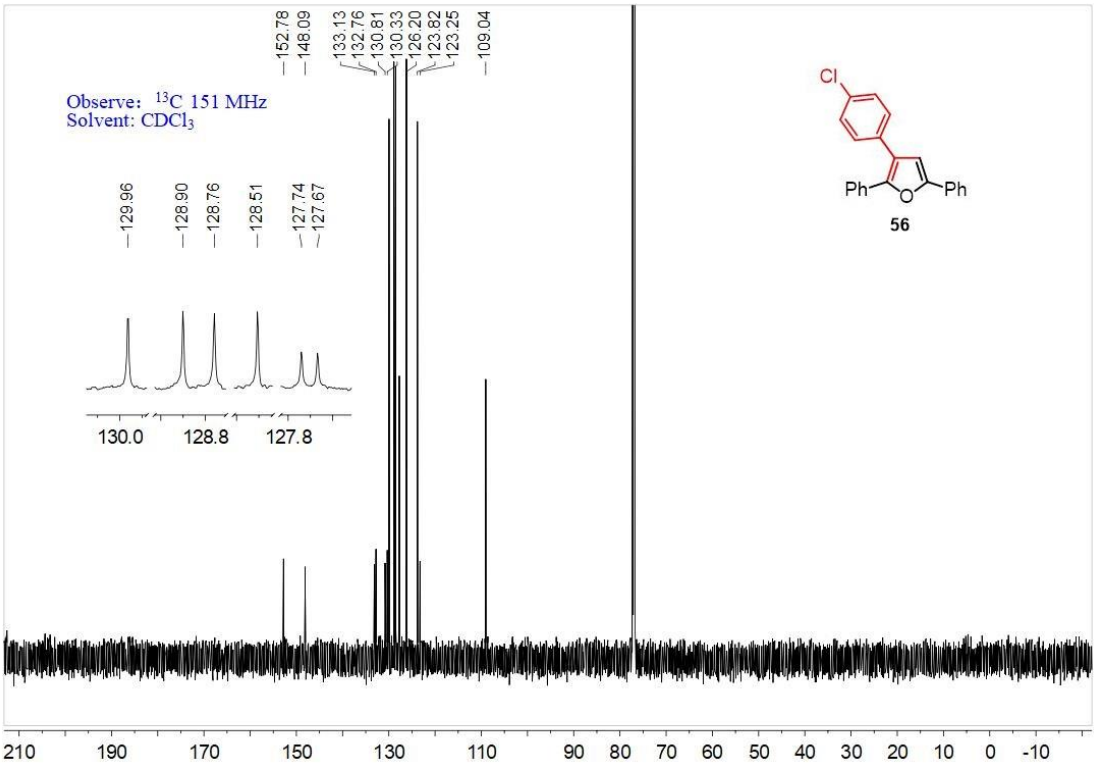

Figure S117. ^{13}C NMR spectrum of compound **56**, related to **Scheme 2.**

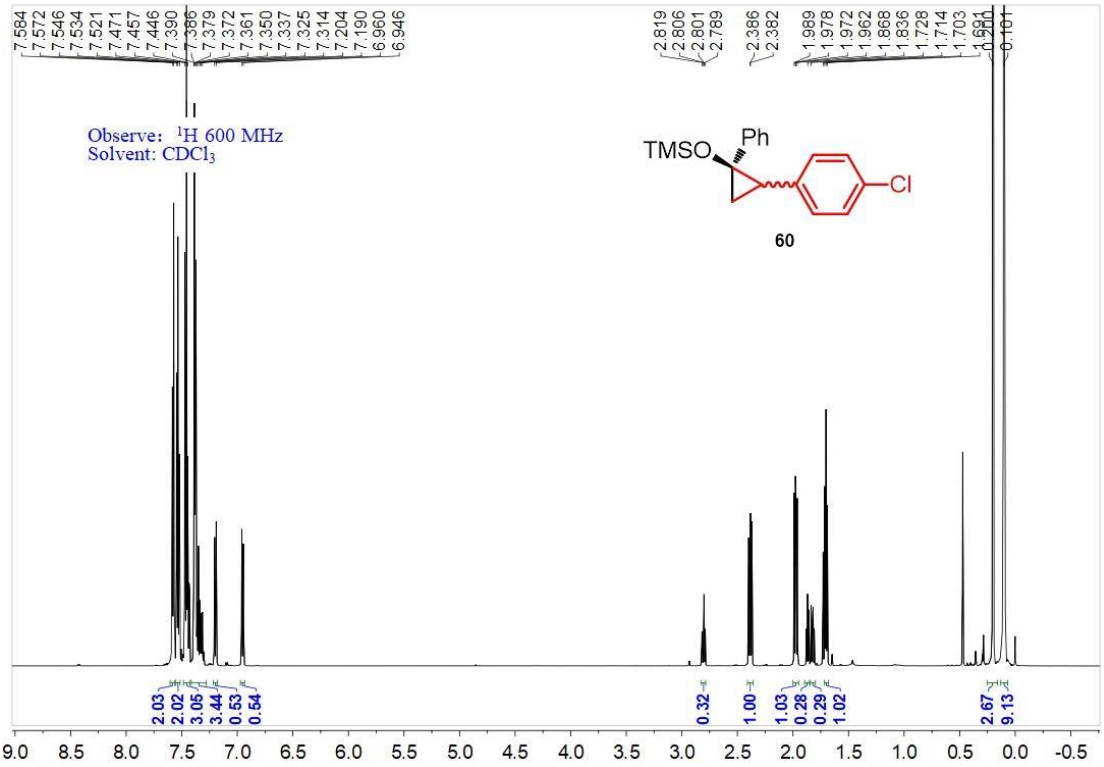

Figure S118. ^{1}H NMR spectrum of compound **60**, related to **Scheme 2.**

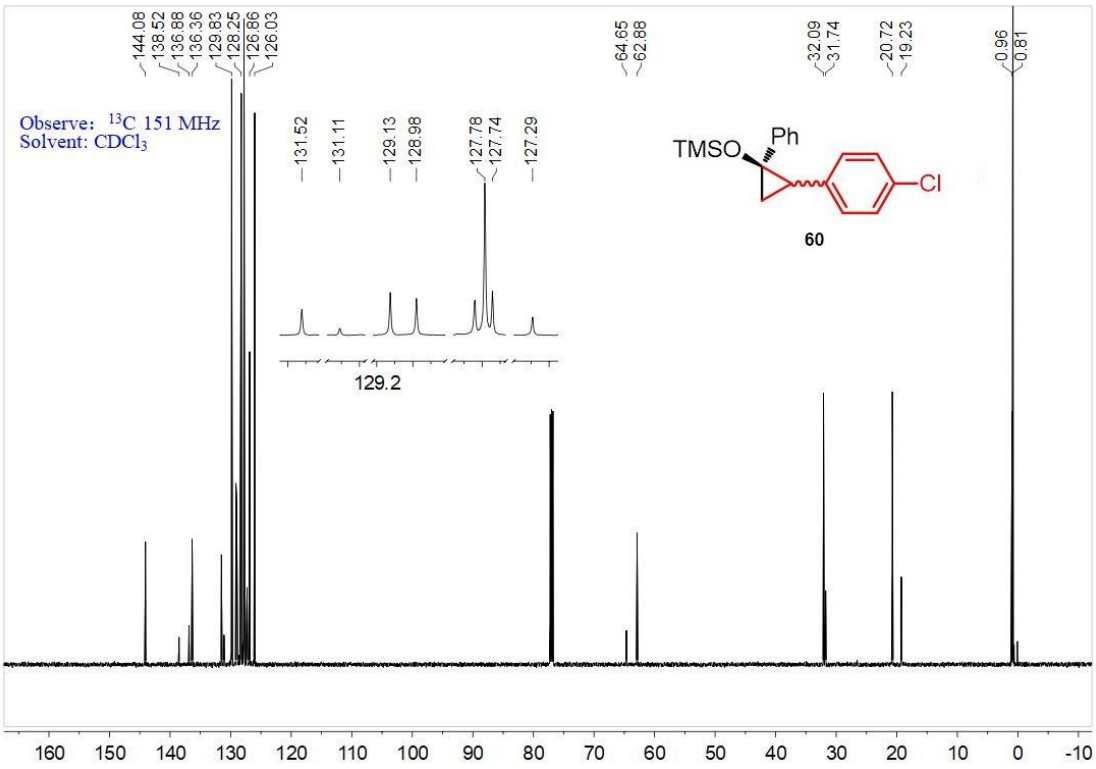

Figure S119. ^{13}C NMR spectrum of compound **60**, related to **Scheme 3.**

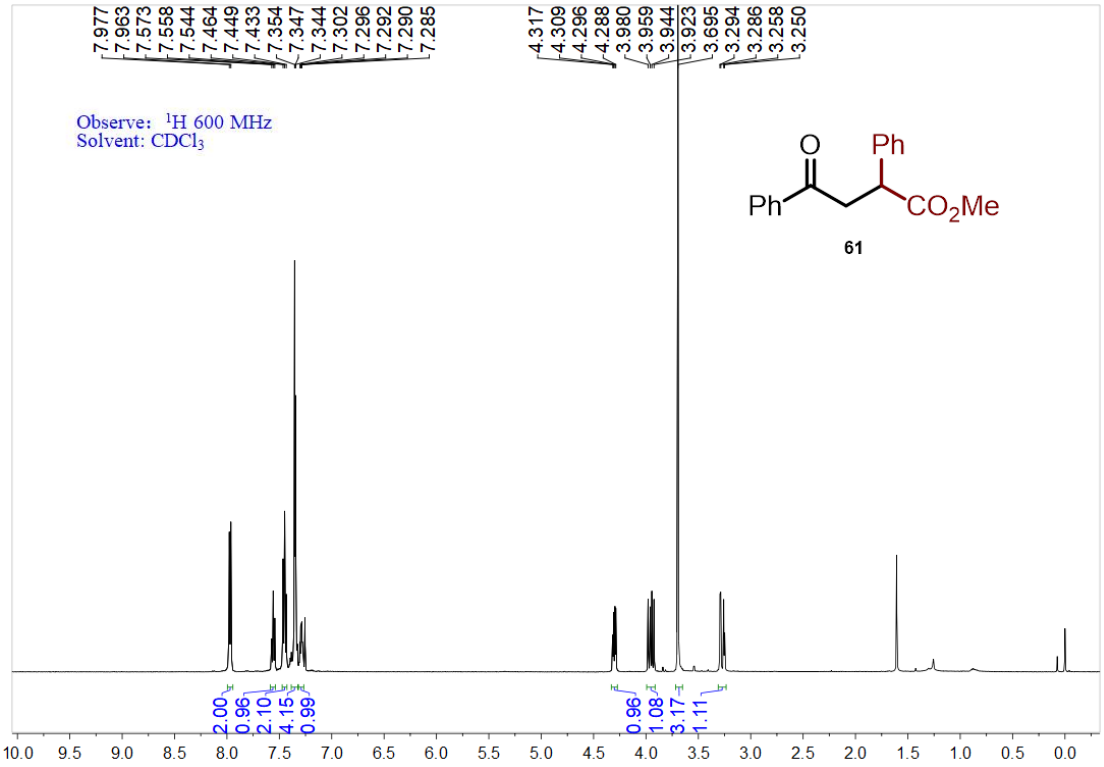

Figure S120. ^{1}H NMR spectrum of compound **61**, related to **Scheme 3.**

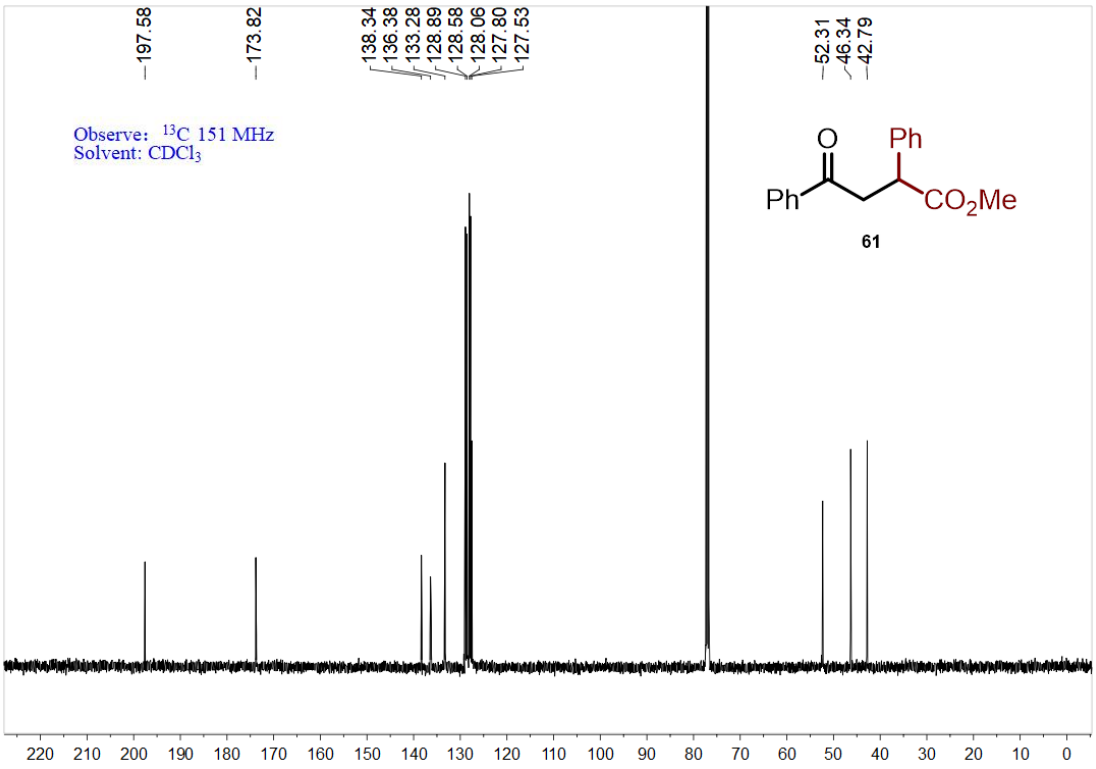

Figure S121. ^{13}C NMR spectrum of compound **61**, related to **Scheme 3.**

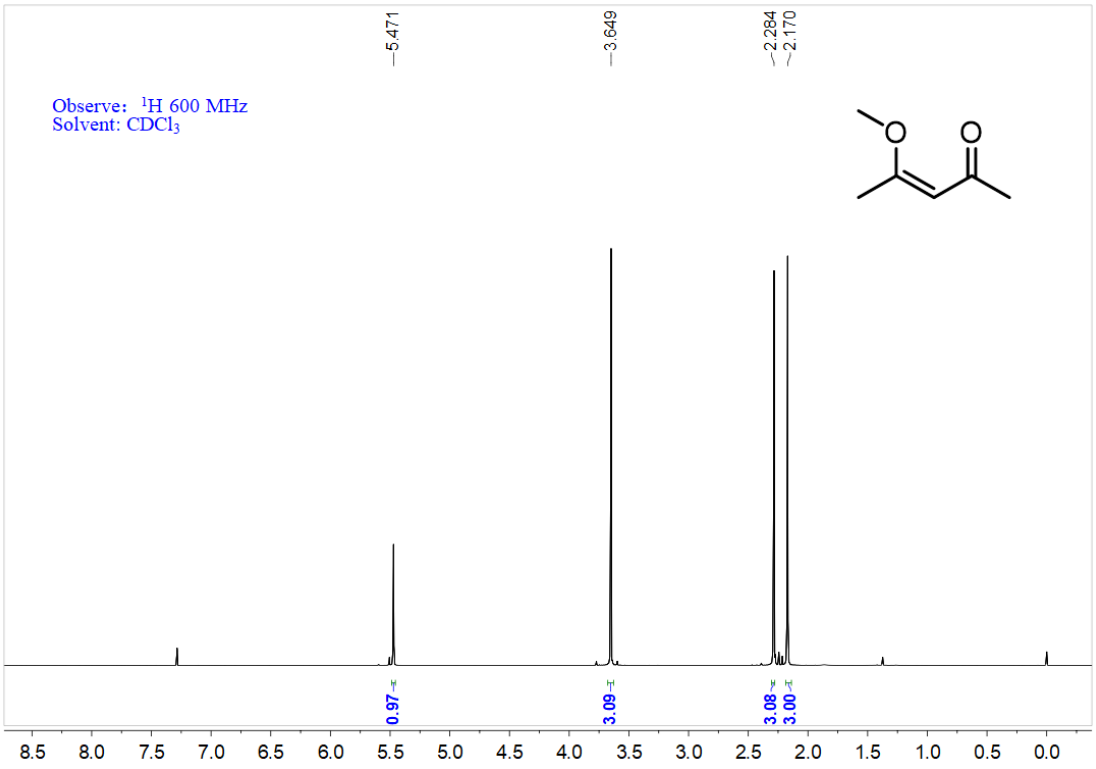

Figure S122. ^{1}H NMR spectrum of compound 4-Methoxy-3-penten-2-one, related to **Scheme 3.**

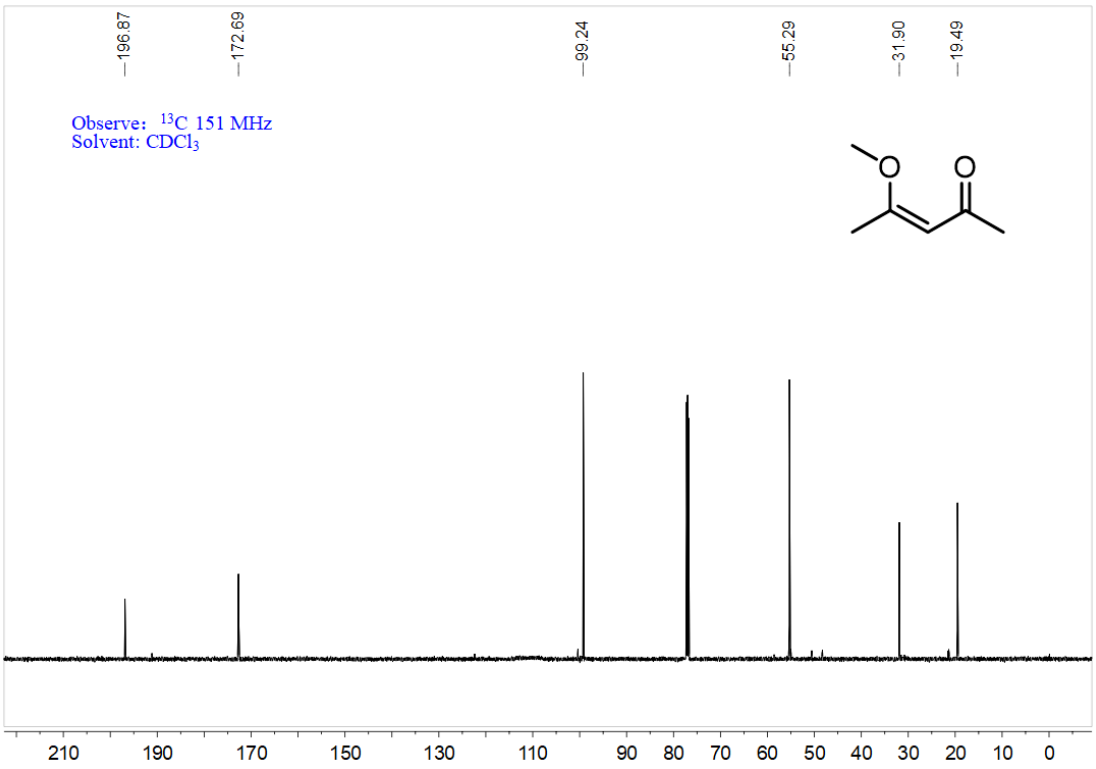

Figure S123. ^{13}C NMR spectrum of compound 4-Methoxy-3-penten-2-one, related to **Scheme 3.**

Supplemental Schemes

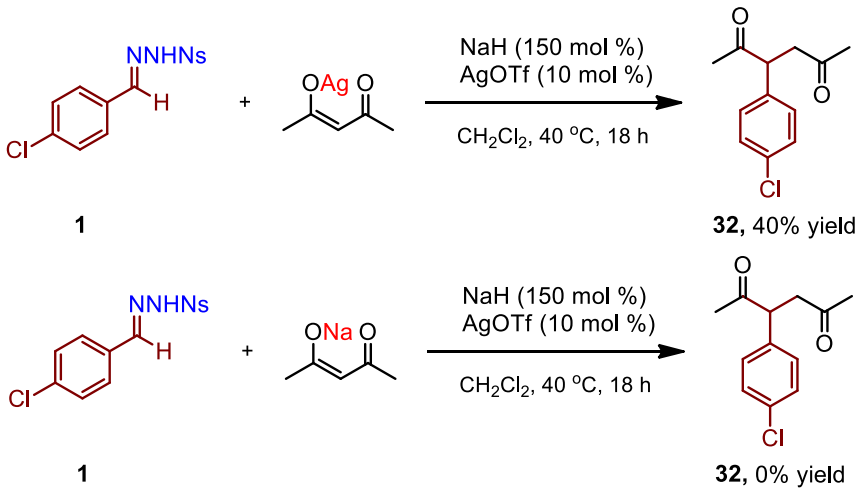

Scheme S1. Mechanistic studies, Related to **Scheme 3.**

Supplemental Tables

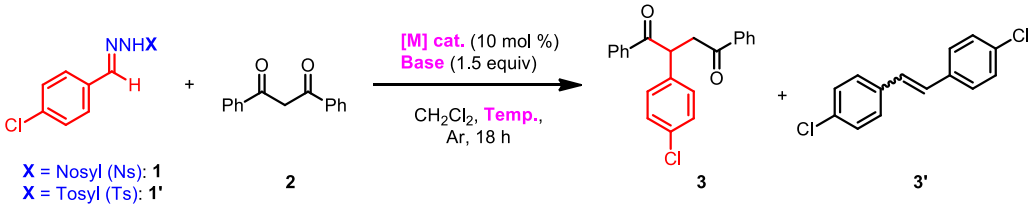

entry	**1/1'**	[M] cat.	base	*t* (℃)	**3** (%)[b]	**3'** (%)[b]
1	1'	AgOTf	NaH	40	54	18
2	**1**	**AgOTf**	**NaH**	**40**	**96 (92)** [c]	**0**
3	1	AgOAc	NaH	40	68	0
4	1	AgTFA	NaH	40	86 (81) [c]	0
5	1	Ag_2CO_3	NaH	40	32	<10
6	1	$Rh_2(OAc)_4$	NaH	40	36	42
7	1	$Cu(OTf)_2$	NaH	40	23	36
8	1	$Pd(OAc)_2$	NaH	40	0	68
9	1	$Sc(OTf)_3$	NaH	40	0	10
10	1	AgOTf	*t*-BuOLi	40	42	30
11	1	AgOTf	K_2CO_3	40	72	14
12	1	AgOTf	Cs_2CO_3	40	67	16
13	1	AgOTf	NaH	80	58	24

Table S1. Optimization of reaction conditions, Related to **Scheme 1**.[a]

[a]Reaction conditions: **1** (0.3 mmol), NaH (0.45 mmol), and CH_2Cl_2 (6 mL) were stirred at rt for 1 h, and then the catalyst and **2** (0.45 mmol) were added, after which the mixture was stirred at 40 ℃ for 18 h.

[b] Yields were calculated from ^{1}H-NMR spectroscopy with CH_2Br_2 as the internal standard.

[c] Isolated yields in parentheses.

Single Crystal Data of 3

Single-crystal X-ray diffraction data for the reported complex was recorded at a temperature of 293(2) K on a Oxford Diffraction Gemini R Ultra diffractometer, using a ω scan technique with Mo-Kα radiation (λ = 0.71073 Å). The structure was solved by Direct Method of SHELXS-97 and refined by full-matrix least-squares techniques using the SHELXL-97 program.1 Non-hydrogen atoms were refined with anisotropic temperature parameters, and hydrogen atoms of the ligands were refined as rigid groups. CCDC 1563346 for **3** contains the supplementary crystallographic data. Basic information pertaining to crystal parameters and structure refinement is summarized in Table S2. These data can be obtained free of charge from the Cambridge Crystallographic Data Centre via www.ccdc.cam.ac.uk/data_request/cif.

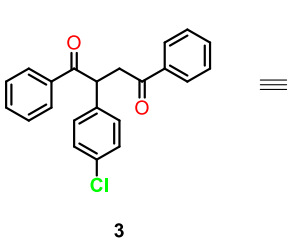

3

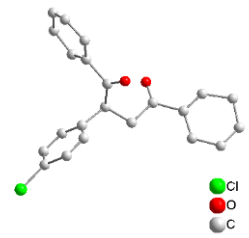

CCDC 1563346

X-ray structure of **3**

Empirical formula	$C_{22}H_{17}ClO_2$
Formula weight	348.80

Temperature	293(2) K
Wavelength	0.71073 Å
Space group	P 1 21/n 1
Unit cell dimensions	a = 11.476(4) Å
	b = 9.529(3) Å
	c = 16.264(6) Å
	alpha = 90.000 deg.
	beta = 93.826(6) deg.
	gamma = 90.000 deg.
Volume	1774.5(10) $Å^3$
Z	4
Calculated density	1.306 Mg/m^3
Absorption coefficient	0.227 mm^{-1}
F(000)	728
Crystal size	0.28 x 0.25 x 0.23 mm^3
Theta range for data collection	2.107 to 26.491 deg.
Reflections collected	9349 /3614 [$R_{(int)}$ = 0.0885]
Completeness to theta = 25.242 deg	99.2%
Data / restraints / parameters	3614 / 0 / 227
Goodness-of-fit on F^2	1.085
Final R indices [I>2sigma(I)]	R_1 = 0.0917, wR_2 = 0.2148
R indices (all data)	R_1 = 0.1194, wR_2 = 0.2256
Largest diff. peak and hole	0.445 and -0.447 $e.Å^{-3}$

Table S2. Crystal data and structure refinement for **3**, Related to **Scheme 1**.

Transparent Methods

Unless otherwise noted, all reactions were carried out in standard Schlenk techniques with magnetic stirring bar under argon atmosphere. All reagents were purchased from commercial sources and used without purification unless otherwise mentioned. The products were purified by column chromatography over silica gel (200-400 size). ^1H and ^{13}C Nuclear Magnetic Resonance (NMR) spectra were recorded at 25 ℃ on a Varian 600 MHz and 151 MHz, and TMS was used as internal standard. Chemical shifts are reported in ppm with the deuterium solvent as the internal standard (e.g. $CDCl_3$: 77.0 ppm). Mass spectra were recorded on BRUKER AutoflexIII Smartbeam MS-spectrometer. IR spectra were recorded on an Nicolet 6700-FTIR spectrometer. High resolution mass spectra (HRMS) were recorded on Bruck microTof by using ESI method.

Procedure for converting carbonyl compounds to *N*-nosylhydrazones.

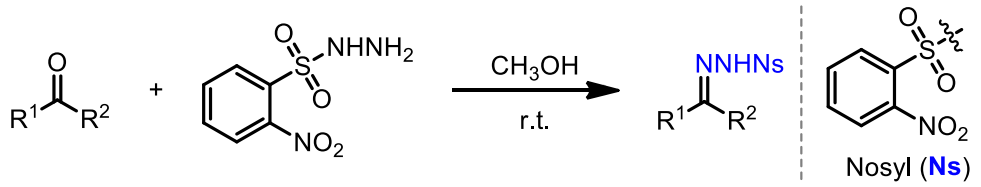

General procedure A (Liu et al., 2017): To a stirred solution of $NsNHNH_2$ (2.0 mmol, 1.0 equiv) in methanol (2 mL) were added carbonyl compounds (2.2 mmol, 1.1 equiv) and the mixture was stirred for 1-2 h at room temperature. The mixture was filtered and the resulting solid was washed with ice cold diethyl ether and dried under reduced pressure to give pure *N*-nosylhydrazones. The yields were around 80% in general.

Procedure for the insertion reaction of aldehyde-derived *N*-nosylhydrazones

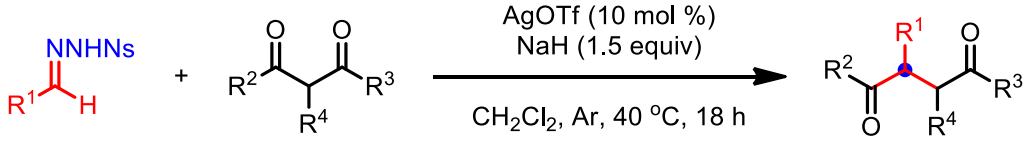

General procedure B: In a screw capped reaction vial, *N*-nosylhydrazone (0.3 mmol, 1.0 equiv) derived from aldehydes and NaH (0.45 mmol, 1.5 equiv, 60 wt%) were added. After sealed the tube was evacuated and backfilled with argon for three times, followed by dry CH_2Cl_2 (6 mL) addition via syringe. The reaction mixture was stirred at room temperature for 1 h. Then, 1,3-dicarbonyl compound (0.45 mmol, 1.5 equiv) and AgOTf (0.03 mmol, 10 mol%) were added. The resulting mixture was allowed to stir at 40 °C until *N*-nosylhydrazone was consumed completely determined by TLC analysis. After being filtrated through celite and concentrated, the residue was purified by column chromatography on silica gel to afford the desired 1,4-dicarbonyl compound.

Procedure for the insertion reaction of ketone-derived *N*-nosylhydrazones

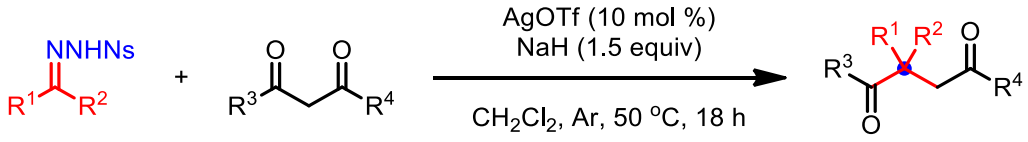

General procedure C: In a screw capped reaction vial, *N*-nosylhydrazone (0.3 mmol, 1.0 equiv) derived from ketones and NaH (0.45 mmol, 1.5 equiv, 60 wt%) were added. After sealed the tube was evacuated and backfilled with argon for three times, followed by dry CH_2Cl_2 (6 mL) addition via syringe. The reaction mixture was stirred at room temperature for 1 h. Then, 1,3-dicarbonyl compound (0.45 mmol, 1.5 equiv) and AgOTf (0.03 mmol, 10 mol%) were added. The resulting mixture was allowed to stir at 50 °C until *N*-nosylhydrazone was consumed completely determined by TLC analysis. After being filtrated through celite and concentrated, the residue was purified by column chromatography on silica gel to afford the desired 1,4-dicarbonyl compound.

Procedure for the insertion reaction of aliphatic aldehyde and ketone-derived *N*-nosylhydrazones

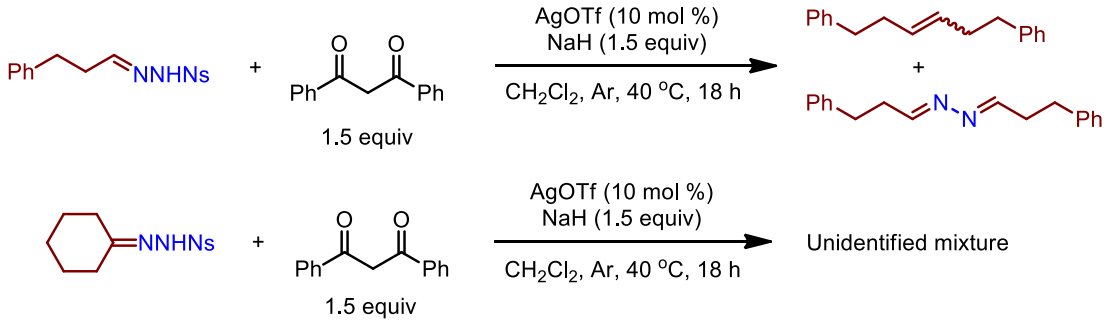

We have carried out the reactions of *N*-nosylhydrazones derived from aliphatic aldehydes and ketones, respectively, but an unidentified mixture was obtained in both reactions. Alkene and azine products were identified to be major products by ^{1}H NMR analysis of the crude reaction mixture in the reaction of the illustrated aldehyde *N*-nosylhydrazone. One of these products clearly appears to be derived from carbene dimerization; the other appears to derive from carbene insertion into the N=N-H bond, potentially forming a C=N bond with elimination of Ns group. In fact, both provide further support for carbene intermediacy, but we have yet to isolate these compounds in sufficient purity to support this.

Gram-scale synthesis

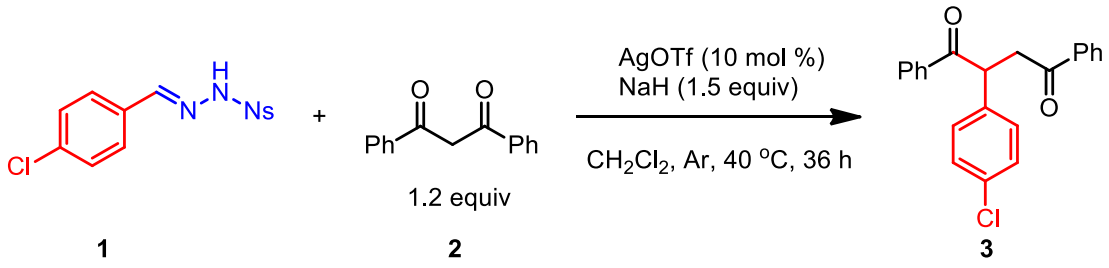

1 **2** **3**

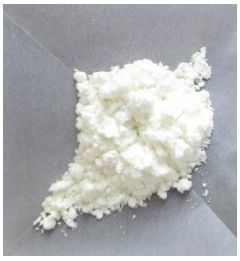

A. (**Left**) *N*-nosylhydrazone **1** (5.10 g, 15 mmol) and (**Right**) NaH (0.90 g, 22.5 mmol) were weighed on the bench top.

B. (**Left**) *N*-nosylhydrazone **1** and NaH were added to an oven-dried three-neck round bottom flask. The bottom was evacuated and refilled with Ar.

(**Right**) After addition of dry CH_2Cl_2 (280 mL) via syringe, the reaction mixture was stirred at room temperature for 1 hour.

C. AgOTf (385.4 mg 1.5 mmol) was weighed in the glovebox and introduced into the reaction mixture under Argon atmosphere.

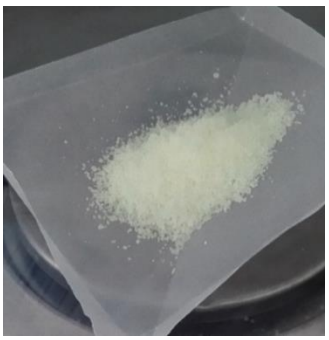

D. (**Left**) Dibenzoylmethane **2** (4.03 g, 18 mmol) was weighed on the bench top and dissolved in 20 mL dry CH_2Cl_2.

(**Right**) The above solution of dibenzoylmethane **2** was added via syringe for 10 min.

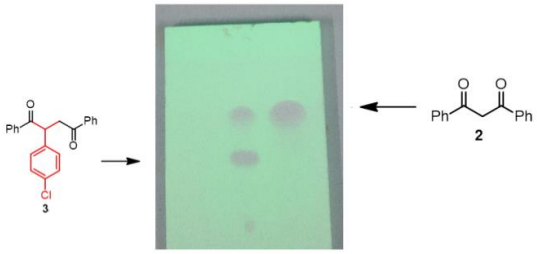

E. (**Left**)The reaction mixture is placed in an oil bath preheated to 40 ℃ and vigorously stirred (> 800 RPM) for 36 h.

(**Right)**TLC of the reaction (10:1 petroleum ether/EtOAc).

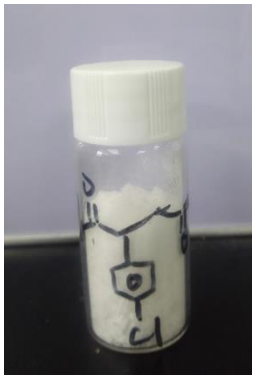

F. Isolated product of **3** (purified by flash column chromatopgrahy, gradient elution of 25:1 petroleum ether/EtOAc to 15:1 petroleum ether/EtOAc).

Experimental procedures for synthetic applications

(a)

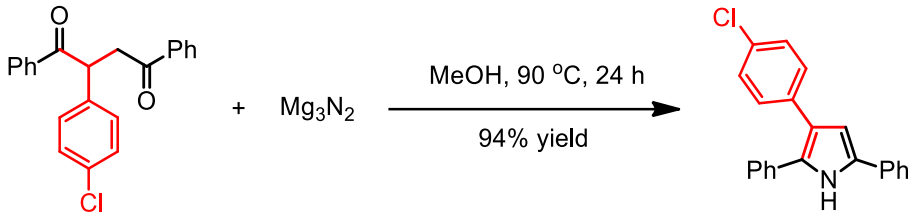

3 54

To a stirred solution of 2-(4-chlorophenyl)-1,4-diphenylbutane-1,4-dione **3** (174.4 mg, 0.5 mmol) in MeOH (5 mL) at 0 ℃ was added magnesium nitride (5.0 mmol). The reaction vessel was sealed and allowed to stir for 10 min before heating to 90 ℃ for 24 h. After cooling to room temperature, the mixture was evaporated in vacuum to leave a crude mixture, which was purified by column chromatography on silica gel to afford **54** (154.8 mg, 94% yield) as a white soild.

(b)

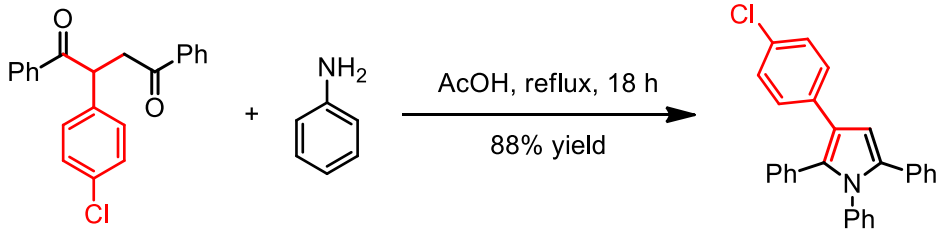

3 55

In a dried glass tube, 2-(4-chlorophenyl)-1,4-diphenylbutane-1,4-dione **3** (104.6 mg, 0.3 mmol), aniline (41.9 mg, 0.45 mmol) and AcOH (2 mL) was added sequentially at room temperature. The reaction mixture was reflux for 18 h. The mixture was cooled to room temperature, added water and extracted with ether three times. The combine ether layer was washed with brine, dried with Na_2SO_4 and concentrated. Purified by column chromatography to afford desired product **55** (107.1 mg, 88% yield) as a white soild.

(c)

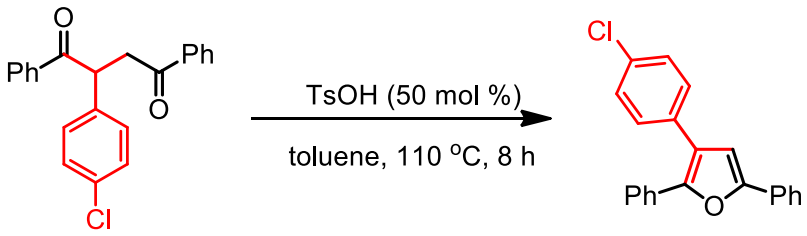

3 56

To a suspension of 2-(4-chlorophenyl)-1,4-diphenylbutane-1,4-dione **3** (104.6 mg, 0.3 mmol) in 2 mL Toluene, was added *p*-toluenesulfonic (25.8 mg, 0.15 mmol), and stirred at 110 °C for 8 h. The mixture was cooled to room temperature and was evaporated in vacuum to leave a crude mixture, which was purified by column chromatography on silica gel (eluting with petroleum ether) to afford **56** (85.3 mg, 86% yield) as a white soild.

Experimental procedures for mechanistic studies

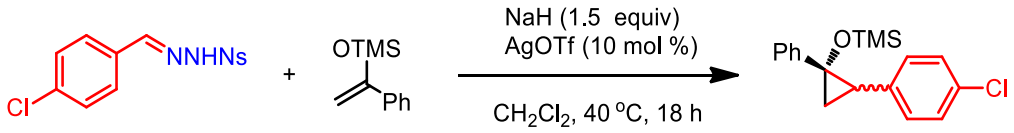

1 **59** (1.5 equiv) **60**, 74%, 3:1

Following the general procedure B, **1** (170 mg, 0.5 mmol), NaH (30 mg, 60 wt%, 0.75 mmol) and CH_2Cl_2 (10 mL) were stirred at rt for 1 h, and then AgOTf (12.9 mg, 0.05 mmol) and **59** (192.3 mg, 1.0 mmol) were added, after which the mixture was stirred at 40 ℃ for 18 h. Cyclopropanated product **60** (116.9 mg, 74%) was obtained as an inseparable mixture with d.r. 3:1.

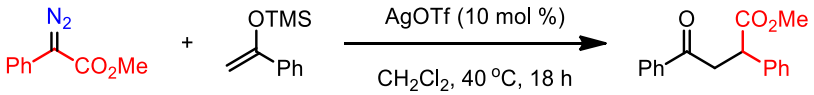

59 (1.5 equiv) **61**, 76%

Under Ar atmosphere, methyl phenyldiazoacetate (52.8 mg, 0.3 mmol) in CH_2Cl_2 (5.0 mL) was added dropwise (for 0.5 h) to a mixture of AgOTf (7.7 mg, 0.03 mmol) and **59** (115.4 mg, 0.6 mmol) in CH_2Cl_2 (1.0 mL), after which the mixture was stirred at 40 ℃ for 18 h. The mixture was concentrated and the residue was purified by column chromatography on silica gel to afford the desired product **61** as a colorless oil (61.1 mg, 76% yield).

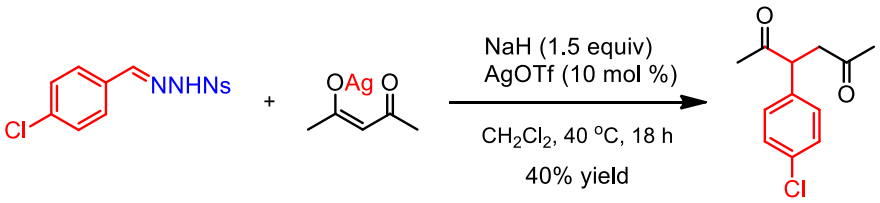

1 **32**

Following the general procedure B, **32** (26.9 mg, 40% yield) was obtained from *N*-nosylhydrazone **1** (101.9 mg, 0.3 mmol) and silver acetylacetonate (93.1 mg, 0.45 mmol), by using NaH (18.0 mg, 0.45 mmol, 60% suspension in paraffin oil), AgOTf (7.7 mg, 0.03 mmol) and CH_2Cl_2 (6 ml, 0.05 M) at 40 °C for 18 h.

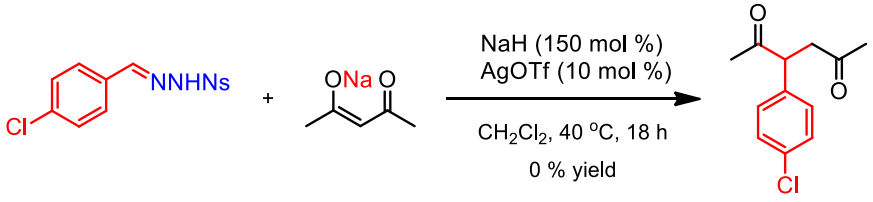

1 **32**

Sodium acetylacetonate (related to **Scheme S1)** (Schroll and König, 2015)**.** Pentane-2,4-dione (5 mmol, 1equiv) was dissolved in dry diethyl ether (20 mL) at room temperature. Sodium hydride (5 mmol, 200 mg, 60% suspension in paraffin oil) was added in portions. After gas evolution had ceased, the mixture was stirred for 30 minutes at ambient temperature. A yellowish precipitate was formed that was filtered, washed with cold diethyl ether (2 x 20 mL), and dried in vacuo.

Following the general procedure B, no product **32** was obtained from *N*-nosylhydrazone **1** (101.9 mg, 0.3 mmol) and sodium acetylacetonate (54.9 mg, 0.45 mmol), by using NaH (18.0 mg, 0.45 mmol, 60% suspension in paraffin oil), AgOTf (7.7 mg, 0.03 mmol) and CH_2Cl_2 (6 ml, 0.05 M) at 40 ^oC for 18 h.

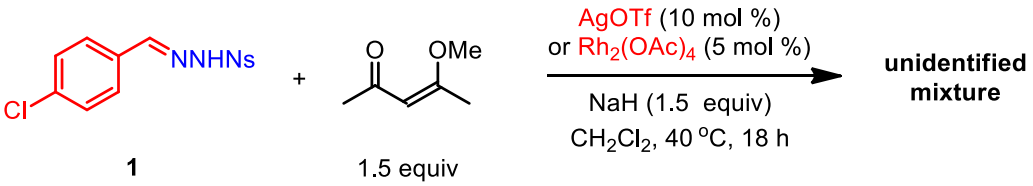

1 1.5 equiv

4-Methoxy-3-penten-2-one. A flame-dried flask is charged with 2,4-pentanedione (2.50 g, 25 mmol),trimethyl orthoformate (2.65 g, 25 mmol), p-toluenesulfonic acid (86 mg, 0.5 mmol), and methanol (10 mL). The flask is placed in an oil bath and heated at 55 ℃ for 5 h. Then 50 mL of CCl4 is added and the solution is again concentrated under reduced pressure. The crude product is distilled via a short-path condenser and collected in a flask cooled in an ice bath. Then, we have further applied 4-Methoxy-3-penten-2-one in the reaction with N-nosylhydrazone 1 under AgOTf or $Rh_2(OAc)_4$ catalysis, respectively; however, both of these two reaction systems gave complex mixtures, without giving the corresponding cyclopropane product.

Experimental procedures for asymmetric insertion

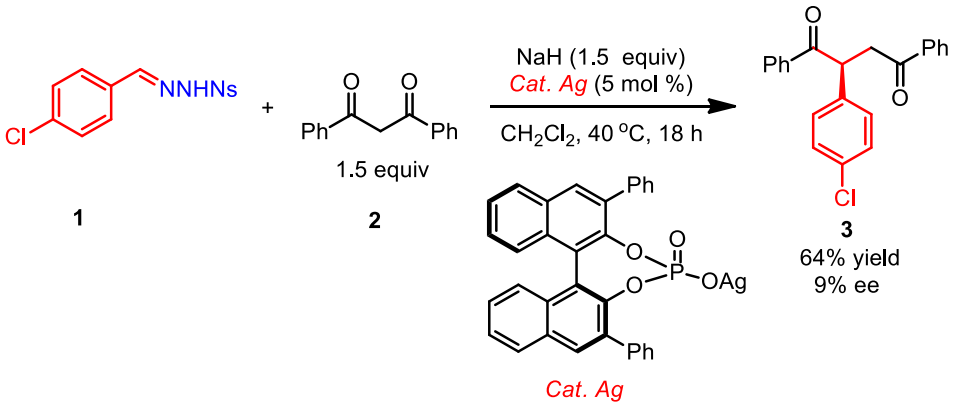

1 1.5 equiv **2** **3** 64% yield 9% ee

Cat. Ag

We indeed have tried this using a chiral silver phosphate catalyst; unfortunately, poor enantioselectivity was observed to date. Further studies to develop an asymmetric variant of this one-carbon homologation reaction are underway in our laboratory.

In a screw capped reaction vial, *N*-nosylhydrazone **1** (101.9 mg, 0.3 mmol) derived from 4-chlorobenzaldehyde and NaH (18 mg, 0.45 mmol, 60 wt%) were added. After sealed the tube was evacuated and backfilled with argon for three times, followed by dry CH_2Cl_2 (6 mL) addition *via* syringe. The reaction mixture was stirred at room temperature for 1 h. Then, 1,3-diphenylpropanedione **2** (100.9 mg, 0.45 mmol) and chiral silver phosphate catalyst (17.8 mg, 0.03 mmol) were added. The resulting mixture was allowed to stir at 40 ^oC until *N*-nosylhydrazone was consumed completely determined by TLC analysis. After being filtrated through celite and concentrated, the residue was purified by column chromatography

on silica gel to afford the desired 2-(4-chlorophenyl)-1,4-diphenylbutane-1,4-dione **3** (66.9 mg, 64%).

Characterization of all compounds

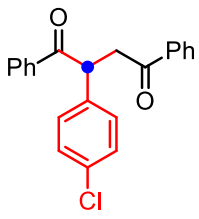

3

Following procedure B, 2-(4-chlorophenyl)-1,4-diphenylbutane-1,4-dione **3** (related to **Scheme 1**) (Mattson et al., 2006) was obtained as a white solid, m.p. 118-120 ^{o}C; **^{1}H-NMR** (600 MHz, $CDCl_3$) δ 8.01 (d, *J* = 7.8 Hz, 2H), 7.97 (d, *J* = 7.2 Hz, 2H), 7.54 (t, *J* = 7.2 Hz, 1H), 7.49 (t, *J* = 7.2 Hz, 1H), 7.43 (t, *J* = 7.8 Hz, 2H), 7.40 (t, *J* = 7.8 Hz, 2H), 7.31-7.24 (m, 4H), 5.31 (dd, *J* = 10.2 Hz, *J* = 3.6 Hz, 1H), 4.16 (dd, *J* = 18.0 Hz, *J* = 10.2 Hz, 1H), 3.29 (dd, *J* = 18.0 Hz, *J* = 3.6 Hz, 1H). **^{13}C-NMR** (151 MHz, $CDCl_3$) δ 198.56, 197.67, 137.07, 136.28, 136.17, 133.30, 133.27, 133.04, 129.55, 129.30, 128.82, 128.56, 128.54, 128.09, 47.87, 43.59. **IR** (KBr, cm^{-1}) 3056, 2919, 1679, 1594, 1488, 1446, 1366, 1233, 717, 687. **HRMS** (ESI) m/z calculated for $C_{22}H_{17}ClNaO_2$ $[M+Na]^+$ 371.0809, found 371.0808.

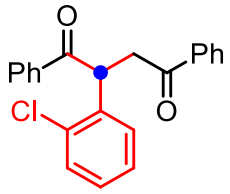

4

Following procedure B, 2-(2-chlorophenyl)-1,4-diphenylbutane-1,4-dione **4** (related to **Figure 2A**) was obtained as a colorless oil; **^{1}H-NMR** (600 MHz, $CDCl_3$) δ 8.00 (t, *J* = 7.8 Hz, 4H), 7.56 (t, *J* = 7.8 Hz, 1H), 7.50 (t, *J* = 7.2 Hz, 1H), 7.45 (t, *J* = 7.8 Hz, 3H), 7.41 (t, *J* = 7.8 Hz, 2H), 7.22-7.15 (m, 3H), 5.79 (dd, *J* = 10.8 Hz, *J* = 3.0 Hz, 1H), 4.10 (dd, *J* = 18.0 Hz, *J* = 10.8 Hz, 1H), 3.24 (dd, *J* = 18.0 Hz, *J* = 3.0 Hz, 1H). **^{13}C-NMR** (151 MHz, $CDCl_3$) δ 198.56, 197.54, 136.38, 136.37, 136.07, 133.26, 133.24, 133.13, 130.30, 129.08, 128.83, 128.72, 128.58, 128.56, 128.19, 127.52, 44.98, 42.21. **IR** (KBr, cm^{-1}) 3062, 2911, 1680, 1596, 1474, 1445, 1234, 718, 689. **HRMS** (ESI) m/z calculated for $C_{22}H_{17}ClNaO_2$ $[M+Na]^+$ 371.0809, found 371.0818.

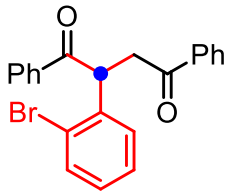

5

Following procedure B, 2-(2-bromophenyl)-1,4-diphenylbutane-1,4-dione **5** (related to **Figure 2A**) was obtained as a yellow oil; **^{1}H-NMR** (600 MHz, $CDCl_3$) δ 8.01-7.98 (m, 4H), 7.64 (d, *J* = 7.8 Hz, 1H), 7.56 (t, *J* = 7.8 Hz, 1H), 7.49 (t, *J* = 7.8 Hz, 1H), 7.45 (t, *J* = 7.8 Hz, 2H), 7.40 (t, *J* = 7.8 Hz, 2H), 7.21-7.18 (m, 2H), 7.12-7.08 (m, 1H), 5.76 (dd, *J* = 10.8 Hz, *J* = 3.0 Hz, 1H), 4.07 (dd, *J* = 18.0 Hz, *J* = 10.8 Hz, 1H), 3.23 (dd, *J* = 18.0 Hz, *J* = 3.0 Hz, 1H). **^{13}C-NMR** (151 MHz, $CDCl_3$) δ 198.48, 197.40, 138.07, 136.31, 136.00, 133.65, 133.22, 133.12, 129.06, 128.97, 128.86, 128.56, 128.54, 128.18, 128.14, 124.09, 47.79, 42.22. **IR** (KBr, cm^{-1}) 3058, 2920, 1680, 1593, 1465, 1442, 1288, 1232, 758, 685. **HRMS** (ESI) m/z calculated for $C_{22}H_{17}BrNaO_2$ $[M+Na]^+$ 415.0304, found 415.0302.

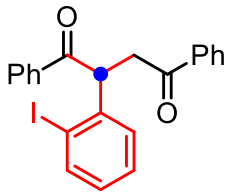

6

Following procedure B, 2-(2-iodophenyl)-1,4-diphenylbutane-1,4-dione **6** (related to **Figure 2A**) was obtained as a yellow oil; **^{1}H-NMR** (600 MHz, $CDCl_3$) δ 8.00-7.97 (m, 4H), 7.91 (dd, *J* = 7.8 Hz, *J* = 1.2 Hz, 1H), 7.54 (t, *J* = 7.2 Hz, 1H), 7.48 (t, *J* = 7.8 Hz, 1H), 7.44 (t, *J* = 7.8 Hz, 2H), 7.39 (t, *J* = 7.8 Hz, 2H), 7.23-7.20 (m, 1H), 7.16 (dd, *J* = 7.8 Hz, *J* = 1.2 Hz, 1H), 6.91 (td, *J* = 7.8 Hz, *J* = 1.2 Hz, 1H), 5.61 (dd, *J* = 10.8 Hz, *J* = 3.0 Hz, 1H), 4.02 (dd, *J* = 18.0 Hz, *J* = 10.8 Hz, 1H), 3.18 (dd, *J* = 18.0 Hz, *J* = 3.0 Hz, 1H). **^{13}C-NMR** (151 MHz, $CDCl_3$) δ 198.48, 197.23, 141.40, 140.44, 136.30, 136.03, 133.19, 133.08, 129.09, 129.00, 128.92, 128.54, 128.52, 128.31, 128.17, 100.98, 53.01, 42.29. **IR** (KBr, cm^{-1}) 3060, 2918, 1680, 1595, 1464, 1439, 1276, 754, 691. **HRMS** (ESI) m/z calculated for $C_{22}H_{17}INaO_2$ $[M+Na]^+$ 463.0166, found 463.0171.

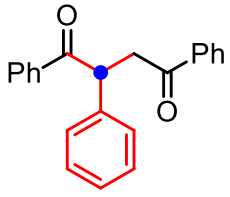

7

Following procedure B, 1,2,4-triphenylbutane-1,4-dione **7** (related to **Figure 2A**) (Mattson et al., 2006) was obtained as a white solid, m.p. 129-130 ^{o}C; **^{1}H-NMR** (600 MHz, $CDCl_3$) δ 7.96-7.94 (m, 2H), 7.90-7.88 (m, 2H), 7.45 (t, *J* = 7.2 Hz, 1H), 7.39 (t, *J* = 7.2 Hz, 1H), 7.34 (t, *J* = 7.8 Hz,

2H), 7.30 (t, *J* = 7.8 Hz, 2H), 7.28-7.26 (m, 2H), 7.22 (t, *J* = 7.8 Hz, 2H), 7.13 (t, *J* = 7.2 Hz, 1H), 5.24 (dd, *J* = 10.2 Hz, *J* = 3.6 Hz, 1H), 4.13 (dd, *J* = 18.0 Hz, *J* = 10.2 Hz, 1H), 3.21 (dd, *J* = 18.0 Hz, *J* = 3.6 Hz, 1H). **^{13}C-NMR** (151 MHz, $CDCl_3$) δ 198.87, 198.00, 138.65, 136.48, 136.47, 133.17, 132.82, 129.15, 128.88, 128.52, 128.45, 128.20, 128.12, 127.31, 48.70, 43.83. **IR** (KBr, cm^{-1}) 3058, 2920, 1678, 1594, 1446, 1229, 761, 699. **HRMS** (ESI) m/z calculated for $C_{22}H_{18}NaO_2$ $[M+Na]^+$ 337.1199, found 337.1210.

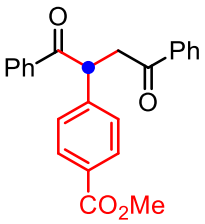

8

Following procedure B, methyl 4-(1,4-dioxo-1,4-diphenylbutan-2-yl)benzoate **8** (related to **Figure 2A**) was obtained as a yellow oil; **^{1}H-NMR** (600 MHz, $CDCl_3$) δ 7.94-7.92 (m, 2H), 7.91-7.88 (m, 4H), 7.47 (t, *J* = 7.8 Hz, 1H), 7.41 (t, *J* = 7.8 Hz, 1H), 7.38-7.34 (m, 4H), 7.32 (t, *J* = 7.8 Hz, 2H), 5.32 (dd, *J* = 10.2 Hz, *J* = 4.2 Hz, 1H), 4.13 (dd, *J* = 18.0 Hz, *J* = 10.2 Hz, 1H), 3.79 (s, 3H), 3.24 (dd, *J* = 18.0 Hz, *J* = 4.2 Hz, 1H). **^{13}C-NMR** (151 MHz, $CDCl_3$) δ 198.33, 197.56, 166.58, 143.83, 136.31, 136.23, 133.33, 133.10, 130.42, 129.30, 128.84, 128.58, 128.56, 128.28, 128.12, 52.07, 48.65, 43.46. **HRMS** (ESI) m/z calculated for $C_{24}H_{20}NaO_4$ $[M+Na]^+$ 395.1254, found 395.1269.

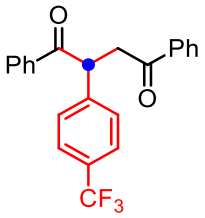

9

Following procedure B, 1,4-diphenyl-2-(4-(trifluoromethyl)phenyl)butane-1,4-dione **9** (related to **Figure 2A**) was obtained as a yellow oil; **^{1}H-NMR** (600 MHz, $CDCl_3$) δ 8.03-8.01 (m, 2H), 7.98-7.96 (m, 2H), 7.58-7.55 (m, 3H), 7.54-7.49 (m, 3H), 7.47-7.41 (m, 4H), 5.41 (dd, *J* = 9.6 Hz, *J* = 3.6 Hz, 1H), 4.21 (dd, *J* = 18.0 Hz, *J* = 9.6 Hz, 1H), 3.34 (dd, *J* = 18.0 Hz, *J* = 3.6 Hz, 1H). **^{13}C-NMR** (151 MHz, $CDCl_3$) δ 198.32, 197.47, 142.69, 136.23, 136.12, 133.43, 133.25, 129.70 (q, *J* = 32.3 Hz), 128.87, 128.66, 128.63, 128.14, 126.11 (q, *J* = 3.6 Hz), 123.94 (q, *J* = 271.2 Hz), 48.31, 43.61. **IR** (KBr, cm^{-1}) 3062, 2919, 1679, 1594, 1447, 1324, 1231, 1118, 750, 693. **HRMS** (ESI) m/z calculated for $C_{23}H_{17}F_3NaO_2$ $[M+Na]^+$ 405.1073, found 405.1078.

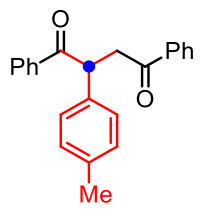

10

Following procedure B, 1,4-diphenyl-2-(*p*-tolyl)butane-1,4-dione **10** (related to **Figure 2A**)[2] was obtained as a white solid, m.p. 77-79 °C; **^{1}H-NMR** (600 MHz, $CDCl_3$) δ 8.04-8.02 (m, 2H), 7.98-7.96 (m, 2H), 7.55-7.52 (m, 1H), 7.47 (t, *J* = 7.2 Hz, 1H), 7.43 (t, *J* = 7.8 Hz, 2H), 7.38 (t, *J* = 7.8 Hz, 2H), 7.25-7.23 (m, 2H), 7.11 (d, *J* = 7.8 Hz, 2H), 5.29 (dd, *J* = 10.2 Hz, *J* = 3.6 Hz, 1H), 4.19 (dd, *J* = 18.0 Hz, *J* = 10.2 Hz, 1H), 3.28 (dd, *J* = 18.0 Hz, *J* = 3.6 Hz, 1H), 2.28 (s, 3H). **^{13}C-NMR** (151 MHz, $CDCl_3$) δ 198.96, 198.10, 137.02, 136.43, 135.52, 133.16, 132.78, 129.85, 128.92, 128.87, 128.51, 128.43, 128.11, 128.05, 48.25, 43.85, 20.99. **IR** (KBr, cm^{-1}) 3027, 2907, 1680, 1594, 1446, 1394, 1341, 1233, 742, 689. **HRMS** (ESI) m/z calculated for $C_{23}H_{20}NaO_2$ $[M+Na]^+$ 351.1356, found 351.1360.

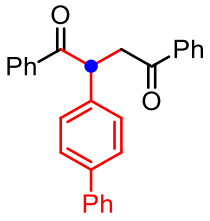

11

Following procedure B, 2-([1,1'-diphenyl]-4-yl)-1,4-diphenylbutane-1,4-dione **11** (related to **Figure 2A**) was obtained as a yellow oil; **^{1}H-NMR** (600 MHz, $CDCl_3$) δ 8.08-8.06 (m, 2H), 8.00-7.98 (m, 2H), 7.55-7.51 (m, 5H), 7.49 (t, *J* = 7.2 Hz, 1H), 7.45-7.38 (m, 8H), 7.31 (t, *J* = 7.2 Hz, 1H), 5.37 (dd, *J* = 10.2 Hz, *J* = 4.2 Hz, 1H), 4.24 (dd, *J* = 18.0 Hz, *J* = 10.2 Hz, 1H), 3.34 (dd, *J* = 18.0 Hz, *J* = 4.2 Hz, 1H). **^{13}C-NMR** (151 MHz, $CDCl_3$) δ 198.84, 197.98, 140.42, 140.27, 137.62, 136.50, 136.48, 133.22, 132.90, 128.93, 128.74, 128.62, 128.55, 128.51, 128.15, 127.85, 127.35, 126.96, 48.31, 43.83. **HRMS** (ESI) m/z calculated for $C_{28}H_{22}NaO_2$ $[M+Na]^+$ 413.1512, found 413.1501.

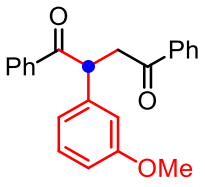

12

Following procedure B, 2-(3-methoxyphenyl)-1,4-diphenylbutane-1,4-dione **12** (related to **Figure 2A**) was obtained as a yellow oil; **^{1}H-NMR** (600 MHz, $CDCl_3$) δ 8.04-8.02 (m, 2H), 7.98-7.96 (m, 2H), 7.56-7.53 (m, 1H), 7.49-7.46 (m, 1H), 7.43 (t, *J* = 7.8 Hz, 2H), 7.39 (t, *J* = 7.8 Hz, 2H), 7.22 (t, *J* = 7.8 Hz, 1H), 6.94 (d, *J* = 7.8 Hz, 1H), 6.89 (t, *J* = 1.8 Hz, 1H), 6.77-6.75 (m, 1H), 5.29 (dd, *J* = 10.2 Hz, *J* = 3.6 Hz, 1H), 4.20 (dd, *J* = 18.0 Hz, *J* = 10.2 Hz, 1H), 3.76 (s, 3H), 3.29 (dd, *J* = 18.0 Hz, *J* = 3.6 Hz, 1H). **^{13}C-NMR** (151 MHz, $CDCl_3$) δ 198.71, 198.00, 160.12, 140.18, 136.51, 136.48, 133.18, 132.84, 130.17, 128.88, 128.53, 128.46, 128.13, 120.57, 113.90, 112.62, 55.19, 48.73, 43.80. **IR** (KBr, cm^{-1}) 3060, 2919, 2842, 1681, 1600, 1576, 1482, 1448, 1246, 1212, 1040, 749, 709. **HRMS** (ESI) m/z calculated for $C_{23}H_{20}NaO_3$ $[M+Na]^+$ 367.1305, found 367.1311.

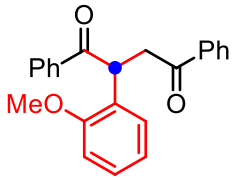

13

Following procedure B, 2-(2-methoxyphenyl)-1,4-diphenylbutane-1,4-dione **13** (related to **Figure 2A**) was obtained as a yellow oil; **^{1}H-NMR** (600 MHz, $CDCl_3$) δ 8.02-8.00 (m, 2H), 7.99-7.97 (m, 2H), 7.53 (t, *J* = 7.8 Hz, 1H), 7.47-7.41 (m, 3H), 7.36 (t, *J* = 7.8 Hz, 2H), 7.22-7.18 (m, 1H), 7.15 (dd, *J* = 7.8 Hz, *J* = 1.8 Hz, 1H), 6.89 (d, *J* = 7.8 Hz, 1H), 6.86 (t, *J* = 7.8 Hz, 1H), 5.75 (dd, *J* = 10.2 Hz, *J* = 3.0 Hz, 1H), 4.11 (dd, *J* = 18.0 Hz, *J* = 10.2 Hz, 1H), 3.89 (s, 3H), 3.19 (dd, *J* = 18.0 Hz, *J* = 3.0 Hz, 1H). **^{13}C-NMR** (151 MHz, $CDCl_3$) δ 199.49, 198.36, 155.96, 136.65, 136.36, 132.99, 132.69, 128.74, 128.65, 128.48, 128.45, 128.30, 128.12, 127.05, 121.01, 110.96, 55.45, 42.21, 41.29. **HRMS** (ESI) m/z calculated for $C_{23}H_{20}NaO_3$ $[M+Na]^+$ 367.1305, found 367.1312.

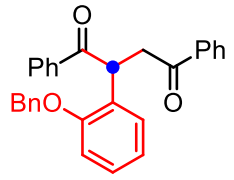

14

Following procedure B, 2-(2-(benzyloxy)phenyl)-1,4-diphenylbutane-1,4-dione **14** (related to **Figure 2A**) was obtained as a white solid, m.p. 108-110 °C; **^{1}H-NMR** (600 MHz, $CDCl_3$) δ 8.03-8.01 (m, 2H), 7.97-7.95 (m, 2H), 7.54 (t, *J* = 7.2 Hz, 1H), 7.48-7.41 (m, 5H), 7.37-7.29 (m, 5H), 7.21-7.16 (m, 2H), 6.96 (d, *J* = 7.8 Hz, 1H), 6.88 (t, *J* = 7.2 Hz, 1H), 5.81 (dd, *J* = 10.2 Hz, *J* = 3.6 Hz, 1H), 5.17 (AB, *J* = 20.4 Hz, *J* = 12.0 Hz, 2H), 4.11 (dd, *J* = 18.0 Hz, *J* = 10.2 Hz, 1H), 3.17 (dd, *J* = 18.0 Hz, *J* = 3.6 Hz, 1H). **^{13}C-NMR** (151 MHz, $CDCl_3$) δ 199.48, 198.23, 155.07, 136.75, 136.62, 136.36, 133.00, 132.72, 128.90, 128.84, 128.67, 128.46, 128.31, 128.14, 128.03, 127.40, 127.27, 121.39, 112.61, 70.35, 42.37, 41.28. **IR** (KBr, cm^{-1}) 3058, 2914, 1674, 1594, 1482, 1449, 1221, 766, 743, 692. **HRMS** (ESI) m/z calculated for $C_{29}H_{24}NaO_3$ $[M+Na]^+$ 443.1618, found 443.1622.

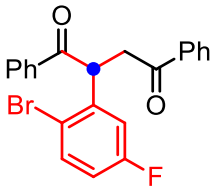

15

Following procedure B, 2-(2-bromo-5-fluorophenyl)-1,4-diphenylbutane-1,4-dione **15** (related to **Figure 2A**) was obtained as a yellow solid, m.p. 99-101 °C; **^{1}H-NMR** (600 MHz, $CDCl_3$) δ 8.02-8.00 (m, 2H), 7.99-7.97 (m, 2H), 7.60-7.55 (m, 2H), 7.52 (t, *J* = 7.2 Hz, 1H), 7.46-7.41 (m, 4H), 6.96 (dd, *J* = 9.6 Hz, *J* = 3.0 Hz, 1H), 6.87-6.82 (m, 1H), 5.73 (dd, *J* = 10.8 Hz, *J* = 3.0 Hz, 1H), 4.06 (dd, *J* = 18.0 Hz, *J* = 10.8 Hz, 1H), 3.23 (dd, *J* = 18.0 Hz, *J* = 3.0 Hz, 1H). **^{13}C-NMR**

(151 MHz, $CDCl_3$) δ 198.08, 197.07, 162.09 (d, *J* = 248.5 Hz), 140.07 (d, *J* = 7.4 Hz), 136.11, 135.80, 134.76 (d, *J* = 8.0 Hz), 133.37, 133.36, 128.84, 128.67, 128.58, 128.17, 118.06 (d, *J* = 3.3 Hz), 116.33 (d, *J* = 22.5 Hz), 116.25 (d, *J* = 23.6 Hz), 47.68, 42.19. **IR** (KBr, cm^{-1}) 3081, 2914, 1679, 1596, 1578, 1468, 1448, 1340, 1245, 1218, 997, 741, 686. **HRMS** (ESI) m/z calculated for $C_{22}H_{16}BrFNaO_2$ $[M+Na]^+$ 433.0210, found 433.0214.

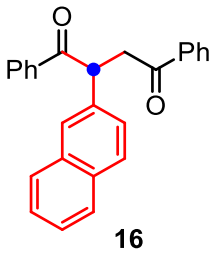

16

Following procedure B, 2-(naphthalen-2-yl)-1,4-diphenylbutane-1,4-dione **16** (related to **Figure 2A**) (Mattson et al., 2006) was obtained as a white solid, m.p. 128-130 °C; **^{1}H-NMR** (600 MHz, $CDCl_3$) δ 8.07 (d, *J* = 7.2 Hz, 2H), 7.99 (d, *J* = 7.2 Hz, 2H), 7.82-7.77 (m, 4H), 7.54 (t, *J* = 7.2 Hz, 1H), 7.50 (dd, *J* = 8.4 Hz, *J* = 1.2 Hz, 1H), 7.47-7.42 (m, 5H), 7.38 (t, *J* = 7.8 Hz, 2H), 5.49 (dd, *J* = 9.6 Hz, *J* = 3.6 Hz, 1H), 4.30 (dd, *J* = 18.0 Hz, *J* = 9.6 Hz, 1H), 3.38 (dd, *J* = 18.0 Hz, *J* = 3.6 Hz, 1H). **^{13}C-NMR** (151 MHz, $CDCl_3$) δ 198.86, 197.99, 136.49, 136.13, 133.66, 133.23, 132.89, 132.53, 129.05, 128.94, 128.67, 128.56, 128.50, 128.16, 127.75, 127.63, 127.12, 126.35, 126.11, 126.04, 48.84, 43.89. **HRMS** (ESI) m/z calculated for $C_{26}H_{20}NaO_2$ $[M+Na]^+$ 387.1356, found 387.1380.

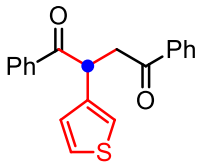

17

Following procedure B, 1,4-diphenyl-2-(thiophen-3-yl)butane-1,4-dione **17** (related to **Figure 2A**) was obtained as a yellow solid, m.p. 85-87 °C; **^{1}H-NMR** (600 MHz, $CDCl_3$) δ 8.04 (d, *J* = 7.2 Hz, 2H), 7.97 (d, *J* = 7.2 Hz, 2H), 7.53 (t, *J* = 7.8 Hz, 1H), 7.49 (t, *J* = 7.2 Hz, 1H), 7.44-7.39 (m, 4H), 7.25 (dd, *J* = 4.8 Hz, *J* = 3.0 Hz, 1H), 7.14-7.13 (m, 1H), 7.05 (dd, *J* = 4.8 Hz, *J* = 0.6 Hz, 1H), 5.46 (dd, *J* = 9.6 Hz, *J* = 3.6 Hz, 1H), 4.17 (dd, *J* = 18.0 Hz, *J* = 9.6 Hz, 1H), 3.34 (dd, *J* = 18.0 Hz, *J* = 3.6 Hz, 1H). **^{13}C-NMR** (151 MHz, $CDCl_3$) δ 198.68, 197.91, 138.55, 136.41, 136.39, 133.21, 132.89, 128.78, 128.52, 128.48, 128.09, 127.15, 126.51, 122.37, 43.67, 43.18. **IR** (KBr, cm^{-1}) 3060, 2904, 2361, 1674, 1591, 1445, 1336, 1227, 996, 770, 726, 689. **HRMS** (ESI) m/z calculated for $C_{20}H_{16}NaO_2S[M+Na]^+$ 343.0763, found 343.0768.

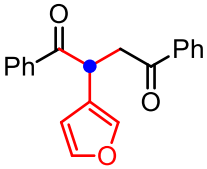

18

Following procedure B, 2-(furan-3-yl)-1,4-diphenylbutane-1,4-dione **18** (related to **Figure 2A**) was obtained as a white solid, m.p. 116-118 ^{o}C; **^{1}H-NMR** (600 MHz, $CDCl_3$) δ 8.06 (d, *J* = 7.2 Hz, 2H), 7.99 (d, *J* = 7.2 Hz, 2H), 7.58-7.53 (m, 2H), 7.47-7.43 (m, 4H), 7.34-7.33 (m, 2H), 6.36 (s, 1H), 5.26 (dd, *J* = 9.6 Hz, *J* = 4.2 Hz, 1H), 4.11 (dd, *J* = 18.0 Hz, *J* = 9.6 Hz, 1H), 3.35 (dd, *J* = 18.0 Hz, *J* = 4.2 Hz, 1H). **^{13}C-NMR** (151 MHz, $CDCl_3$) δ 198.90, 197.95, 143.45, 139.98, 136.38, 136.23, 133.30, 133.04, 128.76, 128.58, 128.56, 128.13, 122.66, 109.96, 42.68, 38.82. **HRMS** (ESI) m/z calculated for $C_{20}H_{16}NaO_3$ $[M+Na]^+$ 327.0992, found 327.0980.

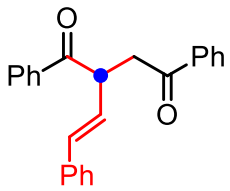

19

Following procedure B, (*E*)-1,4-diphenyl-2-styrylbutane-1,4-dione **19** (related to **Figure 2A**) was obtained as a yellow oil; **^{1}H-NMR** (600 MHz, $CDCl_3$) δ 8.12-8.10 (m, 2H), 7.99 (d, *J* = 7.2 Hz, 2H), 7.56-7.52 (m, 2H), 7.48-7.43 (m, 4H), 7.30 (d, *J* = 7.2 Hz, 2H), 7.26 (t, *J* = 7.8 Hz, 2H), 7.21-7.18 (m, 1H), 6.61 (d, *J* = 15.6 Hz, 1H), 6.29 (d, *J* = 15.6 Hz, *J* = 9.0 Hz, 1H), 4.97-4.93 (m, 1H), 4.01 (dd, *J* = 18.0 Hz, *J* = 9.6 Hz, 1H), 3.30 (dd, *J* = 18.0 Hz, *J* = 4.2 Hz, 1H). **^{13}C-NMR** (151 MHz, $CDCl_3$) δ 199.59, 197.90, 136.58, 136.54, 136.50, 133.61, 133.30, 133.09, 128.80, 128.64, 128.62, 128.58, 128.17, 127.85, 126.84, 126.31, 45.84, 41.70. **IR** (KBr, cm^{-1}) 3080, 3056, 3024, 2918, 1669, 1594, 1493, 1447, 1220, 998, 969, 751, 738. **HRMS** (ESI) m/z calculated for $C_{24}H_{20}NaO_2$ $[M+Na]^+$ 363.1356, found 363.1361.

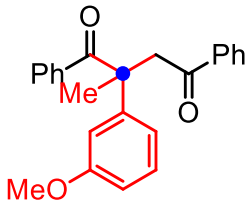

20

Following procedure C, 2-(3-methoxyphenyl)-2-methyl-1,4-diphenylbutane-1,4-dione **20** (related to **Figure 2A**) was obtained as a white solid, m.p. 142-144 ^{o}C; **^{1}H-NMR** (600 MHz, $CDCl_3$) δ 7.89-7.88 (m, 2H), 7.51 (t, *J* = 7.8 Hz, 1H), 7.44-7.43 (m, 2H), 7.40 (t, *J* = 7.8 Hz, 2H), 7.34-7.33 (m, 1H), 7.31 (t, *J* = 8.4 Hz, 1H), 7.23 (t, *J* = 7.8 Hz, 2H), 7.04 (dd, *J* = 7.8 Hz, *J* = 1.2 Hz, 1H), 7.00 (t, *J* = 2.4 Hz, 1H), 6.84 (dd, *J* = 8.4 Hz, *J* = 2.4 Hz, 1H), 3.94 (d, *J* = 17.4 Hz, 1H), 3.79 (s, 3H), 3.55 (d, *J* = 17.4 Hz, 1H), 1.86 (s, 3H). **^{13}C-NMR** (151 MHz, $CDCl_3$) δ 203.15, 197.29, 160.14, 144.65, 137.65, 137.37, 132.86, 131.18, 130.12, 128.84, 128.40, 127.92, 127.88, 118.57, 112.49, 112.17, 55.25, 53.10, 49.33, 24.10. **HRMS** (ESI) m/z calculated for $C_{24}H_{22}NaO_3$ $[M+Na]^+$ 381.1463, found 381.1452.

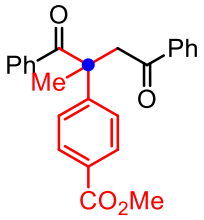

21

Following procedure C, methyl 4-(2-methyl-1,4-dioxo-1,4-diphenylbutan-2-yl)benzoate **21** (related to **Figure 2A**) was obtained as a white solid, m.p. 135-137 ^{o}C; **^{1}H-NMR** (600 MHz, $CDCl_3$) δ 8.05 (d, *J* = 8.4 Hz, 2H), 7.88 (d, *J* = 8.4 Hz, 2H), 7.55 (d, *J* = 8.4 Hz, 2H), 7.51 (t, *J* = 7.5 Hz, 1H), 7.41-7.38 (m, 4H), 7.35 (t, *J* = 7.8 Hz, 1H), 7.22 (t, *J* = 7.8 Hz, 2H), 3.95 (d, *J* = 17.4 Hz, 1H), 3.92 (s, 3H), 3.62 (d, *J* = 17.4 Hz, 1H), 1.91 (s, 3H). **^{13}C-NMR** (151 MHz, $CDCl_3$) δ 202.60, 196.85, 166.61, 148.14, 137.17, 137.13, 133.01, 131.43, 130.29, 129.12, 128.82, 128.45, 127.96, 127.88, 126.40, 53.36, 52.11, 49.06, 24.00. **IR** (KBr, cm^{-1}) 3064, 2987, 2952, 1724, 1678, 1596, 1441, 1408, 1352, 1278, 754, 687. **HRMS** (ESI) m/z calculated for $C_{25}H_{22}NaO_4$ $[M+ Na]^+$ 409.1414, found 409.1406.

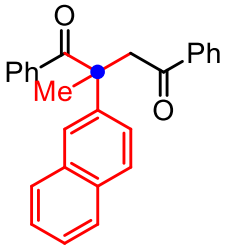

22

Following procedure C, 2-methyl-2-(naphthalen-2-yl)-1,4-diphenylbutane-1,4-dione **22** (related to **Figure 2A**) was obtained as a white solid, m.p. 131-132 ^{o}C; **^{1}H-NMR** (600 MHz, $CDCl_3$) δ 7.93 (d, *J* = 1.2 Hz, 1H), 7.91-7.89 (m, 2H), 7.87-7.83 (m, 3H), 7.58 (dd, *J* = 8.4 Hz, *J* = 1.8 Hz, 1H), 7.51-7.47 (m, 3H), 7.45-7.42 (m, 2H), 7.38 (t, *J* = 7.8 Hz, 2H), 7.31 (t, *J* = 7.2 Hz, 1H), 7.18 (t, *J* = 7.8 Hz, 2H), 4.07 (d, *J* = 17.4 Hz, 1H), 3.64 (d, *J* = 17.4 Hz, 1H), 1.99 (s, 3H). **^{13}C-NMR** (151 MHz, $CDCl_3$) δ 203.36, 197.23, 140.49, 137.69, 137.33, 133.55, 132.88, 132.39, 131.21, 128.94, 128.88, 128.40, 128.10, 127.91, 127.57, 126.41, 126.22, 124.83, 124.42, 53.29, 49.49, 24.17. **IR** (KBr, cm^{-1}) 3058, 2972, 2925, 1677, 1593, 1446, 1345, 1207, 749, 685. **HRMS** (ESI) m/z calculated for $C_{27}H_{22}NaO_2$ $[M+Na]^+$ 401.1512, found 401.1519.

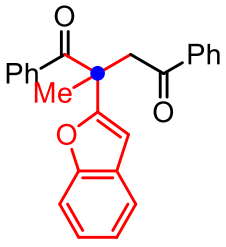

23

Following procedure C, 2-(benzofuran-2-yl)-2-methyl-1,4-diphenylbutane-1,4-dione **23** (related to **Figure 2A**) was obtained as a white solid, m.p. 116-118 ^{o}C; **^{1}H-NMR** (600 MHz, $CDCl_3$) δ

7.93-7.91 (m, 2H), 7.59-7.56 (m, 2H), 7.54-7.49 (m, 2H), 7.44 (d, *J* = 8.4 Hz, 1H), 7.41-7.37 (m, 3H), 7.28-7.25 (m, 3H), 7.22 (td, *J* = 7.2 Hz, *J* = 0.6 Hz, 1H), 6.69 (d, *J* = 0.6 Hz, 1H), 4.10 (d, *J* = 17.4 Hz, 1H), 3.75 (d, *J* = 17.4 Hz, 1H), 1.94 (s, 3H). **^{13}C-NMR** (151 MHz, $CDCl_3$) δ 200.88, 196.93, 158.79, 154.68, 137.66, 136.99, 133.09, 131.39, 128.48, 128.30, 128.26, 128.06, 127.98, 124.21, 122.95, 120.94, 111.34, 103.58, 50.47, 46.82, 22.92. **IR** (KBr, cm^{-1}) 3119, 3061, 2988, 2918, 1686, 1574, 1448, 1348, 1210, 788, 749, 687. **HRMS** (ESI) m/z calculated for $C_{25}H_{20}NaO_3$ $[M+Na]^+$ 391.1308, found 391.1302.

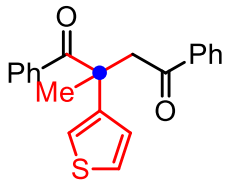

24

Following procedure C, 2-methyl-1,4-diphenyl-2-(thiophen-3-yl)butane-1,4-dione **24** (related to **Figure 2A**) was obtained as a yellow oil; **^{1}H-NMR** (600 MHz, $CDCl_3$) δ 7.90 (d, *J* = 7.2 Hz, 2H), 7.53 (t, *J* = 7.2 Hz, 1H), 7.45-7.33 (m, 6H), 7.28-7.23 (m, 3H), 7.11 (d, *J* = 4.8 Hz, 1H), 4.00 (d, *J* = 17.4 Hz, 1H), 3.57 (d, *J* = 17.4 Hz, 1H), 1.86 (s, 3H). **^{13}C-NMR** (151 MHz, $CDCl_3$) δ 203.78, 197.19, 144.30, 138.23, 137.16, 132.99, 130.99, 128.47, 128.37, 127.94, 127.90, 126.72, 126.55, 120.82, 50.91, 49.38, 24.49. **IR** (KBr, cm^{-1}) 3097, 3062, 2972, 2928, 1680, 1594, 1444, 1346, 1210, 796, 748, 691. **HRMS** (ESI) m/z calculated for $C_{21}H_{18}NaO_2S$ $[M+Na]^+$ 357.0923, found 357.0928.

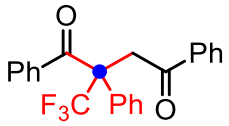

25

Following procedure C, 1,2,4-triphenyl-2-(trifluoromethyl)butane-1,4-dione **25** (related to **Figure 2A**) was obtained as a white solid, m.p. 134-136 °C; **^{1}H-NMR** (600 MHz, $CDCl_3$) δ 7.91 (d, *J* = 7.8 Hz, 2H), 7.57-7.53 (m, 3H), 7.47-7.43 (m, 7H), 7.32 (t, *J* = 7.2 Hz, 1H), 7.19 (t, *J* = 7.8 Hz, 2H), 4.66 (d, *J* = 17.4 Hz, 1H), 4.00 (d, *J* = 17.4 Hz, 1H). **^{13}C-NMR** (151 MHz, $CDCl_3$) δ 193.96, 193.69, 136.61, 136.21, 133.63, 133.58, 131.71, 129.34, 129.19, 129.10, 128.68, 128.39, 128.04, 128.01, 125.38 (q, *J* = 285.0 Hz), 60.80 (q, *J* = 22.6 Hz), 41.24. **IR** (KBr, cm^{-1}) 3063, 2944, 1685, 1595, 1447, 1323, 1217, 1150, 752, 699. **HRMS** (ESI) m/z calculated for $C_{23}H_{18}F_3O_2$ $[M+H]^+$ 383.1255, found 383.1252.

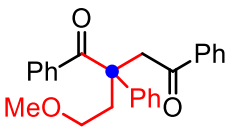

26

Following procedure C, 2-(2-methoxyethyl)-1,2,4-triphenylbutane-1,4-dione **26** (related to **Figure 2A**) was obtained as a white solid, m.p. 134-136 °C; **^{1}H-NMR** (600 MHz, $CDCl_3$) δ 7.86 (d, *J* =

7.2 Hz, 2H), 7.50-7.46 (m, 3H), 7.41-7.37 (m, 4H), 7.33-7.30 (m, 3H), 7.28-7.26 (m, 1H), 7.15 (t, *J* = 7.8 Hz, 2H), 4.38 (d, *J* = 18.0 Hz, 1H), 3.79 (d, *J* = 18.0 Hz, 1H), 3.37-3.32 (m, 1H), 3.18-3.13 (m, 1H), 2.98 (s, 3H), 2.65-2.56 (m, 2H). **^{13}C-NMR** (151 MHz, $CDCl_3$) δ 202.82, 197.05, 141.25, 138.12, 137.26, 132.76, 130.80, 129.14, 128.81, 128.34, 127.85, 127.77, 127.38, 126.71, 69.17, 58.09, 55.00, 43.95, 35.72. **IR** (KBr, cm^{-1}) 3059, 2924, 2872, 1683, 1597, 1448, 1356, 1214, 1114, 785, 754, 694. **HRMS** (ESI) m/z calculated for $C_{25}H_{24}NaO_3$ $[M+Na]^+$ 395.1627, found 395.1618.

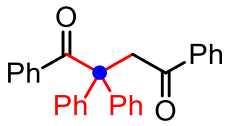

27

Following procedure C, 1,2,2,4-tetraphenylbutane-1,4-dione **27** (related to **Figure 2**) (Bergonzini et al. 2016) was obtained as a white solid, m.p. 159-160 ^oC; **^{1}H-NMR** (600 MHz, $CDCl_3$) δ 7.82-7.79 (m, 2H), 7.50-7.46 (m, 3H), 7.39-7.35 (m, 6H), 7.30-7.26 (m, 5H), 7.25-7.23 (m, 2H), 7.18-7.16 (m, 2H), 4.32 (s, 2H). **^{13}C-NMR** (151 MHz, $CDCl_3$) δ 201.11, 196.33, 142.42, 138.90, 136.99, 133.00, 130.83, 129.32, 129.26, 128.44, 128.20, 127.88, 127.61, 127.00, 62.09, 49.96. **IR** (KBr, cm^{-1}) 3064, 2912, 1673, 1594, 1492, 1446, 1355, 1208, 749, 700, 643. **HRMS** (ESI) m/z calculated for $C_{28}H_{22}NaO_2$ $[M+ Na]^+$ 413.1513, found 413.1520.

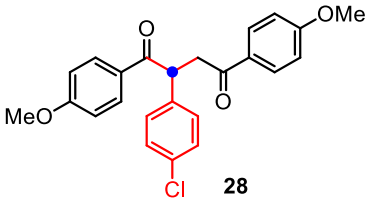

28

Following procedure B, 2-(4-chlorophenyl)-1,4-bis(4-methoxyphenyl)butane-1,4-dione **28** (related to **Figure 2B**) was obtained as a yellow oil; **^{1}H-NMR** (600 MHz, $CDCl_3$) δ 7.90 (d, *J* = 8.4 Hz, 2H), 7.83 (d, *J* = 9.0 Hz, 2H), 7.19 (d, *J* = 8.4 Hz, 2H), 7.14 (d, *J* = 8.4 Hz, 2H), 6.78 (d, *J* = 9.0 Hz, 2H), 6.76 (d, *J* = 9.0 Hz, 2H), 5.17 (dd, *J* = 9.6 Hz, *J* = 3.6 Hz, 1H), 3.99 (dd, *J* = 17.4 Hz, *J* = 9.6 Hz, 1H), 3.71 (s, 3H), 3.68 (s, 3H), 3.12 (dd, *J* = 17.4 Hz, *J* = 3.6 Hz, 1H). **^{13}C-NMR** (151 MHz, $CDCl_3$) δ 197.00, 196.17, 163.49, 163.32, 137.67, 132.94, 131.06, 130.28, 129.44, 129.39, 129.09, 129.04, 113.65, 113.59, 55.30, 55.27, 47.44, 43.07. **HRMS** (ESI) m/z calculated for $C_{24}H_{21}ClNaO_4$ $[M+Na]^+$ 431.1021, found 431.1025.

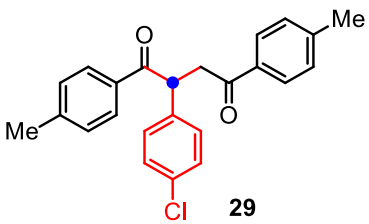

29

Following procedure B, 2-(4-chlorophenyl)-1,4-di-*p*-tolylbutane-1,4-dione **29** (related to **Figure 2B**) was obtained as a yellow oil; **^{1}H-NMR** (600 MHz, $CDCl_3$) δ 7.91 (d, *J* = 8.4 Hz, 2H), 7.86 (d, *J* = 8.4 Hz, 2H), 7.28 (d, *J* = 8.4 Hz, 2H), 7.24 (d, *J* = 8.4 Hz, 2H), 7.21 (d, *J* = 8.4 Hz, 2H), 7.18 (d, *J* = 8.4 Hz, 2H), 5.29 (dd, *J* = 9.6 Hz, *J* = 3.6 Hz, 1H), 4.12 (dd, *J* = 18.0 Hz, *J* = 9.6 Hz, 1H),

3.25 (dd, *J* = 18.0 Hz, *J* = 3.6 Hz, 1H), 2.37 (s, 3H), 2.33 (s, 3H). **^{13}C-NMR** (151 MHz, $CDCl_3$) δ 198.14, 197.27, 144.01, 143.80, 137.43, 133.86, 133.62, 133.07, 129.51, 129.19, 129.18, 129.17, 128.93, 128.17, 47.68, 43.36, 21.56, 21.52. **IR** (KBr, cm^{-1}) 3058, 3031, 2913, 1673, 1569, 1488, 1336, 1232, 1177, 996, 816, 757, 694. **HRMS** (ESI) m/z calculated for $C_{24}H_{21}ClNaO_2$ $[M+Na]^+$ 399.1122, found 399.1130.

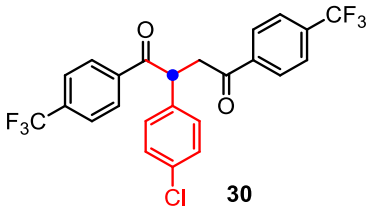

30

Following procedure B, 2-(4-chlorophenyl)-1,4-bis(4-(trifluoromethyl)phenyl)butane-1,4-dione **30** (related to **Figure 2B**) was obtained as a white solid, m.p. 159-160 ^oC; **^{1}H-NMR** (600 MHz, $CDCl_3$) δ 8.09 (d, *J* = 8.4 Hz, 2H), 8.07 (d, *J* = 8.4 Hz, 2H), 7.73 (d, *J* = 8.4 Hz, 2H), 7.68 (d, *J* = 8.4 Hz, 2H), 7.32-7.27 (m, 4H), 5.28 (dd, *J* = 10.2 Hz, *J* = 3.6 Hz, 1H), 4.20 (dd, *J* = 18.0 Hz, *J* = 10.2 Hz, 1H), 3.32 (dd, *J* = 18.0 Hz, *J* = 3.6 Hz, 1H). **^{13}C-NMR** (151 MHz, $CDCl_3$) δ 197.59, 196.75, 138.83, 138.72, 135.87, 134.70 (q, *J* = 32.9 Hz), 134.58 (q, *J* = 32.9 Hz), 133.91, 129.66, 129.48, 129.12, 128.47, 125.74 (q, *J* = 3.6 Hz), 125.72 (q, *J* = 3.6 Hz), 123.50 (q, *J* = 272.7 Hz), 123.48 (q, *J* = 272.7 Hz), 48.35, 43.88. **HRMS** (ESI) m/z calculated for $C_{24}H_{15}ClF_6NaO_2$ $[M+Na]^+$ 507.0557, found 507.0545.

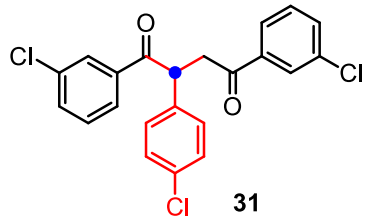

31

Following procedure B, 1,4-Bis(3-chlorophenyl)-2-(4-chlorophenyl)butane-1,4-dione **31** (related to **Figure 2B**) was obtained as a yellow oil; **^{1}H-NMR** (600 MHz, $CDCl_3$) δ 7.96 (t, *J* = 1.2 Hz, 1H), 7.93 (t, *J* = 1.2 Hz, 1H), 7.86 (d, *J* = 7.8 Hz, 1H), 7.83 (d, *J* = 7.8 Hz, 1H), 7.53 (dt, *J* = 8.4 Hz, *J* = 1.2 Hz, 1H), 7.48 (dt, *J* = 7.8 Hz, *J* = 1.2 Hz, 1H), 7.39 (t, *J* = 7.8 Hz, 1H), 7.35 (t, *J* = 7.8 Hz, 1H), 7.31-7.25 (m, 4H), 5.21 (dd, *J* = 9.6 Hz, *J* = 3.6 Hz, 1H), 4.12 (dd, *J* = 18.0 Hz, *J* = 9.6 Hz, 1H), 3.26 (dd, *J* = 18.0 Hz, *J* = 3.6 Hz, 1H). **^{13}C-NMR** (151 MHz, $CDCl_3$) δ 197.23, 196.39, 137.65, 137.61, 136.14, 134.96, 134.94, 133.68, 133.35, 133.07, 129.97, 129.90, 129.52, 129.46, 128.85, 128.23, 126.88, 126.17, 48.05, 43.71. **IR** (KBr, cm^{-1}) 3064, 2918, 1677, 1571, 1489, 1426, 1230, 1196, 1091, 781, 676. **HRMS** (ESI) m/z calculated for $C_{22}H_{15}Cl_3NaO_2$ $[M+Na]^+$ 439.0028, found 439.0030.

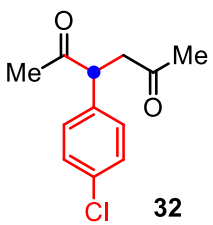

32

Following procedure B, 3-(4-chlorophenyl)hexane-2,5-dione **32** (related to **Figure 2B**) was obtained as a yellow oil**; ^{1}H-NMR** (600 MHz, $CDCl_3$) δ 7.30 (d, *J* = 8.4 Hz, 2H), 7.14 (d, *J* = 8.4 Hz, 2H), 4.20 (dd, *J* = 10.2 Hz, *J* = 3.6 Hz, 1H), 3.40 (dd, *J* = 18.0 Hz, *J* = 10.2 Hz, 1H), 2.56 (dd, *J* = 18.0 Hz, *J* = 3.6 Hz, 1H), 2.16 (s, 3H), 2.12 (s, 3H). **^{13}C-NMR** (151 MHz, $CDCl_3$) δ 206.60, 206.34, 136.22, 133.51, 129.47, 129.23, 53.09, 46.32, 29.84, 28.94. **HRMS** (ESI) m/z calculated for $C_{12}H_{13}ClNaO_2$ $[M+Na]^+$ 247.0498, found 247.0505.

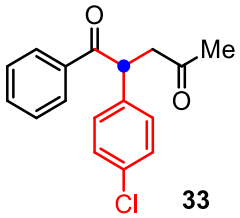

33

Following procedure B, 3-(4-chlorophenyl)-1-phenylpentane-1,4-dione **33** (related to **Figure 2B**) (Blay et al., 2006) was obtained as a yellow solid, m.p. 104-105 ^{o}C; **^{1}H-NMR** (600 MHz, $CDCl_3$) δ 7.94-7.92 (m, 2H), 7.48 (t, *J* = 7.8 Hz, 1H), 7.37 (t, *J* = 7.8 Hz, 2H), 7.24 (d, *J* = 8.4 Hz, 2H), 7.20 (d, *J* = 8.4 Hz, 2H), 5.09 (dd, *J* = 9.6 Hz, *J* = 4.2 Hz, 1H), 3.57 (dd, *J* = 18.0 Hz, *J* = 9.6 Hz, 1H), 2.74 (dd, *J* = 18.0 Hz, *J* = 4.2 Hz, 1H), 2.18 (s, 3H). **^{13}C-NMR** (151 MHz, $CDCl_3$) δ 206.28, 198.51, 137.03, 136.06, 133.24, 133.05, 129.41, 129.29, 128.80, 128.51, 47.93, 47.83, 29.92. **IR** (KBr, cm^{-1}) 3059, 2959, 2913, 2852, 1711, 1678, 1491, 1444, 1330, 1247, 1157, 770, 687. **HRMS** (ESI) m/z calculated for $C_{17}H_{15}ClNaO_2$ $[M+Na]^+$ 309.0653, found 309.0657.

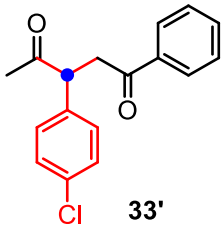

33'

Following procedure B, 2-(4-chlorophenyl)-1-phenylpentane-1,4-dione **33'** (related to **Figure 2B**) was obtained as a yellow oil; **^{1}H-NMR** (600 MHz, $CDCl_3$) δ 7.95-7.93 (m, 2H), 7.55 (t, *J* = 7.8 Hz, 1H), 7.44 (t, *J* = 7.8 Hz, 2H), 7.32 (d, *J* = 8.4 Hz, 2H), 7.23 (d, *J* = 8.4 Hz, 2H), 4.41 (dd, *J* = 9.6 Hz, *J* = 4.2 Hz, 1H), 3.97 (dd, *J* = 18.0 Hz, *J* = 9.6 Hz, 1H), 3.12 (dd, *J* = 18.0 Hz, *J* = 4.2 Hz, 1H), 2.21 (s, 3H). **^{13}C-NMR** (151 MHz, $CDCl_3$) δ 206.70, 197.74, 136.45, 136.35, 133.61, 133.30, 129.64, 129.29, 128.58, 128.04, 53.17, 42.18, 29.16. **IR** (KBr, cm^{-1}) 3061, 2924, 2915, 1715, 1680, 1595, 1490, 1447, 1357, 1245, 1164, 808, 739, 715, 688. **HRMS** (ESI) m/z calculated for $C_{17}H_{15}ClNaO_2$ $[M+Na]^+$ 309.0653, found 309.0649.

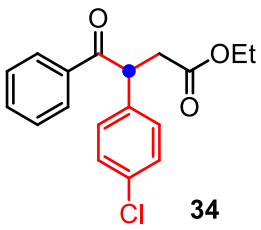

34

Following procedure B, ethyl 3-(4-chlorophenyl)-4-oxo-4-phenylbutanoate **34** (related to **Figure 2B**) (Fujimura et al., 1991) was obtained as a yellow oil; **^{1}H-NMR** (600 MHz, $CDCl_3$) δ 7.94 (d, *J* = 7.2 Hz, 2H), 7.49 (t, *J* = 7.2 Hz, 1H), 7.39 (t, *J* = 7.8 Hz, 2H), 7.26-7.22 (m, 4H), 5.07 (dd, *J* = 9.6 Hz, *J* = 5.4 Hz, 1H), 4.09 (q, *J* = 7.2 Hz, 2H), 3.33 (dd, *J* = 16.8 Hz, *J* = 9.6 Hz, 1H), 2.70 (dd, *J* = 16.8 Hz, *J* = 5.4 Hz, 1H), 1.19 (t, *J* = 7.2 Hz, 3H). **^{13}C-NMR** (151 MHz, $CDCl_3$) δ 198.27, 171.68, 136.57, 136.02, 133.44, 133.12, 129.49, 129.31, 128.78, 128.56, 60.74, 48.74, 38.48, 14.08. **IR** (KBr, cm^{-1}) 3098, 3061, 2928, 1680, 1491, 1344, 1228, 1178, 752, 691. **HRMS** (ESI) m/z calculated for $C_{18}H_{17}ClNaO_3$ $[M+Na]^+$ 339.0758, found 339.0758.

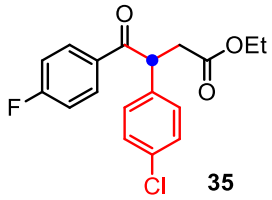

35

Following procedure B, Ethyl 3-(4-chlorophenyl)-4-(4-fluorophenyl)-4-oxobutanoate **35** (related to **Figure 2B**) was obtained as a colorless oil; **^{1}H-NMR** (600 MHz, $CDCl_3$) δ 7.97 (dd, *J* = 8.4 Hz, *J* = 5.4 Hz, 2H), 7.26 (d, *J* = 8.4 Hz, 2H), 7.21 (d, *J* = 8.4 Hz, 2H), 7.08-7.04 (m, 2H), 5.01 (dd, *J* = 9.6 Hz, *J* = 5.4 Hz, 1H), 4.10 (q, *J* = 7.2 Hz, 2H), 3.32 (dd, *J* = 16.8 Hz, *J* = 9.6 Hz, 1H), 2.68 (dd, *J* = 16.8 Hz, *J* = 5.4 Hz, 1H), 1.20 (t, *J* = 7.2 Hz, 3H). **^{13}C-NMR** (151 MHz, $CDCl_3$) δ 196.73, 171.68, 165.68 (d, *J* = 255.4 Hz), 136.39, 133.60, 132.40 (d, *J* = 3.0 Hz), 131.45 (d, *J* = 9.4 Hz), 129.41, 115.73 (d, *J* = 21.9 Hz), 60.81, 48.74, 38.48, 14.08. **IR** (KBr, cm^{-1}) 3072, 2982, 2932, 1731, 1683, 1597, 1490, 1410, 1333, 1235, 830, 768. **HRMS** (ESI) m/z calculated for $C_{18}H_{16}ClFNaO_3$ $[M+Na]^+$ 357.0665, found 357.0658.

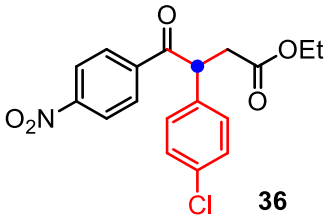

36

Following procedure B, ethyl 3-(4-chlorophenyl)-4-(4-nitrophenyl)-4-oxobutanoate **36** (related to **Figure 2B**) was obtained as a colorless oil; **^{1}H-NMR** (600 MHz, $CDCl_3$) δ 8.23 (d, *J* = 9.0 Hz, 2H), 8.07 (d, *J* = 9.0 Hz, 2H), 7.28 (d, *J* = 9.0 Hz, 2H), 7.20 (d, *J* = 9.0 Hz, 2H), 5.04 (dd, *J* = 9.6 Hz, *J* = 4.8 Hz, 1H), 4.12 (q, *J* = 7.2 Hz, 2H), 3.37 (dd, *J* = 16.8 Hz, *J* = 9.6 Hz, 1H), 2.72 (dd, *J* = 16.8 Hz, *J* = 4.8 Hz, 1H), 1.22 (t, *J* = 7.2 Hz, 3H). **^{13}C-NMR** (151 MHz, $CDCl_3$) δ 197.13, 171.53, 150.20, 140.78, 135.24, 134.06, 129.69, 129.65, 129.44, 123.78, 61.00, 49.44, 38.37, 14.09. **IR** (KBr, cm^{-1}) 3091, 2983, 2906, 1724, 1687, 1611, 1530, 1493, 1351, 1247, 830, 721, 692. **HRMS** (ESI) m/z calculated for $C_{18}H_{16}ClNNaO_5$ $[M+Na]^+$ 384.0609, found 384.0607.

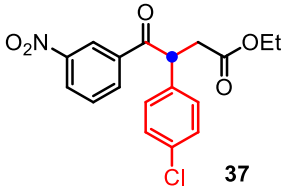

37

Following procedure B, ethyl 3-(4-chlorophenyl)-4-(3-nitrophenyl)-4-oxobutanoate **37** (related to **Figure 2B**) was obtained as a colorless oil; **^{1}H-NMR** (600 MHz, $CDCl_3$) δ 8.79 (s, 1H), 8.35 (dd, *J* = 7.8 Hz, *J* = 1.2 Hz, 1H), 8.25 (d, *J* = 7.8 Hz, 1H), 7.61 (t, *J* = 7.8 Hz, 1H), 7.29 (d, *J* = 8.4 Hz, 2H), 7.24 (d, *J* = 8.4 Hz, 2H), 5.07 (dd, *J* = 9.6 Hz, *J* = 4.8 Hz, 1H), 4.14-4.10 (m, 2H), 3.39 (dd, *J* = 16.8 Hz, *J* = 9.6 Hz, 1H), 2.73 (dd, *J* = 16.8 Hz, *J* = 4.8 Hz, 1H), 1.22 (t, *J* = 7.2 Hz, 3H). **^{13}C-NMR** (151 MHz, $CDCl_3$) δ 196.31, 171.55, 148.40, 137.32, 135.30, 134.19, 134.05, 129.87, 129.68, 129.44, 127.36, 123.67, 61.00, 49.10, 38.39, 14.09. **IR** (KBr, cm^{-1}) 3109, 2982, 2931, 1726, 1691, 1528, 1490, 1347, 1227. **HRMS** (ESI) m/z calculated for $C_{18}H_{16}ClNNaO_5$ $[M+Na]^+$ 384.0607, found 384.0609.

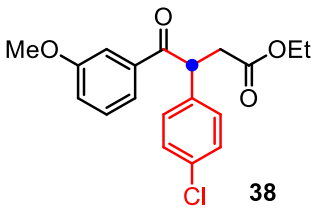

38

Following procedure B, ethyl 3-(4-chlorophenyl)-4-(3-methoxyphenyl)-4-oxobutanoate **38** (related to **Figure 2B**) was obtained as a colorless oil; **^{1}H-NMR** (600 MHz, $CDCl_3$) δ 7.53 (d, *J* = 8.4 Hz, 1H), 7.47 (s, 1H), 7.29 (t, *J* = 8.4 Hz, 1H), 7.25 (d, *J* = 8.4 Hz, 2H), 7.22 (d, *J* = 8.4 Hz, 2H), 7.03 (dd, *J* = 8.4 Hz, *J* = 2.4 Hz, 1H), 5.05 (dd, *J* = 9.6 Hz, *J* = 5.4 Hz, 1H), 4.09 (q, *J* = 7.2 Hz, 2H), 3.79 (s, 3H), 3.32 (dd, *J* = 16.8 Hz, *J* = 9.6 Hz, 1H), 2.70 (dd, *J* = 16.8 Hz, *J* = 5.4 Hz, 1H), 1.19 (t, *J* = 7.2 Hz, 3H). **^{13}C-NMR** (151 MHz, $CDCl_3$) δ 198.02, 171.63, 159.70, 137.23, 136.54, 133.38, 129.49, 129.41, 129.27, 121.36, 119.59, 113.09, 60.72, 55.28, 48.79, 38.43, 14.05. **HRMS** (ESI) m/z calculated for $C_{19}H_{19}ClNaO_4$ $[M+Na]^+$ 369.0865, found 369.0871.

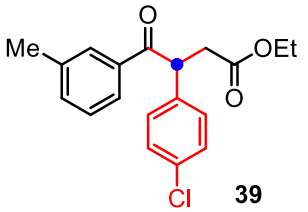

39

Following procedure B, ethyl 3-(4-chlorophenyl)-4-oxo-4-(*m*-tolyl)butanoate **39** (related to **Figure 2B**) was obtained as a yellow oil; **^{1}H-NMR** (600 MHz, $CDCl_3$) δ 7.71 (s, 1H), 7.68 (d, *J* = 7.2 Hz, 1H), 7.25 (d, *J* = 7.2 Hz, 1H), 7.23-7.16 (m, 5H), 5.01 (dd, *J* = 9.0 Hz, *J* = 5.4 Hz, 1H), 4.07-4.02 (m, 2H), 3.27 (dd, *J* = 17.4 Hz, *J* = 9.0 Hz, 1H), 2.64 (dd, *J* = 17.4 Hz, *J* = 5.4 Hz, 1H), 2.30 (s, 3H), 1.14 (t, *J* = 7.2 Hz, 3H). **^{13}C-NMR** (151 MHz, $CDCl_3$) δ 198.48, 171.75, 138.37, 136.62, 135.99, 133.95, 133.36, 129.46, 129.27, 128.40, 126.02, 60.74, 48.66, 38.46, 21.31, 14.08. **IR** (KBr, cm^{-1}) 3052, 2956, 2924, 2854, 1734, 1676, 1583, 1491, 1327, 1233, 1167, 800, 759, 681. **HRMS** (ESI) m/z calculated for $C_{19}H_{19}ClNaO_3$ $[M+Na]^+$ 353.0915, found 353.0923.

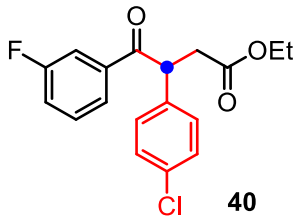

40

Following procedure B, ethyl 3-(4-chlorophenyl)-4-(3-fluorophenyl)-4-oxobutanoate **40** (related to **Figure 2B**) was obtained as a colorless oil; **^{1}H-NMR** (600 MHz, $CDCl_3$) δ 7.72 (d, *J* = 7.8 Hz, 1H), 7.62 (dt, *J* = 9.0 Hz, *J* = 1.8 Hz, 1H), 7.39-7.35 (m, 1H), 7.27 (d, *J* = 8.4 Hz, 2H), 7.21 (d, *J* = 8.4 Hz, 2H), 7.20-7.18 (m, 1H), 5.00 (dd, *J* = 9.6 Hz, *J* = 4.8 Hz, 1H), 4.10 (q, *J* = 7.2 Hz, 2H), 3.33 (dd, *J* = 16.8 Hz, *J* = 9.6 Hz, 1H), 2.69 (dd, *J* = 16.8 Hz, *J* = 4.8 Hz, 1H), 1.20 (t, *J* = 7.2 Hz, 3H). **^{13}C-NMR** (151 MHz, $CDCl_3$) δ 197.15 (d, *J* = 2.0 Hz), 171.60, 162.77 (d, *J* = 248.2 Hz), 138.15 (d, *J* = 6.3 Hz), 136.05, 133.70, 130.24 (d, *J* = 7.7 Hz), 129.46, 129.44, 124.50 (d, *J* = 2.9 Hz), 120.18 (d, *J* = 21.5 Hz), 115.53 (d, *J* = 22.5 Hz), 60.85, 48.98, 38.47, 14.09. **^{19}F-NMR** (564 MHz, $CDCl_3$) δ -111.61-(-111.67). **HRMS** (ESI) m/z calculated for $C_{18}H_{16}ClFNaO_3$ $[M+Na]^+$ 357.0664, found 357.0648.

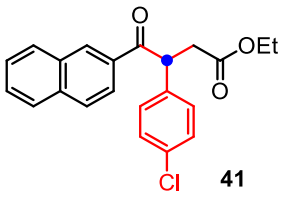

41

Following procedure B, ethyl 3-(4-chlorophenyl)-4-(naphthalen-2-yl)-4-oxobutanoate **41** (related to **Figure 2B**) was obtained as a colorless oil; **^{1}H-NMR** (600 MHz, $CDCl_3$) δ 8.49 (s, 1H), 7.99 (dd, *J* = 8.4 Hz, *J* = 1.8 Hz, 1H), 7.90 (d, *J* = 8.4 Hz, 1H), 7.84-7.81 (m, 2H), 7.58-7.55 (m, 1H), 7.53-7.50 (m, 1H), 7.30-7.28 (m, 2H), 7.26-7.24 (m, 2H), 5.24 (dd, *J* = 9.6 Hz, *J* = 5.4 Hz, 1H), 4.11 (q, *J* = 7.2 Hz, 2H), 3.39 (dd, *J* = 16.8 Hz, *J* = 9.6 Hz, 1H), 2.75 (dd, *J* = 16.8 Hz, *J* = 5.4 Hz, 1H), 1.20 (t, *J* = 7.2 Hz, 3H). **^{13}C-NMR** (151 MHz, $CDCl_3$) δ 198.26, 171.78, 136.68, 135.54, 133.45, 133.32, 132.39, 130.63, 129.64, 129.49, 129.34, 128.58, 128.47, 127.68, 126.74, 124.37, 60.80, 48.79, 38.51, 14.11. **HRMS** (ESI) m/z calculated for $C_{22}H_{19}ClNaO_3$ $[M+Na]^+$ 389.0915, found 389.0927.

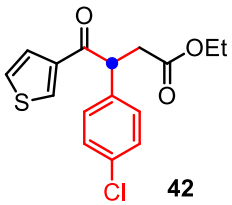

42

Following procedure B, ethyl 3-(4-chlorophenyl)-4-oxo-4-(thiophen-3-yl)butanoate **42** (related to **Figure 2B**) was obtained as a colorless oil; **^{1}H-NMR** (600 MHz, $CDCl_3$) δ 8.04 (dd, *J* = 3.0 Hz, *J* = 1.2 Hz, 1H), 7.50 (dd, *J* = 4.8 Hz, *J* = 1.2 Hz, 1H), 7.28-7.26 (m, 2H), 7.25-7.23 (m, 3H), 4.85 (dd, *J* = 9.6 Hz, *J* = 5.4 Hz, 1H), 4.12-4.08 (m, 2H), 3.29 (dd, *J* = 16.8 Hz, *J* = 9.6 Hz, 1H), 2.67 (dd, *J* = 16.8 Hz, *J* = 5.4 Hz, 1H), 1.20 (t, *J* = 7.2 Hz, 3H). **^{13}C-NMR** (151 MHz, $CDCl_3$) δ 192.30,

171.68, 140.97, 136.69, 133.55, 133.09, 129.44, 129.34, 127.36, 126.30, 60.79, 50.46, 38.16, 14.09. **HRMS** (ESI) m/z calculated for $C_{16}H_{15}ClNaO_3S$ $[M+Na]^+$ 345.0323, found 345.0339.

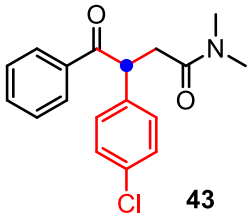

43

Following procedure B, 3-(4-chlorophenyl)-*N*,*N*-dimethyl-4-oxo-4-phenylbutanamide **43** (related to **Figure 2B**) was obtained as a yellow oil; **^{1}H-NMR** (600 MHz, $CDCl_3$) δ 7.91-7.88 (m, 2H), 7.58-7.54 (m, 1H), 7.45 (t, *J* = 7.8 Hz, 2H), 7.22 (d, *J* = 8.4 Hz, 2H), 7.18 (d, *J* = 8.4 Hz, 2H), 4.62 (dd, *J* = 8.4 Hz, *J* = 6.0 Hz, 1H), 3.35 (dd, *J* = 13.8 Hz, *J* = 8.4 Hz, 1H), 3.26 (dd, *J* = 13.8 Hz, *J* = 6.0 Hz, 1H), 2.90 (s, 3H), 2.82 (s, 3H). **^{13}C-NMR** (151 MHz, $CDCl_3$) δ 194.95, 168.76, 137.58, 135.84, 133.36, 132.35, 130.40, 128.77, 128.52, 128.14, 54.43, 37.25, 35.83, 34.62. **IR** (KBr, cm^{-1}) 3367, 3056, 3026, 2935, 1690, 1634, 1489, 1443, 1392, 1226, 1087, 813, 755, 684. **HRMS** (ESI) m/z calculated for $C_{18}H_{16}ClNNaO_2$ $[M+Na]^+$ 338.0918, found 338.0929.

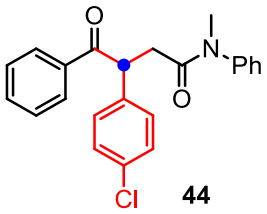

44

Following procedure B, 3-(4-chlorophenyl)-N-methyl-4-oxo-N,4-diphenylbutanamide **44** (related to **Figure 2B**) was obtained as a yellow oil; **^{1}H-NMR** (600 MHz, $CDCl_3$) δ 7.98-7.95 (m, 2H), 7.47 (t, *J* = 7.2 Hz, 1H), 7.42-7.36 (m, 4H), 7.33 (t, *J* = 7.2 Hz, 1H), 7.19-7.16 (m, 4H), 7.10 (d, *J* = 8.4 Hz, 2H), 5.21 (dd, *J* = 9.6 Hz, *J* = 4.8 Hz, 1H), 3.22 (s, 3H), 3.11 (dd, *J* = 16.2 Hz, *J* = 9.6 Hz, 1H), 2.38 (dd, *J* = 16.2 Hz, *J* = 4.8 Hz, 1H). **^{13}C-NMR** (151 MHz, $CDCl_3$) δ 199.00, 170.73, 143.55, 136.96, 136.15, 133.10, 132.93, 129.84, 129.54, 129.09, 128.81, 128.49, 127.94, 127.34, 49.15, 39.00, 37.35. **IR** (KBr, cm^{-1}) 3060, 2923, 2361, 1650, 1594, 1540,1492, 1443, 1413, 1357, 1279, 843, 705. **HRMS** (ESI) m/z calculated for $C_{23}H_{20}ClNNaO_2$ $[M+Na]^+$ 400.1075, found 400.1081.

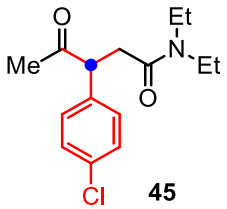

45

Following procedure B, 3-(4-chlorophenyl)-N,N-diethyl-4-oxopentanamide **45** (related to **Figure 2B**) was obtained as a colorless oil; **^{1}H-NMR** (600 MHz, $CDCl_3$) δ 7.32-7.29 (m, 2H), 7.22-7.20 (m, 2H), 4.36 (dd, *J* = 10.2 Hz, *J* = 4.2 Hz, 1H), 3.40-3.23 (m, 5H), 2.70 (dd, *J* = 16.2 Hz, *J* = 4.2 Hz, 1H), 2.19-2.18 (m, 3H), 1.18-1.16 (m, 3H), 1.09-1.07 (m, 3H). **^{13}C-NMR** (151 MHz, $CDCl_3$)

δ 207.43, 169.65, 136.53, 133.39, 129.60, 129.09, 53.89, 41.82, 40.22, 36.96, 29.35, 14.01, 12.96. **HRMS** (ESI) m/z calculated for $C_{15}H_{20}ClNNaO_2$ $[M+Na]^+$ 304.1075, found 304.1081.

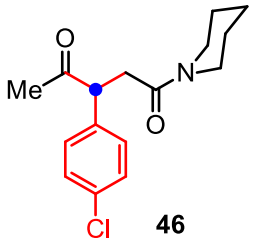

46

Following procedure B, 3-(4-chlorophenyl)-1-(piperidin-1-yl)pentane-1,4-dione **46** (related to **Figure 2B**) was obtained as a colorless oil; **^{1}H-NMR** (600 MHz, $CDCl_3$) δ 7.30 (d, *J* = 8.4 Hz, 2H), 7.20 (d, *J* = 8.4 Hz, 2H), 4.33 (dd, *J* = 10.2 Hz, *J* = 3.6 Hz, 1H), 3.56-3.45 (m, 2H), 3.41-3.34 (m, 2H), 3.27 (dd, *J* = 16.2 Hz, *J* = 10.2 Hz, 1H), 2.44 (dd, *J* = 16.2 Hz, *J* = 3.6 Hz, 1H), 2.19 (s, 3H), 1.64-1.43 (m, 6H). **^{13}C-NMR** (151 MHz, $CDCl_3$) δ 207.46, 168.80, 136.53, 133.42, 129.61, 129.11, 53.87, 46.41, 42.84, 37.05, 29.39, 26.21, 25.44, 24.41. **HRMS** (ESI) m/z calculated for $C_{16}H_{20}ClNNaO_2$ $[M+Na]^+$ 316.1075, found 316.1061.

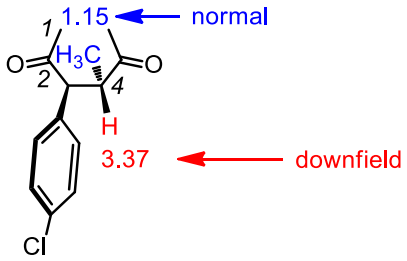

anti-**47**

Following procedure B, major product **(*anti*-47)** (related to **Figure 2C**) was obtained as a colorless oil; **^{1}H-NMR** (600 MHz, $CDCl_3$) δ 7.28 (d, *J* = 8.4 Hz, 2H), 7.17 (d, *J* = 8.4 Hz , 2H), 3.94 (d, *J* = 10.8 Hz, 1H), 3.40-3.35 (m, 1H), 2.10 (s, 3H), 1.88 (s, 3H), 1.15 (d, *J* = 6.6 Hz, 3H). **^{13}C-NMR** (151 MHz, $CDCl_3$) δ 210.77, 206.52, 135.07, 133.70, 130.04, 129.13, 60.47, 49.08, 30.30, 30.26, 15.72. **IR** (KBr, cm^{-1}) 3737, 2970, 2935, 1710, 1490, 1458, 1355, 824. **HRMS** (ESI) m/z calculated for $C_{13}H_{16}ClO_2$ $[M+H]^+$ 239.0834, found 239.0829.

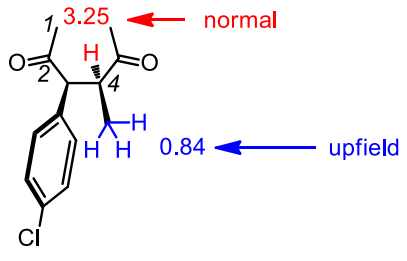

syn-**47**

Following procedure B, minor product ***syn*-47** (related to **Figure 2C**) was obtained as a colorless oil; **^{1}H-NMR** (600 MHz, $CDCl_3$) δ 7.32 (d, *J* = 8.4 Hz, 2H), 7.13 (d, *J* = 8.4 Hz, 2H), 3.94 (d, *J* = 10.8 Hz, 1H), 3.28-3.22 (m, 1H), 2.28 (s, 3H), 2.05 (s, 3H), 0.84 (d, *J* = 7.2 Hz, 3H). **^{13}C-NMR** (151 MHz, $CDCl_3$) δ 211.96, 207.67, 134.82, 133.74, 130.08, 129.31, 61.10, 48.71, 29.18, 28.94,

14.53. **IR** (KBr, cm^{-1}) 3736, 2972, 1712, 1557, 1490, 1457, 1357, 1224, 821. **HRMS** (ESI) m/z calculated for $C_{13}H_{16}ClO_2$ $[M+H]^+$ 239.0834, found 239.0839.

(1) The large chemical shift difference between *syn*-**47** and *anti*-**47** was observed. For *syn*-**47**, the Me doublet is unusually at upfield (0.84 ppm), whereas the CHMe multiplet is normally at 3.25 ppm. For *anti*-**47**, the CHMe multiplet is unusually at downfield (3.37 ppm), and the Me group is normally at 1.15 ppm. This observation was ascribed to a large anisotropy effect of the phenyl group of *syn*-**47** and *anti*-**47**.

(2) The **Figure S93** and **Figure S96** (NOESY experiments of *anti*-**47** and syn-**47)** were used to confirm the configuration of compound **47**. Spatially, H^7 is far from H^8 in *anti*-**47** but H^7 is colse to H^8 in *syn*-**47**.

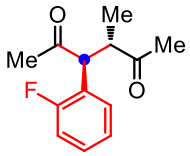

***anti*-48**

Following procedure B, 3-(2-fluorophenyl)-4-methylhexane-2,5-dione ***anti*-48** (related to **Figure 2C**) was obtained as a yellow oil; **^{1}H-NMR** (600 MHz, $CDCl_3$) δ 7.25-7.22 (m, 1H), 7.19 (dt, *J* = 7.2 Hz, *J* = 1.8 Hz, 1H), 7.11-7.05 (m, 2H), 4.35 (d, *J* = 10.2 Hz, 1H), 3.43-3.37 (m, 1H), 2.12 (s, 3H), 1.97 (s, 3H), 1.20 (d, *J* = 7.2 Hz, 3H). **^{13}C-NMR** (151 MHz, $CDCl_3$) δ 210.33, 205.88, 160.54 (d, *J* = 246.9 Hz), 129.41 (d, *J* = 6.4 Hz), 129.39 (d, *J* = 5.6 Hz) 124.64 (d, *J* = 3.5 Hz), 123.86 (d, *J* = 15.2 Hz), 115.95 (d, *J* = 22.9 Hz), 52.88, 48.13, 29.99, 29.22, 15.53. **HRMS** (ESI) m/z calculated for $C_{13}H_{15}FNaO_2$ $[M+Na]^+$ 245.0949, found 245.0955.

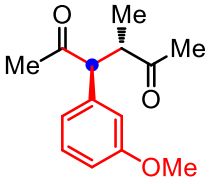

***anti*-49**

Following procedure B, 3-(3-methoxyphenyl)-4-methylhexane-2,5-dione ***anti*-49** (related to **Figure 2C**) was obtained as a yellow oil; **^{1}H-NMR** (600 MHz, $CDCl_3$) δ 7.22 (t, *J* = 7.8 Hz, 1H), 6.81-6.78 (m, 2H), 6.76 (t, *J* = 1.8 Hz, 1H), 3.91 (d, *J* = 10.8 Hz, 1H), 3.78 (s, 3H), 3.43-3.38 (m, 1H), 2.10 (s, 3H), 1.86 (s, 3H), 1.15 (d, *J* = 6.6 Hz, 3H). **^{13}C-NMR** (151 MHz, $CDCl_3$) δ 211.20, 206.64, 159.90, 137.95, 129.93, 121.07, 114.36, 113.06, 61.46, 55.18, 48.83, 30.33, 30.09, 15.71. **IR** (KBr, cm^{-1}) 3061, 2979, 2934, 2836, 1681, 1578, 1490, 1452, 1218, 747. **HRMS** (ESI) m/z calculated for $C_{14}H_{19}O_3$ $[M+H]^+$ 235.1329, found 235.132 6.

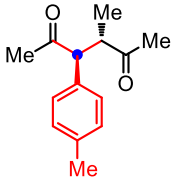

***anti*-50**

Following procedure B, 3-methyl-4-(*p*-tolyl)hexane-2,5-dione ***anti*-50** (related to **Figure 2C**) was obtained as a yellow oil; **^{1}H-NMR** (600 MHz, $CDCl_3$) δ 7.12-7.08 (m, 4H), 3.89 (d, *J* = 10.8 Hz, 1H), 3.42-3.37 (m, 1H), 2.30 (s, 3H), 2.08 (s, 3H), 1.83 (s, 3H), 1.15 (d, *J* = 6.6 Hz, 3H). **^{13}C-NMR** (151 MHz, $CDCl_3$) δ 211.37, 206.90, 137.41, 133.40, 129.65, 128.55, 61.13, 48.87, 30.31, 30.01, 21.00, 15.71. **HRMS** (ESI) m/z calculated for $C_{14}H_{18}NaO_2$ $[M+Na]^+$ 241.1199, found 241.1202.

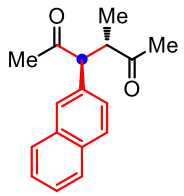

***anti*-51**

Following procedure B, major product ***anti*-51** (related to **Figure 2C**) was obtained as a colorless oil; **^{1}H-NMR** (600 MHz, $CDCl_3$) δ 7.81-7.78 (m, 3H), 7.69 (s, 1H), 7.50-7.45 (m, 2H), 7.36 (dd, *J* = 9.0 Hz, *J* = 1.8 Hz, 1H), 4.12 (d, *J* = 10.2 Hz, 1H), 3.56-3.50 (m, 1H), 2.12 (s, 3H), 1.82 (s, 3H), 1.21 (d, *J* = 7.2 Hz, 3H). **^{13}C-NMR** (151 MHz, $CDCl_3$) δ 211.16, 206.79, 133.98, 133.42, 132.70, 128.79, 127.93, 127.84, 127.63, 126.39, 126.33, 126.22, 61.51, 49.07, 30.36, 30.27, 15.81. **IR** (KBr, cm^{-1}) 3055, 2969, 2935, 1707, 1506, 1458, 1421, 1355, 1271, 1118, 820, 748. **HRMS** (ESI) m/z calculated for $C_{17}H_{18}NaO_2$ $[M+Na]^+$ 227.1199, found 227.1199.

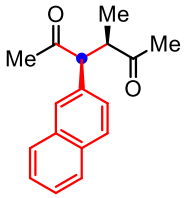

***syn*-51**

Following procedure B, minor product ***syn*-51** (related to **Figure 2C**) was obtained as a colorless oil; **^{1}H-NMR** (600 MHz, $CDCl_3$) δ 7.84-7.81 (m, 3H), 7.68 (s, 1H), 7.53-7.47 (m, 2H), 7.28 (dd, *J* = 8.4 Hz, *J* = 1.8 Hz, 1H), 4.14 (d, *J* = 10.8 Hz, 1H), 3.43-3.37 (m, 1H), 2.32 (s, 3H), 2.08 (s, 3H), 0.86 (d, *J* = 7.2 Hz, 3H). **^{13}C-NMR** (151 MHz, $CDCl_3$) δ 212.32, 208.09, 133.83, 133.59, 132.81, 128.97, 128.18, 127.72, 127.71, 126.50, 126.19, 126.11, 62.04, 48.67, 29.25, 29.06, 14.71. **IR** (KBr, cm^{-1}) 3055, 2970, 2931, 1709, 1507, 1456, 1422, 1356, 1268, 1159, 818, 750. **HRMS** (ESI) m/z calculated for $C_{17}H_{18}NaO_2$ $[M+Na]^+$ 227.1199, found 227.1206.

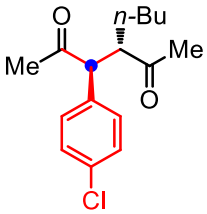

***anti*-52**

Following procedure B, major product ***anti*-52** (related to **Figure 2C**) was obtained as a colorless oil; **^{1}H-NMR** (600 MHz, $CDCl_3$) δ 7.33 (d, *J* = 8.4 Hz, 2H), 7.14 (d, *J* = 8.4 Hz, 2H), 4.06 (d, *J* =

10.8 Hz, 1H), 3.32-3.28 (m, 1H), 2.29 (s, 3H), 2.03 (s, 3H), 1.38-1.29 (m, 1H), 1.23-1.07 (m, 4H), 1.02-0.96 (m, 1H), 0.76 (t, *J* = 7.2 Hz, 3H). **^{13}C-NMR** (151 MHz, $CDCl_3$) δ 212.27, 207.69, 134.79, 133.70, 130.08, 129.29, 59.68, 53.43, 30.69, 29.20, 28.61, 27.91, 22.73, 13.66. **HRMS** (ESI) m/z calculated for $C_{16}H_{22}NaO_2$ $[M+Na]^+$ 269.1512, found 269.1529.

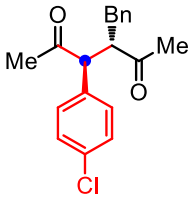

***anti*-53**

Following procedure B, major product ***anti*-53** (related to **Figure 2C**) was obtained as a colorless oil; **^{1}H-NMR** (600 MHz, $CDCl_3$) δ 7.38 (d, *J* = 8.4 Hz, 2H), 7.24-7.20 (m, 4H), 7.18 (t, *J* = 7.2 Hz, 1H), 6.94 (d, *J* = 7.2 Hz, 2H), 4.09 (d, *J* = 10.8 Hz, 1H), 3.51 (td, *J* = 10.8 Hz, *J* = 4.2 Hz, 1H), 2.50 (dd, *J* = 13.2 Hz, *J* = 4.2 Hz, 1H), 2.41 (dd, *J* = 13.2 Hz, *J* = 4.2 Hz, 1H), 2.00 (s, 3H), 1.83 (s, 3H). **^{13}C-NMR** (151 MHz, $CDCl_3$) δ 213.10, 207.33, 138.15, 134.69, 134.01, 130.21, 129.54, 128.67, 128.56, 126.63, 61.63, 55.63, 36.83, 32.36, 29.07. **HRMS** (ESI) m/z calculated for $C_{19}H_{20}ClO_2$ $[M+H]^+$ 315.1147, found 315.1153.

The **Figure S93** (NOESY experiments of *anti*-53) was used to confirm the configuration of compound **53**. Spatially, H^4 is more colse H^8 than H^{10}; H^7 is colse to H^{10} and far from H^8.

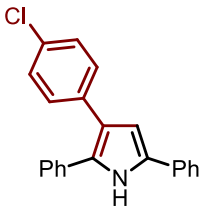

54

Compound **54** (related to **Scheme 2**) (Shen et al., 2013)**.** White solid; m.p. 145-147 ^{o}C; **^{1}H-NMR** (600 MHz, $CDCl_3$) δ 8.40 (s, 1H), 7.54-7.52 (m, 2H), 7.41-7.36 (m, 4H), 7.35-7.32 (m, 2H), 7.31-7.29 (m, 2H), 7.29-7.27 (m, 1H), 7.26-7.23 (m, 3H), 6.66 (d, *J* = 3.0 Hz, 1H).**^{13}C-NMR** (151 MHz, $CDCl_3$) δ 134.82, 132.76, 132.40, 132.01, 131.63, 129.58, 129.49, 129.00, 128.83, 128.49, 127.51, 127.21, 126.67, 123.80, 122.53, 108.24. **HRMS** (ESI) m/z calculated for $C_{22}H_{17}ClN$ $[M+H]^+$ 330.1044, found 330.1047.

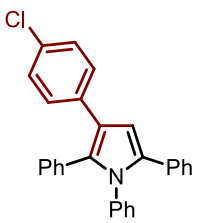

55

Compound **55** (related to **Scheme 2**) (Bharadwaj and Scheidt, 2004)**.** White soild; m.p. 178-180 ^{o}C; **^{1}H-NMR** (600 MHz, $CDCl_3$) δ 7.19-7.14 (m, 13H), 7.12-7.10 (m, 2H), 7.03-7.01 (m, 2H),

6.98-6.95 (m, 2H), 6.67 (s, 1H).**^{13}C-NMR** (151 MHz, $CDCl_3$) δ 138.59, 134.97, 134.63, 132.67, 132.33, 132.29, 131.37, 131.15, 129.31, 129.01, 128.53, 128.49, 128.27, 127.98, 127.97, 127.20, 127.15, 126.46, 122.24, 109.61. **HRMS** (ESI) m/z calculated for $C_{28}H_{21}ClN$ $[M+H]^+$ 406.1357, found 406.1342.

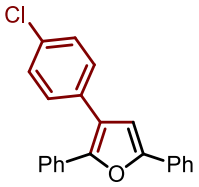

56

Compound **56** (related to **Scheme 2**) ()**.** White solid; m.p. 125-127 ^{o}C. **^{1}H-NMR** (600 MHz, $CDCl_3$) δ 7.77-7.74 (m, 2H), 7.59-7.57 (m, 2H), 7.43-7.38 (m, 4H), 7.36-7.29 (m, 5H), 7.28-7.27 (m, 1H), 6.78 (s, 1H). **^{13}C-NMR** (151 MHz, $CDCl_3$) δ 152.78, 148.09, 133.13, 132.76, 130.81, 130.33, 129.96, 128.90, 128.76, 128.51, 127.74, 127.67, 126.20, 123.82, 123.25, 109.04. **HRMS** (ESI) m/z calculated for $C_{22}H_{16}ClO$ $[M+H]^+$ 331.0884, found 331.0899.

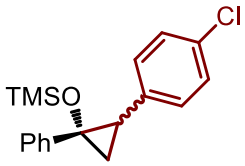

60

Compound **60** (related to **Scheme 3**). Major product: **^{1}H-NMR** (600 MHz, $CDCl_3$) δ 7.57 (d, *J* = 7.2 Hz, 2H), 7.53 (7, *J* = 7.2 Hz, 2H), 7.47-7.43 (m, 2H), 7.39-7.30 (m, 3H), 2.40-2.37 (m, 1H), 1.99-1.96 (m, 1H), 1.71-1.69 (m, 1H), 0.10 (s, 9H). **^{13}C-NMR** (151 MHz, $CDCl_3$) δ 144.08, 136.36, 131.52, 129.83, 128.25, 127.78, 126.86, 126.03, 62.88, 32.09, 20.72, 0.81. Minor product: **^{1}H-NMR** (600 MHz, $CDCl_3$) δ 7.47-7.43 (m, 3H), 7.37-7.30 (m, 2H), 7.20 (d, *J* = 8.4 Hz, 2H), 6.95 (d, *J* = 8.4 Hz, 2H), 2.80 (dd, *J* = 7.2 Hz, *J* = 11.2 Hz, 1H), 1.87 (t, *J* = 6.6 Hz, 1H), 1.82 (dd, *J* = 6.6 Hz, *J* = 11.2 Hz, 1H), 0.20 (s, 9H). **^{13}C-NMR** (151 MHz, $CDCl_3$) δ 138.52, 136.88, 131.11, 129.13, 128.98, 127.84, 127.74, 127.29, 64.65, 31.74, 19.23, 0.96. **IR** (KBr, cm^{-1}) 3736, 3649, 3060, 3029, 2958, 1493, 1449, 1249. **HRMS** (ESI) m/z calculated for $C_{18}H_{22}ClOSi$ $[M+H]^+$ 317.1124, found 317.1136.

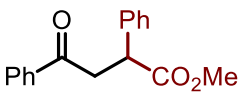

61

Compound **61** (related to **Scheme 3**) (Zhao et al., 2017). **^{1}H-NMR** (600 MHz, $CDCl_3$) δ 7.99-7.96 (m, 2H), 7.56 (t, *J* = 8.4 Hz, 1H), 7.45 (t, *J* = 9.0 Hz, 2H), 7.36-7.34 (m, 4H), 7.31-7.27 (m, 1H), 4.30 (dd, *J* = 4.8 Hz, *J* = 12.6 Hz, 1H), 3.95 (dd, *J* = 12.6 Hz, *J* = 21.6 Hz, 1H), 3.70 (s, 3H), 3.27 (dd, *J* = 4.8 Hz, *J* = 21.6 Hz, 1H). **^{13}C-NMR** (151 MHz, $CDCl_3$) δ 197.58, 173.82, 138.34, 136.38, 133.28, 128.89, 128.58, 128.06, 127.80, 127.53, 52.31, 46.34, 42.79. **HRMS** (ESI) m/z calculated for $C_{17}H_{17}O_3$ $[M+H]^+$ 269.1174, found 269.1176.

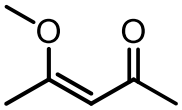

4-Methoxy-3-penten-2-one (related to **Scheme 3**)(Kraus et al., 1989)**.** **^{1}H-NMR** (600 MHz, $CDCl_3$) δ 5.47 (s, 1H), 3.65 (s, 3H), 2.28 (s, 3H), 2.17 (s, 3H). **^{13}C-NMR** (151 MHz, $CDCl_3$) δ 196.87, 172.69, 99.24, 55.29, 31.90, 19.49.

Supplemental References

Bergonzini, G., Cassani, C., Lorimer-Olsson, H., Hörberg, J., and Wallentin, D.-J. (2016). Visible-light-mediated photocatalytic difunctionalization of olefins by radical acyl/arylation and tandem acylation/semipinacol rearrangement. Chem. Eur. J. *22*, 3292-3295.

Bharadwaj, A.R., and Scheidt, K.A. (2004). Catalytic multicomponent synthesis of highly substituted pyrroles utilizing a one-pot Sila-Stetter/Paal-Knorr strategy. Org. Lett. *6*, 2465–2468.

Blay, G., Fernandez, I., Monje, B., Munoz, M.C., Pedro, J.R., Vila, C. (2006). Enantioselective synthesis of 2-substituted-1,4-diketones from (*S*)-mandelic acid enolate and α,β-enones research article. Tetrahedron *62*, 9174-9182.

Fujimura, T., Aoki, S., and Nakamura, E. (1991). Synthesis of 1,4-keto esters and 1,4-diketones *via* palladium-catalyzed acylation of siloxycyclopropanes. Synthetic and mechanistic studies. J. Org. Chem. 1991, *56*, 2809-2821.

Kraus, G.A., Krolski, M.E., and Sy, J. (1989). 4-Methoxy-3-penten-2-one. Org. Syn. *67*, 202-203.

Liu, Z., Li, Q., Yang, Y., and Bi, X. (2017). Silver(I)-promoted insertion into X–H (X = Si, Sn, and Ge) bonds with *N*-nosylhydrazones. Chem. Commun. *53*, 2503-2506.

Mattson, A.E., Bharadwaj, A.R., Zuhl, A.M., and Scheidt, K.A. (2006). Thiazolium-catalyzed additions of acylsilanes: a general strategy for acyl anion addition reactions. J. Org. Chem. *71* 5715-5724.

Schroll, P., and König, B. (2015). Photocatalytic α-oxyamination of stable enolates, silyl enol ethers, and 2-oxoalkane phosphonic esters. Eur. J. Org. Chem. *2015*, 309-313.

Shen, J., Cheng, G., and Cui, X. (2013). "One pot" regionspecific synthesis of polysubstituted pyrroles from benzylamines and ynones under metal free conditions. Chem. Commun. *49*, 10641-10643.

Zhao, F., Li, N., Zhang, T., Han Z., Luo, S., and Gong, L. (2017). Enantioselective Aza-Ene-type reactions of enamides with gold carbenes generated from α-diazoesters. Angew. Chem. Int. Ed. *56*, 3247-3251.